MDC E0647

N73-17646

IMPROVEMENT OF REUSABLE SURFACE INSULATION (RSI) MATERIALS

FINAL REPORT

MCDONNELL DOUGLAS ASTRONAUTICS COMPANY • EAST

MCDONNELL DOUGLAS CORPORATION

Page Intentionally Left Blank

COPY NO. 2

IMPROVEMENT OF REUSABLE SURFACE INSULATION (RSI) MATERIALS

4 AUGUST 1972 MDC E0647

FINAL REPORT
23 JUNE 1971 TO 23 JUNE 1972

J.C. Blome

Submitted in Accordance with
Requirements of Contract
NAS 8-27688

MCDONNELL DOUGLAS ASTRONAUTICS COMPANY - EAST
Saint Louis, Missouri 63166 (314) 232-0232

MCDONNELL DOUGLAS CORPORATION

Page Intentionally Left Blank

FOREWORD

This final report was prepared by the McDonnell Douglas Astronautics Company - East under NASA Contract NAS 8-27688 and covers work performed during the period 23 June 1971 to 23 June 1972. This work was administered under the direction of the Astronautics Laboratory, NASA George C. Marshall Space Flight Center, Alabama, with Harry M. King as the Contracting Officer's Representative.

The author wishes to acknowledge the contributions of the following personnel who were responsible for the program's efforts that fell in their respective fields of endeavor: H. E. Christensen and J. M. Buchanan (Therodynamics), J. K. Lehman and J. A. Smittkamp (Strength), E. L. Rusert, C. J. Goodbrake, J. F. Preston, M. W. Vance, T. M. Day (Materials and Processes), E. F. Disser, B. J. Myers (Manufacturing), D. N. Drennan, R. Patterson, H. W. Jacobus, W. C. Mayden, L. E. McCrary, E. Cox, R. H. Brooks, Jr., R. Wilcox, W. B. Munsell (Engineering Laboratories), and J. Jortner (MDAC-West).

ABSTRACT

The mullite fiber based hardened compacted fibers (HCF) type of reusable surface insulation was further developed for use in the Space Shuttle Program. Two hundred fifty formulations of fiber mixtures, fillers, binders, and organic processing aids were made using mullite fibers as the basic ingredient. Most of the work was accomplished on 15-lb/ft^3 material. It was established that higher density materials are stronger with strength values as high as 250 lb/in^2 in tension. New measurement techniques and equipment were developed for accurate determination of strength and strain to failure. Room temperature to 2300°F stress-strain relationships were made. The room temperature tensile modulus of elasticity is 61,700 lb/in^2 and the strain at failure is 0.165 percent, typically, when measured longitudinally parallel to the long axes of the fibers. Thermal insulating effectiveness was increased 20 percent by reducing the diameter of some of the fibers in the material. Improvements were made in density uniformity and strength uniformity in a block of HCF by mixing improvements and by the use of organic additives. Specifications were established on the materials and processes used in making the insulation. Metal wire reinforcement techniques were developed, and it was demonstrated that the reinforcement would hold cracked pieces together without appreciably increasing density or thermal conductivity. Improvements were made in the glassy reusable liquid-waterproof coating by decreasing density from 0.24 to 0.15 lb/ft^2 and increasing surface smoothness and reproducibility. Organic coatings applied over the HCF provided liquid-waterproofing.

Page Intentionally Left Blank

TABLE OF CONTENTS

Page Intentionally Left Blank

TABLE OF CONTENTS (Continued)

LIST OF PAGES

Title Page
ii thru v
1-1 thru 1-4
2-1 thru 2-35
3-1 thru 3-45
4-1 thru 4-16
5-1 thru 5-20
6-1 thru 6-20
7-1 thru 7-3
8-1

1.0 INTRODUCTION AND SUMMARY

This final report covers the activities and progress made in this one-year program, ending 23 June 1972, in the improvement and evaluation of a reusable surface insulation (RSI) material for the thermal protection system (TPS) for the Space Shuttle.

The 15-lb/ft^3 mullite hardened compacted fibers (HCF) RSI material was improved and evaluated for this program. A reusable liquid-waterproof inorganic coating that had been previously developed was also studied and improved.

Approximately 250 different formulations of mullite HCF-RSI were evaluated; strength improvement and thermal conductivity reduction were the major goals.

Improvements were made in the strength of mullite HCF material. Tensile strength was increased from approximately 75 to 101-lb/in^2 for material with a density of 15-lb/ft^3, and laboratory formulations have had tensile strengths of as high as 250-lb/in^2 for 16-lb/ft^3 materials. It was also verified by testing that strength and modulus of elasticity are dependent on density. It was necessary in this program to develop new measurement techniques and equipment for the accurate determination of strength and strain to failure. Both room temperature and elevated temperature stress-strain relationships were established. At room temperature, typical longitudinal and transverse tensile moduli of elasticity for a 15-lb/ft^3 HCF material, measured using the new technique, are 61,700 and 13,700-lb/in^2, respectively. Longitudinal strains at failure are typically 0.165 percent.

Thermal insulating performance testing was conducted on selected formulations of HCF which had demonstrated adequate strength and processability. Both steady state and transient thermal performance tests were conducted. The modes of heat transfer were modeled in our computer program in an attempt to better describe the insulating effectiveness of RSI. These studies and tests indicated that the thermal insulating efficiency of HCF can be increased approximately 20 percent by

reducing the fiber diameter of about 20 percent of the fibers to below 2μ diameter and by reducing the fraction of filler (glassy spheres). A still lower thermal conductivity would be expected if all of the fibers were below 2μ diameter.

Improvements in material density and strength uniformity were constant goals during this program. We concentrated first on density uniformity and then on reducing the strength gradients in the material. Several cases were found where the density gradients were near zero, but, surprisingly, the strength gradients were severe: the weak areas were usually near the center of the HCF block. This problem was alleviated by changing the processing: two organic materials were added, the mixing procedure was improved, and the HCF felts were turned during drying.

Processing and materials improvements, such as mixing and additives, have resulted in a stronger and more uniform product. Binder solids control and wet density control have both proven to be successful in improving the strength reproducibility of HCF. Reimpregnation of fired felts with binder to improve the strength was unsuccessful.

We have tightened controls on the incoming raw materials, and have improved in-process and postprocessing controls in the fabrication of HCF. Two process specifications have been prepared which define the process operations and control parameters necessary for HCF fabrication and for the application of the inorganic coating.

A summary of the designations of the major materials formulated and tested in this program is given in Figure 1-1.

Reinforcement techniques (to hold the pieces together in case of separation or delamination within the HCF material, and not as a strengthening device for the HCF material), have been investigated. We have successfully processed reinforced HCF tiles using ceramic yarn and metal wires in a 3-D array using the standard HCF

MDAC-EAST DESIGNATION	FORMULATION*					COMMENTS
	FIBERS	FILLERS	OPACIFIERS	BINDER	OTHER**	
MOD I	6μ MULLITE	ECCOSPHERES	ZIRCON	RSB-2	-	BASELINE MATERIAL
MOD II	6μ MULLITE	CENOSPHERES	-	RSB-2	-	HIGHER MULLITE FRACTION IN COMPOSITION
MOD III	4.7μ MULLITE	ECCOSPHERES	ZIRCON	RSB-2	-	UNIFORMITY UNACCEPTABLE
MOD IIIA	4.7μ MULLITE	ECCOSPHERES	ZIRCON	RSB-2	HMT + CELLU-LOSE	BASELINE SELECTED AT END OF PROGRAM; VERY UNIFORM
MOD IV	2.5μ MULLITE	ECCOSPHERES	-	RSB-2	HMT + CELLU-LOSE	DIFFICULT TO PROCESS; FIBERS NOT AVAILABLE IN QUANTITY
MOD V	4.7μ MULLITE +1.2μ SILICA	-	-	RSB-2	HMT + CELLU-LOSE	BEST THERMAL PERFORMANCE; PROCESSING VARIABLES NOT YET DEFINED

*THE FORMULATIONS LISTED HERE ARE NOMINAL AND WERE VARIED DURING THE COURSE OF THIS PROGRAM.

** PROCESSING ADDITIVES WHICH DO NOT BECOME PART OF THE FINISHED PRODUCT BECAUSE THEY BURN OUT DURING FIRING CYCLE

MATERIALS DESIGNATIONS
FIGURE 1-1

felting process; no voids or cavities were found in the HCF tile, based on X-ray and visual examination. An increase in density of 1.5-lb/ft^3 resulted from the use of a columbium wire reinforcement. One sample of wire reinforced HCF was tested to 2500°F without any sign of damage. This reinforcement effort led to the concept of strengthening HCF by including metallic trusses in the HCF. When metallic trusses are used in the HCF combined with the use of an efficient low-density insulation, they could save up to 50 percent of the weight of an unreinforced RSI thermal protection system.

The reusable liquid-waterproof coating previously developed had a high modulus

of elasticity and a low strain to failure because it was sealed with a glass overcoating. Therefore, the coating tended to crack unless the coated HCF was isolated from the structural strains. We were not successful in increasing the strain to failure or lowering the modulus of this reusable liquid-waterproof coating, but the surface density was decreased from 0.24 to 0.15-lb/ft^2 by eliminating one layer of the coating. The coating was also made smoother.

The coating improvement effort included the development of a new base coating which does not exhibit a permanent expansion as did previous coatings. Reusable coatings were evaluated by testing tiles as large as 6 by 6 by 3 inches, coated on five sides, under simulated temperature and pressure cycles. These coatings were then evaluated for appearance, smoothness, cracking and waterproofness. Our liquid-waterproof coating was successfully cycled 100 times to 2300°F in a typical Shuttle temperature profile. Textured coatings were studied as a method to reduce their effective stiffness and, therefore, to make the coatings more compatible with HCF. A one-step coating was developed which reduced coating time and the number of required firing cycles.

Organic coatings applied directly to the HCF or applied as an overcoating for an inorganic base coating have been successful in providing liquid-waterproofing. The organic coatings have an advantage over the inorganic, glass coatings because of their lower moduli, but the organic coatings would have to be refurbished after every flight in areas that exceed 700 to 900°F during ascent or entry.

2.0 HCF DEVELOPMENT

The major goals of this program were to improve mullite HCF in the areas of strength, thermal performance, uniformity in density and strength, and processability. To accomplish these tasks we evaluated and selected raw materials, formulated various compositions, and instituted and developed quality control procedures and practices.

2.1 RAW MATERIALS - Mullite fibers of different diameters, various fillers (hollow ceramic spheres), several inorganic binders, opacifiers, and several organic processing aids were evaluated. Micrographic examination and other methods were used to aid in the selection of the various materials. The materials were classified as to appearance and dimensions both as received and after exposure to several selected high temperatures.

Fibers - In addition to mullite fibers, which are currently available from Babcock and Wilcox (B&W) in a variety of fiber diameters, fine diameter silica fibers were evaluated as a substitute for the hollow silica spheres (filler) (Mod V).

The mullite fiber grades which were investigated included:

- Standard - 5 to 6-μ average fiber diameter
- Intermediate - 4.25 to 5.25-μ average fiber diameter
- Fine - 4.0-μ average fiber diameter
- Very fine - 2.5-μ average fiber diameter

Figures 2-1, 2-2, 2-3, and 2-4 show the photomicrographs of representative fiber specimens in conjunction with the distribution of fiber diameters for each grade of fiber as supplied by the vendor. The differences between the standard, intermediate and fine fibers seem to be due to the selective removal of the coarser fibers, while the very fine (2.5-μ diameter) fibers appear to be more uniformly finer (more normally distributed fibers) than the other grades of fibers.

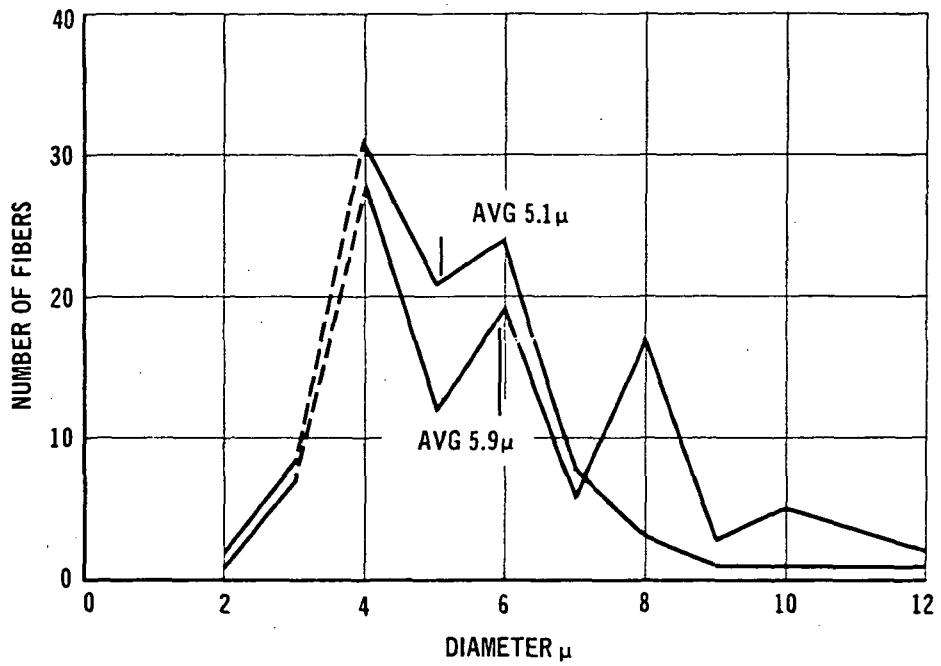

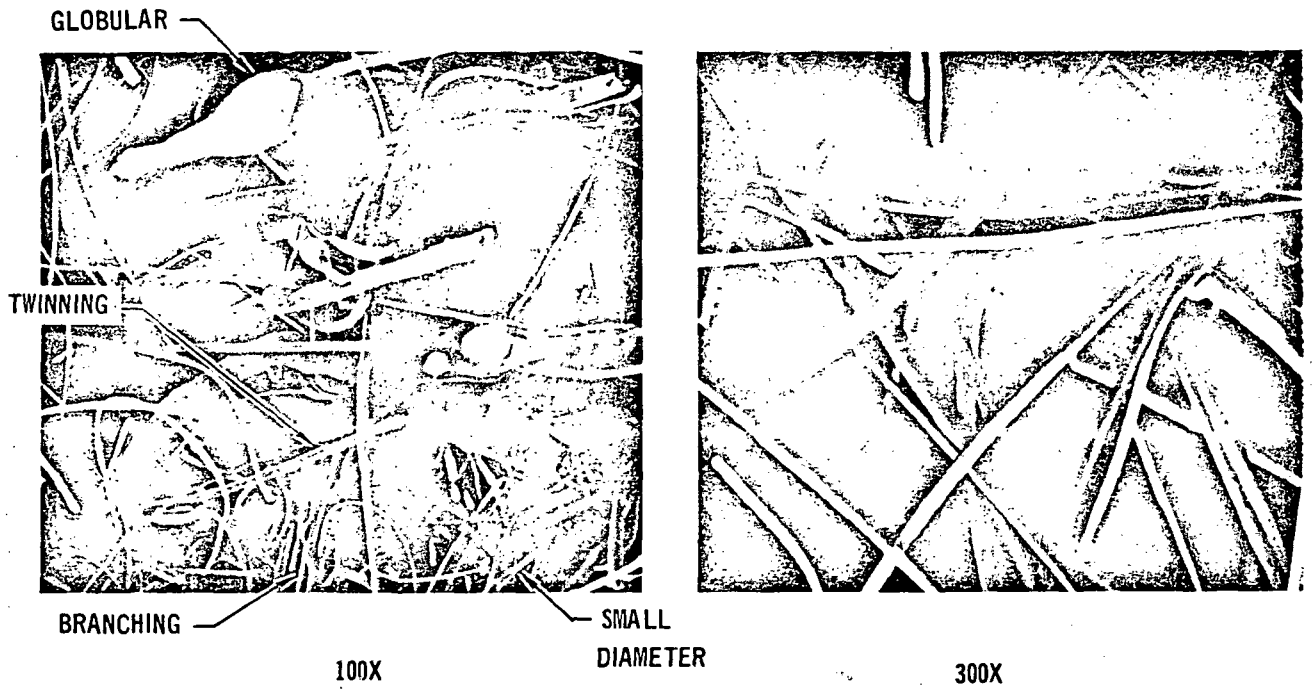

FIGURE 2-1

FIBER DISTRIBUTION AND PHOTOMICROGRAPHS OF STANDARD B&W MULLITE FIBERS (5-6 μ AVERAGE DIAMETER)

457-1605

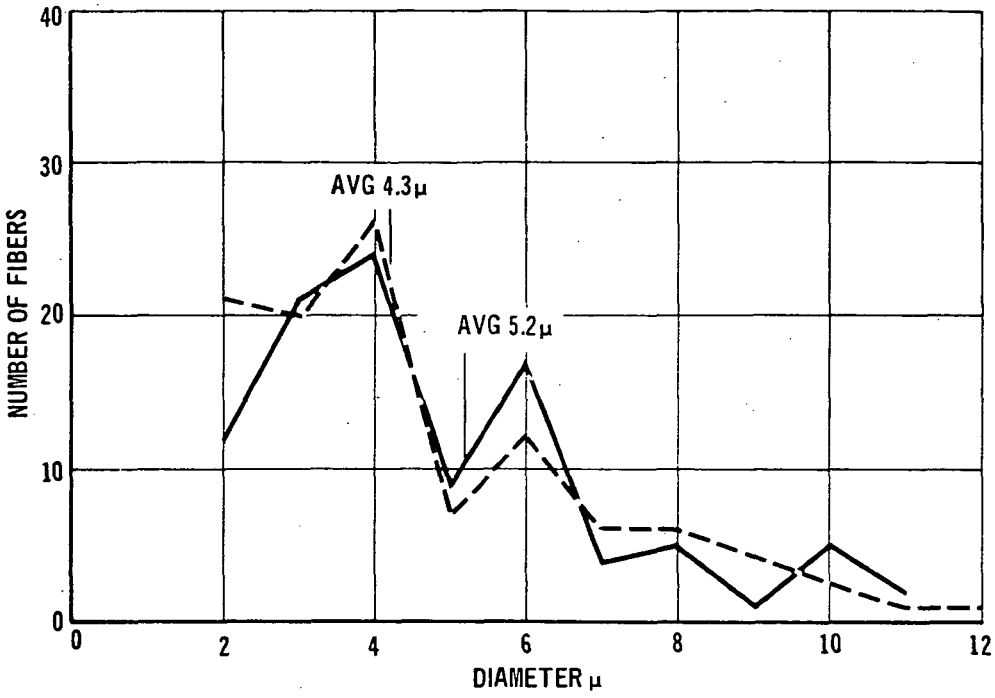

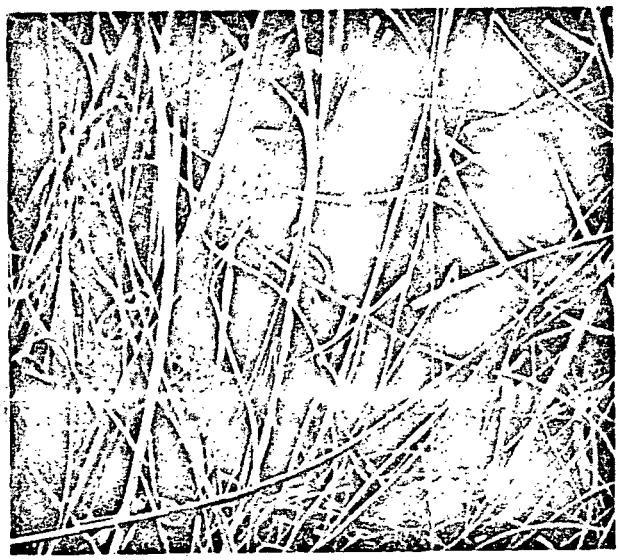

100X

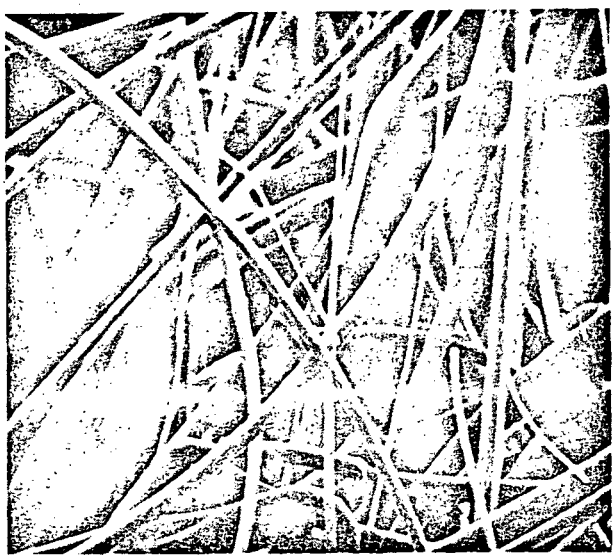

300X

FIGURE 2–2

FIBER DISTRIBUTION AND PHOTOMICROGRAPHS OF INTERMEDIATE B&W MULLITE FIBERS (4.25–5.25 AVERAGE DIAMETER)

457–1004

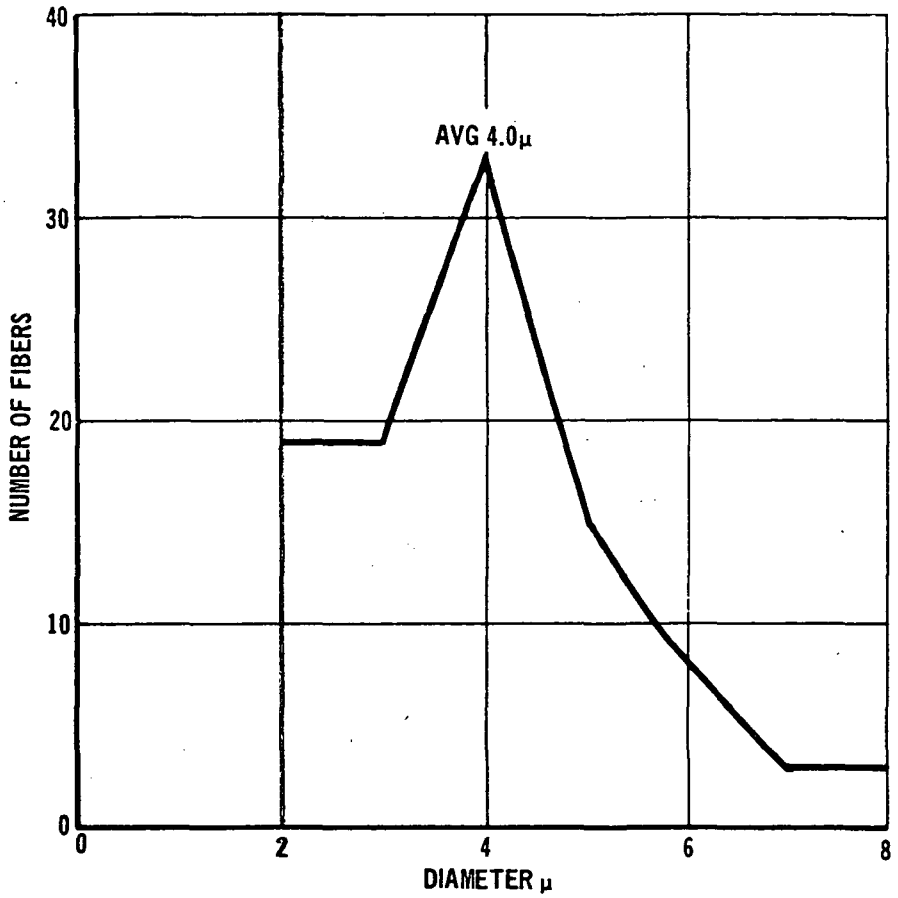

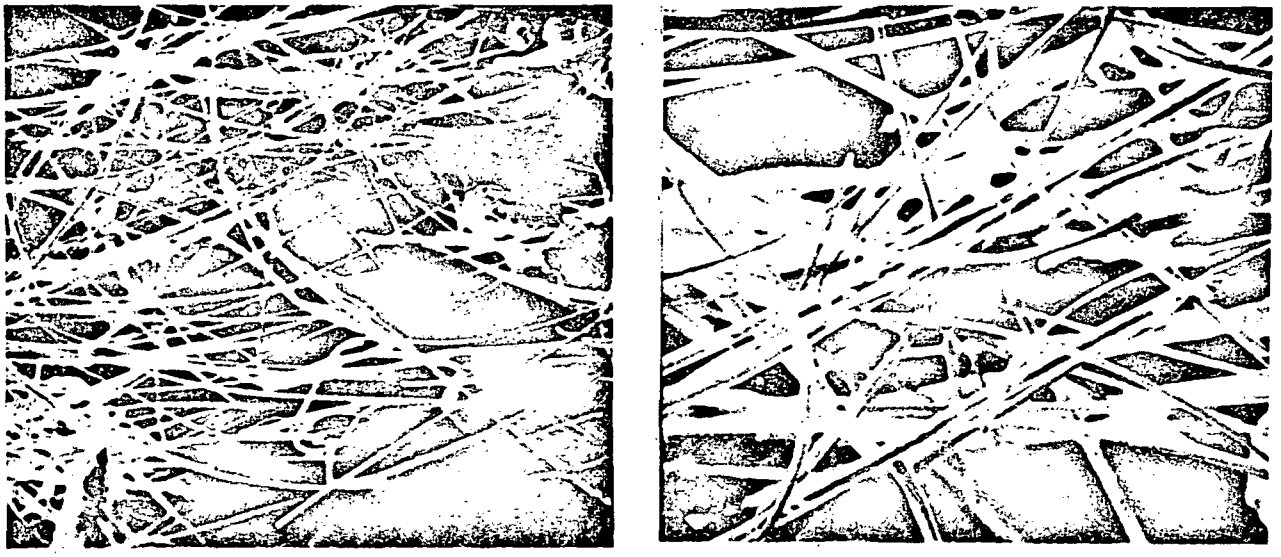

100X 300X

FIGURE 2–3

FIBER DISTRIBUTION AND PHOTOMICROGRAPHS OF FINE B&W MULLITE FIBERS (4.0 AVERAGE DIAMETER)

457–1568

100X

300X

FIBER DIAMETER DISTRIBUTION:
- 80% LESS THAN 4μ
- 65% LESS THAN 3μ
- 30% LESS THAN 2.5μ
- MODE = 2.5μ

FIGURE 2-4

FIBER DIAMETER DISTRIBUTION AND PHOTOMICROGRAPHS OF VERY FINE B & W MULLITE FIBERS (2.5 μ DIAMETER)

457-2561

Silica fibers, as shown in Figure 2-5, with an average fiber diameter of 1.2-μ have a much softer texture than the coarser mullite fibers and are more difficult to chop.

Fillers - Some of the inherent advantages and disadvantages of candidate fillers for HCF are indicated in Figure 2-6. SI grade Eccospheres*, while lightweight, sinter rapidly at 2500°F as shown in Figure 2-7. Although Cenospheres sinter more slowly at 2500°F (See Figure 2-8), they are significantly heavier than SI Eccospheres. The "floaters," a fly ash product similar to Cenospheres

* Emerson & Cuming, Inc.

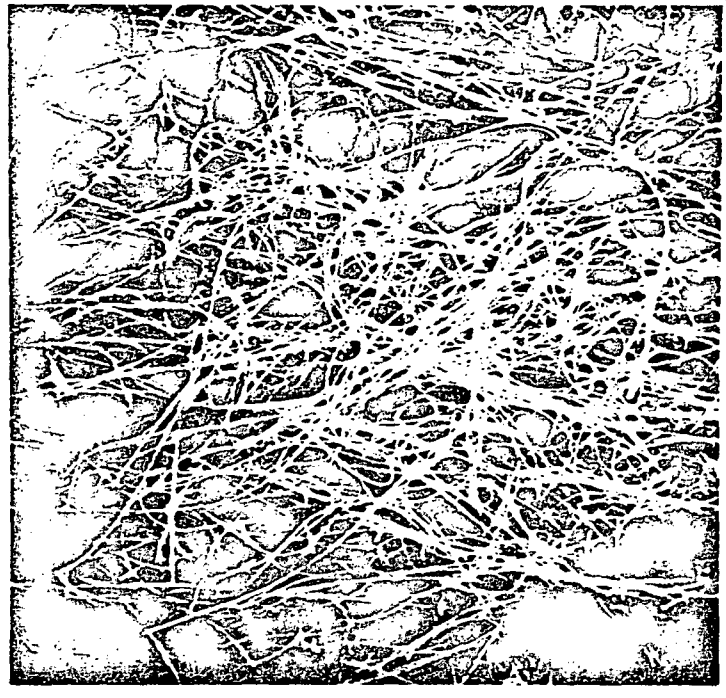

100 X

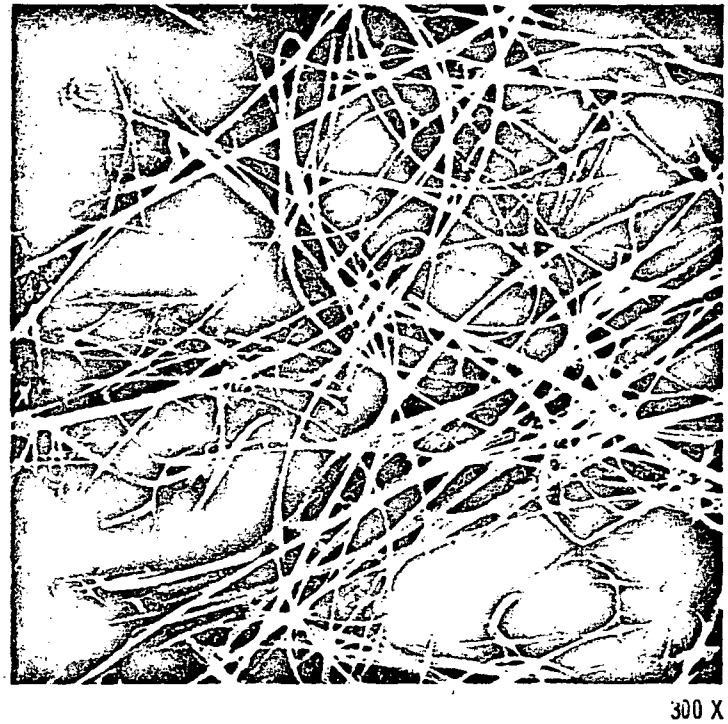

300 X

FIGURE 2–5

PHOTOMICROGRAPHS OF SILICA FIBERS (1.2 μ AVERAGE DIAMETER)

457-2537

FILLER TYPE	SI ECCOSPHERES	LOW ρ CENOSPHERES	"FLOATERS" *	FA-A ECCOSPHERES
COMPOSITION	$SiO_2 \sim 90\%$	$SiO_2 \sim 60\%$ $Al_2O_3 \sim 30\%$	$SiO_2 \sim 53\%$ $Al_2O_3 \sim 33\%$	NOT AVAILABLE
PARTICLE SIZE (DIAMETER)	30 TO 125μ	50 TO 150μ	40 TO 180μ	60 TO 325μ
BULK DENSITY	11 PCF	17 PCF	28 PCF	25 PCF
PARTICLE DENSITY	16 PCF	22 PCF	37 PCF	35 PCF
SINTERING TEMPERATURE	~2300°F	~2500°F	~2500°F	1800°F

*A FLY ASH COMPONENT FROM LOCAL ELECTRICITY GENERATING STATION OF UNION ELECTRIC CO.

457-2540

FIGURE 2-6

PROPERTIES OF CANDIDATE FILLERS

but from a local power plant, were much denser than the Cenospheres.

2.2 FORMULATION AND PROCESSING - Five new general mullite HCF compositions were formulated and their properties were evaluated relative to Mod I HCF, our baseline HCF at the beginning of this period. Figure 2-9 shows the basic properties of Mod I and the properties of the newer HCF materials. The new HCF insulations were tested for strength, impact indentation, uniformity, density, processability, and thermal performance. Specimens of 3.3-inch diameter were formed to determine the initial fabrication parameters for each new HCF composition. Factors which were controlled included blending time, binder specific gravity, slurry viscosity, drain time, batch size, height and weight of the felt, drying cycle and firing cycle. Initial strength and density gradient data were obtained from the 3.3-inch diameter specimens. The felting and testing procedures were later scaled up to 9 and 11-inch diameter specimens. The most promising HCF compositions (Mod IIIA and Mod V) were scaled up to 14 by 16 by 4-1/2-inch specimens. Mechanical

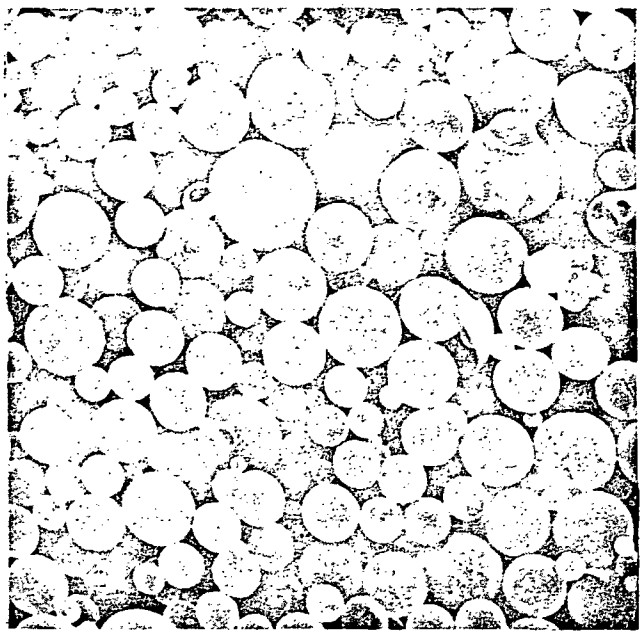

SI ECCOSPHERES AS RECEIVED

457-1271 100 X

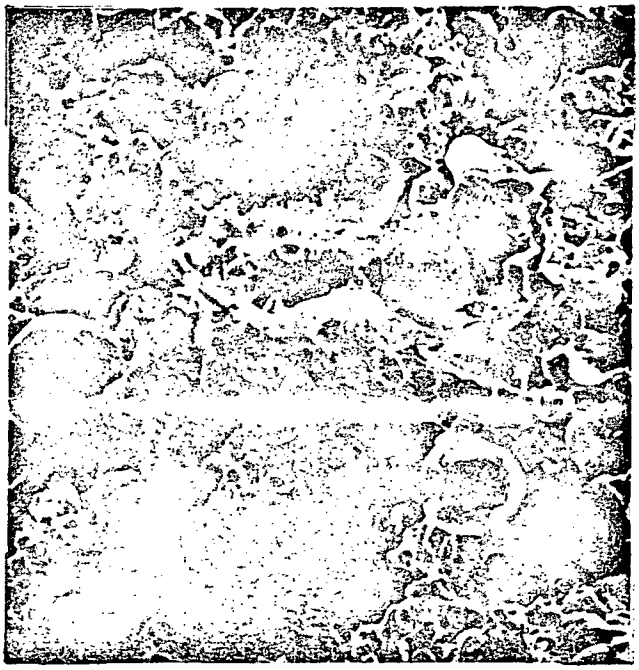

SI ECCOSPHERES FIRED AT
457-1272 2500°F FOR 1 HOUR
100 X

FIGURE 2-7

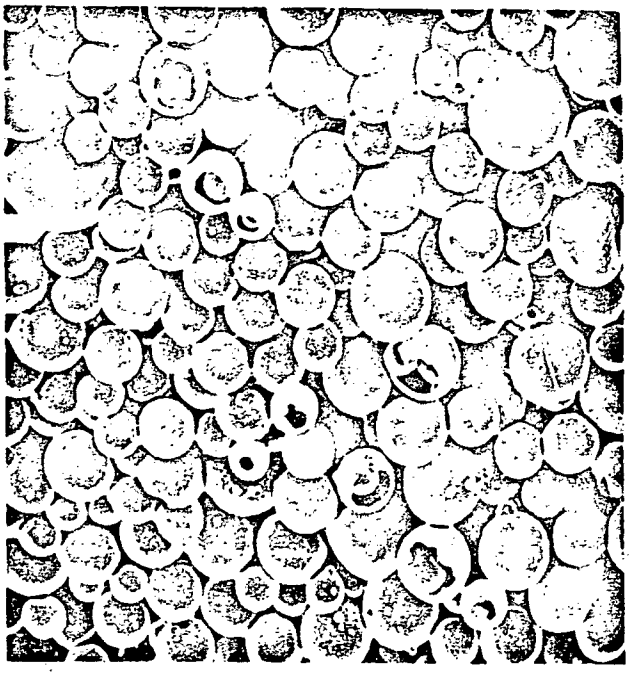

LOW DENSITY CENOSPHERES
AS RECEIVED

457-1273

100 X

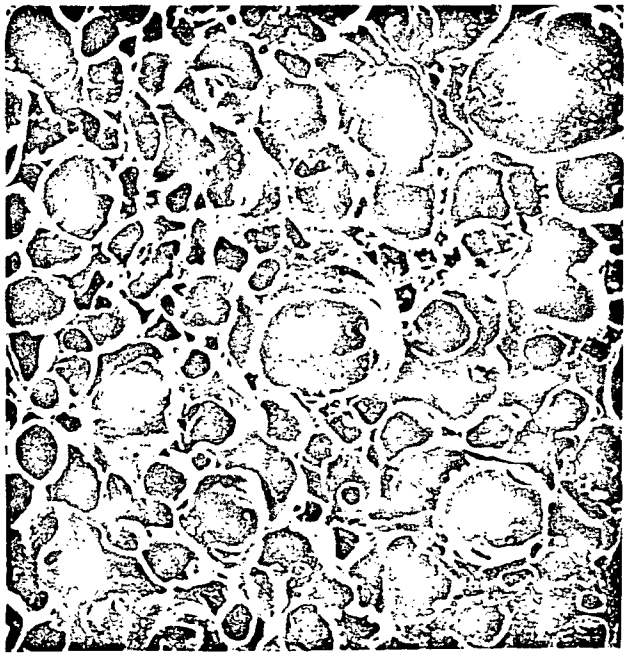

457-1274 LOW DENSITY CENOSPHERES
AFTER FIRING AT 2500°F FOR 15 MINUTES

100 X

FIGURE 2-8

MATERIAL DESIGNATION	FORMULATION	STRENGTH (PSI) TENSION AVERAGE	UNIFORMITY DENSITY GRADIENT LB/FT^3	THERMAL PERFORMANCE BONDLINE TEMPERATURE (^{0}F) OXY ACETYLENE TORCH	REHEAT SHRINKAGE (1 HR 2300^{0}F)		COEFFICIENT OF THERMAL EXPANSION IN/IN/^{0}F		PROCESSABILITY	COMMENTS
					IN X-Y DIRECTION	IN Z DIRECTION	X-Y DIRECTION	Z DIRECTION		
MOD I BASELINE MATERIAL	6μ DIA MULLITE FIBER SiO_2 SPHERES RSB-2 BINDER TiO_2 OPACIFIER	σ_L = 114 σ_T = 33	15-17 BULK DENSITY $\Delta\rho$= 1-3 PCF	540^{0}F 2 IN. THICK 2300^{0}F REENTRY PROFILE	+0.08%	-0.28%	3.0×10^{-6}	NOT DETERMINED	GOOD	CHANGED FROM MOD I TO MOD II AND MOD IIIA USING 4.7μ FIBERS TO IMPROVE THERMAL PERFORMANCE AND STRENGTH
MOD II	4.7μ MULLITE FIBER Al_2O_3: SiO_2 SPHERES RSB-2 BINDER ZIRCON OPACIFIER	σ_L = 140 σ_T = 28	15-17 BULK DENSITY $\Delta\rho$= 2-5 PCF	480^{0}F 2 IN. THICK 2300^{0}F REENTRY PROFILE	+0.18%	-0.33%	3.3×10^{-6}	NOT DETERMINED	FAIR	1) SOFT SPOTS IN THE CENTER OF THE FELTS 2) NEED TO APPLY MOD IIIA PROCESSING TECHNIQUES
MOD III	4.7μ MULLITE FIBER SiO_2 SPHERES RSB-2 BINDER ZIRCON OPACIFIER	σ_L = 121 σ_T = 51	14-16 BULK DENSITY $\Delta\rho$= 2-4 PCF	465^{0}F 2 IN. THICK 2300^{0}F REENTRY PROFILE	+0.02%	-0.33%	3.4×10^{-6}	NOT DETERMINED	GOOD	1) POOR DENSITY GRADIENTS 2) LACKED IN PROCESS CONTROL 3) SOFT AREAS
MOD IIIA	4.7μ MULLITE FIBER SiO_2 SPHERES RSB-2 BINDER ZIRCON OPACIFIER THICKENING AGENT	σ_L = 87 σ_T = 54	14-16 BULK DENSITY $\Delta\rho$= 2.0 PCF	480^{0}F 2 IN. THICK 2300^{0}F REENTRY PROFILE	+0.07%	-0.63%	3.2×10^{-6}	2.5×10^{-6}	VERY GOOD	1) VERY GOOD UNIFORMITY 2) NEED TO IMPROVE OVERALL STRENGTH
MOD IV	2.5μ MULLITE FIBER SiO_2 SPHERES RSB-2 BINDER ZIRCON OPACIFIER	σ_L = 128 σ_T = 63	16-24 BULK DENSITY $\Delta\rho$= 5-8 PCF	NOT TESTED DIRECTLY OPTICAL SCATTERING DATA SHOWED 2.5μ MULLITE FIBERS 50% BETTER THAN MOD IIIA	+0.27%	-0.8%	NOT DETERMINED		POOR HIGH BULK DENSITY HIGH DENSITY GRADIENTS	1) 2.5μ MULLITE FIBER SHOWS PROMISE TO LOWER THERMAL CONDUCTIVITY 2) NEED TO IMPROVE PROCESS
MOD V	4.7μ MULLITE FIBER 1.2μ SiO_2 FIBER RSB-2 BINDER NO OPACIFIER THICKENING AGENT	σ_L = 43 (250)* σ_T = 29 (105)*	15-16 BULK DENSITY $\Delta\rho$= 2-5	380^{0}F 2 IN. THICK 2300^{0}F REENTRY PROFILE	+0.11%	-0.75%	2.7×10^{-6}	2.4×10^{-6}	FAIR-POOR DIFFICULT TO FELT AND FIRE TO GET GOOD STRENGTH	1) HAS BETTER THERMAL PERFORMANCE THAN MOD I - MOD IV 2) NEED TO REFINE PROCESS AND CONTROL SiO_2 FIBER QUALITY

LONGITUDINAL - (L) PARALLEL TO FIBERS
TRANSVERSE - (T) PERPENDICULAR TO FIBERS

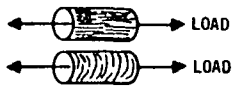

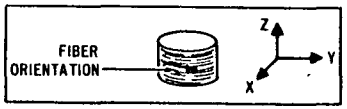

+ EXPANSION
- SHRINKAGE

*MADE WITH EXPERIMENTAL LOT OF SiO_2 FIBERS

$\Delta\rho$= DENSITY GRADIENT

FIGURE 2-9

HCF NOMINAL PROPERTIES

properties testing and coating development were conducted using the larger HCF specimens (9-inch diameter or 14 by 16-inch sizes).

Mod II HCF - Mod II HCF was formulated as a totally mullite reusable surface insulation. Initially, Mod II consisted of 6.0-μ mullite fibers, mullite binder and aluminosilicate glass spheres. Several 3.3 and 9.0-inch diameter all-mullite specimens were processed. X-ray diffraction studies showed the Mod II to be gamma Al_2O_3 and mullite. No silica (cristobalite) was detected. The strength of the Mod II with mullite binder was low. An evaluation of slurry viscosities, blending procedures, and firing cycles indicated that the strength properties desired could not be obtained with this all-mullite system. A silica binder, RSB-2, that had been used successfully with Mod I HCF to improve its strength was tried. Strength values did increase substantially when the new binder was used. With the addition of the silica, X-ray diffraction showed some cristobalite formation after firing. At the same time, we began using 4.7-μ diameter mullite fibers. The 4.7-μ mullite fibers seemed to improve the thermal performance during early screening tests. The altered Mod II consisted of 4.7-μ mullite fibers, aluminosilicate spheres, RSB-2 binder, and zircon opacifier. The only compositional change from the Mod I material was the substitution of aluminosilicate glass spheres for the silica spheres. Two types of aluminosilicate glass spheres were tested. The first was a fly ash derivative from a local source (Union Electric "Floaters"). The second was fly ash spheres from England (Cenospheres). The Cenospheres had a higher degradation temperature than the SiO_2 spheres due to the greater wall thickness and the composition of the Cenospheres (see Section 2.1).

Mod II specimens were produced in two diameters, 3.3 and 9.0-inches. The Mod II felts processed much differently than the Mod I; i.e., nearly every Mod II felt retained excessive binder on the top and bottom surface, causing a soft center problem. Photomicrographs clearly showed the lack of binder in the center

of the Mod II specimen. Figure 2-10 shows a typical density gradient, through a sample of Mod II. We believe the binder deficiency was caused by a binder, fiber, Cenosphere wetting phenomenon, and binder migration during drying. To correct the soft center problem in Mod II, we varied the slurry viscosity and the solids content in the binder. The results of these studies showed that an increase in blending time decreased the slurry viscosity and increased the bulk density of the Mod II specimen. The soft center condition was partially controlled by longer blending times, but many Mod II felts were unacceptably dense (16-18 lb/ft^3). Work on Mod II was suspended because it did not appear that an acceptable product could be made using this formulation.

Mod III HCF - Mod III was the next series of HCF materials formulated, and it consisted of 4.7-μ diameter mullite fibers, SiO_2 spheres, RSB-2 silica binder and zircon opacifier. Mod III processed easily but the uniformity of the material and the reproducibility of the process were erratic as shown in Figure 2-11. The most serious problems with Mod III were the densified surfaces and the soft centers of many felts.

We processed Mod III HCF to obtain felts which had 15 $\pm$ 1.5-lb/ft^3 bulk fired density with a minimum density gradient through and across the specimen. Figure 2-12 shows typical gradients encountered in a typical Mod III felt. We also noticed the tendency of coated Mod III blocks to fail during reentry simulation due to delamination cracks in the X-Y plane. Many of the cracks occurred through the soft center portion of the Mod III tiles.

Mod IIIA HCF - Mod IIIA has the same composition after firing as Mod III. The basic change was the use of additives (processing aids) to make fabrication of Mod IIIA easier and to improve the uniformity of the HCF. The first additive tested was propylcellulose[(1)]. When added in small quantities (less than 0.2 percent by

[(1)] Propylcellulose - Klucel, Hercules Corp.

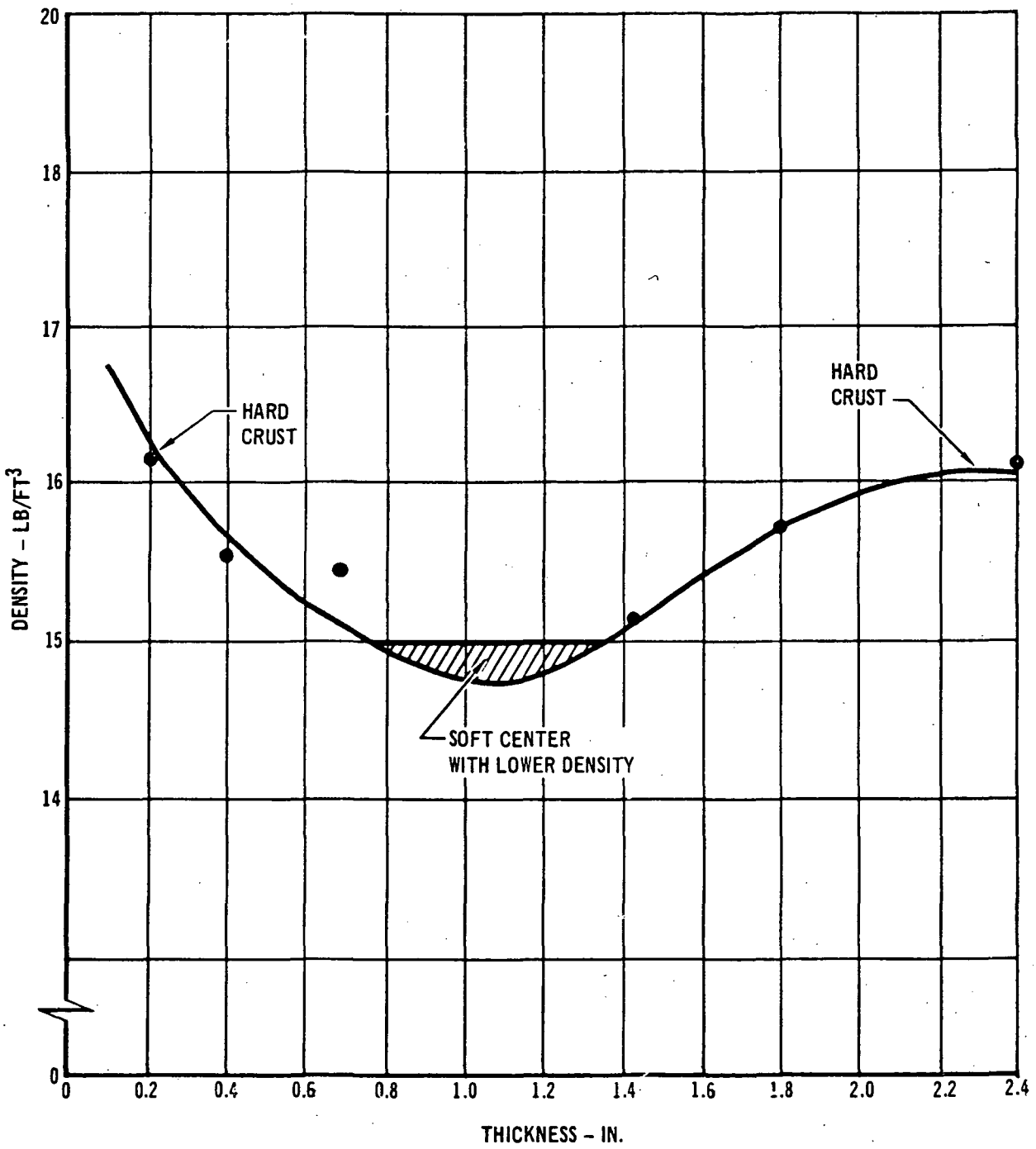

FIGURE 2-10

DENSITY GRADIENT OF MOD II HCF

457-2557

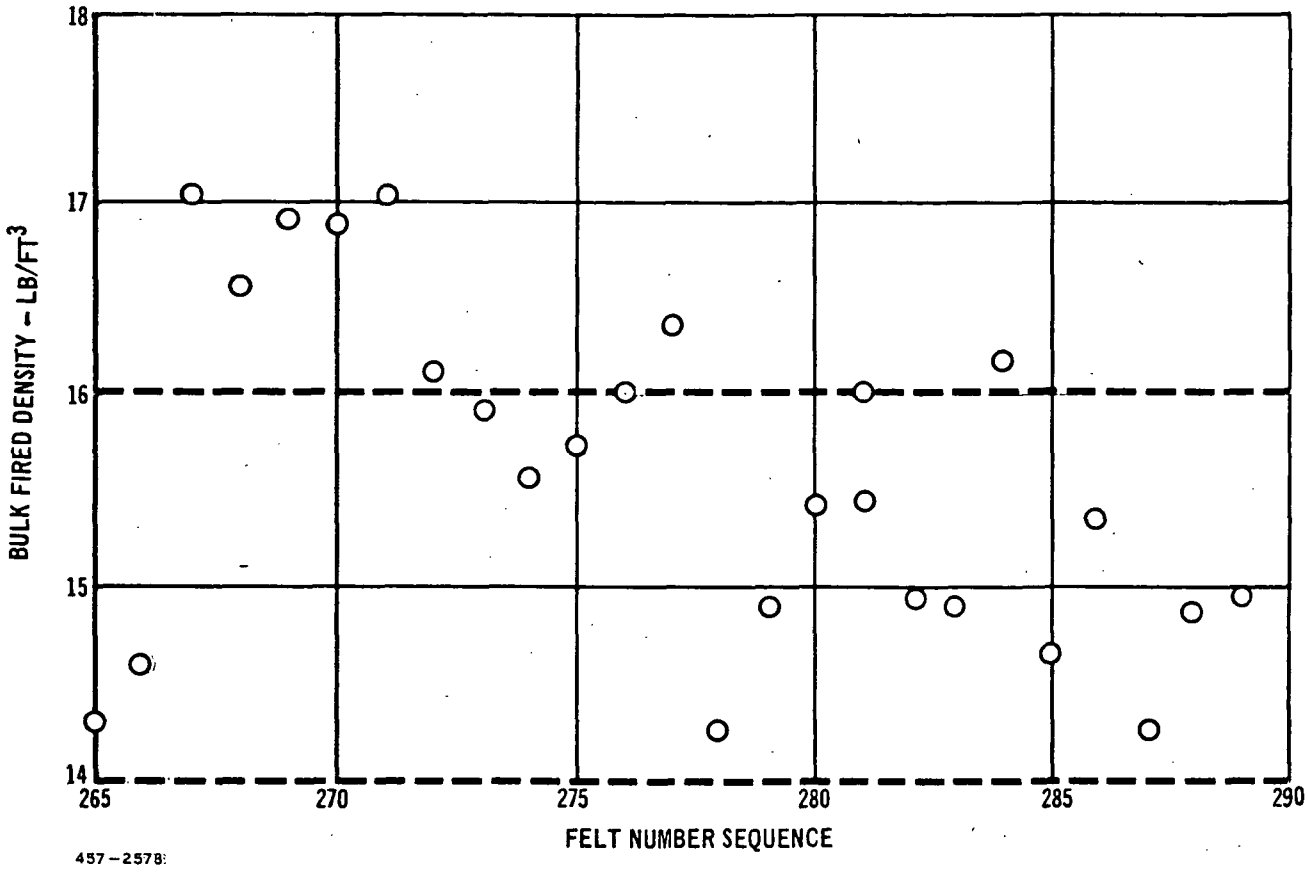

FIGURE 2-11

PROCESS VARIABILITY OF MOD III WITH NO PROCESSING AIDS

weight of binder), the cellulose decreased the felting and drain time and drastically reduced the density gradient through and across the Mod IIIA specimens. In concentrations greater than 0.2 weight percent, the cellulose additive thickens and foams the slurry. Figure 2-13 shows the improved uniformity in Mod IIIA compared to Mod III. The cellulose additive did not correct the soft centers even though the density of the Mod IIIA was extremely uniform and the final fired densities became controllable. Photomicrographs showed two conditions which caused soft spots. One was less binder in the central portion of the felt, the other was silica sphere migration. It was found that the 4.7-μ fibers pulled away from the felting column as soon as the felt formed, preventing adequate drainage around the edge of the specimen due to air leakage. The center of the specimen was still well

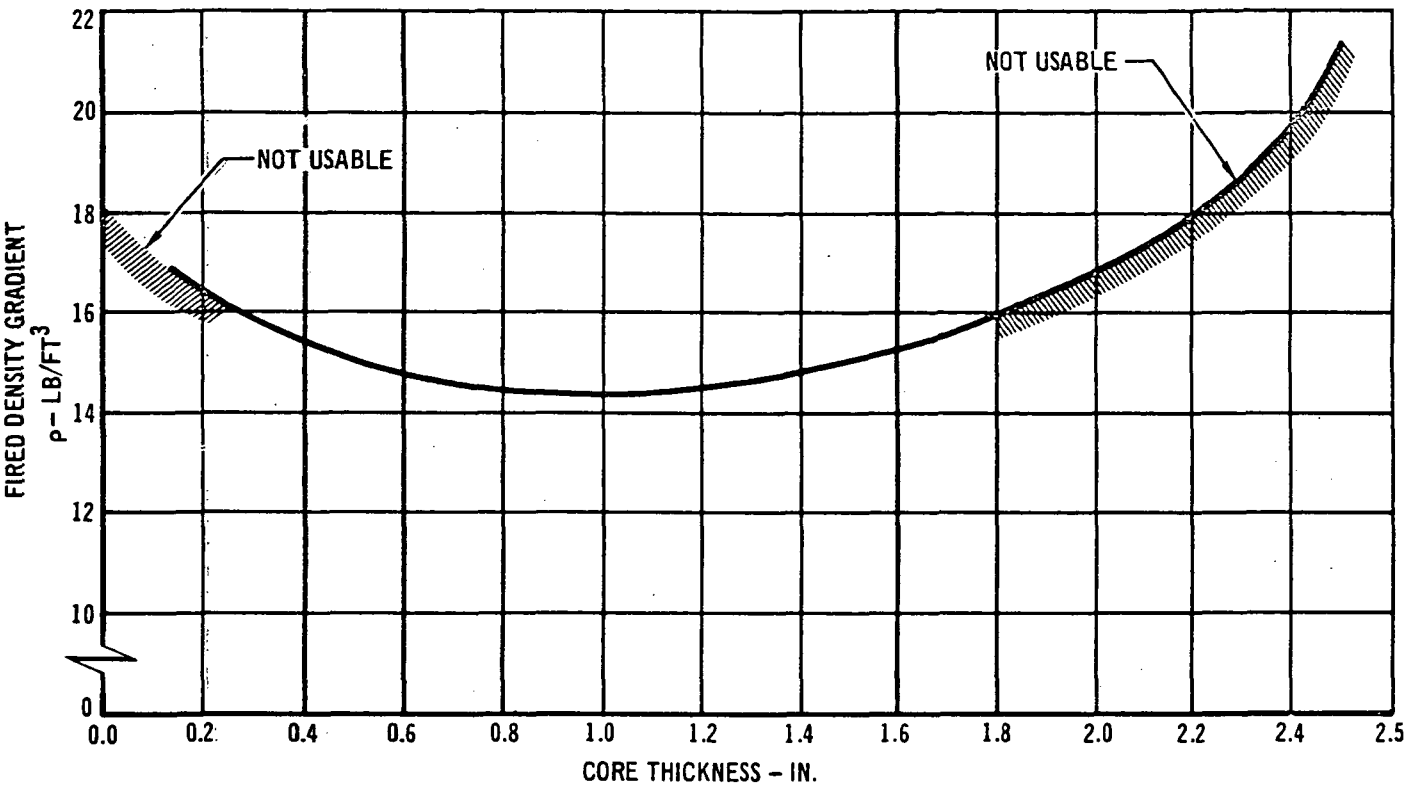

FIGURE 2-12

457-2556 BULK DENSITY GRADIENT MEASUREMENTS OF Mod III

sealed and drained more completely, resulting in binder deficiency. This condition was eliminated by adjusting the concentration of propylcellulose.

The nonuniform distribution of SiO_2 spheres was corrected by additional mixing before felting and by instituting a faster felting procedure to prevent the hollow SiO_2 spheres from floating to the top during felting. Mod IIIA was more uniform than Mod I but still not as hard and strong as desired.

To increase the strength throughout the felts, a second additive, hexamethylenetetramine (HMT), was added to the Mod IIIA slurry. A 1.5-percent solution of this amine compound was used which, when heated, produces ammonia gas that raises the pH of the silica binder system, causing it to gel. This additive successfully

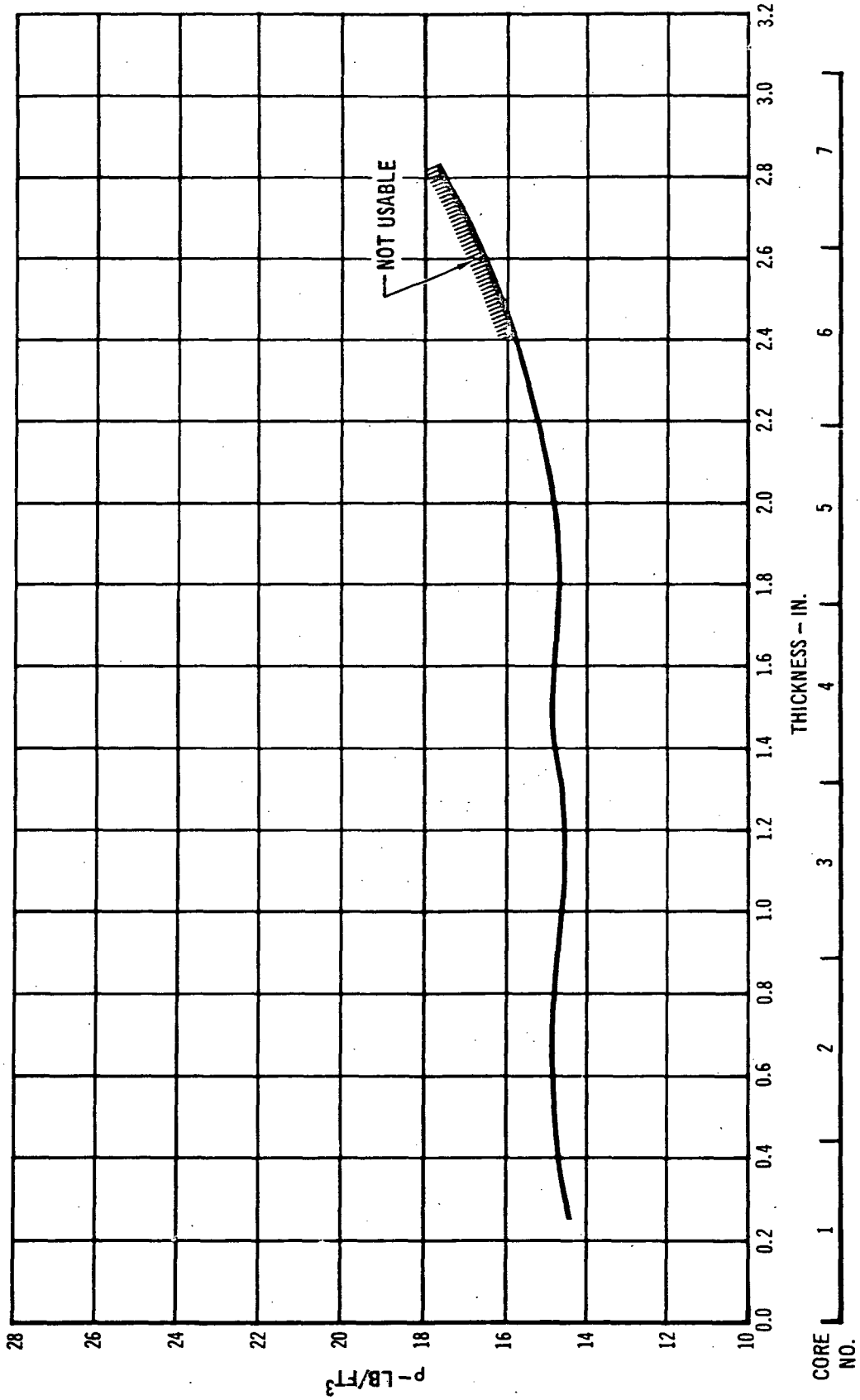

FIGURE 2-13
BULK DENSITY GRADIENT OF Mod III A

457-2366

set the binder, but it did not totally eliminate the strength gradients through larger (14 by 16 by 4.5-inch) HCF felts. The edges of the felts were consistently stronger than the centers, even when the density was uniform. Binder migration is believed to have caused this for three reasons:

1. transporting of binder solids caused by drying at the surfaces
2. excessive draining in certain areas caused by location of drain holes in the felting apparatus
3. settling to one side caused by gravity prior to curing.

The binder migration was significantly reduced, but not completely eliminated by adding the hexamethylenetetramine (HMT).

Figure 2-14 shows the effects of temperature and HMT concentration on gel time. The circled points are actual data; the remainders of the curves are extrapolations based upon Arrhenius' theory $K = Ae^{\frac{-E}{RT}}$. In the temperature range used (140 to 190°F), the time to gel is rather short, ranging from 3 to 13 minutes.

An in-process control which eliminated excessive draining was the weighing of the felt during the vacuum drain portion of the felt forming operation. The wet weight, monitored during the drain period, was used as a measure of the amount of the binder left in the felt. When a predetermined wet weight was reached, the vacuum pumping was discontinued, stopping the flow of liquid binder from the felt. A series of 154 felts was made using this additional control; a significant improvement in HCF strength, and a narrowing of the strength scatter band resulted. The continual monitoring of the wet weight of all felts during production has improved the reproducibility of the processing.

Manufacturing facilities for Mod IIIA have been scaled up, and many 14 by 16 by 4-1/2-inch tiles have been produced for coating evaluation and basic property testing. Mod IIIA has finer texture and is easier to coat than Mod III. The addition of the cellulose thickener allows longer blending times and permits drain-

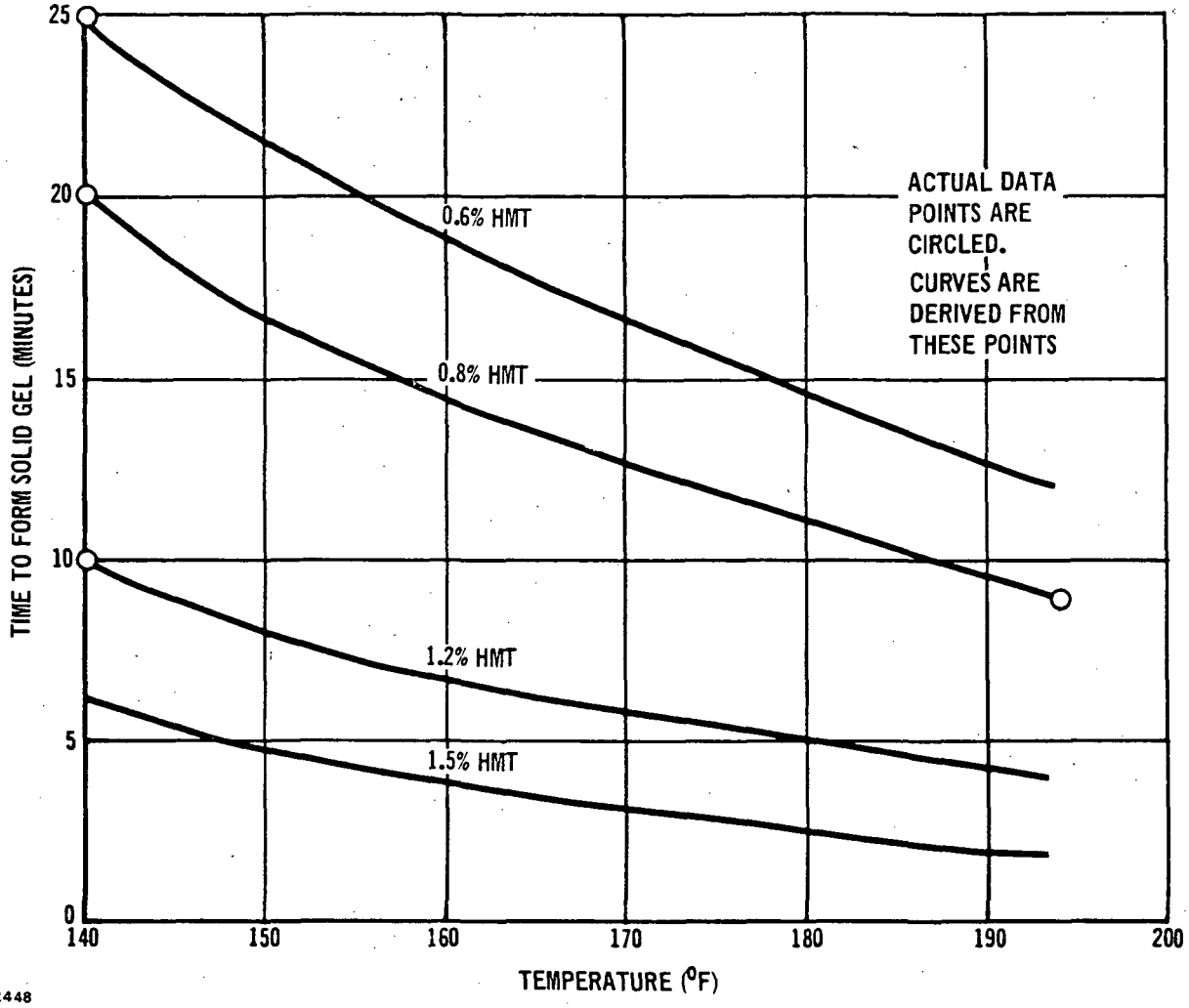

FIGURE 2-14
REACTION RATE OF HMT AND COLLOIDAL SILICA BINDER

$$K = Ae^{\frac{-E}{RT}}$$ ARRHENIUS' RATE EQUATION

WHERE K = SPECIFIC REACTION RATE (SEC^{-1})
A = NUMBER OF MOLECULES COLLIDING PER GRAM MOLECULAR WEIGHT PER SECOND
e = 2.718
E = ACTIVATION ENERGY (CAL./GM. MOL. WT.)
R = GAS CONSTANT (CAL./GM.MOL.WT.-^{0}K)
T = ABSOLUTE TEMPERATURE (^{0}K)

ing of excess binder.

Mod IV HCF - Mod IV HCF consisted of 2.5-μ mullite fibers, SiO_2 spheres, and RSB-2 binder. Its strength was nearly the same as Mod III, but its calculated thermal performance was better. Actual thermal performance was determined from optical scattering data and oxyacetylene torch tests. The finer fiber mullite was much more difficult to process than the fiber used for Mod IIIA HCF. The use of additives (propylcellulose and HMT) hindered binder drainage.

Work on Mod IV HCF was suspended because a sufficient quantity of the 2.5-μ mullite fiber was not available during the contract period. More work is needed to determine the full potential of Mod IV HCF.

Mod V HCF - Mod V was pursued to improve the thermal performance of HCF insulation. All of the HCFs (Mod II, Mod III, Mod IIIA and Mod IV) had a spherical hollow glassy filler as part of their formulation. By substituting the very small diameter silica fiber for the glassy spheres, a reduction in radiant heat transfer seemed likely. The basic formulation of Mod V was set at 80-percent mullite fibers and 20-percent SiO_2 fibers by weight. Because the SiO_2 may devitrify and undergo disruptive volume change upon heating and cooling, an upper limit of 25 weight percent was set for experimentation. Mod V was fired at 2300°F.

The texture of Mod V was superior to any other HCF composition tested, and it was also easily coated. Mod V had thermal performance superior to the other HCFs. (See Section 3.3.) This is due to the increased heat radiation scattering caused by the 1.2-μ SiO_2 fibers. An HCF composed entirely of SiO_2 fiber HCF had somewhat lower thermal conductivity than Mod V, but an all-SiO_2 HCF exhibited considerable shrinkage and some cracking when heated to 2500°F. The mixture of mullite and SiO_2 fibers seems to produce both good thermal performance and good physical stability.

The microstructure of Mod V is much more compact than any previous HCF. This

compactness required long felting and drain times and mechanical pressing of the fibers. Figure 2-15 shows a density profile through a Mod V specimen and the effect of pressing. The Mod V felts were very difficult to remove from the felting apparatus. During felting, the Mod V would pull away from the column walls. This sealing problem was solved by pouring mixed slurry into the gap between the wet felt and felting column immediately after felting. Resealing the Mod V felts allowed proper binder drainage. The problem of removing the Mod V felt from the column without damage was accomplished by lining the felting apparatus with a removable liner and mechanically forcing the felt backward out of the felting column.

Another processing procedure which affected the compounding of Mod V was the propylcellulose. On all other HCF compositions, the cellulose additive was added to and mixed with the entire slurry batch. In processing Mod V, the cellulose thickener and HMT processing aids were dissolved in water and then added to the binder. The dissolved additives were discovered to be much more active when they were dissolved prior to use. Mod V, however, because it was a totally fibrous system, had to be mixed longer than other HCF compositions. The energy imparted by the mixer during longer mixing heated the slurry to over 120°F. The cellulose material had higher solubilities when cool, so the binder was cooled to 40°F before processing. Figure 2-16 shows the temperature rise of the binder during mixing Mod V.

The most important processing step during manufacturing Mod V was the firing cycle. Once Mod V is properly fired, it is very stable through coating processing and reentry simulation cycling. Mod V, however, is sensitive to the initial firing cycle and a quick firing cycle appears to be best overall. Mod V HCF has good potential as a reusable surface insulation. Specimens up to 16 by 14 by 4-1/2 inches have been fabricated and tested. When properly formed and fired, the

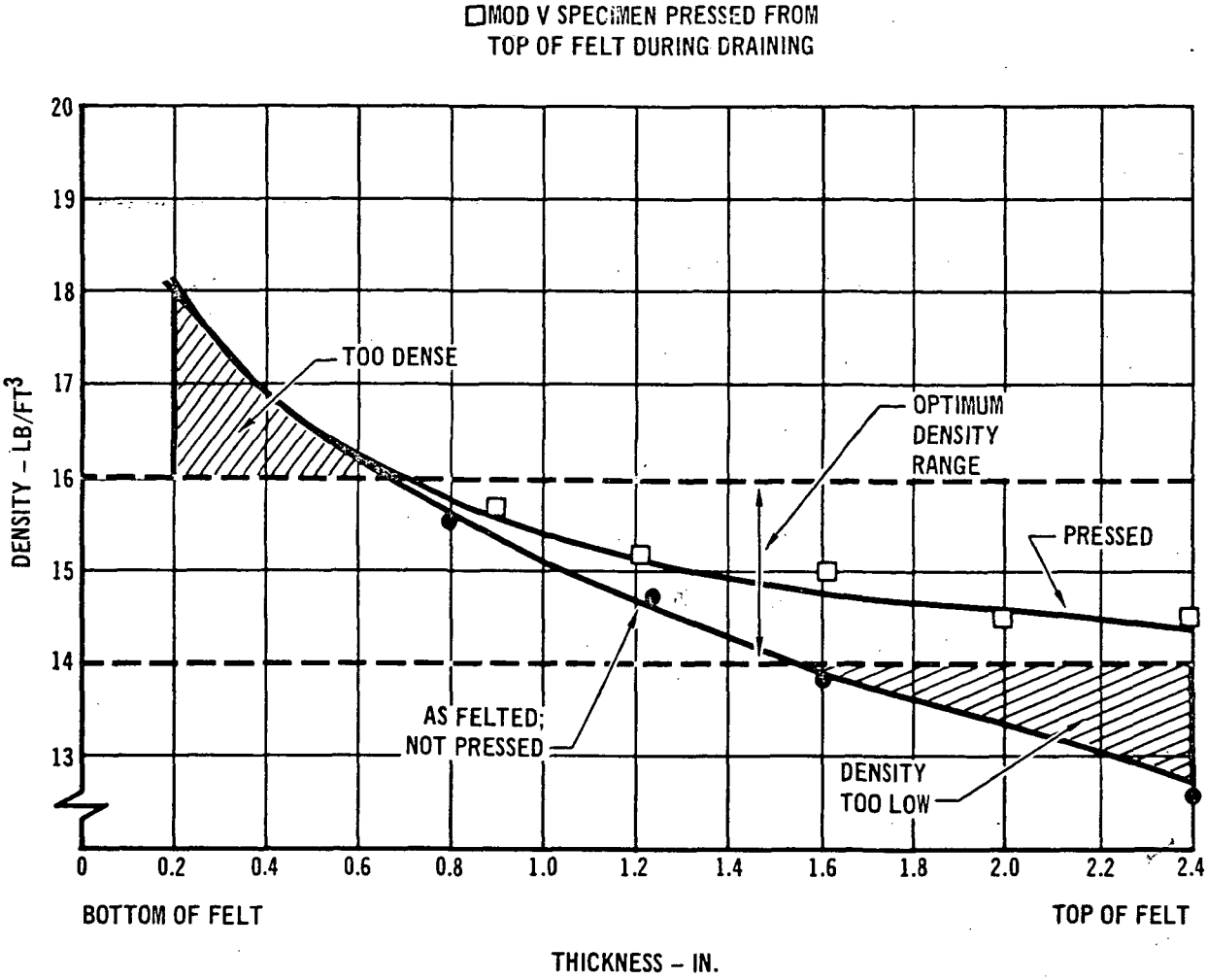

457-2558

FIGURE 2-15

TYPICAL DENSITY GRADIENT THROUGH MOD V HCF SHOWING THE EFFECT OF MECHANICAL PRESSING DURING FABRICATION

thermal shock resistance and strength of processed Mod V was equal to that of Mod IIIA. However, a major difficulty with Mod V was establishing an acceptable initial firing cycle due to the batch-to-batch variation in the heat stability of the SiO_2 fibers. The prior processing history of the SiO_2 fibers was the major remaining problem preventing production of good quality Mod V in quantity.

Opacifiers - Many HCF specimens were formulated, fabricated and evaluated to improve the thermal performance of HCF by reducing radiant heat transfer, as shown in Figure 2-17. Oxides such as Cr_2O_3, Co_3O_4 and NiO colored the HCF: Cr_2O_3

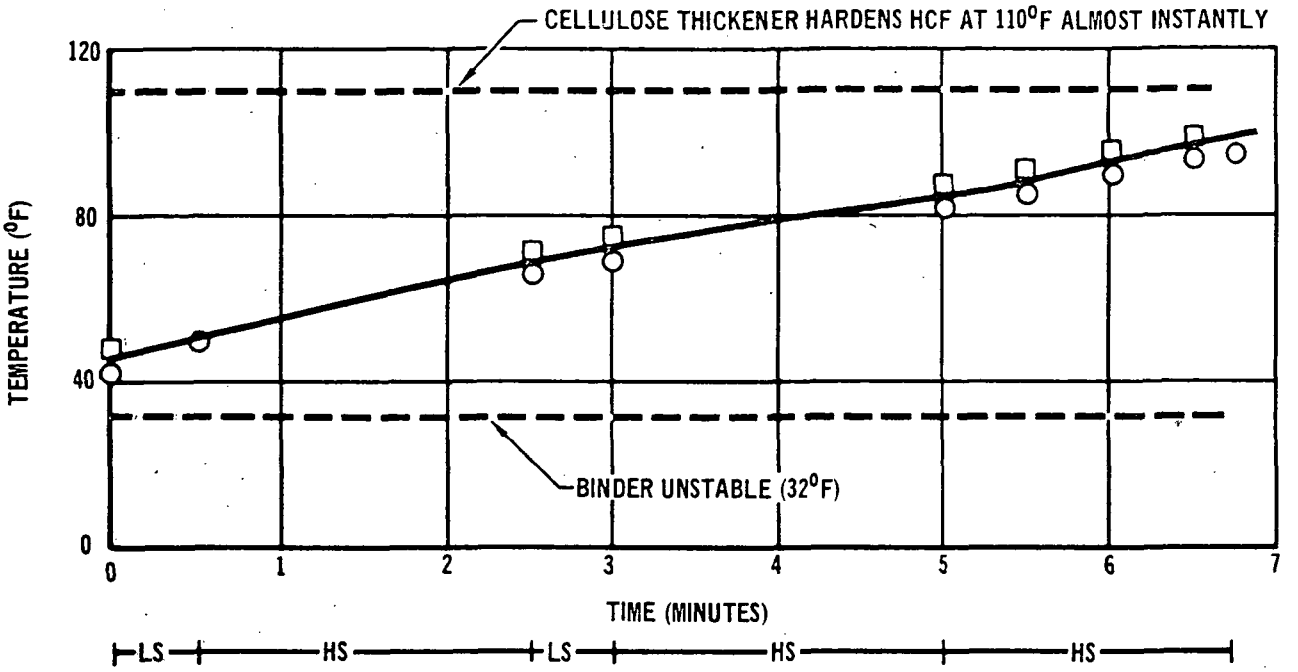

NOTE: LS – LOW SPEED ON HOBART 80
HS – HIGH SPEED ON HOBART 80

457-2560

FIGURE 2-16
SLURRY TEMPERATURE INCREASES WITH MIXING TIME IN HOBART 80 MIXER

(green), Co_3O_4 (blue) and NiO (black), and all caused some local fluxing of the HCF and increased its strength. Cr_2O_3, Co_3O_4, and NiO very likely increased the emittance of the mullite fibers but also increased the heat transfer through the HCF slightly. The best ceramic opacifiers were TiO_2 and $ZrSiO_4$. Both TiO_2 and $ZrSiO_4$ are white, have a high refractive index (scatter heat radiation well), and are thermally stable in the HCF composition. One, three and ten percent additions by weight were added to the baseline Mod IIIA composition and evaluated for thermal performance in 3.3-inch diameter "hockey puck" tests (see Section 3.3). In these evaluations the maximum surface temperature of the specimens was 2300°F and the time as a function of backface temperature was recorded. The best results were obtained using 3-percent by weight $ZrSiO_4$ (zircon) opacifier. (In comparison to basic Mod IIIA, the opacifiers had relatively little effect on thermal performance.)

The second method of opacification was to vary the fiber diameter. Studies

SPECIMEN NO.	COMPOSITION	FIRING TEMP °F (AND TIME)	FIRED DENSITY (LB/FT^3)	TESTING		REMARKS
15–1	MF–ECCO, RSB–2	2300	17.00	THERMAL CONDUCTIVITY AS A FUNCTION OF TEMPERATURE & PRESSURE, RESULTS: SAME AS PREVIOUS 15 PCF MULLITE HCF. NO DISCERNABLE CHANGE IN "K"		CONDUCTIVITY SPECIMENS (9" DIAMETER)
2	(TiO_2 OPACIFIER 3% ADDITION)	2300 1 HR	14.10			
	ADDITIONS			BONDLINE TEMPERATURE RECORDED IN OXY–ACETYLENE TORCH	TIME TO 480°F	
23–1	CONTROL	2300	13.8		185	OPACIFICATION STUDY – ALL SPECIMENS COATED WITH $Cr_2O_3 + AlPO_4$ FOR HIGH EMITTANCE. ALL SPECIMEN CUT DOWN TO A SURFACE DENSITY OF 1.3 LB/FT^2 INCLUDING THE COATING. TESTED IN OXY-ACETYLENE TORCH, $T_{SURFACE}=2300°F$ RECORDED TIME TO BACKFACE TEMPERATURE OF 480°F. Co_3O_4 SPECIMENS WERE QUITE STRONG
2	CONTROL	1 HR	14.2		183	
3	1% ZrO_2		13.6		224	
4	3% ZrO_2		13.6		218	
5	6% ZrO_2		14.3		195	
23–6	1% NiO		13.9		188	
7	3% NiO		14.7		205	
8	6% NiO		15.5		172	
9	1% TiO_2		14.0		187	
10	3% TiO_2		14.5		175	
11	6% TiO_2		14.6		204	
12	1% Co_3O_4 & CoO		14.4		214	
13	3% Co_3O_4 & CoO		14.3		222	
14	6% Co_3O_4 & CoO		15.4		197	
	BASIC MATERIAL MF, ECCO, RSB–2					
	ADDITIONS		WITH ε COATING	BONDLINE TEMPERATURE RECORDED		
27–1	1% BN	2300	16.0		219	OPACIFICATION STUDY – ALL SPECIMENS COATED WITH $Cr_2O_3 + AlPO_4$ FOR HIGH EMITTANCE. ALL SPECIMENS CUT DOWN TO A SURFACE DENSITY OF 1.3 LB/ FT^2 INCLUDING THE COATING. TESTED AT O/A TORCH $T_{SURFACE}$ = 2300°F. RECORDED TIME TO BACKFACE TEMPERATURE OF 480°F.
2	3% BN		15.8		188	
3	6% BN	1 HR	17.0		200	
4	1% $ZrSiO_4$		15.5		236	
5	3% $ZrSiO_4$		15.6		227	
6	6% $ZrSiO_4$		16.3		194	
7	1% C BLACK		15.5		210	
8	3% C BLACK		15.3		227	
9	6% C BLACK		16.4		190	
10	1% Cr_2O_3		15.5		202	
11	3% Cr_2O_3		15.9		216	
12	6% Cr_2O_3		16.3		203	
13	1% SiC		15.4		236	
14	3% SiC		15.7		194	
15	6% SiC		15.9		207	
27–16	1% $K_2O \cdot XTiO_2$		17.4		168	BECAME STRATIFIED DURING FORMING $K_2O \cdot XTiO_2$ FILLED MANY PORES.
17	3% $K_2O \cdot XTiO_2$		16.1		218	
18	6% $K_2O \cdot XTiO_2$		16.4		206	
19	1% SnO_2		15.4		217	
20	3% SnO_2		16.1		208	
21	6% SnO_2		15.9		177	
	BASIC MATERIAL MF, ECCO, RSB–2					

457–2530

FIGURE 2–17

HCF COMPOSITIONS CONTAINING OPACIFIERS

(Reference a) showed that thermal performance improved (lower thermal conductivity) as the fiber diameter decreased. Mullite fibers of 2.5, 4.7 and 6.0-μ diameters were evaluated for thermal performance by optical scattering measurements. The 2.5-μ mullite fibers were the most promising fibers of the group and were used to make several Mod IV felts. However, no thermal conductivity tests were run on Mod IV (2.5-μ diameter fibers) because not enough fibers were available to fabricate specimens.

Because of availability, small fiber diameter, and a composition somewhat similar to mullite, we evaluated SKX Fiberfrax* (2.5-μ aluminosilicate fiber) mixed with 4.7-μ mullite fibers. From a radiation scattering standpoint, the SKX fibers were found to be approximately equal to the SiO_2 fibers (reference a). However, the SKX fibers were harder to process and did not survive thermal cycling as well as SiO_2 fibers. We also evaluated a 1.2-μ mullite type fiber, Fiberfrax HT†, which was extremely hard to process and the resultant HCF specimens were very weak. The HT fiber contained fiberized material and it was judged unsuitable for producing HCF.

Of all the fibers additions evaluated, the 1.2-μ SiO_2 fibers (Microquartz) were the most effective radiation scatterer. The Mod V HCF contained 20-percent SiO_2 fiber substituted for the SiO_2 spheres and was discussed previously.

Reaction Sintering - The opacification studies indicated that the strength of HCF might be improved by using reactive metal additives. By adding a selected metal to the HCF a desired ceramic oxide might be formed in place within the insulation during the firing cycle. This oxide then would react with the ceramic fibers and filler as the block is fired and it would affect the strength. Certain oxidized metals slightly improved the radiation scattering of the Mod IIIA material (see Figure 2-18). Strengths of over 200-lb/in^2 in tension were obtained with a

* Experimental Fiber - Carborundum Co.

† Carborundum Co.

METALLIC ADDITIVE	CERAMIC OXIDE FORMED DURING FIRING	RESULTS
Zn	ZnO	IMPROVED THERMAL RADIATION SCATTERING*, POOR STRENGTH
Sn	SnO	IMPROVED THERMAL RADIATION SCATTERING, POOR STRENGTH
Al	Al_2O_3	NO IMPROVEMENT IN SCATTERING, POOR STRENGTH
Si	SiO_2	NO IMPROVEMENT IN SCATTERING, POOR STRENGTH
Ti	TiO_2	NO IMPROVEMENT IN SCATTERING, POOR STRENGTH
Zr	ZrO_2	NO IMPROVEMENT IN SCATTERING, POOR STRENGTH
Mg	MgO	SLIGHT IMPROVEMENT IN LIGHT SCATTERING, POOR STRENGTH
Ni	NiO	BLACK OXIDE, VERY STRONG

10% BY WEIGHT ADDITION OF EACH METAL
*2.0μ THERMAL RADIATION

457-2568

FIGURE 2-18

REACTIVE SINTERING EFFECT ON MOD IIIA HCF

10-percent weight addition of nickel metal. However, the NiO modified Mod IIIA shrank unpredictably. All of the other reactive metal sintering aids tested failed to improve the strength of HCF.

2.3 QUALITY ASSURANCE PROVISIONS - To manufacture reliable and reproducible HCF, all the raw materials and their associated processing must be controlled. Many variables were recorded and studied in both small laboratory formulations and in the larger pilot plant, in order to determine which variables were most significant. Several of the more important variables which were identified are discussed in this section.

Raw Material Control - We routinely analyzed HCF raw materials (SiO_2 spheres, mullite fibers and binder) for quality before processing. The Na_2O content of the spheres was checked along with the melting point and wettability of the mullite fibers. Normally, the SiO_2 spheres contain 8-percent or less Na_2O. One shipment

of SiO_2 spheres was rejected because of high Na_2O content.

Quantitative analysis was performed by atomic absorption spectrophotometry after dissolving each specimen using the Bedrick Bernas method.* The test results for various fibers follows. All values are reported in weight percent of the oxide and the silica content was obtained by difference.

	#1 Early Batch - SI Eccospheres	#2 Intermediate Batch - SI Eccospheres	#3 Contaminated Batch Eccospheres	#4 Local Spheres (Union Electric)
Aluminum (Al_2O_3)	0.08	0.11	0.10	32.6
Lithium (Li_2O)	0.02	0.02	0.02	0.04
Potassium (K_2O)	0.03	0.03	0.02	4.05
Sodium (Na_2O)	8.1	12.4	15.4	4.1
Iron (Fe_2O_3)	0.04	0.05	0.05	5.1
Magnesium (MgO)	0.03	0.12	0.09	0.90
Calcium (CaO)	0.04	0.04	0.04	0.42
Silicon (SiO_2)	91.7	87.2	84.4	52.8

The variation of sodium (Na_2O) content is apparent between Eccosphere batches and especially in the contaminated material (material contaminated during processing by Emerson and Cuming). The local fly ash taken from the Union Electric material has a high alumina (Al_2O_3) content as expected.

The "as processed" Mod II HCF was also analyzed by the same process as the Eccospheres and the test results are given as follows:

	Samples	
	Standard	#122
Aluminum (Al_2O_3)	32.9	35.9
Lithium (Li_2O)	< 0.01	< 0.01
Potassium (K_2O)	< 0.06	< 0.06

* Bernas, Bedrick, Anal. Chem. 40, 1682, October 1969.

Sodium (Na_2O)	2.47	2.10
Iron (Fe_2O_3)	0.05	0.07
Magnesium (MgO)	0.23	0.20
Calcium (CaO)	< 0.01	< 0.01
Titanium (TiO_2)	< 0.02	0.53
Silicon (SiO_2)	64.3	61.1

NOTE: Percent silicon calculated by difference.

The specific gravity and solids content of the silica binder were monitored. These two properties help control the final density and strength of the HCF. For a given HCF formulation, the final density of the material can be predictably raised or lowered. The binder is generally diluted to a fixed specific gravity before processing. Specific gravity is adjusted by adding deionized water or fresh binder as necessary. Figure 2-19 shows the relationship between specific gravity and solids content. In spite of the replenishment, the binder can only be reused once before it becomes deficient in silica and degrades the strength of the product.

Analyses have been run on samples of binder which had been used various numbers of times. The results of these analyses are shown in Figure 2-20. The solids remained constant but the silica (SiO_2) containing binder phase was removed with reuse. Figure 2-21 shows the binder analysis when cellulose thickener is added to the RSB-2 binder. Again silica was depleted with reuse.

During the felting process, the opacifiers (TiO_2 or $ZrSiO_4$) collected in the binder. The analysis of binder for the TiO_2 opacifier in Mod I is shown below:

	Fresh Binder	1 Reuse
Magnesium (MgO)	0.23	0.20
Calcium (CaO)	<0.01	<0.01
Titanium (TiO_2)	<0.02	0.53
Silicon (SiO_2)	64.3	61.1

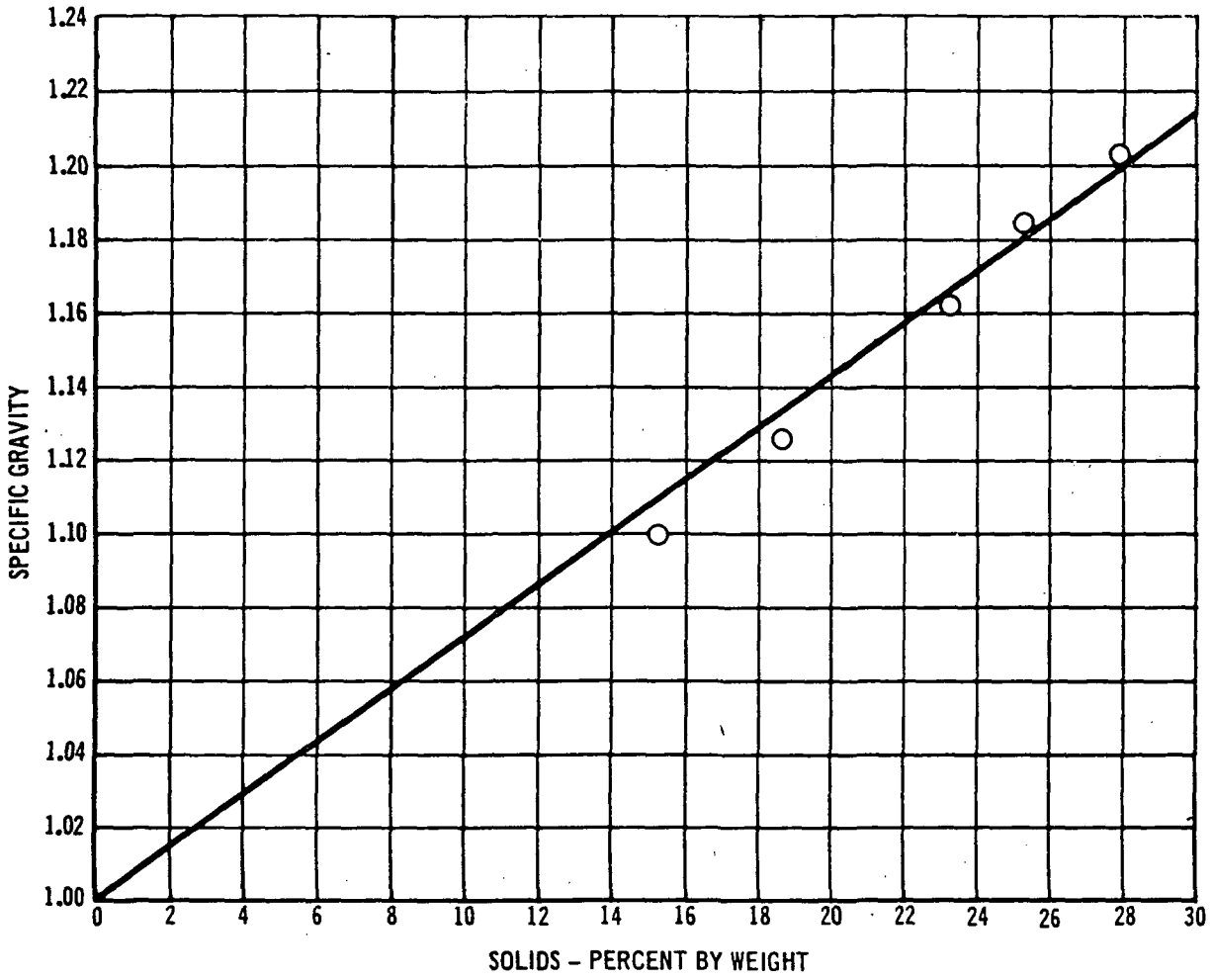

NOTE: BINDER AS RECEIVED – 30% SOLIDS/1.23 SG

457-2447

FIGURE 2-19

SPECIFIC GRAVITY OF COLLOIDAL SILICA BINDER AS A FUNCTION OF SOLIDS CONTENT

Three percent by weight TiO_2 was added to the slurry before felting. The standard material had no opacifier added. Specimen #122 (Mod I) retained only about 18-percent of the 3-percent added to the felting slurry. The TiO_2 opacifier had no effect on the strength of the Mod I HCF.

The mullite fibers were checked for melting point and wettability. The melting point was determined by fusing mullite fibers with an oxyacetylene torch. This test indicates the impurity levels in the fibers. Some batches of fiber are

NO. OF REUSES	% SOLIDS	% OF SOLIDS – MEASURED AS METALLIC CATION				
		Mg	Na	Al	Si	Zr
FRESH	29.0%	0.13	1.0	7.0	52.5	< 2
1	29.3%	0.09	1.1	6.0	51.2	< 2
2	29.0%	0.37	1.0	6.1	48.7	< 2
3	29.0%	0.48	1.2	6.4	47.2	< 2
4	29.1%	0.37	1.0	5.8	47.8	< 2
5	29.4%	0.18	0.9	4.8	42.7	< 2

FIGURE 2–20

VARIATION IN BINDER CONSTITUENTS vs REUSE

SPECIMEN NUMBER	PERCENT SOLIDS	PERCENT OF SOLID			
		Si	Al	Mg	Zr
1 – FRESH BINDER WITH CELLULOSE THICKENER*	28.4	32.0	3.88	0.67	<0.2
2 – 1 REUSE CELLULOSE THICKENER	27.2	29.6	4.43	0.80	<0.2
3 – 3 REUSES CELLULOSE THICKENER	26.4	28.0	4.03	0.53	0.8

*THE CELLULOSE THICKENER LEAVES NO SOLID RESIDUE

457-2553

FIGURE 2–21

BINDER SOLIDS ANALYSIS

wetted by binder easier than others. It is necessary for the binder to set the fibers where they intersect each other and the SiO_2 spheres to obtain a strong, uniform material. Wetting of the fibers by the binder also affects fiber chopping, slurry dispersion, and binder retention. Wetting of batch materials was examined prior to mixing; some fibers floated on the binder and some sank. In some slurry batches the silica spheres floated in an unwetted mass after partial blending.

Wetting varied from lot to lot.

Chopping and mixing operations affect HCF homogeneity and texture. Figure 2-22 shows the results of a viscosity - fiber length study. Both fiber length and viscosity decrease as chopping time increases. After a certain chopping time is reached, the viscosity is relatively insensitive to further blending even though more short fibers are formed. The fired density of the HCF formed from different viscosity slurries was checked. The fired density increased proportionally as viscosity decreased. The long blending time associated with short fibers also produced a finely textured material which was superior for coating and proved to be quite strong. The short fibers and the associated finer texture increased the strength of all HCFs. Proper control of both chopping and mixing is necessary to form a good block of HCF. Decreasing fiber length forms a fine textured material, but thorough mixing of the slurry is equally important to minimize density variation throughout the felted block. The chopping action of the blades of the blenders reduces the lengths of the fibers, but equally important, it disperses clumps of fibers. The longer chopping or blending time produced fewer clumps of fibers.

In Process Control - During the HCF fabrication process, mullite fibers are chopped and mixed with filler and binder. A 1-gallon mixer was used and the fiber length distribution for a specific mixing time and speed is shown in Figure 2-23. A larger capacity mixer (3-gallon) was evaluated which produced a fiber length distribution, Figure 2-24, similar to that from 1-gallon blender. Because of the close comparison of the fiber lengths, a 20-gallon mixer was procured which allowed mixing and chopping of enough material at one time to make a 14 by 16 by 4-1/2-inch thick HCF felt from a single mixer batch.

During processing, certain parameters - such as slurry viscosity, blending time and weight of the wet HCF felt are controlled. Viscosity is kept low to

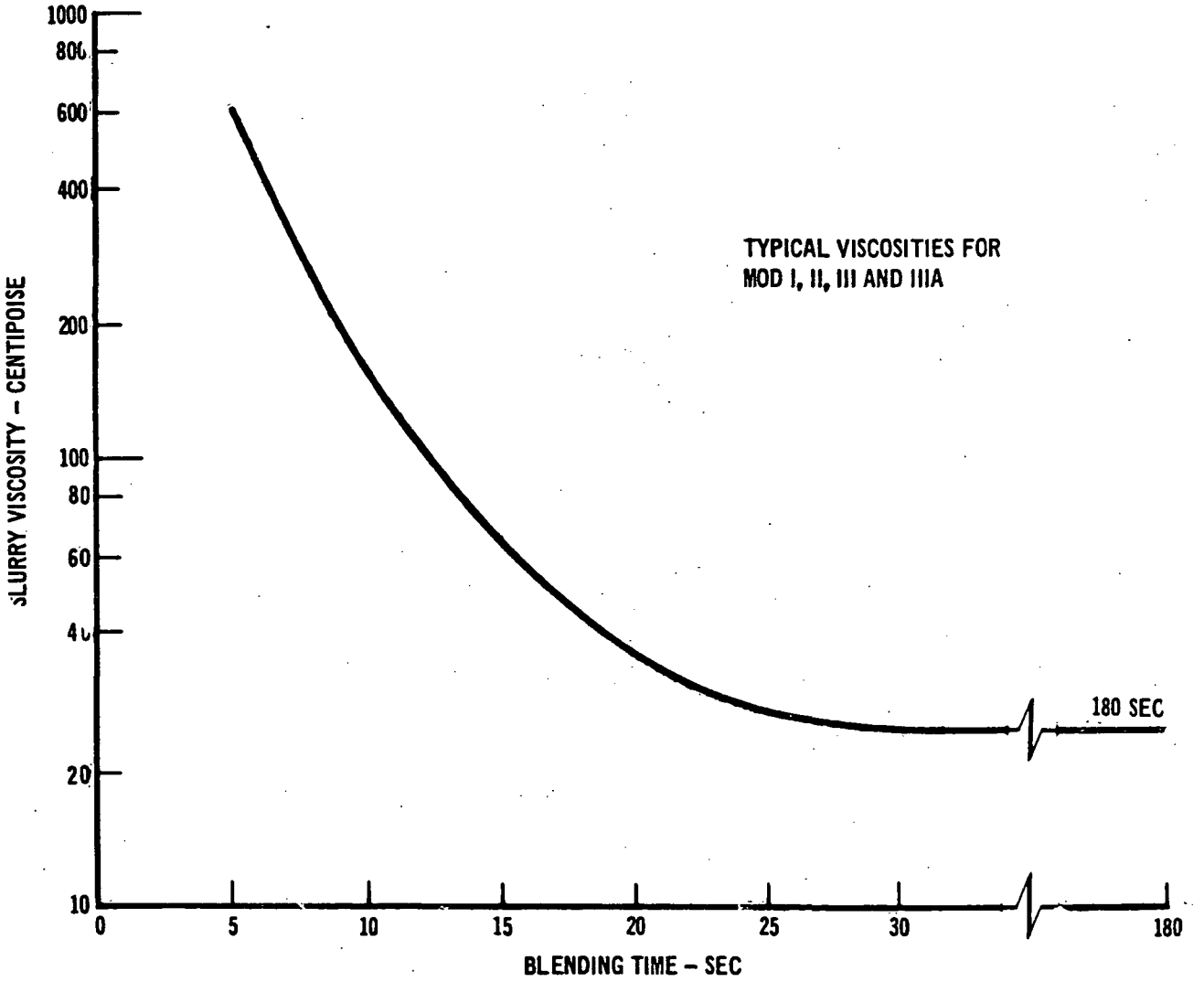

457-2531

FIGURE 2-22

HCF CHOPPING PARAMETERS

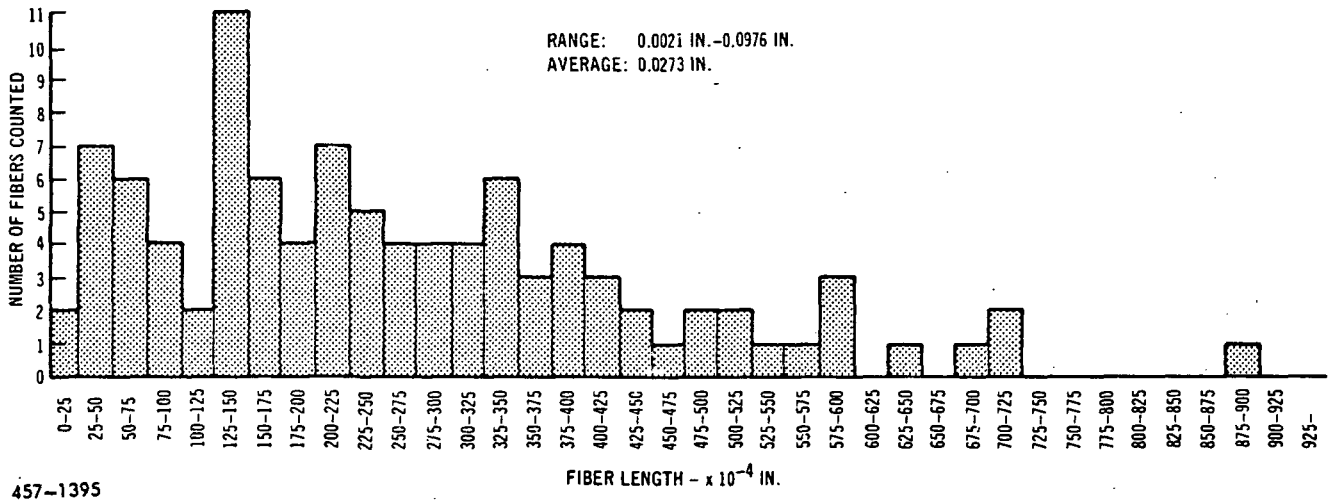

FIGURE 2-23
ONE GALLON MIXER

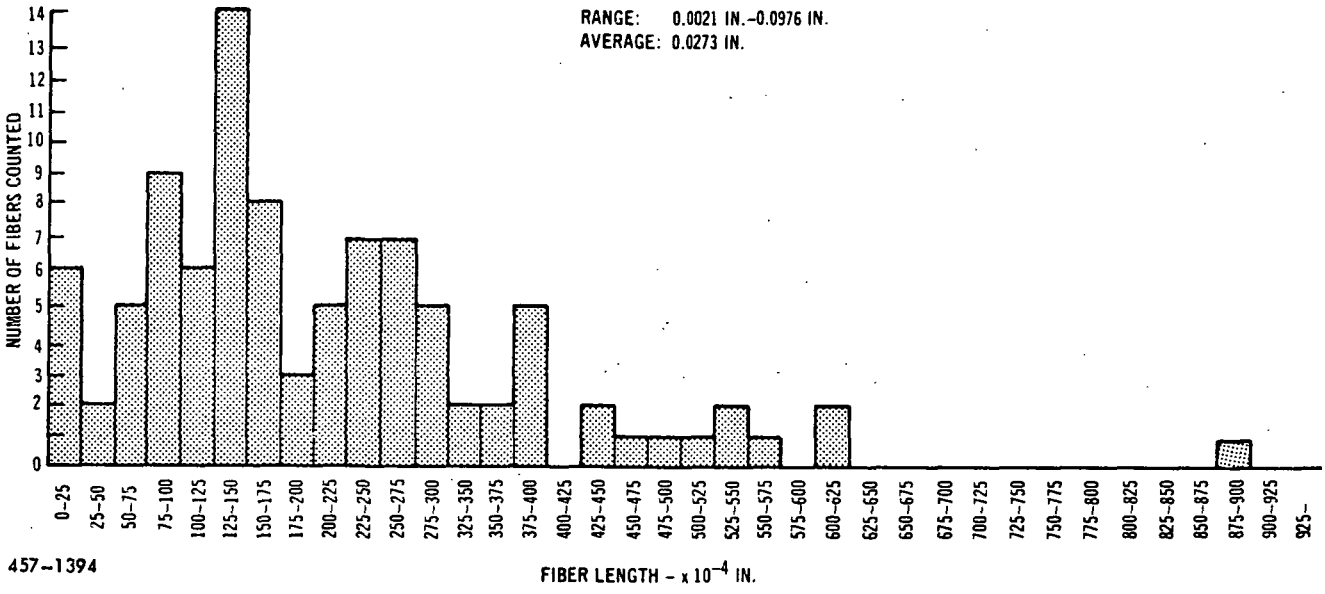

FIGURE 2-24
THREE GALLON MIXER

prevent excessive felting time. The control having the greatest effect on the density uniformity finished product is the wet weight of the HCF blocks. By keeping the wet weight within a predetermined band, the density and the strength of the final product can be controlled.

As mentioned previously, a processing aid was added to prevent binder migration in the felt. The compound (hexamethylenetetramine) decomposes on heating, and produces ammonia which gels the binder. During the heat-up cycle, the HCF felts are inverted every 15 minutes to prevent binder migration due to gravity.

Since HCF is formed in a high speed mixer, the possibility of breaking the hollow SiO_2 spheres during processing was analyzed. An experimental batch of HCF slurry (binder, fibers and spheres) was mixed for about 60 seconds (about twice the normal mixing time) and the whole spheres were separated by water flotation. Less than 7-percent of the total batch of spheres was broken during mixing. The test was repeated using only distilled water and Eccospheres to remove the effect of the fibers. Again, the slurry was blended 60 seconds. Less than 5-percent of the spheres batch was broken during this test. It was concluded that the broken spheres, as seen in SEM the photomicrographs, are not broken primarily by the mixing operation. See Figure 2-25.

Post Processing Control - Each processed HCF felt is cored and the density and hardness gradients are determined for each large felt. Density gradient records were kept to aid in the selection of acceptable HCF and to monitor processing variations. If variation in density occurs, the HCF is evaluated for acceptability. The hardness through and across each HCF felt is measured by the ball drop test as discussed in Section 3.2.

In order to determine the reason for variation in strength, HCF specimens were examined with a scanning electron microscope (SEM) to locate the filler (hollow silica spheres) and binder. Figure 2-26 shows a specimen of HCF with a density of

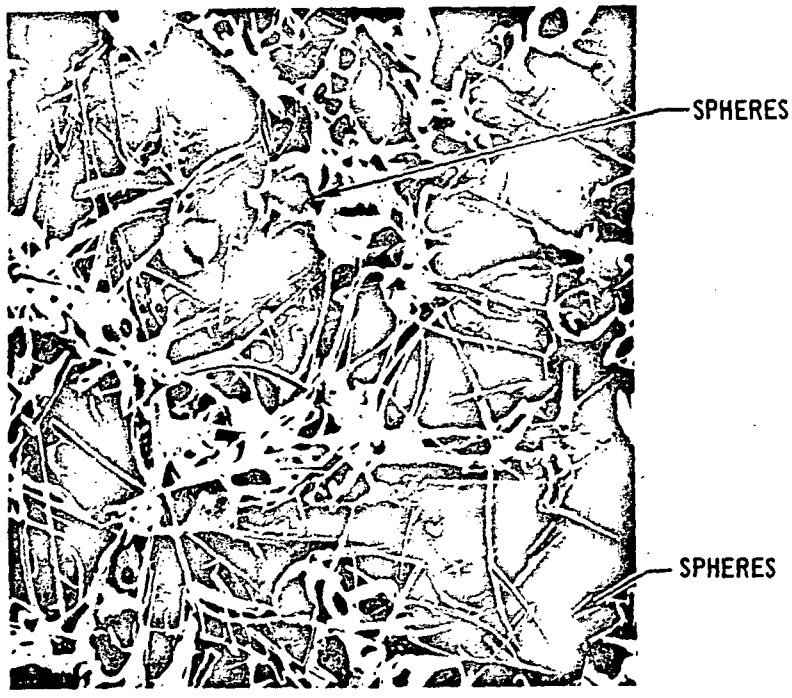

457-2443

FIGURE 2-25

HOLLOW SPHERE MORPHOLOGY IN PROCESSED MOD IIIA HCF (100X)

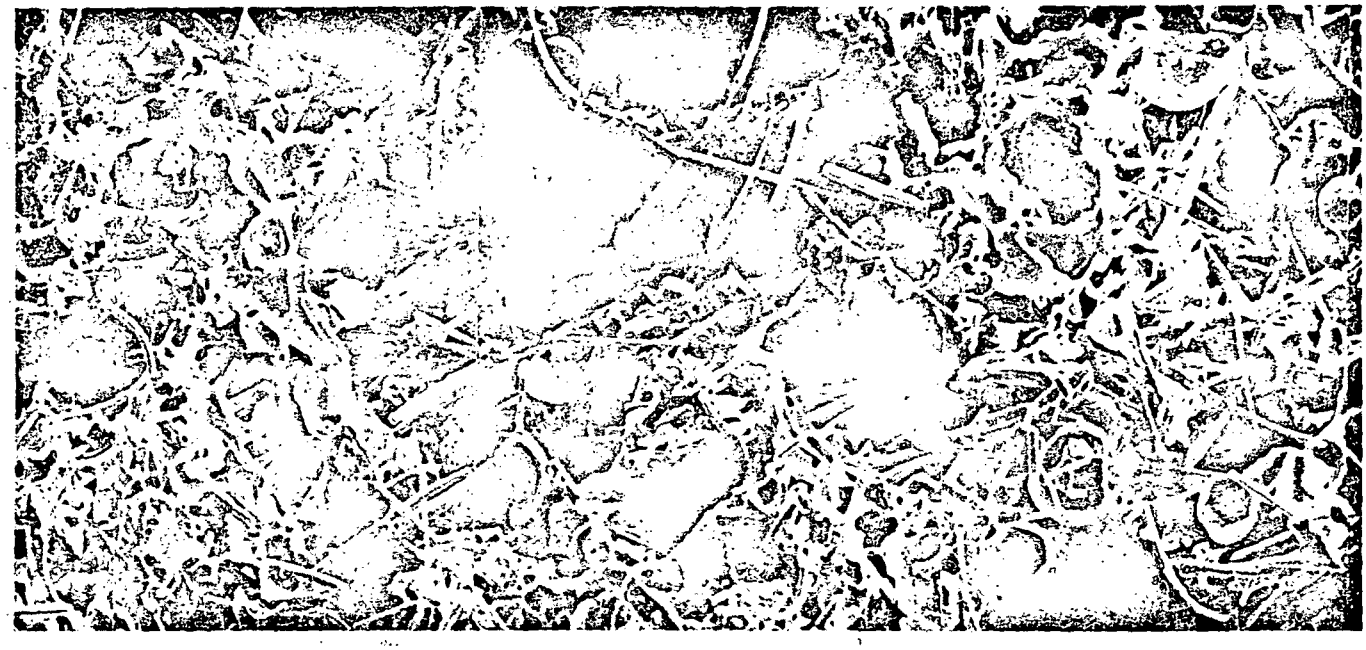

457-2445

FIGURE 2-26

(300 X)

NORMAL FILLER AND BINDER DISTRIBUTION IN MOD IIIA HCF

• AS FIRED AT 2300°F FOR 3 HOURS

15-lb/ft^3 and a longitudinal tensile strength of 120-lb/in^2. This piece of HCF had well distributed filler and an adequate amount of binder located at fiber intersections. This specimen also survived 20 thermal cycles without cracking. Figure 2-27 shows softer HCF with a density of 13.5 pcf and a longitudinal tensile strength of 77-lb/in^2. This specimen cracked during thermal cycling. The photomicrograph shows very few spheres and very little binder. As a result of this data and other observations, processing parameters were varied to insure binder retention and better dispersion of filler. Processing aids, such as HMT, were also added to reduce binder migration as discussed in Section 2.2.

Extra chopping during processing improved the strength properties of all the HCFs. Increased chopping also increased the fired bulk density. Tradeoff studies were conducted on the most promising HCF compositions (Mod IIIA and Mod V). HCFs formed from low viscosity slurries (20 to 40 cps) were usually stronger than HCFs processed from higher viscosity (50 to 200 cps) slurries. The target density of 15-lb/ft^3 could be obtained using both the low and high range of viscosity.

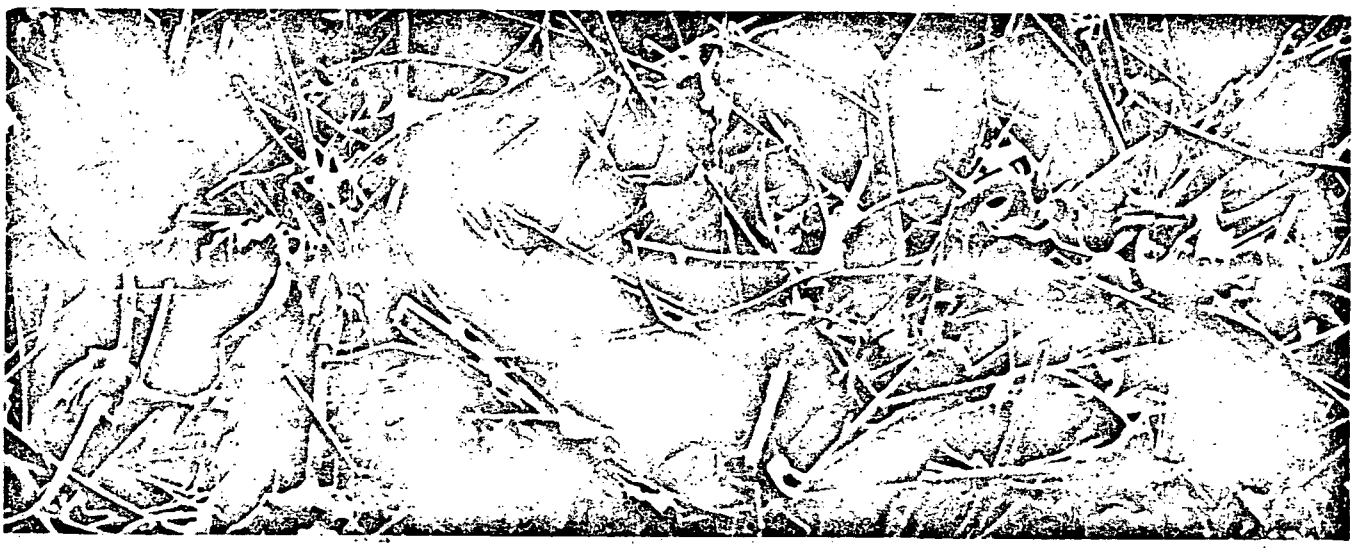

FIGURE 2-27 (300 X)

457-2444

MOD IIIA HCF-DEFICIENT IN BINDER AND FILLER

- AS FIRED AT 2300°F FOR 3 HOURS
- EXTREMELY WEAK

3.0 HCF PROPERTIES

In this section are presented the results of the efforts to achieve the goals of this program to improve mullite HCF in the following areas:

density control,

density gradients reduction,

strength increase,

strength gradients reduction,

thermal conductivity decrease.

3.1 PHYSICAL PROPERTIES - Overall density control and density gradient reduction were the major two physical properties of HCF which were concentrated on during this program. The results of the efforts in these two areas are discussed in detail in Section 2.0.

The efforts in both of these areas were successful. The overall density was controlled to 15 $\pm$1 lb/ft^3. Density gradients, which were prevalent during the early part of the program, were essentially eliminated. The organic processing aids and the density control during draining were two major factors which contributed to the elimination of density gradients.

3.2 MECHANICAL PROPERTIES - HCF mechanical properties were measured throughout this program to aid in screening materials. Various test methods were evaluated for accurately determining mechanical properties. This section includes discussions of the various formulations of HCF tested, test methods used and results.

Strength Screening Tests - Mechanical property tests of various HCF formulations were conducted to aid in guiding HCF development. Tensile and compressive properties were determined at room and elevated temperatures and both longitudinal and transverse fiber orientations were tested. During this program several improvements were made in test methods which resulted in more precise mechanical property

measurements. Room temperature tests discussed in this section were conducted at MDAC-E. Elevated temperature tests which utilized an optical extensometer to measure strains were conducted at MDAC-W and are discussed later in this section.

Test Methods - MDAC-E HCF mechanical property test specimens are illustrated in Figure 3-1. All specimens were loaded to failure at 0.01 to 0.02 inches per minute loading rate. Specimen densities, approximately 15 $\pm$1 lb/ft^3, are listed with test results.

Tensile Tests - Room temperature tensile tests were conducted on cylindrically shaped HCF specimens 1.29 inches in diameter by 1.0 inch long. Both longitudinal and transverse fiber orientations were tested. Aluminum loading blocks were bonded to the specimens with Scotchweld 2216 adhesive.* Loads were applied to the aluminum blocks through universal joints to eliminate bending loads. Load and strain were continuously monitored for room temperature specimens.

Methods for determining tensile strain were improved during this program. Early in the program, strains were measured using test machine crosshead travel. This original test setup is illustrated in Figure 3-2. Unreasonably low elastic

* 3M Corporation

ROOM TEMPERATURE TENSION AND ROOM AND ELEVATED TEMPERATURE COMPRESSION

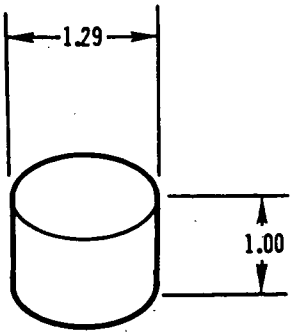

ELEVATED TEMPERATURE TENSION

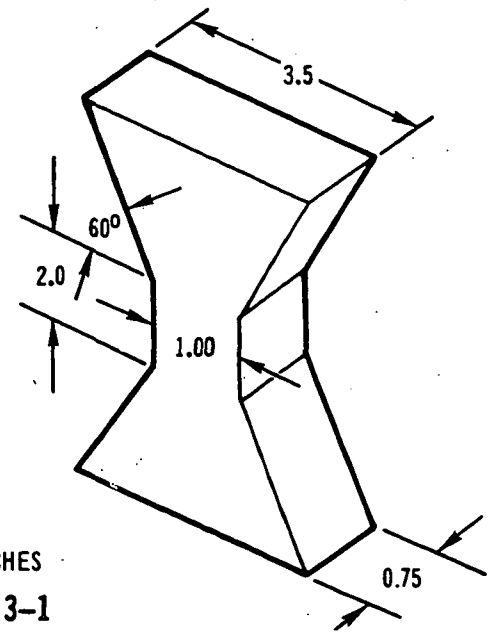

NOTE: ALL DIMENSIONS IN INCHES

457-2436

FIGURE 3-1
HCF MECHANICAL PROPERTY SPECIMENS

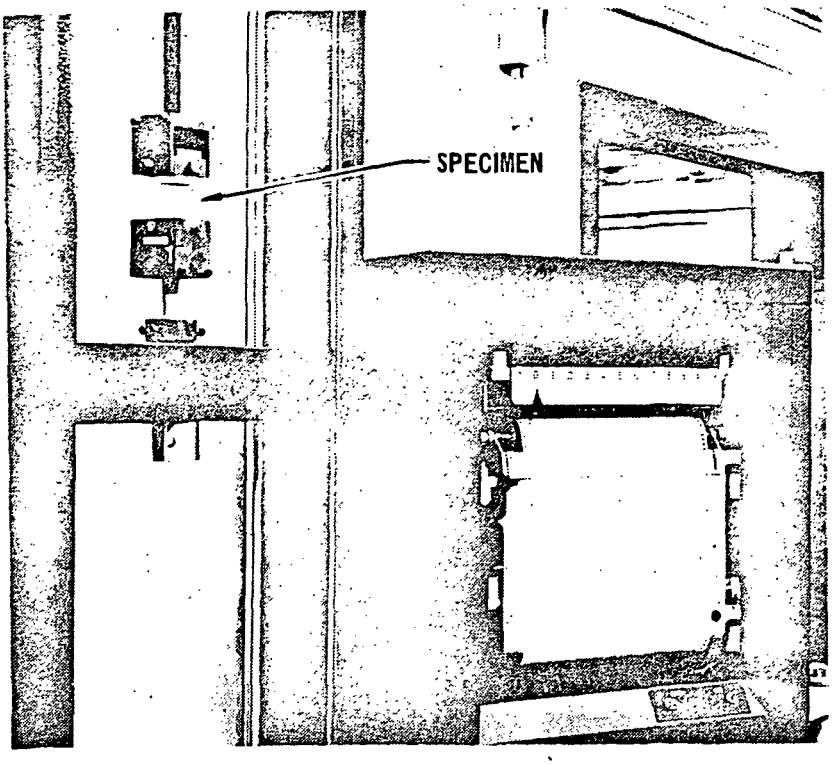

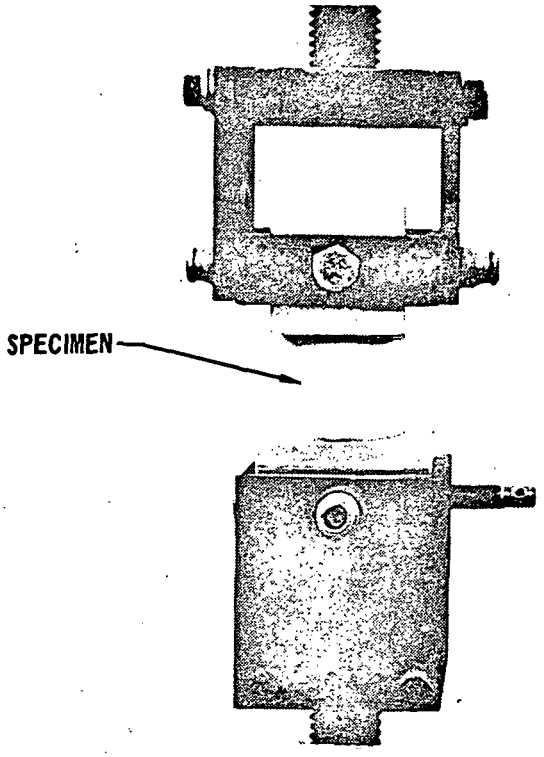

FIGURE 3–2

ORIGINAL HCF ROOM TEMPERATURE TENSION TEST SETUP

457–1264

moduli were obtained using this test method, and it was concluded that machine crosshead travel could not be used satisfactorily to compute strains. As a result, the test setup was changed to include the use of a clip-on displacement gage attached between loading blocks. Two clip-on displacement gages were used on opposite sides of each specimen as illustrated in Figure 3-3, in order to compensate for cocking of specimens.

The double cantilever clip-on displacement gages are composed of strain gages bonded to cantilever arms. The displacement gages were calibrated by relating strain gage output to displacement of the cantilever arms. The gages were attached to two sides of each specimen to compensate for differential strains due to specimen misalignment or nonuniform specimen density. The gages were accurate to within 0.0003 inch per inch.

Elevated temperature tensile tests were conducted at 1200°F, 1800°F, and 2300°F. The test setup is illustrated in Figure 3-4. Coated columbium grips were used to load the specimens. Ten-inch quartz lamps rated at three hundred sixty watts per inch were used to heat the specimens. Specimens were heated to test temperature in approximately 3 minutes and allowed to soak at test temperature for 3 minutes prior to testing.

Compression Tests - HCF compression tests were conducted on cylindrically shaped specimens 1.29 inches in diameter by 1.0 inch long. Both longitudinal and transverse fiber orientations were tested. Tests were conducted at room temperature, 1200°F, 1800°F, and 2300°F. Load and strain were continuously monitored for room temperature specimens.

Methods for determining compression strain were also improved during this program. The original test setup is shown in Figure 3-5. Specimens were compressed between machine loading heads and strains were determined from machine cross-head travel. It was found that a large portion of the strain obtained from

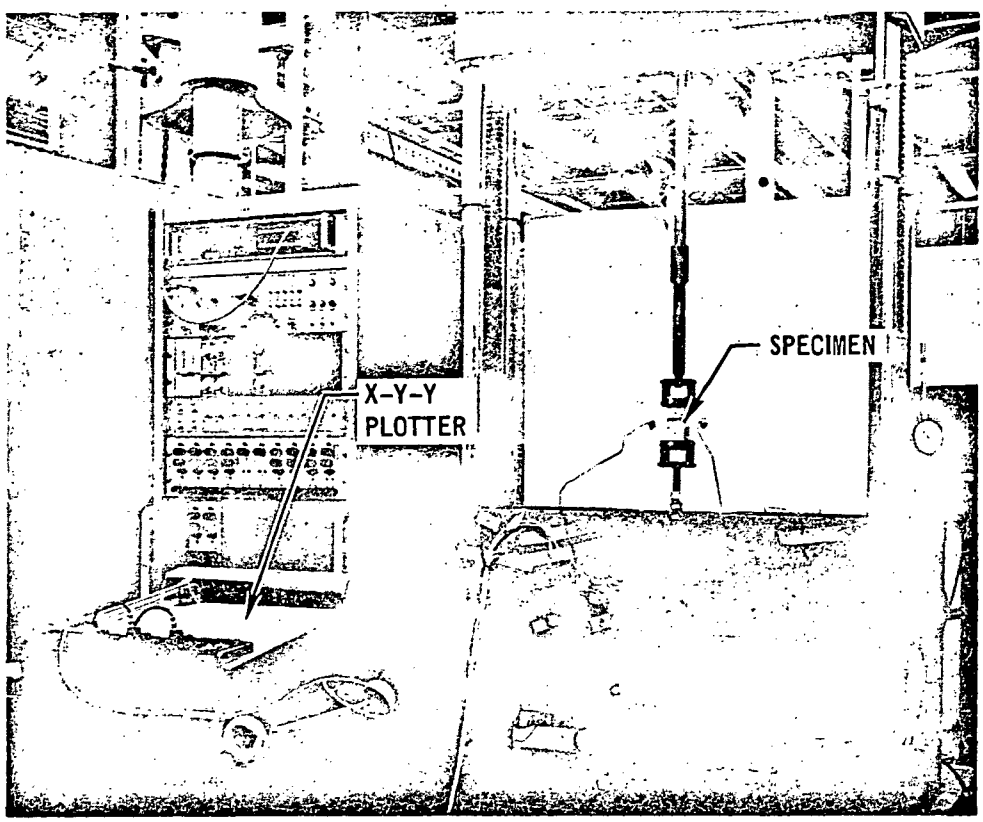

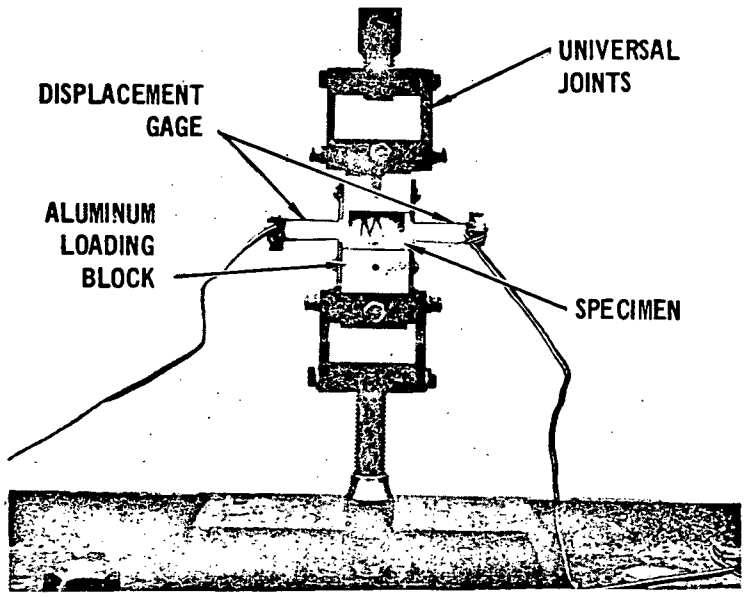

457-2170

FIGURE 3-3

IMPROVED HCF ROOM TEMPERATURE TENSION TEST SETUP

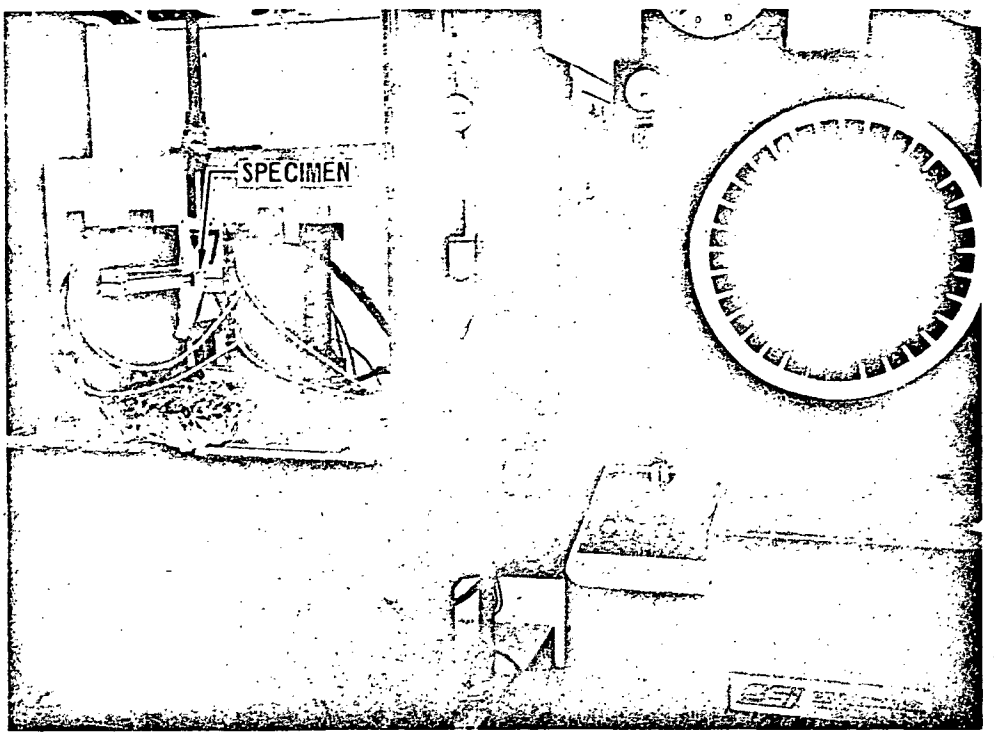

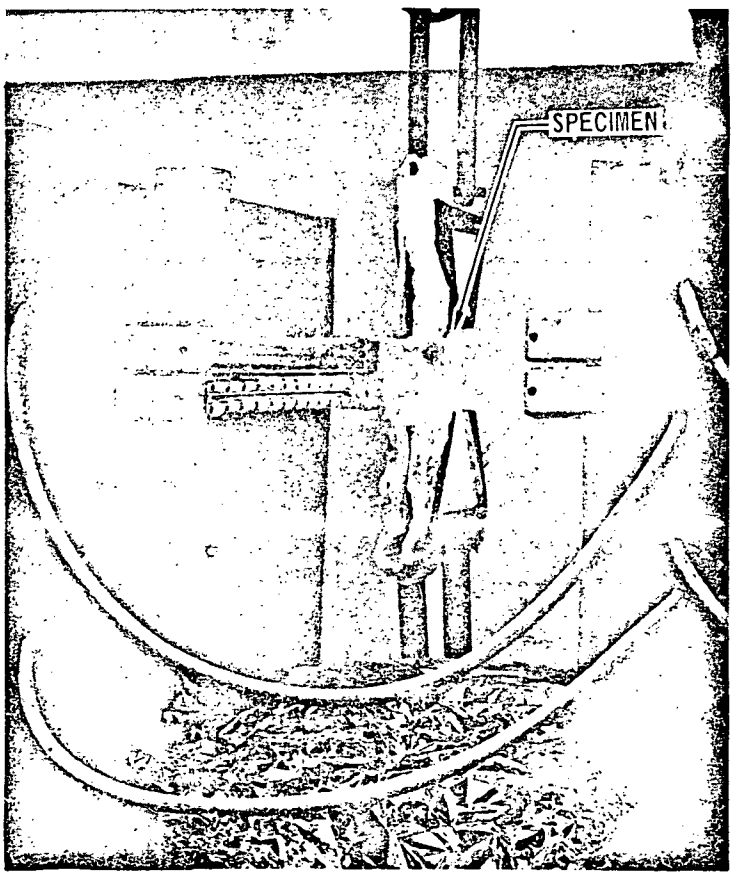

457-2109

FIGURE 3-4
HCF ELEVATED TEMPERATURE TENSION TEST SETUP

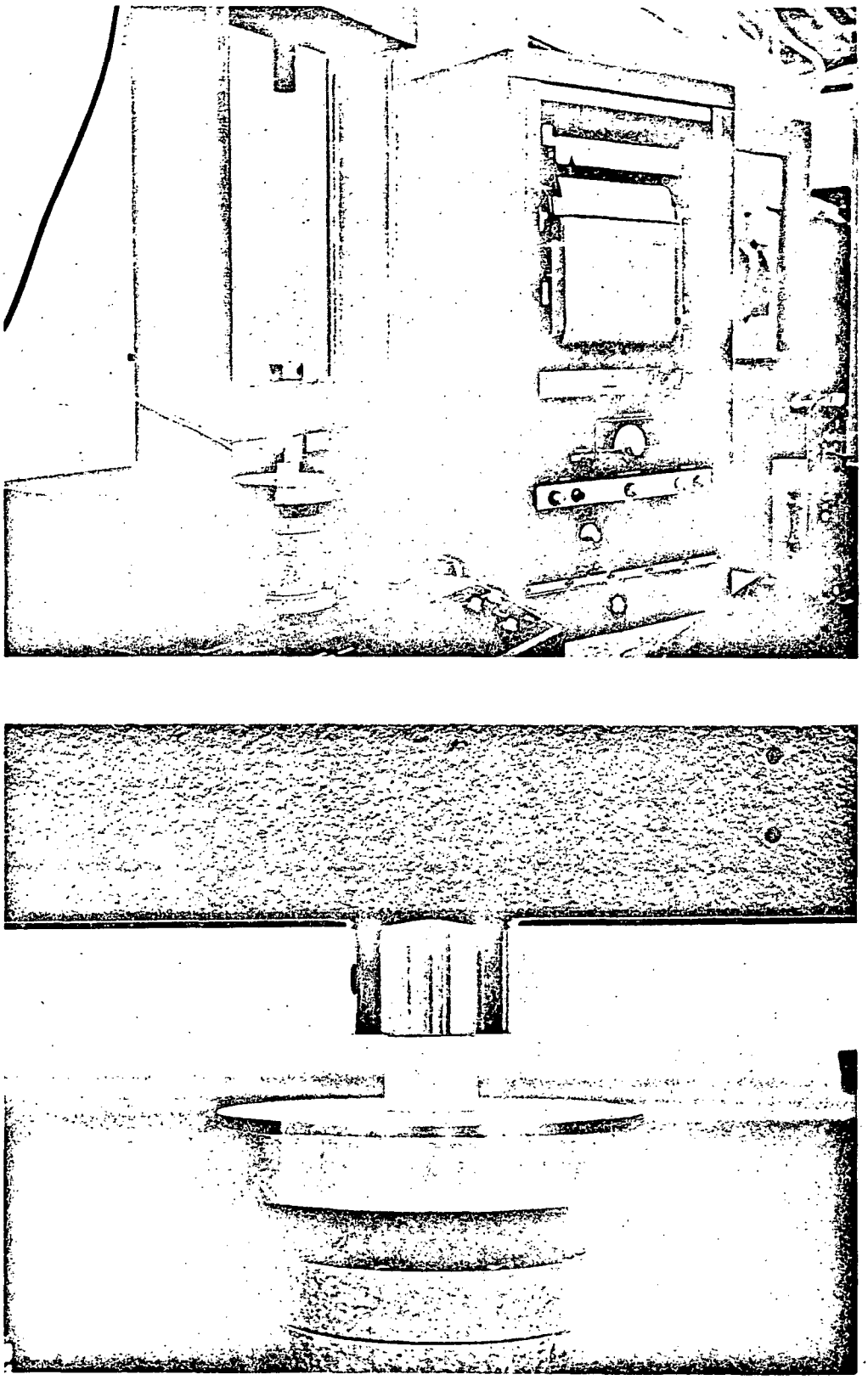

FIGURE 3–5
ORIGINAL HCF ROOM TEMPERATURE COMPRESSION TEST SETUP

457–1265

machine cross-head travel was due to local crushing at the ends of specimens. The crushing was eliminated by bonding the specimens to aluminum loading blocks with Scotchweld 2216 adhesive. Strain measurement accuracy was improved by using a clip-on extensometer attached between the loading blocks. The final test setup used two double cantilever clip-on displacement gages as illustrated in Figure 3-6.

The elevated temperature compression test setup is illustrated in Figure 3-7. The ends of the specimens were coated with Sauereisen No. 78* ceramic cement to prevent crushing. ATJ graphite cylinders were used to load specimens and 10-inch quartz lamps were used to provide heat. Specimens were heated to test temperature in approximately 5 minutes and allowed to soak for 3 minutes prior to testing.

Test Results - Mechanical property screening test results are listed in Figure 3-8. Properties were determined for a group of experimental materials with different fillers, Mod I, Mod II, Mod III, Mod IIIA and Mod V materials. The composition of each material, as well as firing temperature and density are defined. Specimens were tested in the "as fabricated" condition and all specimens were loaded to failure. Both longitudinal and transverse fiber orientations were tested. Ultimate strengths were obtained by dividing ultimate load by specimen cross sectional area. Elastic moduli represent the slope of the linear portion of the stress-strain curve, and the footnotes used in Figure 3-8 indicate the various types of strain measurement used. Stress-strain curves for both tension and compression are generally linear to failure. Typical stress-strain curves are shown in Figure 3-9. Stress-strain data were recorded for all room temperature test specimens. Typical tensile and compressive failures are illustrated in Figure 3-10.

Elevated Temperature Mechanical Properties of Mod IIIA HCF - One goal of this program was to develop methods for accurately determining HCF mechanical

* Sauereisen Cements Company

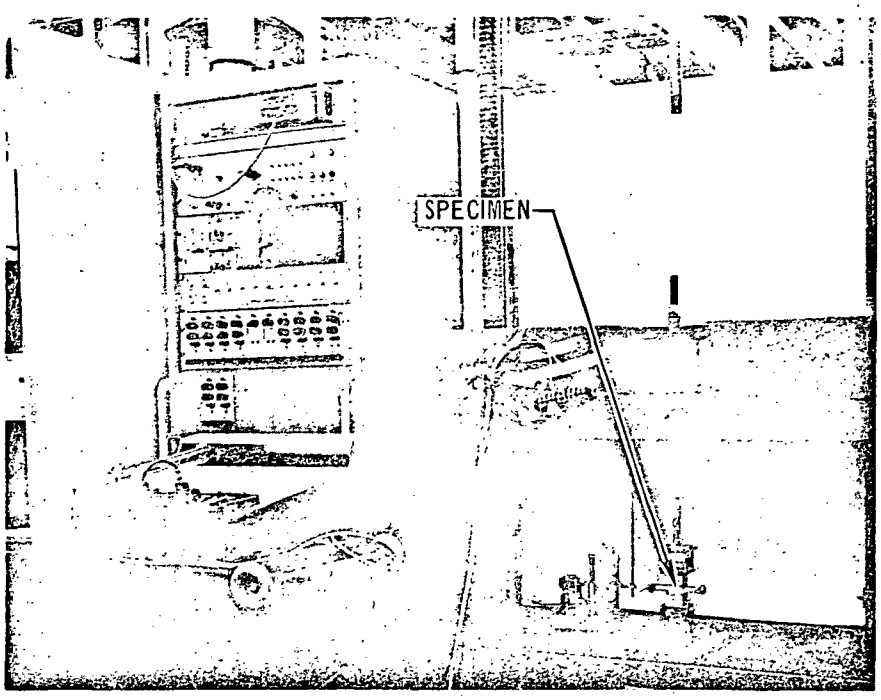

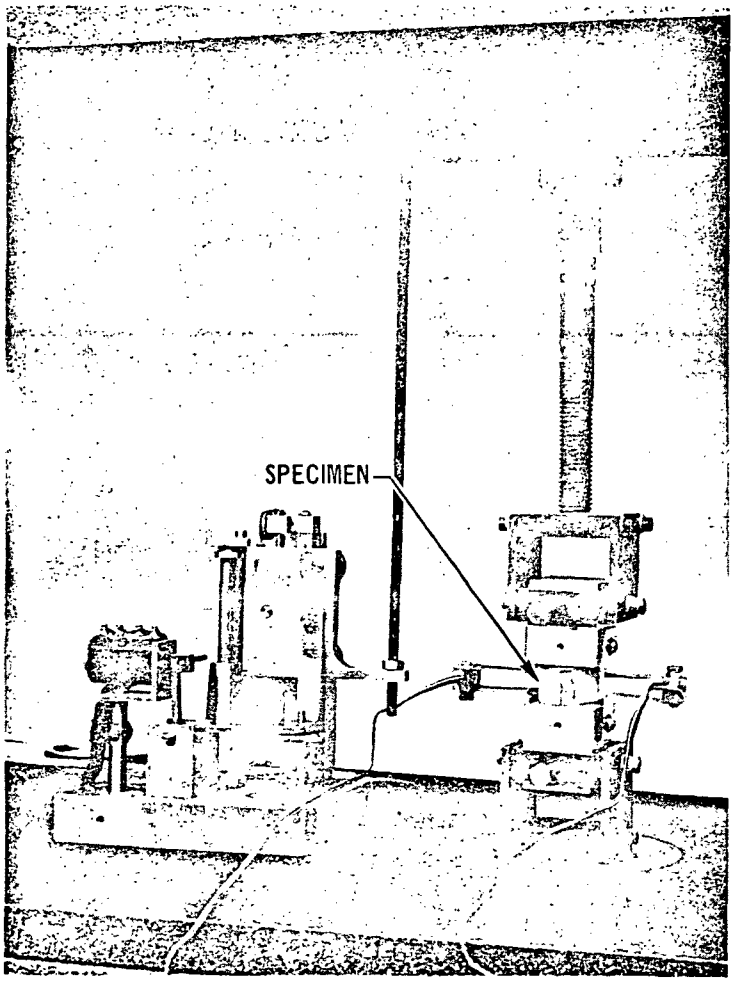

457-2111

FIGURE 3-6
IMPROVED HCF ROOM TEMPERATURE COMPRESSION TEST SETUP

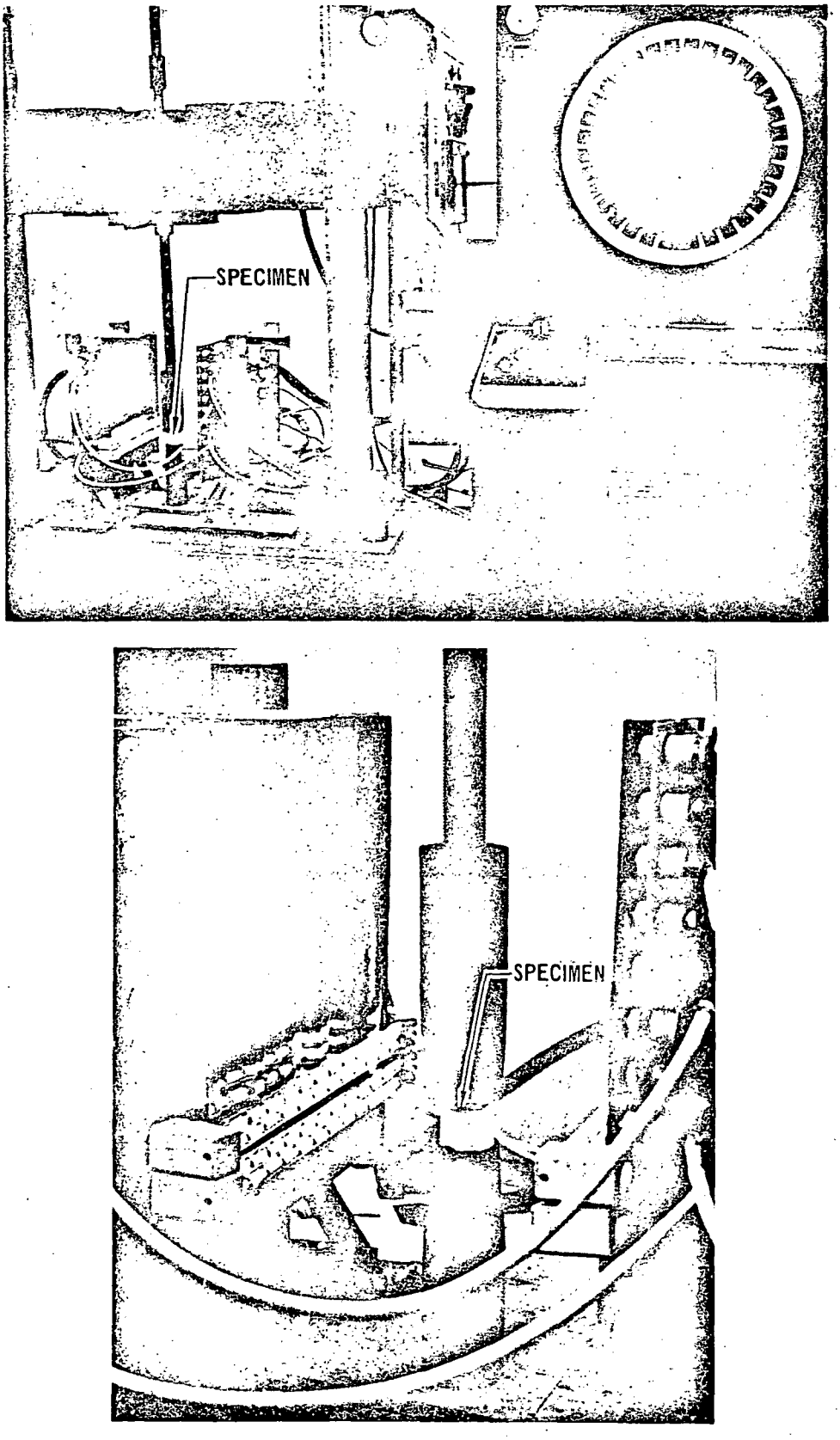

457-2110

FIGURE 3-7
HCF ELEVATED TEMPERATURE COMPRESSION TEST SETUP

MATERIAL DESIGNATION	SPECIMEN NUMBER	COMPOSITION (1)	FIRING TEMPERATURE (°F)	DENSITY (LB/FT³)	LONGITUDINAL PROPERTIES				TRANSVERSE PROPERTIES				REMARKS AND REASONS FOR TESTS
					TENSION		COMPRESSION		TENSION		COMPRESSION		
					F_{tu}	E_t	F_{cu}	E_c	F_{tu}	E_t	F_{cu}	E_c	
EXPERIMENTAL FORMULATIONS (COMPARISON OF FILLERS)		ALL SPECIMEN MB-MF (FILLERS LISTED BELOW)											ALL SPECIMENS USED MULLITE BINDER
	13-1	ECCO	2,100	16.0	75	7,500	89	3,600					SYSTEMATIC VARIATION OF PROCESSING PARAMETERS USING MULLITE BINDER, 13-1 THRU 13-12; 30 SEC BLENDING TIME
	-2	ECCO	2,100	17.3	89	6,360	108	6,100					
	-3	ECCO	2,300	15.8	52	5,000	55	1,800					
	-4	ECCO	2,300	16.2	60	6,500	54	2,000					
	-5	ECCO	2,500	16.3	62	6,250	64	1,250					
	-6	AL_2O_3 FIBERS	2,300	15.6	34	4,170	44	1,110					
	-7	CENO, PHENOLIC MICROBALLOONS	2,100	14.1	NA	NA	15	715					13-13 THRU 13-18; 15 SEC BLENDING TIME
	-8	↕	2,100	15.7	NA	NA	17	1,070					
	-9	↕	2,300	15.0	15	2,500	20	835					
	-10	↕	2,300	13.3	14	2,500	20	938					
	-11	↕	2,500	13.9	NA	NA	17	715					
	-12	CENO, PHENOLIC MICROBALLOONS	2,500	13.4	6	555	13	715					
	-13	NO FILLER	2,100	13.7	14	2,500	19	715					
	-14	↕	2,100	13.4	16	3,333 (2)	19	835 (2)					
	-15	↕	2,300	13.3	18	4,000	18	835					
	-16	↕	2,300	13.3	16	5,000	17	750					
	-17	↕	2,500	14.6	24	3,570	19	625					
	-18	NO FILLER	2,500	13.1	16	4,160	19	835					
	-19	ECCO	2,500	14.9	46	6,000	36	1,150					
	-20	ECCO, AL_2O_3 FIBERS	2,300	15.5	47	5,570	34	1,137					
	-21	ECCO, FINE MF	↕	12.9	NA	NA	38	1,315					
	-22	ECCO, FINE MF	↕	12.2	NA	NA	29	1,153					
	-23	AL_2O_3 FIBERS	↕	14.9	NA	NA	25	770					
	-24	AL_2O_3 FIBERS	↕	14.3	NA	NA	21	535					
	-25	FAA, ECCO	↕	16.7	35	5,100	43	1,875					
	-26	FAA, ECCO	↕	18.1	50	3,000	42	1,820					
	-27	FAA, ECCO	↕	16.2	28	2,500	27	834					
	13-28	FAA, ECCO	2,300	16.3	32	3,750	24	1,231					
MOD I	21-7	6μ MF, ECCO, RSB-2	2,300	14.8	90 (a)	8,000	164 (b)	9,585					(a) BOND FAILURE (b) SPECIMEN STRENGTH EXCEEDED CAPABILITY OF TEST MACHINE
	-8	↕	↕	14.1	100 (a)	9,000	163 (b)	5,460					
	-11	↕	↕	15.9	123 (a)	10,000	163 (b)	5,000					
	21-12	↕	↕	15.8	112	8,000	152	3,750					
	13-1	6μ MF, ECCO, RSB-2	↕	14.1	102	13,500	209	9,000					
	-2	6μ MF, ECCO, RSB-2	↕	14.6	153	15,250	237	7,300					
	-4	SAME AS -2 WITH 3% Co_3O_4	↕	15.8	186	17,000	216	8,000					
	-6	↕	2,300	14.7	122	13,000	190	5,500					
	-10	↕	2,000	14.9	110	11,500 (2)	172	10,000					
	-11	↕	2,000	15.8	154	14,000	198	9,000					
	-12	↕	2,150	15.2	137	14,500	193	10,500					
	13-13	SAME AS-2 WITH 3% Co_3O_4	2,150	14.9	145	15,500	213	11,000					
	37-1-F	6μ MF, ECCO, RSB-2	2,300	17.3	175	7,500							
	-G	↕	↕	13.3	106	10,500							
	-H	↕	↕	13.3			202	3,250					6μ MF TESTED FOR STRENGTH AND TO EVALUATE NEW TESTING TECHNIQUES
	37-1-I	6μ MF, ECCO, RSB-2	↕	16.4			258	5,000					
	37-4-F	SAME AS -G WITH 1% ZIRCON	↕	12.9	83	8,750							
	49-17-B	6μ MF, ECCO, RSB-2	↕	16.1					27	18,500			
	49-17-C	↕	↕	15.8				(2)			46	3,150	
	49-17-D	↕	↕	15.8							43	3,500	
	49-18-B	↕	↕	15.1	81	73,400							
	49-18-C	↕	↕	15.2			115	5,000					
	49-19-B	↕	↕	15.9					32	16,000			
	49-19-C	↕	↕	15.8						(3)	55	3,750	
	49-20-B	↕	↕	15.6	73	190,000							
	49-20-C	↕	↕	15.1			123	6,100				(2)	
	49-20-D	6μ MF, ECCO, RSB-2	2,300	15.0			116	6,000					

FIGURE 3-8

STRENGTH SCREENING TEST RESULTS

MATERIAL DESIGNATION	SPECIMEN NUMBER	COMPOSITION (1)	FIRING TEMPERATURE (°F)	DENSITY (LB/FT³)	LONGITUDINAL PROPERTIES				TRANSVERSE PROPERTIES				REMARKS AND REASONS FOR TESTS
					TENSION		COMPRESSION		TENSION		COMPRESSION		
					F_{tu}	E_t	F_{cu}	E_c	F_{tu}	E_t	F_{cu}	E_c	
MOD III	41-1-D	4.7μ MF, ECCO, RSB-2, 1% ZIRCON	2,300	15.3	133	16,500							TESTED STRENGTH OF OPACIFIED HCF
	-E			15.5	184	13,000							
	-F			14.8			128	8,250					
	41-1-G	4.7μ MF, ECCO, RSB-2, 1% ZIRCON		15.3		(2)	187	6,000					
	41-2-B	4.7μ MF, ECCO, RSB-2, 3% ZIRCON		16.7					51	155,000 (3)			
	-C			15.2							55	5,000 (2)	
	-D			15.4	156	17,000							
	-E			15.6	66	155,000		(2)					
	-F			14.5			158	3,375					
	-G			15.5			199	4,500					
	-X			14.2			120	6,500					
	-Y			14.8			113	10,000					
	41-2-Z			15.2	67	155,000							
	349P7			15.9	37	NA							TESTED AT 2300°F
	336P4			14.9	9	NA							
	336P5			15.4	13	NA							
	336P6	4.7μ MF, ECCO, RSB-2, 3% ZIRCON	2,300	15.6	20	NA							TESTED AT 2300°F
	AVERAGE				121	71,390 (4)	151	6,400 (4)	51	156,000 (4)	55	5,000 (4)	ROOM TEMPERATURE TESTS ONLY
MOD IIIA	49-7-B	4.7μ MF, ECCO, RSB-2, CELLULOSE THICKENER, HMT	2,300	14.4					43	100,000 (3)			
	49-7-C			13.8							62	3,500 (2)	
	49-8-A			16.2	131	160,000							
	49-8-C			16.4			169	3,750					
	75-1A			17.1	161	178,000							COMPARISON OF MECHANICAL PROPERTIES OF HCF WITH CELLULOSE THICKENING AGENT VS HCF MOD I
	-1C			15.2	136	91,000							
	-2C			14.8	120	48,000							
	-2D			14.9	114	NA							
	-1F			15.1					38	84,100			
	-1G			15.8					46	20,000			
	-2E			14.2					51	41,400 (3)			
	-2H			14.5					49	49,000			
	-1B			14.7		(3)	162	7,000					
	-1D			14.5			152	8,500					
	-2A			14.2			141	7,270					
	-2B			13.9			134	6,660					
	-1E			14.1				(2)			61	5,900	
	-1H			14.6							64	6,660	
	-2F			13.8							56	5,550 (2)	
	-2G			13.6							67	6,660	
	-1BB			15.2	97	970,000							
	-1DD			14.0	84	83,500							
	-1FF			16.2					54	36,600			
	-1GG			14.7					42	32,500			
	-2BB			13.9	84	153,000				(3)			
	-2CC			14.8	92	163,500							
	-2FF			14.4					39	224,000			
	-2HH			15.1					46	840,000			
	-1CHH			14.7			137	7,270					
	-1AHH			14.6			141	7,300					
	-2AHH			14.6			131	8,000					
	-2DHH			14.6			145	4,000					
	-1EVV			14.9							61	5,710	
	-2EVV			14.6							71	5,670 (2)	
	75-2GVV			14.9							67	5,710	
	289BP12			14.3	51	46,600							COMPARISON OF SHOP PROCESSED MOD IIIA VS LAB PROCESSED MOD IIIA
	2			14.3	72	51,600							
	4	4.7μ MF, ECCO, RSB-2, CELLULOSE THICKENER, HMT		15.7	89	61,000							
	289BP15		2,300	14.6			160	55,300					

457-2579 (CONT'D)

STRENGTH SCREENING TEST RESULTS (Continued)

MATERIAL DESIGNATION	SPECIMEN NUMBER	COMPOSITION (1)	FIRING TEMPERATURE (°F)	DENSITY (LB/FT³)	LONGITUDINAL PROPERTIES				TRANSVERSE PROPERTIES				REMARKS AND REASONS FOR TESTS
					TENSION		COMPRESSION		TENSION		COMPRESSION		
					F_{tu}	E_t	F_{cu}	E_c	F_{tu}	E_t	F_{cu}	E_c	
			2,300										
	143-A	6μ MF, ECCO, RSB-2, 3% TiO_2		19.3		(3)			59	82,200			
	-C			19.3					11	180,000			
	-D			19.8					34	340,000			
	-E			15.1							98	14,500	
	-F			15.0							79	6,500	
	-G			15.0							83	7,000	
MOD I	-J			16.0	89	115,000							
	-K			16.0	86	132,000							
	-L			15.2	83	81,300							
	-M			20.1			148	5,500					
	-N			15.7			106	6,000					
	-O			18.4			156	5,500					
	-W			16.0	114	14,000 (2)							
	-X			17.9	92	14,500							
	-Y			15.9			158	9,000					
	143-Z	6μ MF, ECCO, RSB-2, 3% TiO_2	2,300	18.3			117	7,500					
	AVERAGE				114	36,200 (4)	171	7,000 (4)	33	127,300 (4)	67	6,400 (4)	
	25-1	6μ MF, CENO, RSB-2	2,300	18.8	128	9,000	127	2,725					TEST STRENGTH OF ALL MULLITE FILLER
	-2	6μ MF, CENO, RSB-2	2,300	18.2	133	8,340	142	2,500					
	-3	6μ MF, CENO, Li_2CO_3, RSB-2	2,300	19.4	132	7,500	172	2,900					
	25-4	6μ MF, CENO, H_3BO_3, RSB-2	2,300	18.1	142	9,000	117	3,360					
	35-1-A	6μ MF, E-CENO, RSB-2	2,150	14.8	106	12,000							
	-B		2,150	14.9	123	10,000							
	-C		2,150	14.2			145	2,250					
	35-1-D		2,150	13.9			130	2,500					
	35-2-A		2,300	15.2	124	14,500							
	-B		2,300	14.9	144	15,000							
	-C		2,300	15.3			162	2,375					
	35-2-D		2,300	15.2			182	2,500					
MOD II	35-3-A		2,150	15.1	129	16,600 (2)							
	-B		2,150	16.0	151	18,000							
	-C		2,150	16.3			212	5,500					
	35-3-D		2,150	15.6			205	3,750					
	35-4-A		2,300	16.0	168	12,000							
	-B		2,300	16.3	162	19,500							
	-C		2,300	16.0			224	4,250					
	35-4-D		2,300	16.2			255	4,625 (2)					
	35-5-A		2,150	17.6	155	19,600							
	-B		2,150	16.9	162	17,000							
	-C		2,150	16.7			221	8,000					
	35-5-D		2,150	17.3			246	6,000					
	35-6-A		2,300	16.9	220	18,000							
	-B			16.9	177	20,500							
	-C			16.1			228	3,750					
	35-6-D	6μ MF, E-CENO, RSB-2		16.8			250	3,750					
	47-1-B	4.7μ MF, E-CENO, RSB-2		13.1					41	12,800			
	-C			12.7							41	1,500	
	47-1-D			NA							43	2,750	
	47-4-C			13.5			106	4,000		(3)			
	47-4-D	4.7μ MF, E-CENO, RSB-2		14.0			111	3,250				(2)	
	51-1-A	4.7μ MF, E-CENO, RSB-2, 3% ZIRCON		14.9					19	11,600			
	-B			14.5					23	17,000			
	-C			13.6							31	2,000	
	-E			12.7	78	53,000 (3)							
	-F			12.9	88	82,000							
	51-1-G	4.7μ MF, E-CENO, RSB-2, 3% ZIRCON	2,300	13.7			85	5,000					
	AVERAGE				140	20,100 (4)	175	3,800 (4)	28	13,800 (4)	38	2,100 (4)	

457-2579 (CONT'D)

STRENGTH SCREENING TEST RESULTS (Continued)

MATERIAL DESIGNATION	SPECIMEN NUMBER	COMPOSITION (1)	FIRING TEMPERATURE (°F)	DENSITY (LB/FT³)	LONGITUDINAL PROPERTIES				TRANSVERSE PROPERTIES				REMARKS AND REASONS FOR TESTS
					TENSION		COMPRESSION		TENSION		COMPRESSION		
					F_{tu}	E_t	F_{cu}	E_c	F_{tu}	E_t	F_{cu}	E_c	
MOD IIIA	125-2-1P	4.7μ MF, ECCO, RSB-2, CELLULOSE THICKENER, HMT	2,300	16.2							171	36,900	
	-2P			15.4					65	32,500			EVALUATION OF STRENGTH AND SHRINKAGE OF MOD IIIA
	-3P			15.7					61	28,200			
	-4P			15.5					81	39,100			
	-1N			16.2			231	70,000					
	-2N			15.0	103	65,000							
	-3N			15.5	125	65,300							
	125-2-4N			15.9	163	88,500							
	147-5-A			14.2	62	31,900							
	-B			14.1	64	33,200							EVALUATION OF STRENGTH OF BINDER DEFICIENT MOD IIIA
	147-5-C			14.3			96	32,200					
	147-7-A			14.4	71	36,800							
	-B			14.2			111	33,600					
	147-7-C			14.1			120	35,000					
	11-1-C			13.4	103	65,200							EVALUATION OF MECHANICAL PROPERTIES OF HIGH STRENGTH MOD IIIA
	11-1-D			13.2			206	59,250					
	11-2-C			16.3	NA	68,500							
	11-2-D			16.0			285	65,300					
	129-1-A			15.6	88	56,800							
	129-1-B			15.6			187	57,520					
	147-1			15.0	77	42,700							EVALUATION OF STRENGTH OF BINDER DEFICIENT MOD IIIA
	-2			15.5	77	46,400							
	-3			15.4	90	56,000							
	147-4			15.8	71	46,500							
	19-5A			15.3					54	33,200			
	19-5B			16.1					60	42,200			
	19-6			15.2					50	31,500			
	23-1			17.0					80	36,400			
	23-2			15.0					63	30,000			
	119-1A			15.9							151	45,000	
	119-1B			16.4							205	56,700	
	25-1S			14.4							154	NA	
	25-1C			15.7							200	NA	
	25-1F			14.7							108	NA	
	408P1			14.6	32	NA							TESTED AT 1200°F
	408P2			14.1	45	NA							TESTED AT 1200°F
	408P3			14.0	20	NA							TESTED AT 2300°F
	119-1C			15.2			221	NA					TESTED AT 1200°F
	119-1D			14.5			83	NA					TESTED AT 1800°F
	119-1P			15.6			81	NA					TESTED AT 2300°F
	430P6			NA	53	NA							TESTED AT 1200°F
	5			NA	45	NA							TESTED AT 1200°F
	1			NA	8	NA							TESTED AT 2300°F
	3			NA	23	NA							TESTED AT 2300°F
	430P4			NA	8	NA							TESTED AT 2300°F
	47-1B	4.7μ MF, ECCO, RSB-2, CELLULOSE THICKENER, HMT	2,300	15.9			120	NA					TESTED AT 1200°F
	47-1E			15.6			158	NA					TESTED AT 1200°F
	AVERAGE				87 (5)	53,900 (5)	175 (5)	51,000 (5)	54 (5)	34,100 (5)	165 (5)	46,200 (5)	ROOM TEMPERATURE TESTS ONLY
MOD V	C69-1-L1	4.7μ MF, 1.2μ SiO_2, RSB-2, CELLULOSE THICKENING AGENT, HMT	2,300	16.3	221	103,300							LAB PROCESSED
	-L2			16.2	273	102,700							
	-N1			16.3					103	24,200			
	C69-1-N2			16.2					109	27,800			
	455APT1			15.6	32	22,100							
	455APT2			16.1	30	21,300							SHOP PROCESSED
	455BPT1	4.7μ MF, 1.2μ SiO_2, RSB-2, CELLULOSE THICKENING AGENT, HMT	2,300	16.7	37	26,000							
	455BPT2			16.4	31	NA							
	455ANT1			15.5					16	12,900			

457-2579 (CONT'D)

STRENGTH SCREENING TEST RESULTS (Continued)

MATERIAL DESIGNATION	SPECIMEN NUMBER	COMPOSITION (1)	FIRING TEMPERATURE (°F)	DENSITY (LB/FT³)	LONGITUDINAL PROPERTIES				TRANSVERSE PROPERTIES				REMARKS AND REASONS FOR TESTS
					TENSION		COMPRESSION		TENSION		COMPRESSION		
					F_{tu}	E_t	F_{cu}	E_c	F_{tu}	E_t	F_{cu}	E_c	
MOD IV	455ANT2	4.7μ MF, 1.2μ SiO_2, RSB-2, CELLULOSE THICKENING AGENT, HMT	2,300	15.6					15	13,200			TESTED EFFECT OF FIRING CYCLE ON STRENGTH
	455ANB1			18.6					20	16,200			
	455ANB2			17.3					18	11,800			
	455BPB1			18.3	59	32,500							
	455DPB2			18.5	48	34,300							
	455APB1			18.6	43	29,200							
	455APB2			18.9	39	NA							
	455AN1			19.7					52	16,900			
	455BN1			15.7					44	17,900			
	455BN2			19.3					40	17,600			
	463AP1			15.1	35	24,500							
	463AP2			15.9	34	30,300							
	463BP1			15.9	61	NA							
	463BP2			15.6	66	51,000							
	463BN1			16.7					38	15,500			
	463BN2	4.7μ MF, 1.2μ SiO_2, RSB-2, CELLULOSE THICKENING AGENT, HMT		17.0					43	15,500			
	463AN1			15.2					15	5,740			
	463AN2		2,300	15.3					15	6,700			
	AVERAGE				72	43,400			41	15,500			

(1) KEY
MB – MULLITE BINDER
MF – MULLITE FIBERS
ECCO – SI ECCOSPHERES
CENO – FLY ASH SPHERES FROM UNION ELECTRIC (FLOATERS)
E-CENO – ENGLISH CENOSPHERES
NA – NOT AVAILABLE
RSB-1 – ETHYL SILICATE
RSB-2 – COLLOIDAL SILICA
FAA ECCO – GRADE OF ECCOSPHERES
FAS ECCO – GRADE OF ECCOSPHERES
(2) ERROR CAUSED BY USING MACHINE CROSS-HEAD TRAVEL TO DETERMINE SPECIMEN STRAIN
(3) POSSIBLE ERROR CAUSED BY USING ONLY ONE EXTENSOMETER
(4) AVERAGED RESULTS INCLUDE ERRORS CAUSED BY STRAIN MEASUREMENT TECHNIQUES
(5) AVERAGED RESULTS INCLUDE ONLY SPECIMENS TESTED WITH TWO EXTENSOMETERS AT ROOM TEMPERATURE

457–2579 (CONT'D)

STRENGTH SCREENING TEST RESULTS (Continued)

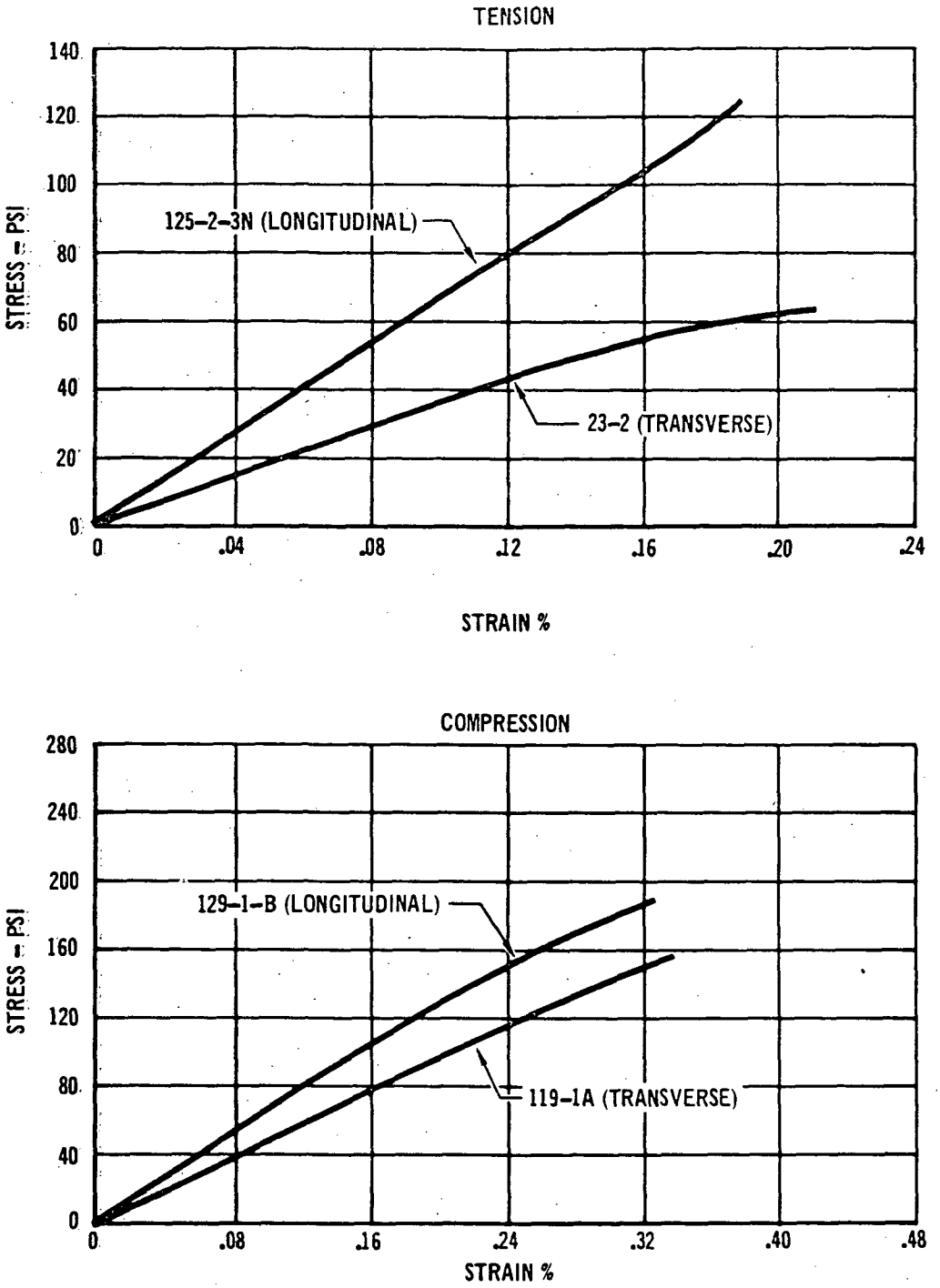

FIGURE 3–9

TYPICAL HCF STRESS STRAIN CURVES
MOD IIIA HCF

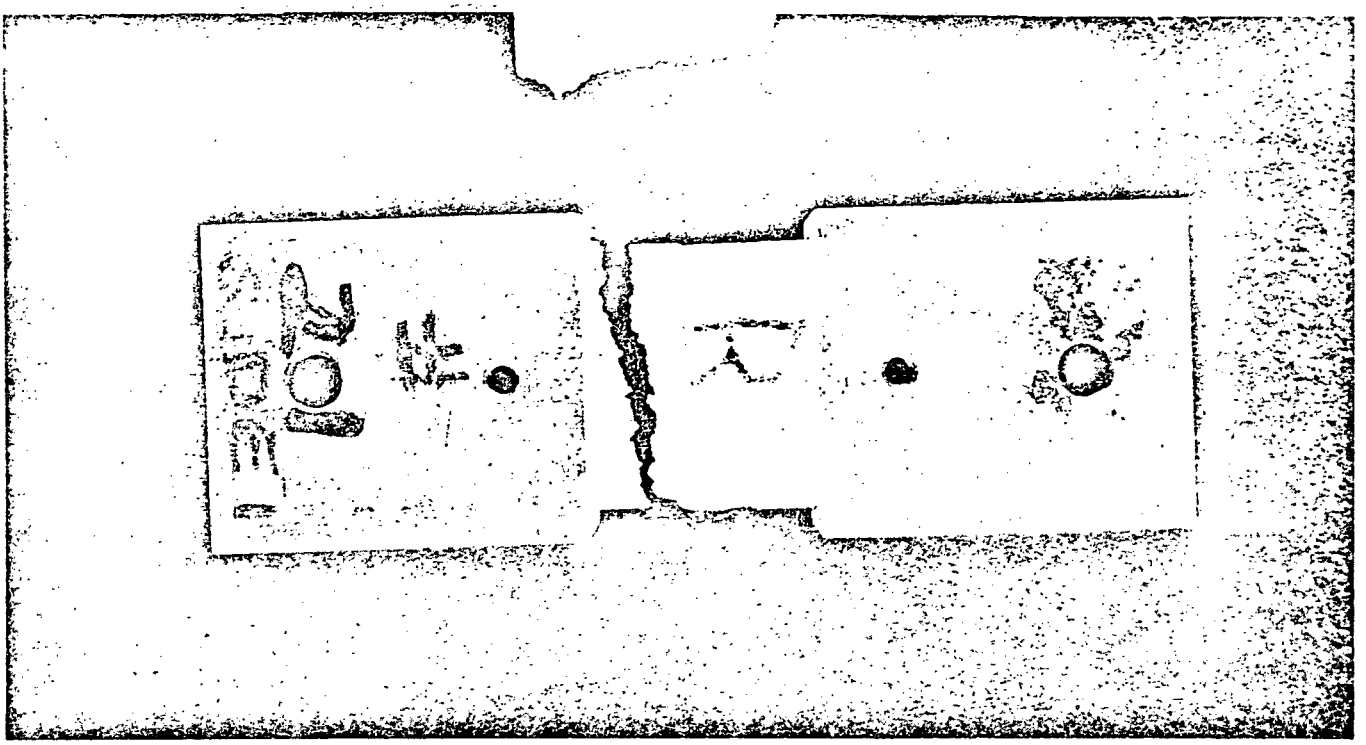

SPECIMEN NO. 322R
(REF B)

Tension

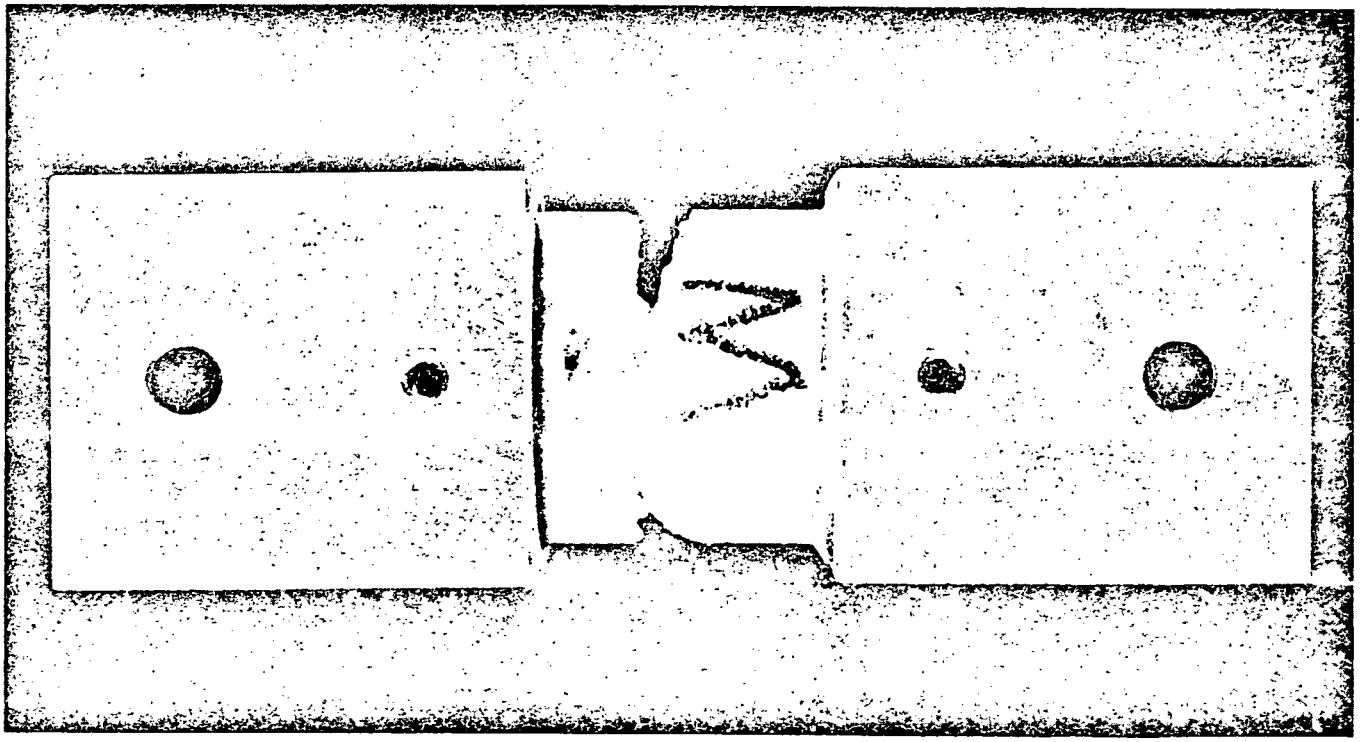

457-2368

Compression

SPECIMEN NO. 322M
(REF B)

FIGURE 3-10
TYPICAL FAILED SPECIMENS

properties. Results reported in this section were obtained using an optical extensometer to measure strains which is thought to be the most accurate means of determining elevated temperature strains. All of this series of tests were conducted at MDAC-W on Mod IIIA material. Properties were measured to 2300°F.

The above results and those from tests conducted at MDAC-E were used to derive curves of strength and modulus of Mod IIIA HCF as a function of temperature. The MDAC-E tests were conducted during the Reference (b) program using the latest procedures described in this section. In the Reference (b) program, room temperature strains were measured using mechanical techniques, and elevated temperature strains were not determined.

Elevated Temperature Test Methods - Test specimen configurations are illustrated in Figure 3-11. All specimens were loaded to failure at a loading rate of approximately 0.05 inch/minute. Specimen densities were approximately 15 lb/ft^3 and are listed along with mechanical properties.

Tests were conducted in the elevated temperature fixture shown in Figure 3-12 mounted in an Instron test machine. Load rods were closely fitted to guide bushings in the yoke to ensure good alignment. The yoke and guide bushings were water cooled for dimensional stability.

Heating was provided by radiation from electrically heated graphite bars. The furnace was purged with argon for 2 hours prior to heating the specimens to test temperature. Heat was applied slowly (approximately 30 minutes) and the temperature was held for approximately 20 minutes before applying loads. The furnace contained quartz windows for sighting with optical instrumentation. A chromel-alumel thermocouple, imbedded in a small block of HCF clamped to each specimen was used to measure temperatures to 1900°F. An Ircon infrared pyrometer, sighted at the specimen gage section, was used at 2300°F. The pyrometer was calibrated against thermocouples at lower temperatures.

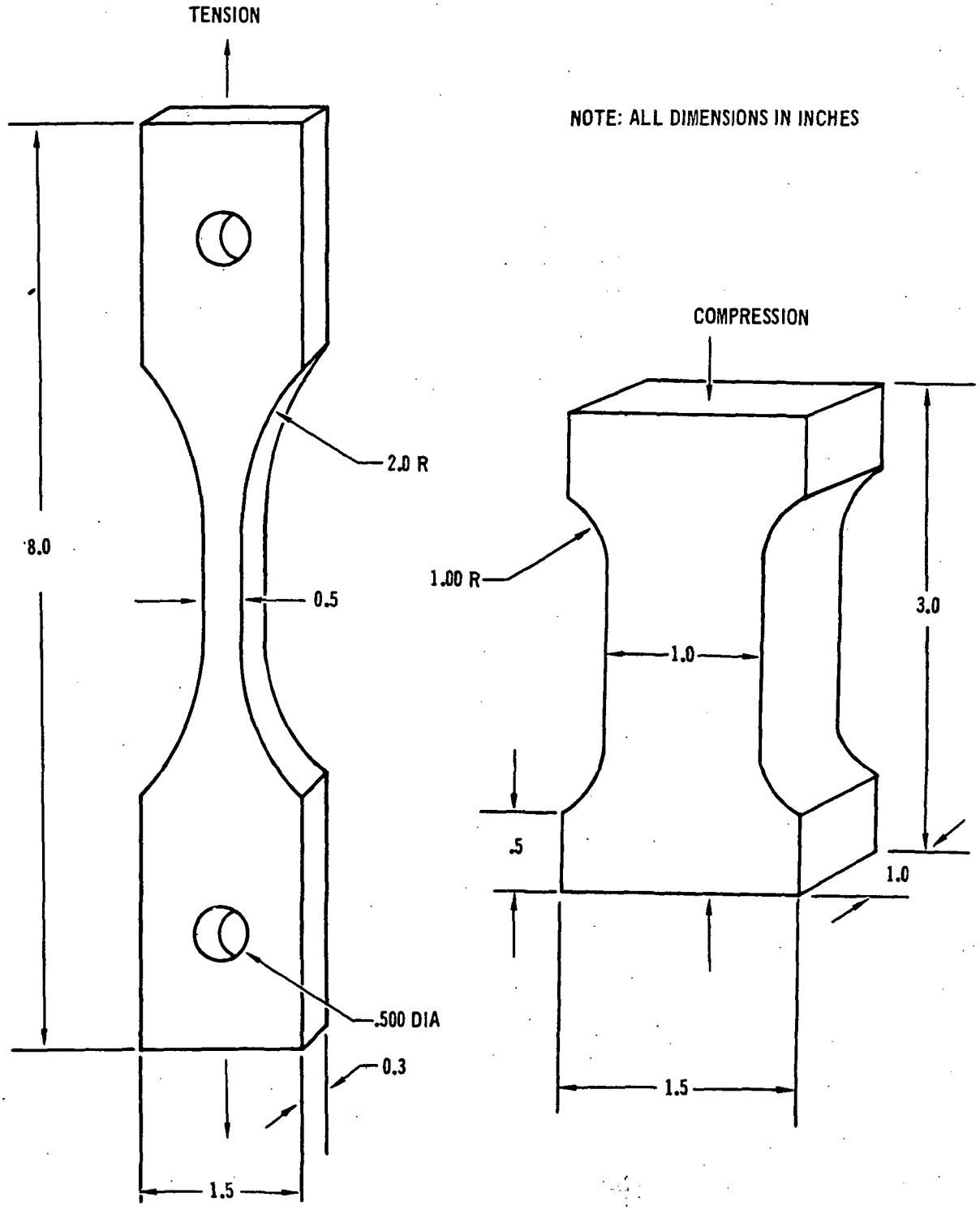

FIGURE 3-11
HCF ELEVATED TEMPERATURE MECHANICAL PROPERTY SPECIMENS

457-2545

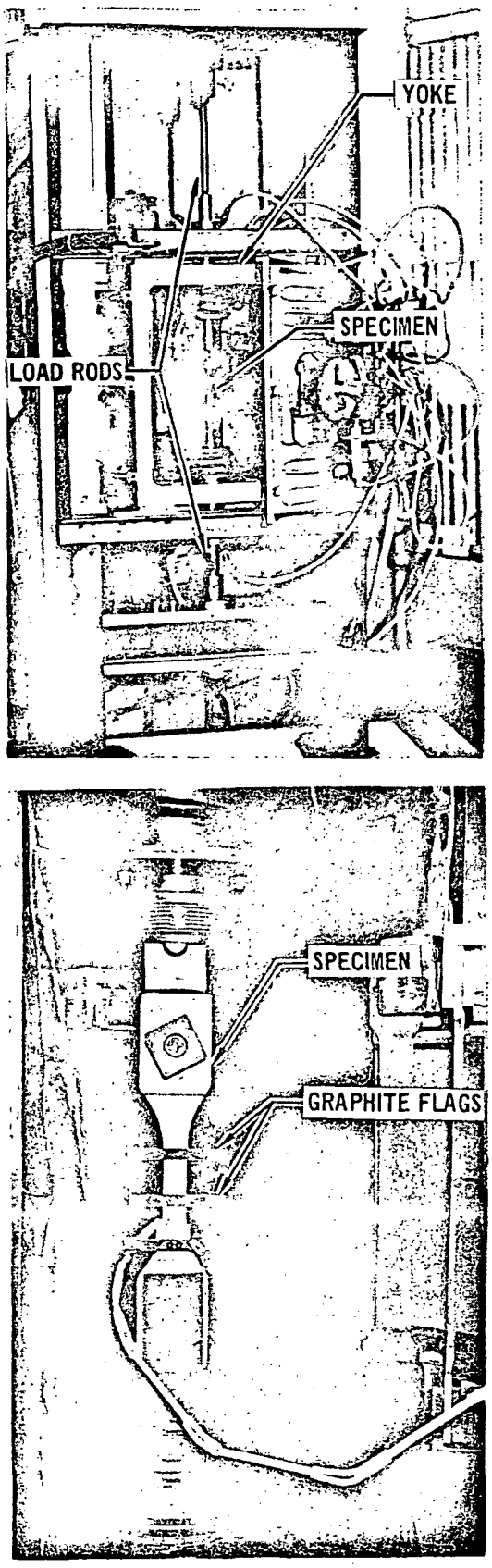

457-2544

FIGURE 3-12
HIGH TEMPERATURE STRENGTH TEST SETUP

Axial strains were measured with an Optron Model 800 optical extensometer aimed at graphite flags attached to the specimen. Figure 3-12 shows the flags mounted on a tensile specimen; also shown is the thermocouple block clamped to the lower part of the specimen. Similar flags were used in compression. Poisson's ratios were measured for two room temperature compression samples by recording the axial strain from the Optron against the transverse strain as determined with a mechanical extensometer.

The close fit between load rods and guide bushings gives rise to frictional loads. In these tests two load cells were used; one at the top and the other at the bottom of the fixture, to monitor the magnitude of friction. The difference between load cell readings was less than 5 percent at failure except in tension tests at 2300°F where the 0.3 to 0.5-lb load due to friction represents a larger portion of the load. The top load cell reading, which was the lesser of the two loads, was used to compute stress.

Test Results - Results of tensile tests are presented in Figure 3-13. All specimens were tested in the "as fabricated" condition and all specimens were loaded to failure. Specimen densities, ultimate strength, strain at failure and elastic modulus are listed for each specimen tested.

At the highest test temperature (2300°F) the tensile strength was only about 8 psi and the material shredded rather than broke as in the typical room temperature failure. Elongation of the 2300°F specimens exceeded the 0.050-inch limit of the optical extensometer. Typical fractures at the different test temperatures are shown in Figure 3-14. The grayish discoloration of the specimens tested at elevated temperature is believed due to graphite deposition from the furnace heating elements.

Tensile strength and modulus are plotted as a function of test temperature in Figures 3-15 and 3-16. Also shown are results of tests of the MOD IIIA material on the Reference (b) program. A computer program entitled "General Least Squares

TEST TEMPERATURE (°F)	FIBER DIRECTION	SPECIMEN NO.	DENSITY (LB/FT^3)	ULTIMATE STRENGTH LB/IN^2	STRAIN AT FAILURE (PERCENT)	ELASTIC MODULUS LB/IN^2	COMMENTS
ROOM TEMPERATURE	LONGITUDINAL	1	15.5	–	–	–	SPECIMEN BROKE DURING INSTALLATION
		2	15.5	71(1)	–	67,000	PREMATURE FAILURE AT FLAG
		3	16.1	109	–	–	FLAG SLIPPED
		AVERAGE	15.7	109	–	67,000	–
1200	LONGITUDINAL	5	–	54(1)	–	32,000	PREMATURE FAILURE AT FLAG
		6	15.6	112	0.37	30,000	
		8	15.9	84(1)	>0.13(1)	35,000	PREMATURE FAILURE AT THERMOCOUPLE ATTACHMENT
		AVERAGE	15.8	112	0.37	32,300	–
1900	LONGITUDINAL	9	15.6	53	>3.00	6,000	STRAIN EXCEEDED EXTENSOMETER LIMIT
2300	LONGITUDINAL	4	15.4	8	>5.00	< 1,000	STRAIN EXCEEDED EXTENSOMETER LIMIT
		7	15.8	8	>5.00	< 1,000	STRAIN EXCEEDED EXTENSOMETER LIMIT
		AVERAGE	15.6	8	>5.00	< 1,000	–

(1) – DATA NOT USED IN AVERAGE

FIGURE 3–13
MOD IIIA TENSION TEST RESULTS

457–2539

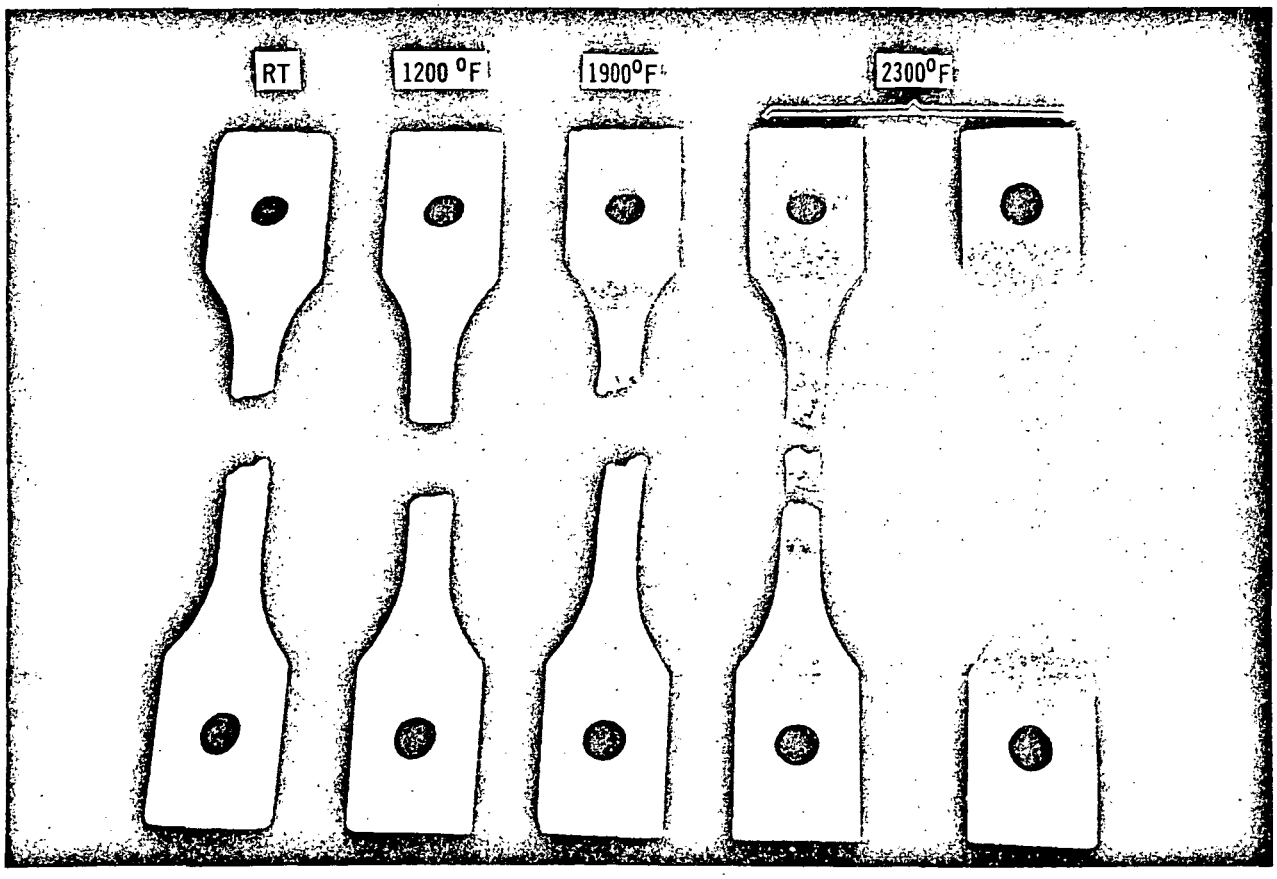

FIGURE 3-14

TYPICAL FAILED TENSILE SPECIMENS

457-2551

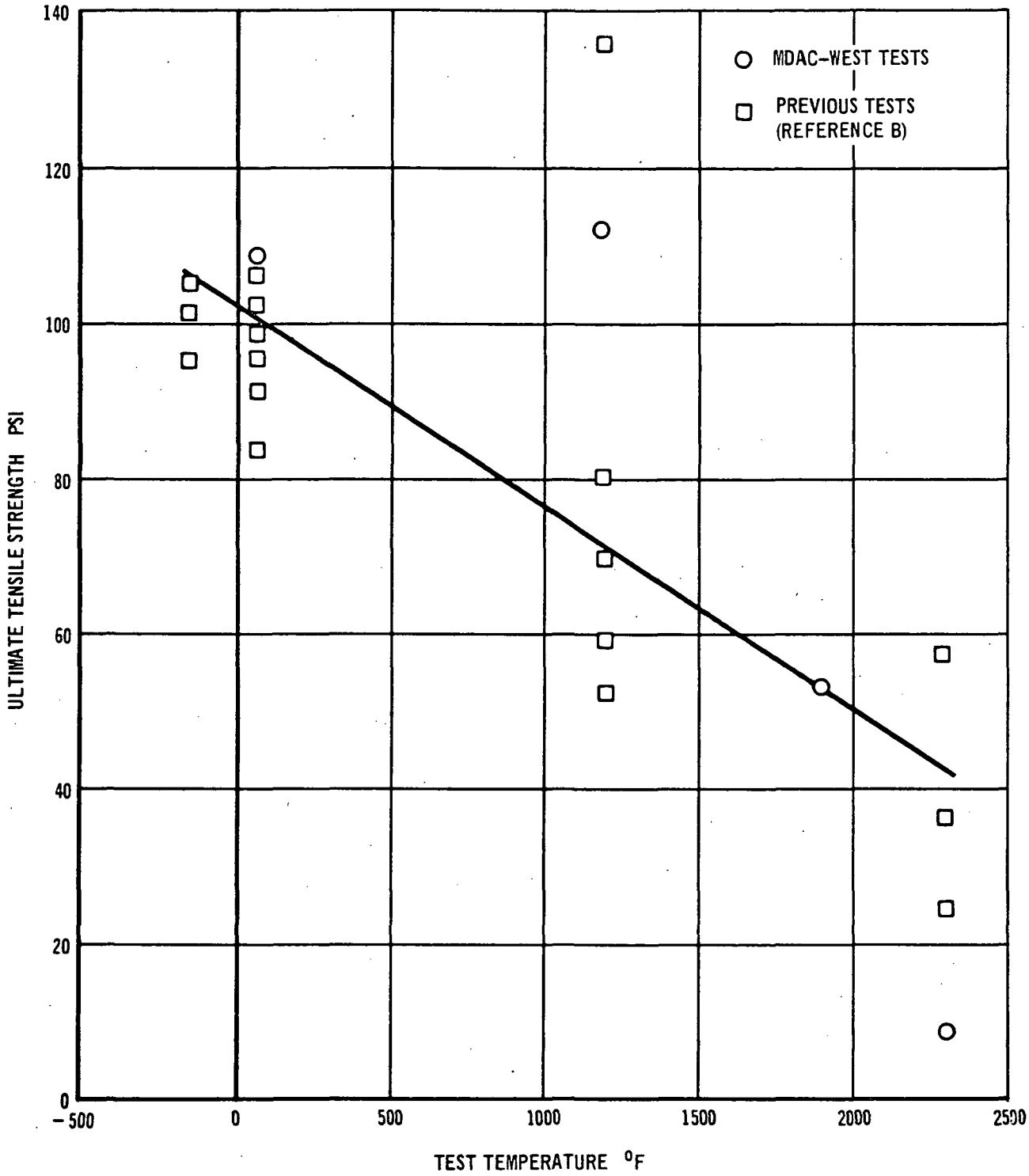

FIGURE 3-15

HCF LONGITUDINAL TENSION STRENGTH
Mod III A

457-2543

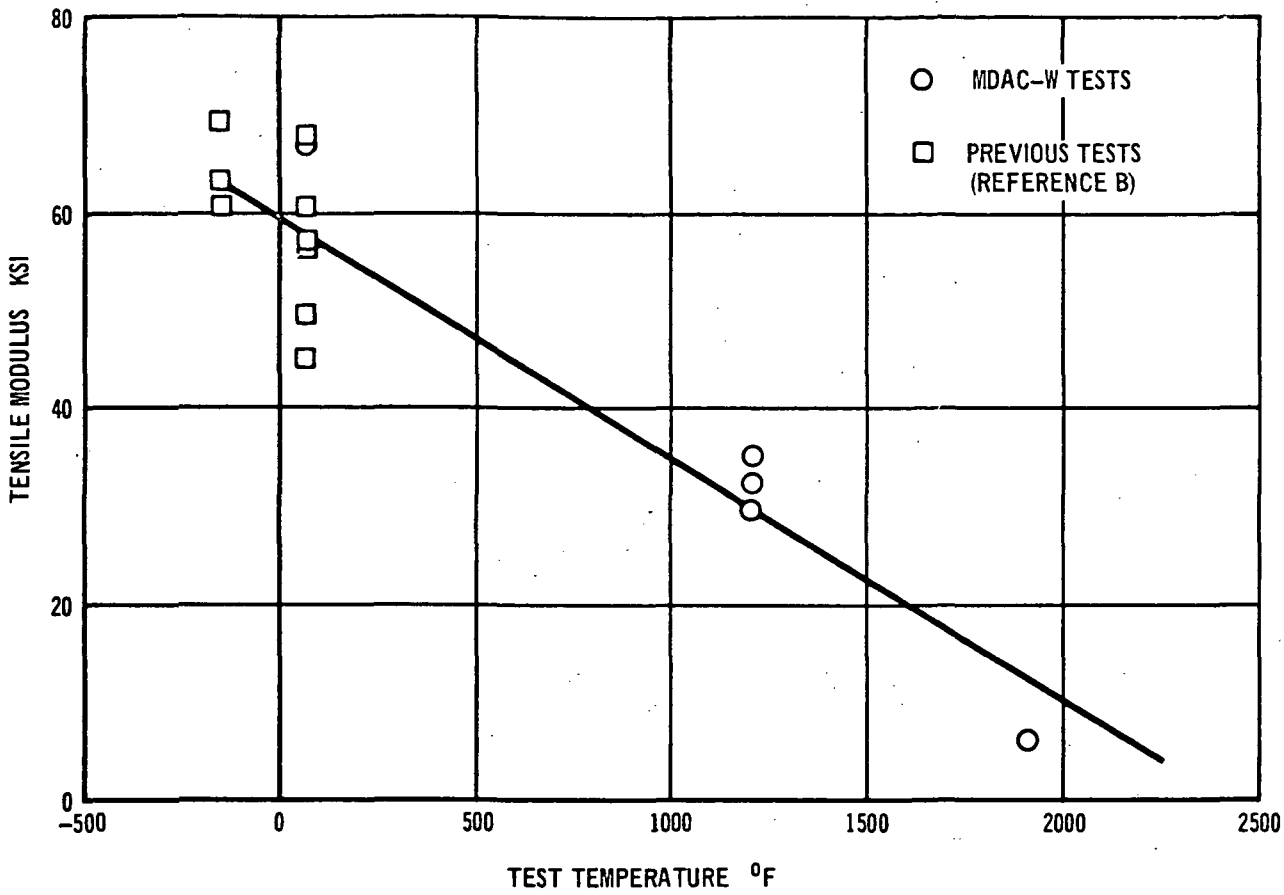

FIGURE 3-16
HCF LONGITUDINAL TENSION MODULUS
Mod III A

Analysis" was used to fit the data to linear least squares curves. The data fit a straight line relationship adequately; therefore, it was not necessary to consider higher order equations.

Compression test results are given in Figure 3-17. Typical compression failures are illustrated in Figure 3-18. At the higher test temperatures the longitudinal specimens did not break but only bulged. As can be seen in Figure 3-18, there was an appreciable expansion in the transverse direction at the center of these specimens.

Longitudinal compression strength and modulus are plotted in Figures 3-19 and 3-20 and transverse compression strength and modulus are plotted in Figures 3-21 and 3-22 as a function of temperature. Also shown are results of previous tests of

TEST TEMP. (°F)	FIBER DIRECTION	SPECIMEN NO.	DENSITY (LB/FT^3)	ULTIMATE STRENGTH LB/IN^2	STRAIN AT FAILURE (%)	ELASTIC MODULUS LB/IN^2	COMMENTS
ROOM TEMP.	LONGITUDINAL	2	15.8	230	0.17	145,000	
		3	15.5	247	0.22	114,000	μ = 0.160(2)
		AVERAGE	15.6	238	0.20	130,000	—
	TRANSVERSE	4	15.0	97	—	36,000	
		5	15.8	96	0.43	25,000	
		6	15.9	105	0.30	37,000	μ = 0.093(2)
		AVERAGE	15.5	100	0.35	32,700	—
1200	LONGITUDINAL	13	15.9 (1)	—	—	—	ENDS OF SPECIMEN CRUSHED DURING LOADING
		14	16.0	233	0.15	127,000	
		15	15.3	227	0.13	81,000	
		AVERAGE	15.7	230	0.14	104,000	—
1900	LONGITUDINAL	8	16.6	36	—	91,000	
		9	15.8	57	—	120,000	
		AVERAGE	16.2	47	—	106,000	—
	TRANSVERSE	10	16.5	27	—	1,800	
		11	17.0	24	—	900	
		12	17.1	30	—	1,100	
		AVERAGE	16.9	27	—	1,300	—
2300	LONGITUDINAL	7	16.7	10	—	—	

(1) DATA NOT USED IN AVERAGE
(2) POISSON'S RATIO

FIGURE 3-17

COMPRESSION TEST RESULTS

MOD III A

457-2549

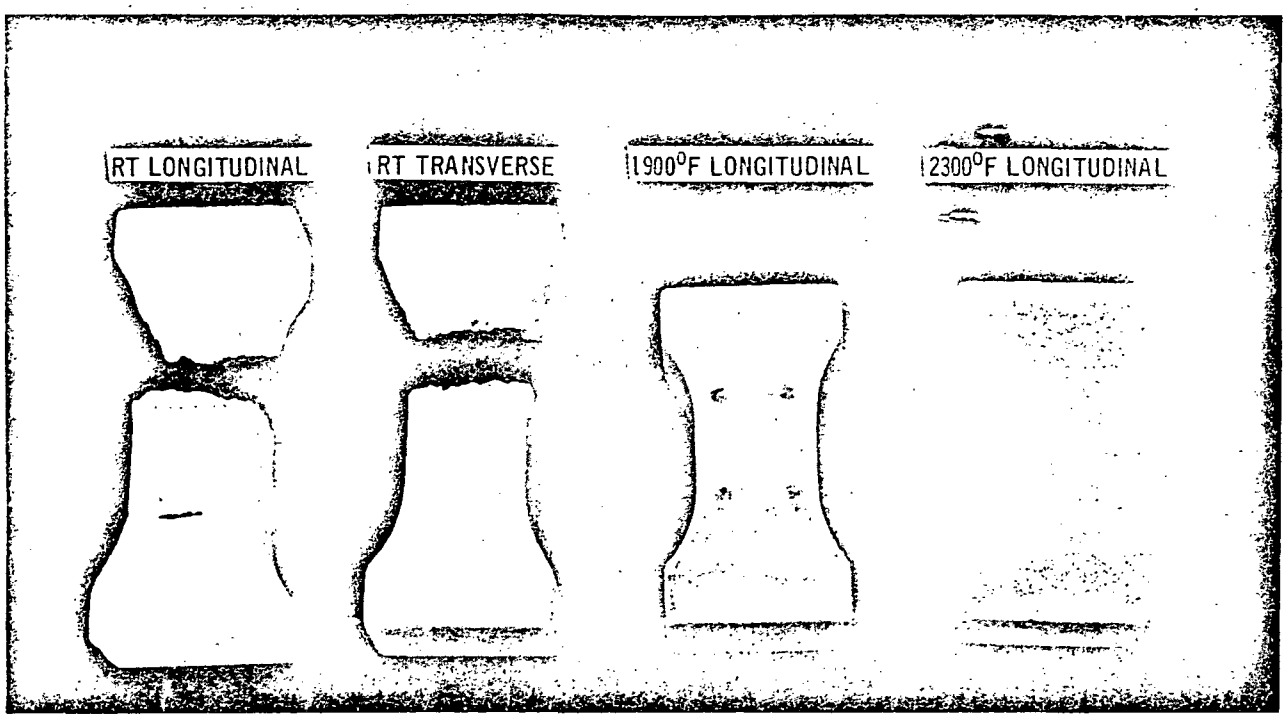

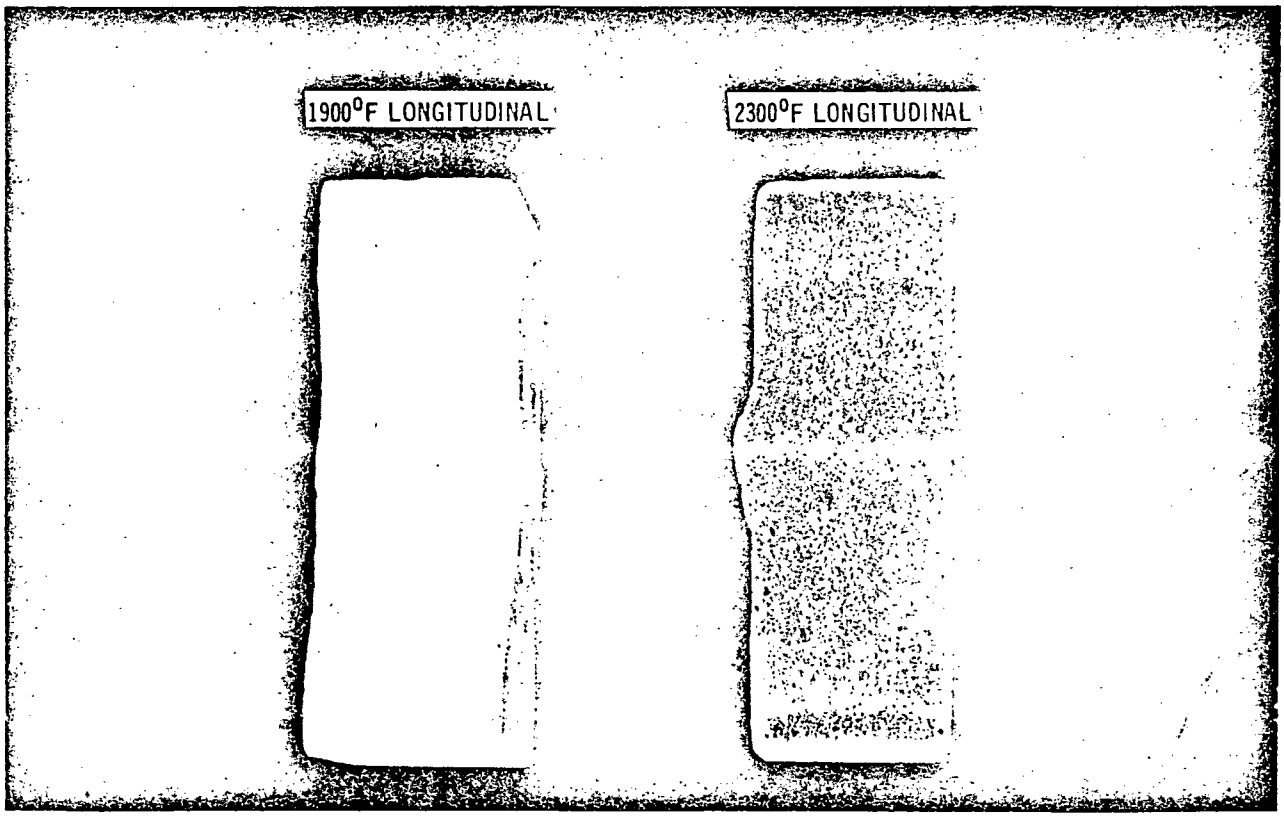

FIGURE 3-18

457-2532

TYPICAL FAILED COMPRESSION SPECIMENS

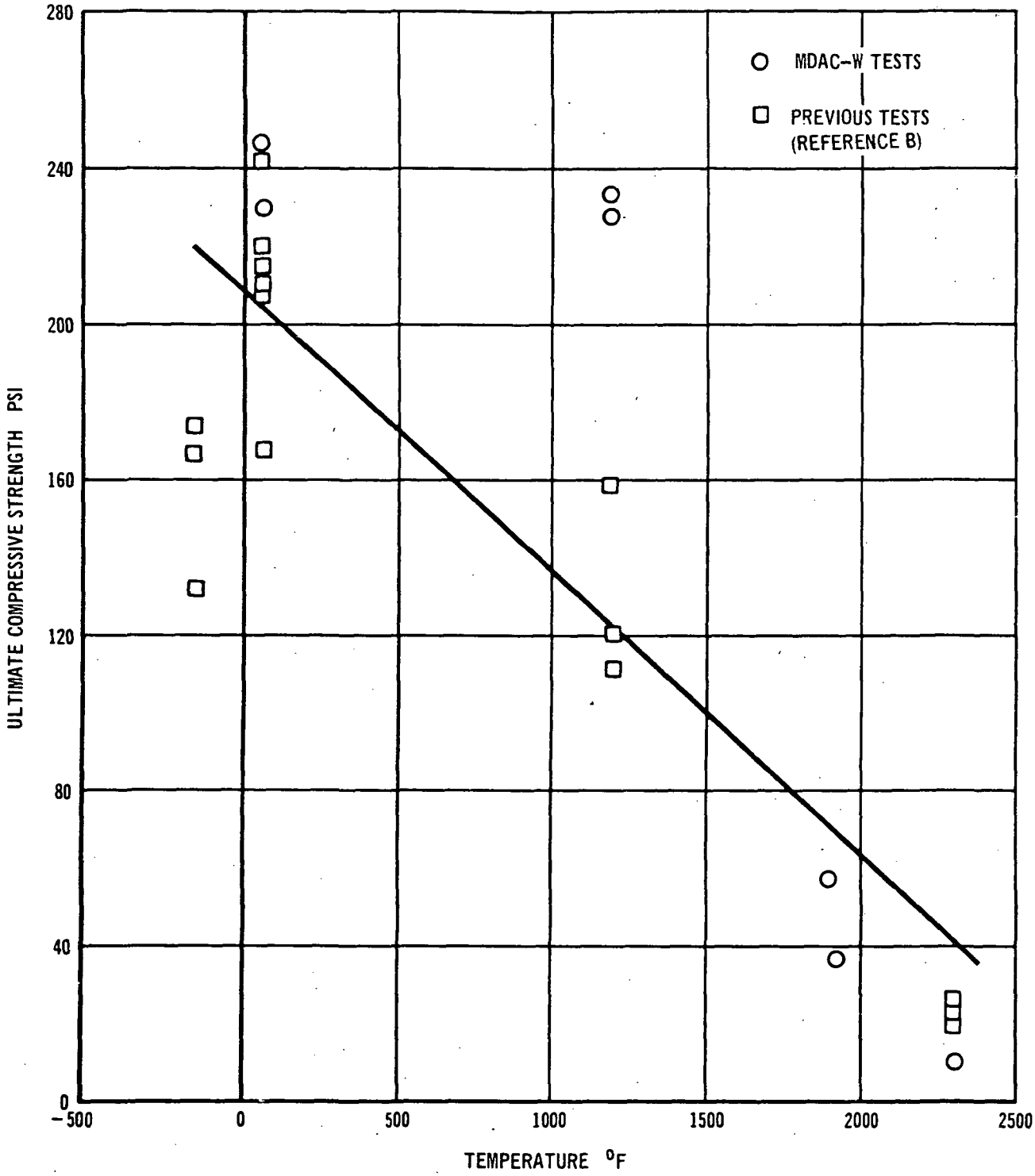

FIGURE 3-19
HCF LONGITUDINAL COMPRESSION STRENGTH
Mod III A

457-2550

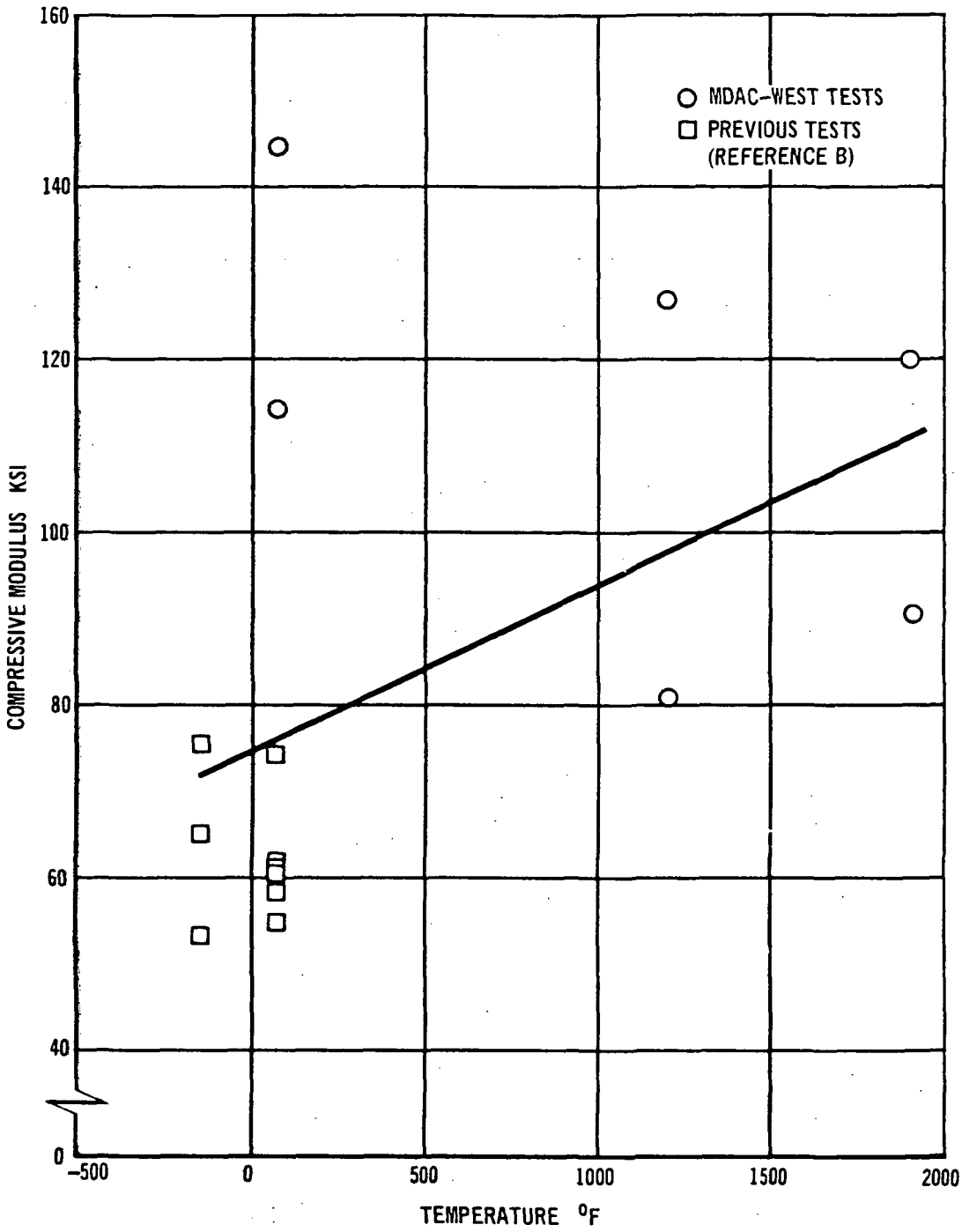

FIGURE 3-20
HCF LONGITUDINAL COMPRESSION MODULUS
Mod III A

457-2541

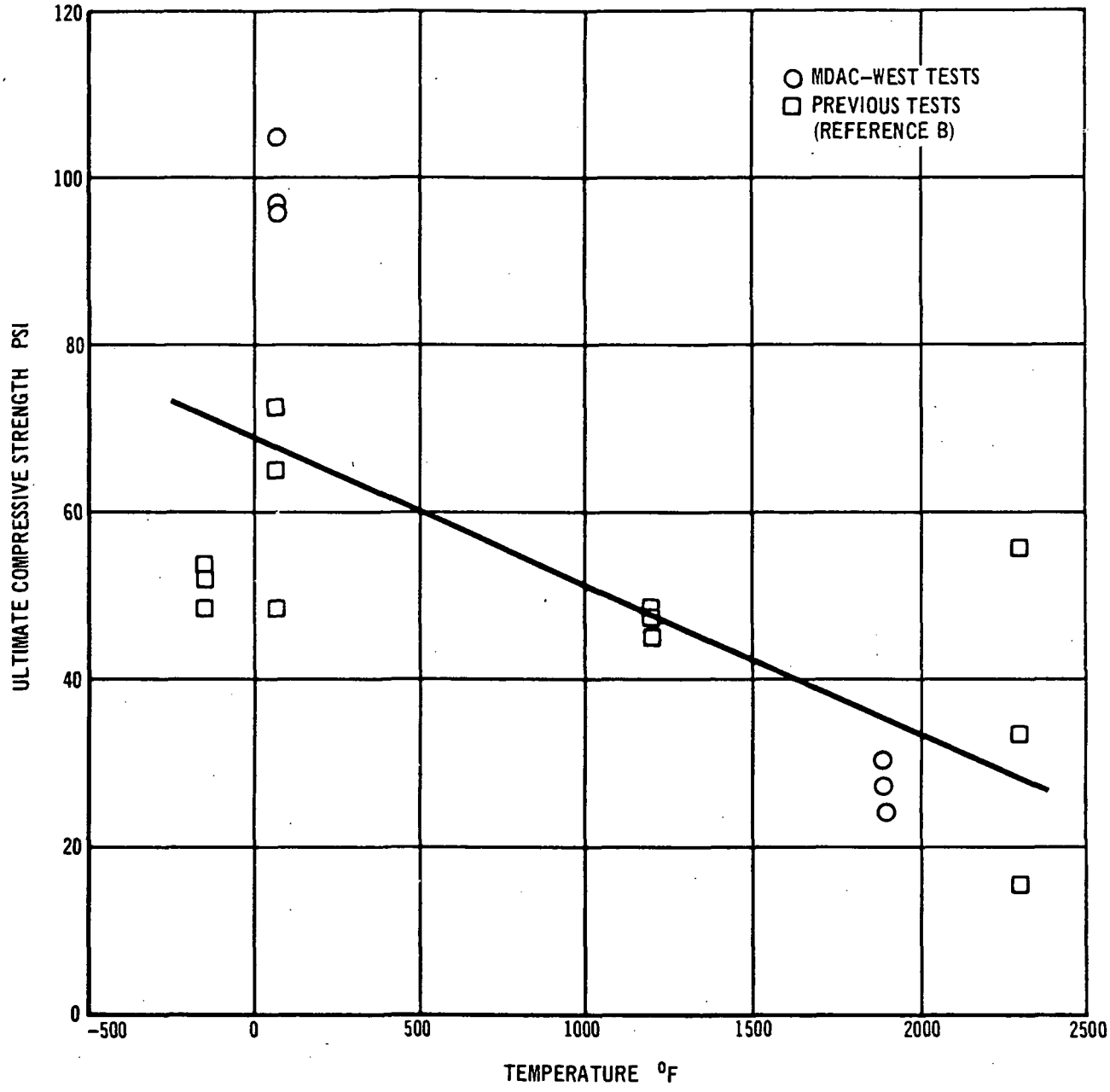

FIGURE 3-21

HCF TRANSVERSE COMPRESSIVE STRENGTH
Mod III A

457-2542

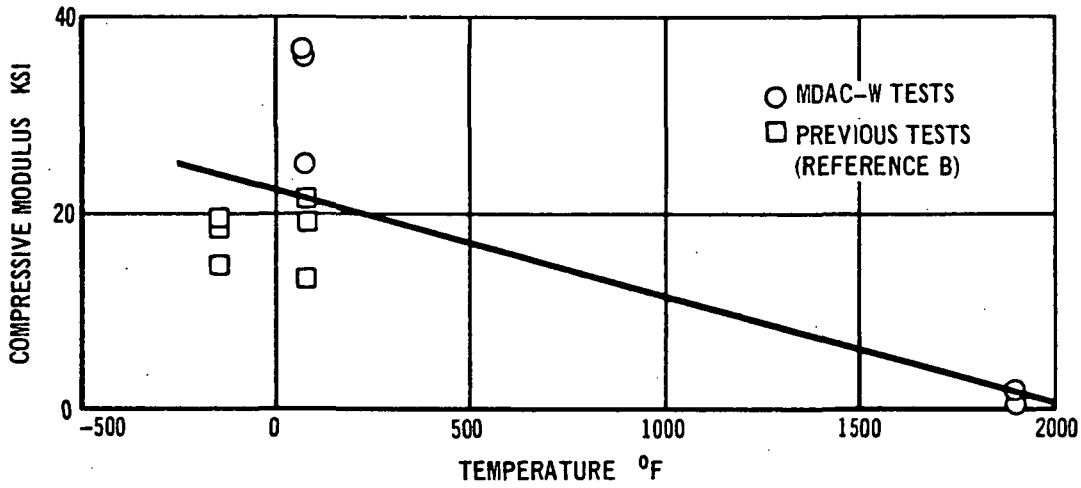

FIGURE 3-22

HCF TRANSVERSE COMPRESSIVE MODULUS

Mod III A

457-2552

MOD IIIA material from the Reference (b) program. Straight line least squares curve fits are also shown. The curve for the longitudinal compression modulus, shown in Figure 3-20, indicates that modulus increases with test temperature. This does not seem reasonable and is therefore questionable. Other curves show both strength and modulus decreasing with temperature. The large scatter in test results is characteristic of brittle ceramics.

Strength Gradient Improvements - As discussed in Section 2.2, density gradients were reduced and overall uniformity less improved; however, some HCF specimens which were uniformly dense were still weak in the center of the felt. Therefore, causes were identified and problem areas were isolated and the strength uniformity was improved.

The problem was approached by attempting to obtain a more uniform felt composition. Two components of the HCF were suspected of not being uniformly distributed: the binder and the hollow silica spheres. The binder was suspected because the surfaces were stronger than the center; this condition is characteristic of the migration mechanism which occurs during the drying of this type of binder. When liquid migrates to the surface to evaporate, it carries with it some of the binder solids phase which is then deposited near the surface. The hollow spheres in HCF were considered to be a cause of nonuniformity because they could be seen floating during the felting process when the felting time became excessive. Also, micrographic examination revealed that the concentration of the spheres was higher near the top surface in some cases.

Rapid Strength Screening Test - Several techniques were investigated for quickly measuring the strength uality of HCF material. (See Figure 3-23.) Such subjective techniques as simply observing, squeezing, and rubbing the material may be satisfactory for determining variations across the surface area of a tile, but they are not adequate in quantitizing differences from tile to tile. The most

promising method evaluated for providing a rapid, quantitative indication of strength was a free falling sphere impact indentation test.

The impact indentation test (Figure 3-24) utilizes a dial micrometer with an 85-gram load and a 0.25-inch ball tip (per ASTM D395, method B) to measure the specimen thickness before and after a glass sphere impacts the surface of the HCF. A glass sphere with a weight of 5.05 grams and a diameter of 0.616 inch is dropped through a tube from a height of 25.4 inches onto the HCF specimen. The measurement of the depth of the impact depression (in mils) is reported as the impact indentation number. A range of acceptable impact indentation numbers was established. based on observation and strength data:

Impact Indentation (Mils)	Remarks
20-30	Very Strong
30-40	Strong
40-50	Fair
50-60	Barely acceptable
60 and above	Weak

METHOD	PROS	CONS
(1) VISUAL AND PHYSICAL OBSERVATION	FAST, SLIGHT VARIATIONS IN TILE SEEN	SUBJECT TO OBSERVER ERROR, NON-REPRODUCIBLE
(2) IMPACT INDENTATION TEST	RELIABLY CALIBRATED, REPRODUCIBLE, FAST	NOT DIRECT MEASURE OF STRENGTH, CHECK ONLY SMALL AREA
(3) TENSILE/COMPRESSIVE STRENGTH TESTS	ACCURATE MEASURE OF STRENGTH, REPRODUCIBLE	SLOW, CHECKS ONLY SMALL AREA
(4) X-RAY	CAN DETECT GRAIN, DENSE INCLUSIONS, VOIDS, LARGE AREA VISIBLE	SLOW, NEED 2 VIEWS TO ACCURATELY LOCATE DEFECTS EDGE AFFECT DISTORTION. CANNOT PROVIDE ESTIMATE OF STRENGTH

FIGURE 3-23

HCF QUALITY MEASUREMENT METHODS

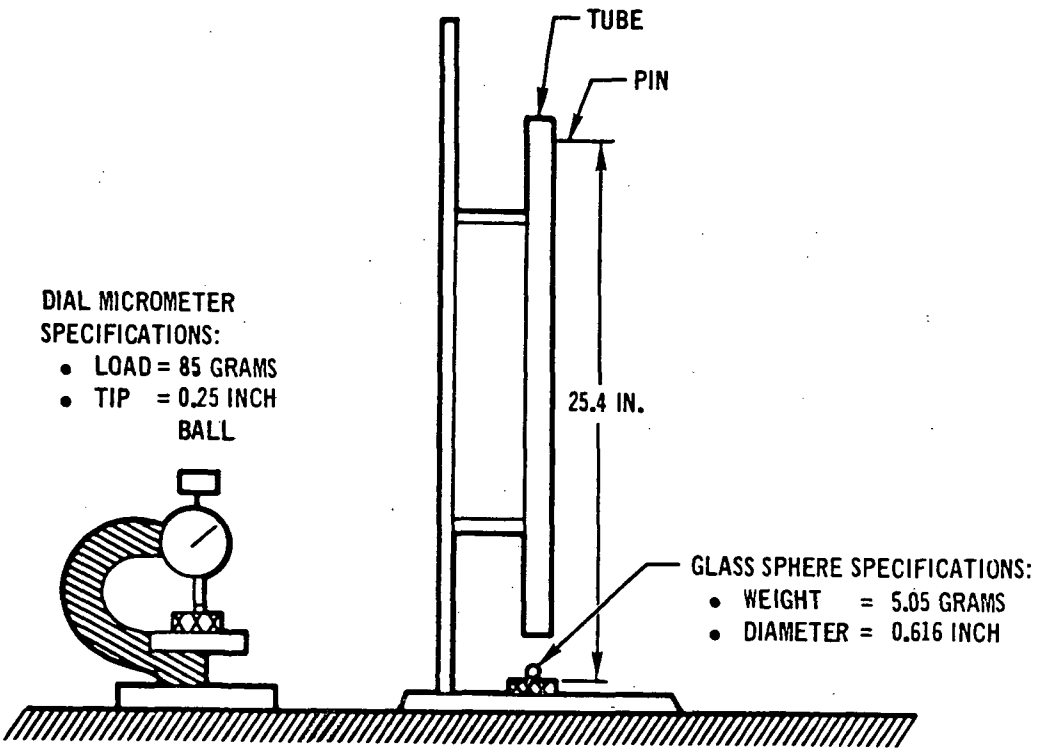

457-2437

FIGURE 3-24

HCF IMPACT HARDNESS TEST DEVICE

3.3 THERMAL PROPERTIES - The thermal properties improvement of candidate HCF formulations was measured by thermal shock tests using the oxyacetylene torch and by thermal performance tests using radiant graphite heaters.

Thermal Shock Testing - Mullite HCF specimens with four candidate binders were exposed to the calibrated oxyacetylene torch simulating the chock obtained from plasma jet testing performed at NASA centers where a large thermal gradient in the surface plane and rapid heat-up and cool-down were experienced. The specimens were held at 2300°F for 5 minutes during each cycle.

Specimens made with RSB-1 (silicate binder) survived 6 to 9 cycles before cracking, while RSB-2 (silica binder) specimens lasted 17 to 19 cycles before cracking. While RSB-3 (mullite binder) specimens lasted 30 cycles before testing was terminated, they had very low measured strength values. RSB-4 (alumina binder) specimens failed after 9 cycles.

Thermal Performance Testing - Candidate materials were tested and ranked according to performance, and an effective thermal conductivity was computed for comparison with guarded hot plate measurements which indicated an additional mode of heat transfer through RSI, probably direct short wavelength radiation. In this section, details of the thermal performance testing and a comparison of effective and guarded hot plate conductivities are discussed.

To determine if a candidate HCF formulation had improved performance, a comparative test method was established and used in which seven 3.3-inch diameter specimens were exposed to the same environment at one time. The heat source was a radiant graphite heater, which heats a coated columbium susceptor plate (21.5 by 21.5 inches) which in turn heats the seven HCF specimens. It was employed for these tests because of its heat flux uniformity at atmospheric as well as at reduced pressure. The test specimen consisted of a disk of HCF bonded to a honeycomb backup structure. Thermocouples were installed at intervals through the test specimen for

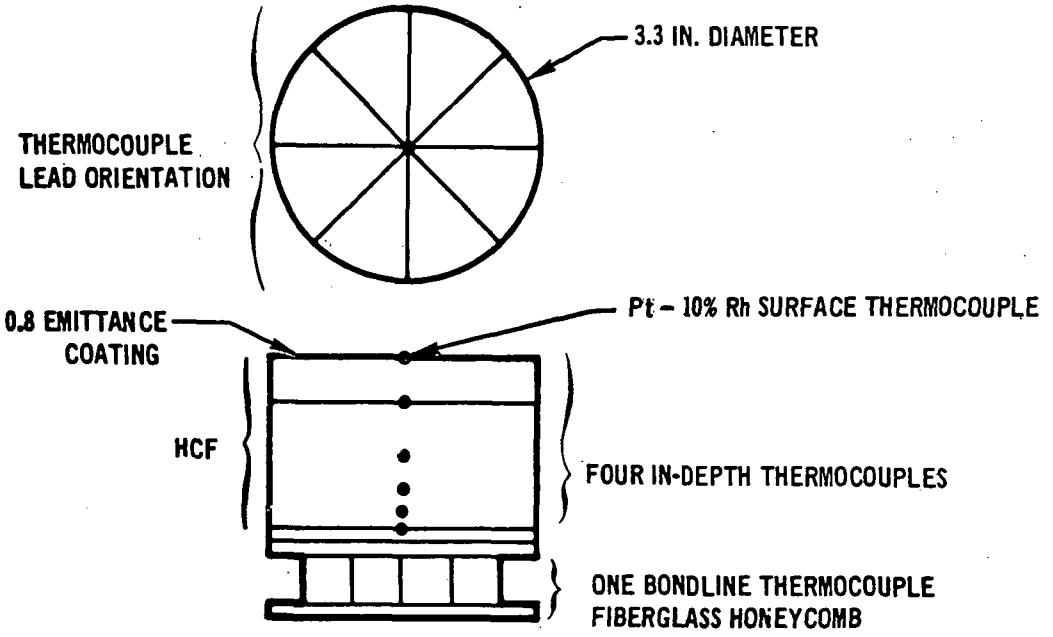

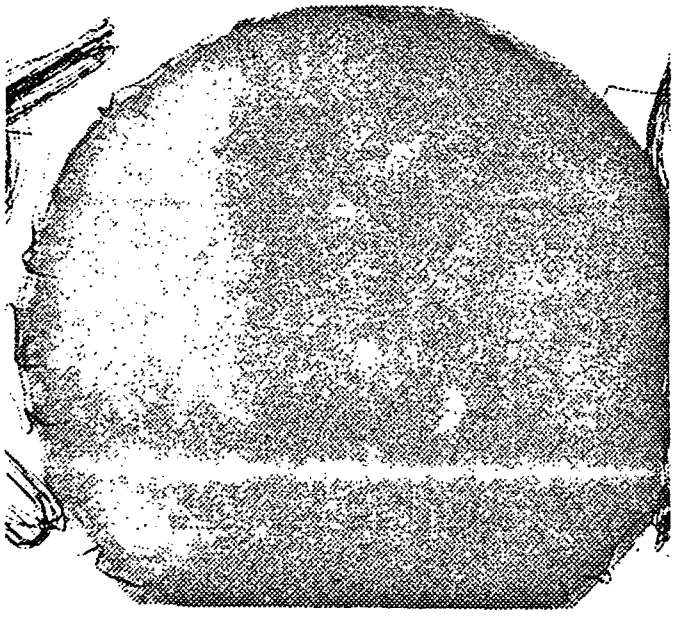

X-RAY PLAN VIEW

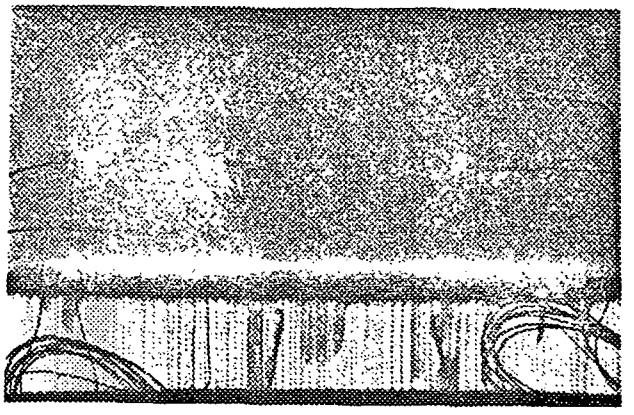

X-RAY SIDE VIEW

(SPECIMEN 101-2)

457-2440

FIGURE 3-25

COMPARATIVE THERMAL PERFORMANCE TEST SPECIMEN

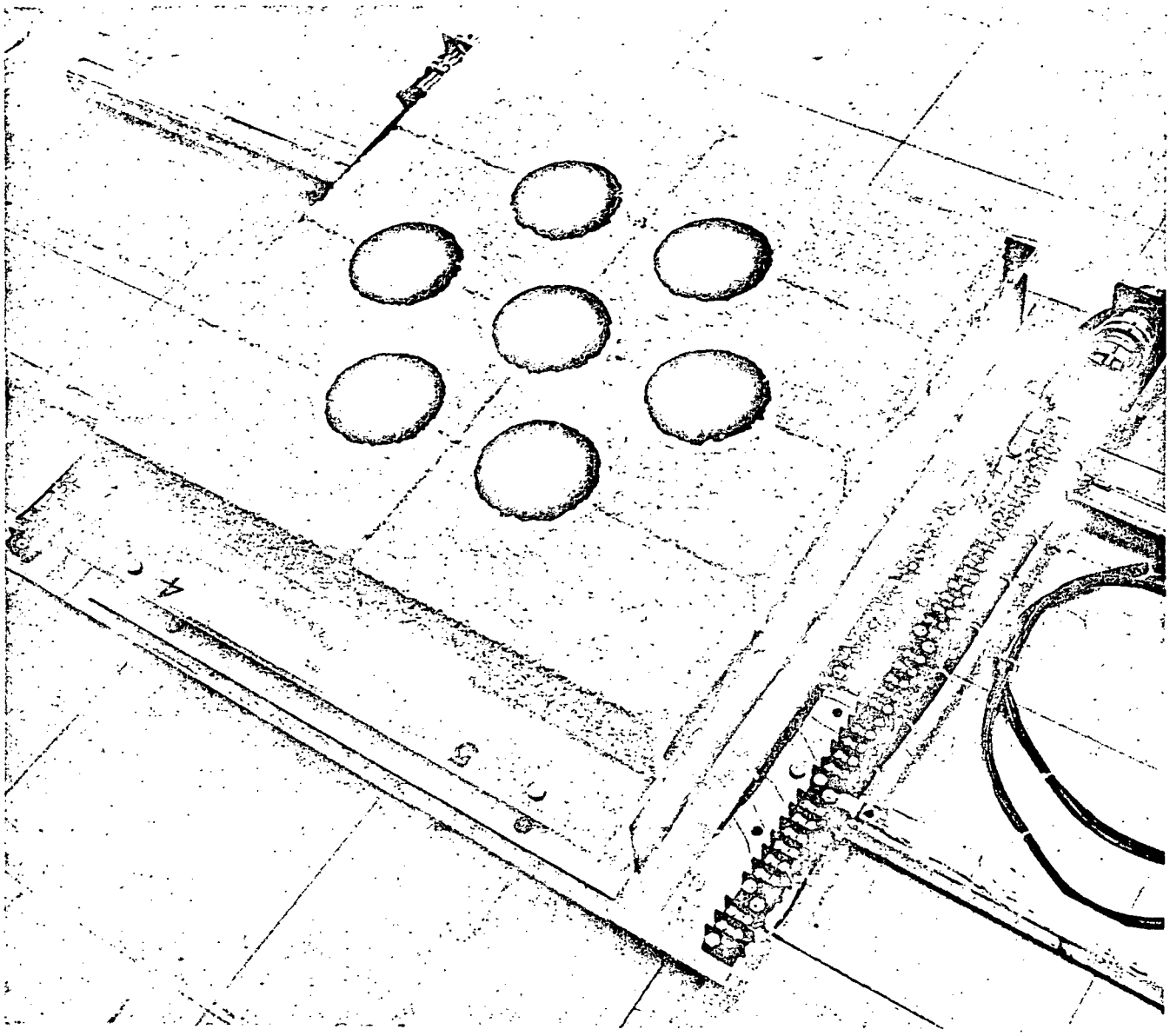

457-2441

FIGURE 3-26
THERMAL PERFORMANCE TEST SPECIMENS MOUNTED IN SPECIMEN HOLDER

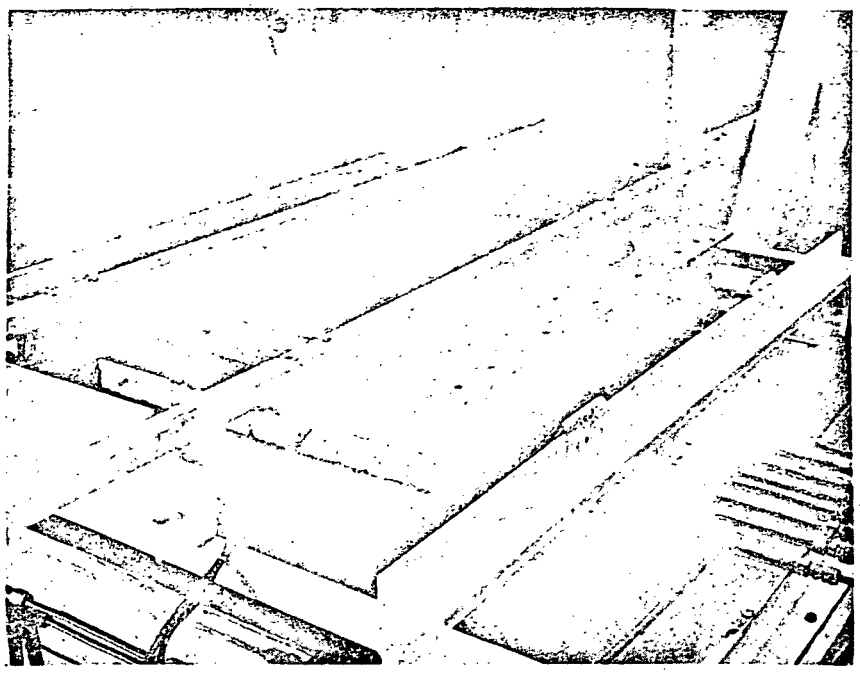

- RADIANT HEATER TESTS
- ATMOSPHERIC AND REDUCED PRESSURE
- TEST FIXTURE OVER HEATER
- DIRECT COMPARISON BETWEEN SEVEN SPECIMENS IN SAME TEST

FIGURE 3–27
OPACIFIED HCF – THERMAL PERFORMANCE TESTS

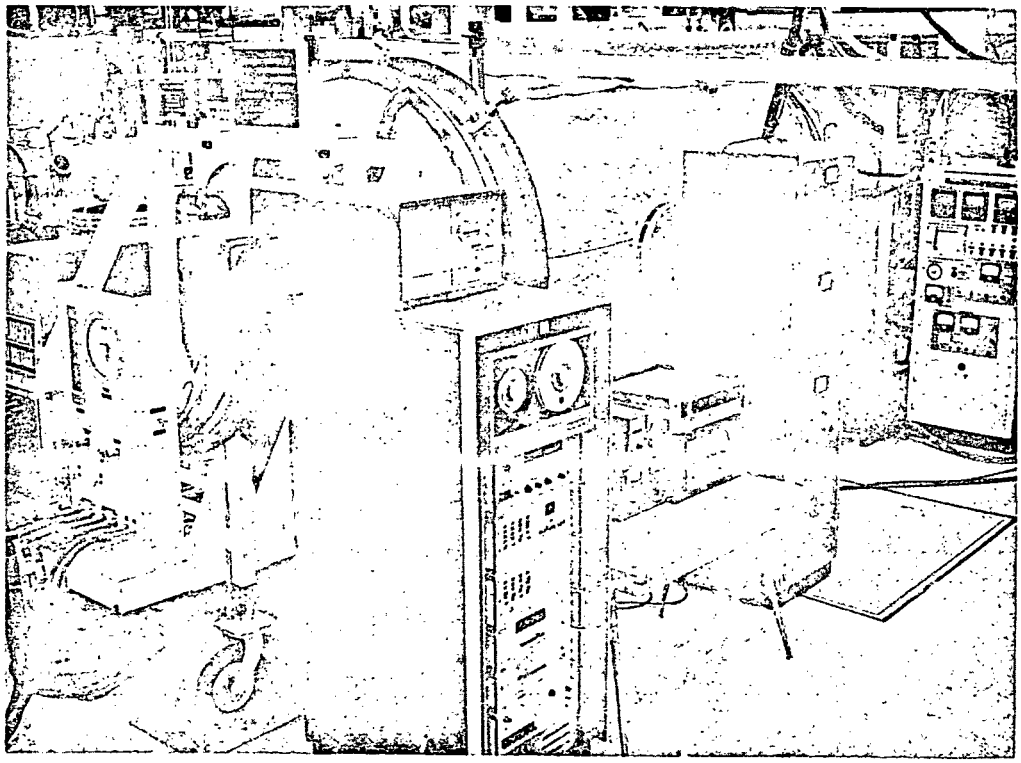

FIGURE 3–28
HCF TEST FIXTURES IN SPACE CHAMBER

recording thermal response. The test specimen configuration and an X-ray of a specimen are shown in Figure 3-25. Various degrees of instrumentation were used with the configuration shown in Figure 3-25. An opaque emittance coating was applied to each specimen to prevent direct radiation from the heater through the material and each specimen also had a surface thermocouple. The test specimens were installed in a test fixture (Figure 3-26) which shows the HCF guard insulation around the specimens. The test fixture was positioned over the radiant heater (Figure 3-27), which in turn operated in a vacuum chamber (Figure 3-28) for reduced pressure testing. The radiant heater was programmed to force the specimen surfaces to follow a specified temperature-time curve (at constant pressures of 10, 100, and 760 torr air pressure) representative of Shuttle entry.

Various formulations of HCF were evaluated simultaneously, generally using specimens with the same surface density. Due to tolerances during fabrication, the bulk density of the candidate materials did not come out exactly 15 lb/ft^3 so the specimens were cut to the same surface density for the tests. Four series of HCF formulations were extensively evaluated over a range of temperaturcs up to 2300°F and over a range of test pressures from 10 to 760 torr. Specimens with 4.7 and 6.0-μ diameter mullite fibers along with several opacifiers were investigated in the first series. In this test, shown in Figure 3-29, the major driver in the thermal performance at constant surface density appears to be density and not mullite fiber diameter or opacifiers. To investigate the influence of density, a second set of specimens was fabricated including different densities of the same formulation. Again, there is a strong indication that on the basis of constant surface density the lower the density of the HCF, the better the thermal performance, as shown in Figure 3-30. Because the lower density specimens are thicker, they provide more thermal blockage.

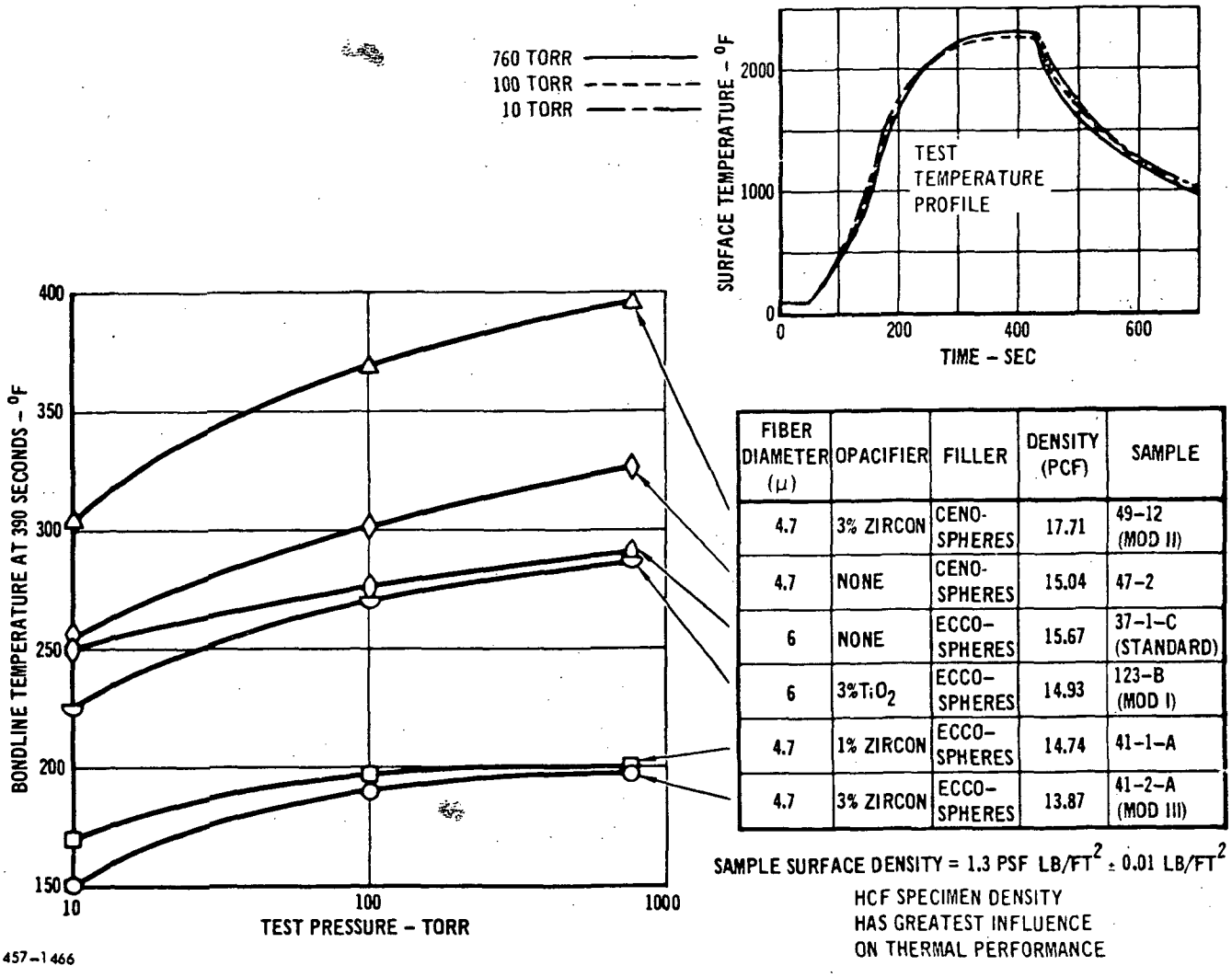

FIBER DIAMETER (μ)	OPACIFIER	FILLER	DENSITY (PCF)	SAMPLE
4.7	3% ZIRCON	CENO-SPHERES	17.71	49-12 (MOD II)
4.7	NONE	CENO-SPHERES	15.04	47-2
6	NONE	ECCO-SPHERES	15.67	37-1-C (STANDARD)
6	3% $Ti O_2$	ECCO-SPHERES	14.93	123-B (MOD I)
4.7	1% ZIRCON	ECCO-SPHERES	14.74	41-1-A
4.7	3% ZIRCON	ECCO-SPHERES	13.87	41-2-A (MOD III)

SAMPLE SURFACE DENSITY = 1.3 PSF LB/FT^2 ± 0.01 LB/FT^2

HCF SPECIMEN DENSITY
HAS GREATEST INFLUENCE
ON THERMAL PERFORMANCE

FIGURE 3-29

DECREASED HCF DENSITY IMPROVES THERMAL PERFORMANCE FOR CONSTANT SURFACE DENSITY USING VARYING FORMULATIONS

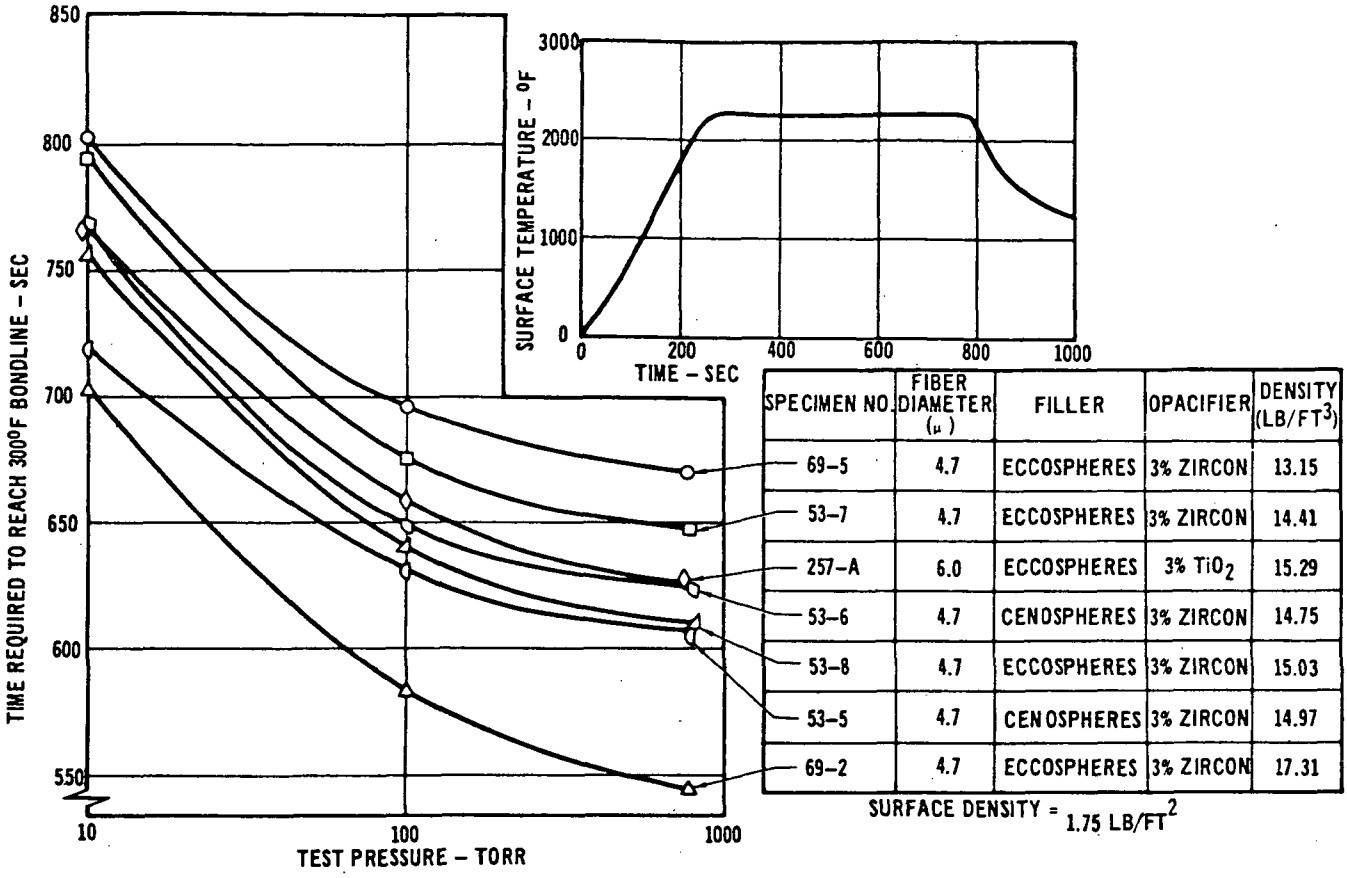

SPECIMEN NO.	FIBER DIAMETER (μ)	FILLER	OPACIFIER	DENSITY (LB/FT^3)
69-5	4.7	ECCOSPHERES	3% ZIRCON	13.15
53-7	4.7	ECCOSPHERES	3% ZIRCON	14.41
257-A	6.0	ECCOSPHERES	3% TiO_2	15.29
53-6	4.7	CENOSPHERES	3% ZIRCON	14.75
53-8	4.7	ECCOSPHERES	3% ZIRCON	15.03
53-5	4.7	CENOSPHERES	3% ZIRCON	14.97
69-2	4.7	ECCOSPHERES	3% ZIRCON	17.31

SURFACE DENSITY = 1.75 LB/FT^2

457-2533

FIGURE 3-30

DECREASED HCF DENSITY IMPROVES THERMAL PERFORMANCE FOR CONSTANT SURFACE DENSITY USING VARYING FORMULATION

Figure 3-31 shows the results of testing a set of specimens of identical composition, but varying bulk density and surface density. To separate actual density effects from those resulting from increased or decreased HCF thickness, the specimens were cut to the same thickness; and surface density was, therefore, not constant among specimens. In general, the results indicate that (for constant HCF thickness) higher density specimens perform better. The trend, however, is not conclusive; it has a large amount of scatter.

Effective thermal conductivities for MOD IIIA were calculated using the measured temperature histories of the heated surface and of the bondline

as the boundary conditions for a thermal model. The thermal conductivity curve (a function of temperature) was adjusted to produce computed temperature histories for all the thermocouples throughout the specimen that best correlated with the measured response by producing the smallest least-squares error. This procedure was employed for the three test pressures and the resulting effective conductivity is compared with the guarded hot plate data in Figure 3-32. Similar results were obtained for arc tunnel and radiant heater tests using the Thermal Property Analyzer Computer Method. For these tests it can be concluded that an additional mechanism of heat transfer exists within RSI other than conduction measured by the guarded hot plate device.

A fourth test was conducted using mullite specimens with the addition of fine fibers, opacifiers and with the deletion of the normal silica spheres. (See Figure 3-33.) The addition of fine silica fibers appeared to improve the thermal performance of mullite HCF as indicated by specimen B103-1 (MOD V type), compared with the baseline MOD IIIA specimens.

These test results agree with the Reference (a) work, which showed that the radiant heat transfer in 6-μ diameter mullite fibers is considerably higher than 2.5-μ diameter fibers of the same chemical composition. The Reference (a) work found this same relationship using silica fibers of two different diameters.

- MOD III HCF: 4.7-μ MULLITE FIBERS, ZIRCON OPACIFIER
  ECCOSPHERE FILLER, THICKNESS = 1.5 INCHES
  PRODUCTION-MAGNITUDE DENSITY GRADIENTS

SPECIMEN NO.	SYMBOL	DENSITY LB/FT^3	LOCATION OF DENSER SURFACE
2	◇	15.65	HEATED SURFACE
9	◁	16.70	BONDLINE
6C	△	13.90	BONDLINE
3	□	14.99	BONDLINE
1	◇	14.00	BONDLINE
7	○	13.30	BONDLINE
4	◁	12.84	HEATED SURFACE

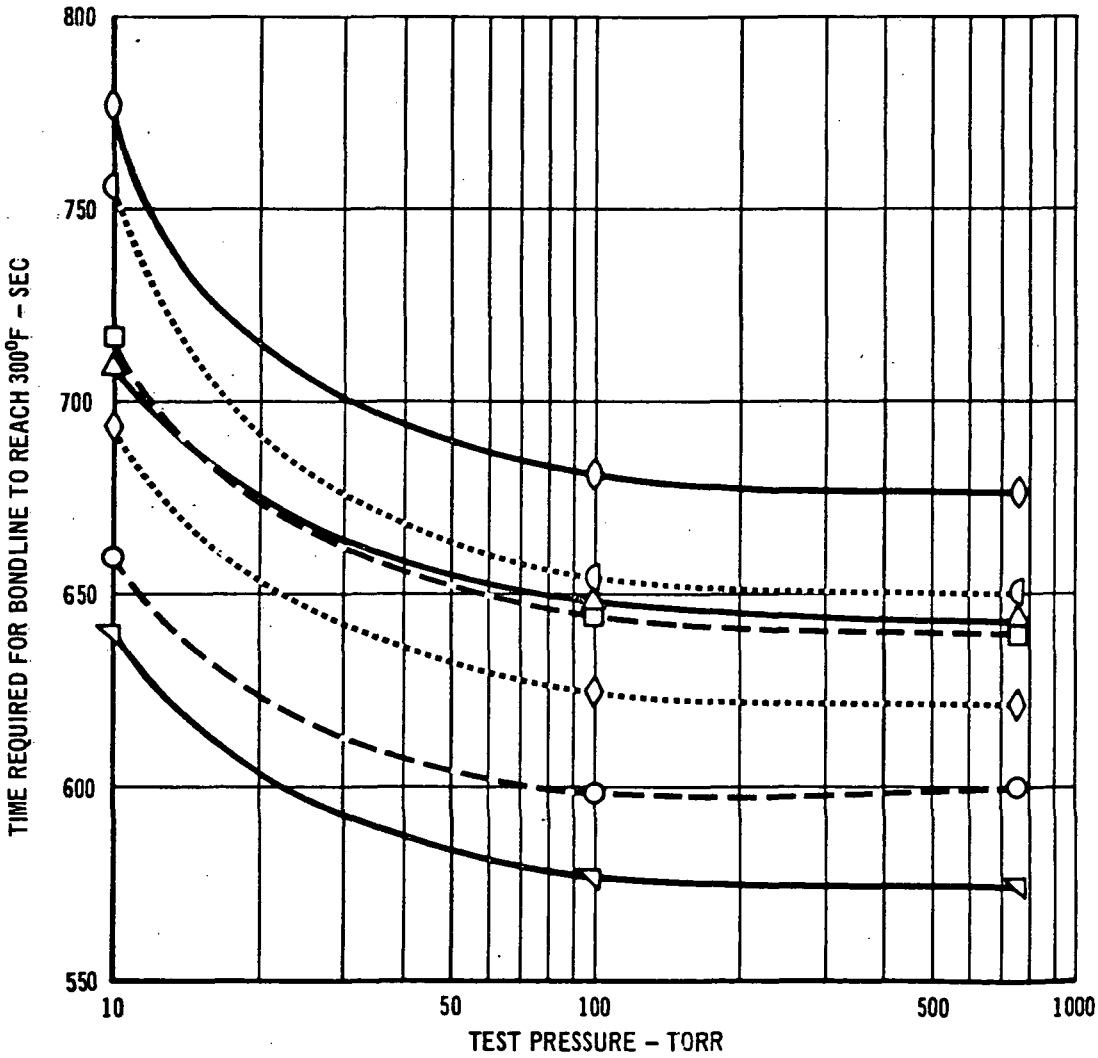

FIGURE 3-31

EFFECT OF DENSITY ON HCF THERMAL PERFORMANCE
USING CONSTANT FORMULATION

457-2538

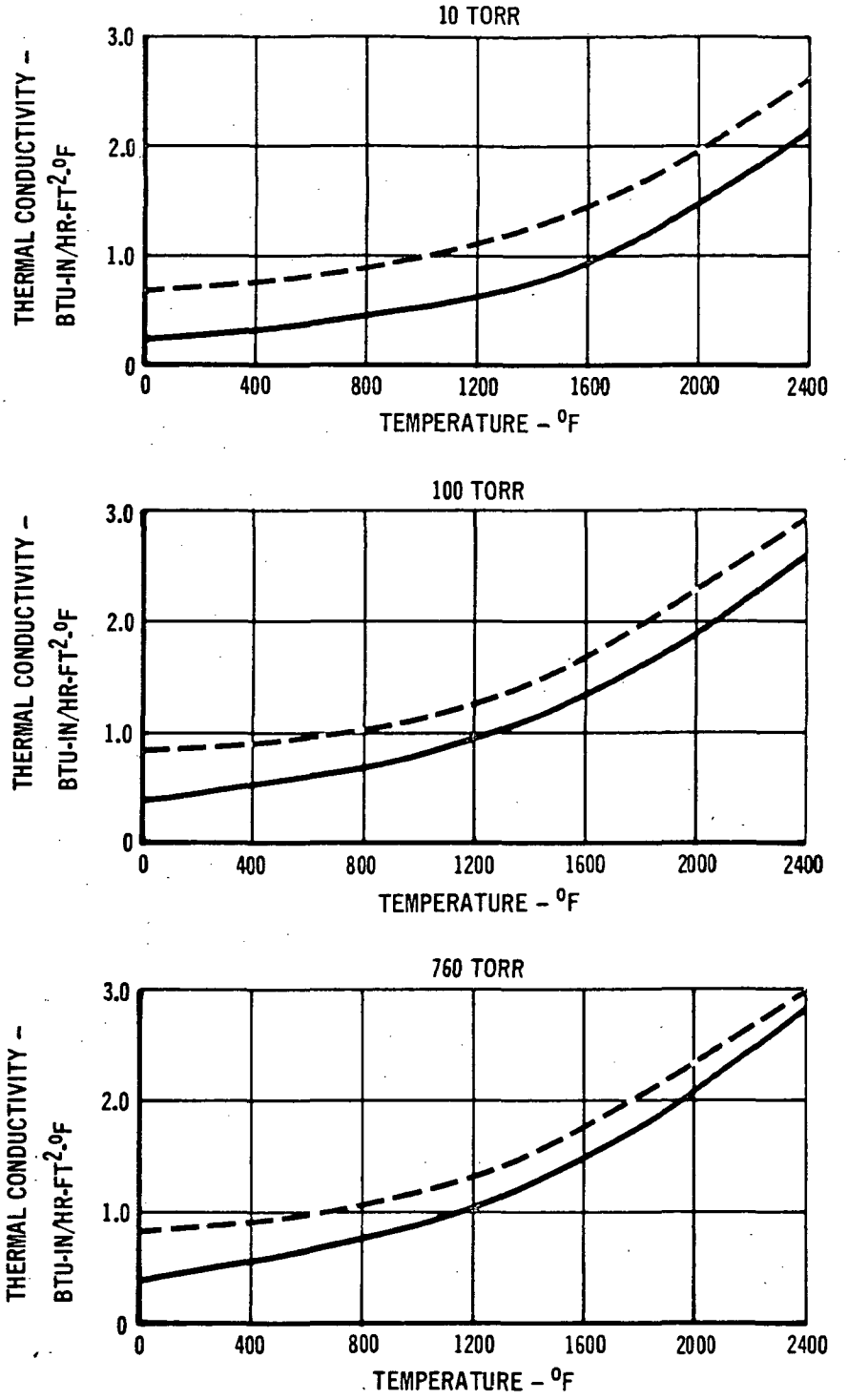

457-2161

FIGURE 3-32
EFFECT OF PRESSURE ON THERMAL CONDUCTIVITY

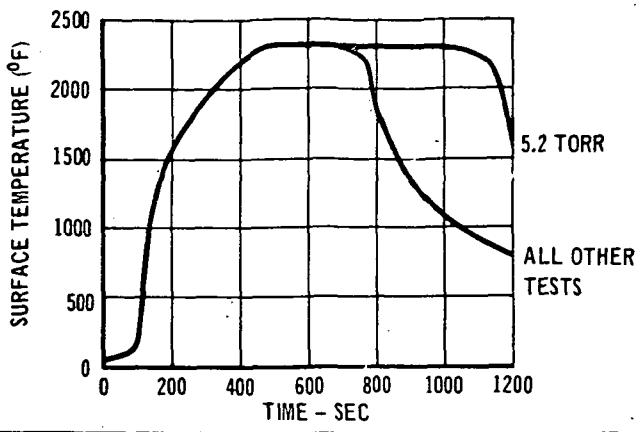

SPEC. NO.		COMPOSITION	LB/FT^3	h (IN)
C37–1	◇	100% SILICA FIBERS – ZIRCON OPACIFIER – NO ECCOSPHERES	16.28	1.300
B103–1	△	80% 4.7–μ MULLITE – 20% SILICA FIBERS – ZIRCON OPACIFIER – NO ECCOSPHERES	15.59	1.398
B101–2	○	100% 4.7–μ MULLITE – ZIRCON OPACIFIER – NO ECCOSPHERES	15.19	1.399
C37–3	◁	80% 4.7–μ MULLITE – 20% SKX (1.6 μ $Al_2O_3 \cdot SiO_2$) – ZIRCON OPACIFIER – NO ECCOSPHERES	17.2	1.302
MOD III A	◇	100% 4.7–μ MULLITE – ZIRCON OPACIFIER – WITH ECCOSPHERES	14.48	1.502
C31–1	□	100% 4.7–μ MULLITE – Ni FLAKE OPACIFIER – WITH ECCOSPHERES	16.87	1.301
C39–3	◁	80% 4.7–μ MULLITE – 20% SILICA FIBERS – ZIRCON OPACIFIER – WITH ECCOSPHERES	16.3	1.365

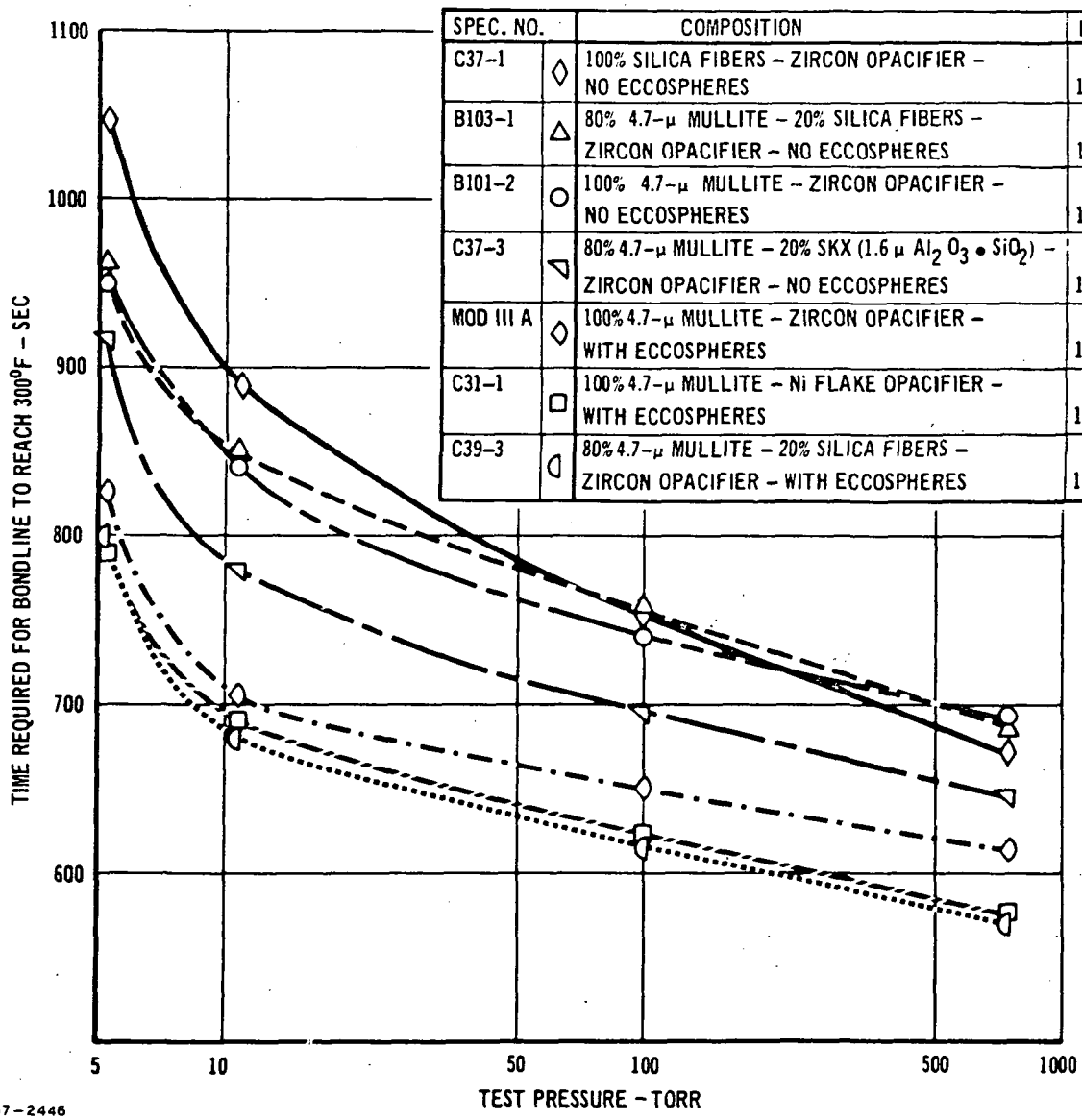

FIGURE 3–33

COMPARATIVE THERMAL PERFORMANCE OF SEVERAL HCF – RSI FORMULATIONS

(Data From Graphite Heater Tests of 3.3 Inch Diameter Cylindrical Specimens)

4.0 COATING DEVELOPMENT

Prior to this program, a liquid waterproof high emittance inorganic coating system, designated M25A7, was developed for the mullite HCF. This was a multi-layered, gradated density coating which was successfully scaled up and tested on 6 by 6 by 1.5-inch and 12 by 12 by 1.5-inch tiles.

In this and in the concurrent MSC program (Reference (b)), new concepts were investigated to improve the reusable liquid waterproof coating (glass sealed). The basic problem with a glassy coating is cracking due to: (1) high thermal stresses in the coating caused by thermal gradients during entry heating; and (2) residual stresses in the coating resulting from differential thermal expansion of the coating relative to the HCF.

Factors which aggravate this cracking tendency are:

a. increased tile thickness,

b. inorganic coating on five sides of a tile,

c. variations in insulation material strength,

d. nonuniform surface texture of the HCF material.

During this program and related programs, the following methods were used to evaluate the high temperature resistance of the HCF coatings:

a. screening of coatings applied to 2 by 2 by 1/2-inch HCF coupons using an oxyacetylene torch,

b. application of the coatings to full-size tiles for testing in the graphite heater or quartz lamps,

c. thermal expansion measurements,

d. low pressure tests in the graphite heater.

The major tasks to reduce cracking of the coating which were performed in each respective program were:

NASA-MSC

1. M25A7 Coating Improvements,
2. liquid waterproof coating development,

NASA-MSFC

1. reinforcement techniques in base coating,
2. grooves in coating,
3. nonglassy seal coatings,

MDAC-IN-HOUSE-EFFORT

1. one-step glassy coatings,
2. coating properties measurements.

4.1 COATING IMPROVEMENTS - A summary of early coating development work performed on 2 by 2 by 1/2-inch HCF coupons is given in Figure 4-1. The main index of improvement was thermal shock resistance determined by using the oxyacetylene torch to rapidly heat the surface. A maximum test temperature of 2300°F was maintained over a 5-minute period to complete the test cycle. The M25A7 coated Phase I Mullite HCF was used as a standard for gaging improvement.

During this phase of the work, the coating weight was reduced by eliminating the "intermediate coating" in the M25A7 coating system. Improved coating texture resulted from a smoother base coating. The thermal expansion of the base coating was measured and was found to closely match that of the mullite HCF; and changing the expansion coefficient of the base coating did not improve the thermal cycling resistance of the coating. Reducing the base coating modulus did not improve the thermal shock resistance because more glass sealer was required to obtain a waterproof coating.

The current trend of the development work has been toward the one-step coatings which offer potential weight and cost improvements over the multistep coatings (M25A7, MMpP7). The basic structure of the multistep coatings compared with the

ACTIVITY	PROS	CONS
• IMPROVE M25A7 COATING SYSTEM BY ELIMINATING INTERMEDIATE COATING.	• USE OF STRONGER, MOD-HIA HCF ELIMINATES INTERMEDIATE COATING. • NEW DESIGNATION M5A7. • LOWER WEIGHT (0.24, 0.16 LB FT^2). • IMPROVED THERMAL SHOCK RESISTANCE OVER THE M25A7 COATING.	• NONE
• BASE COATING IMPROVEMENT		
1. VARYING PERCENTAGE OF MULLITE FIBERS IN BASE COATING.	• NONE	• NO IMPROVEMENT IN THERMAL CYCLING RESISTANCE.
2. ADDING LOW EXPANSION MATERIALS	• NONE	• NO IMPROVEMENT IN THERMAL CYCLING RESISTANCE.
3. ADDING ORGANIC BURN-OUT MATERIALS TO REDUCE COATING MODULUS.	• NONE	• NO IMPROVEMENT IN THERMAL CYCLING RESISTANCE.
4. FILLING VOIDS IN BASE COATING TO REDUCE AMOUNT OF GLASS FOR WATERPROOFING.	• NONE	• NO IMPROVEMENT IN THERMAL CYCLING RESISTANCE OR REDUCTION OF SEALER REQUIRED FOR LIQUID WATERPROOFING.
5. CLOSE CONTROL OF BASE COATING THICKNESS AND SMOOTH BASE COAT.	• IMPROVED THERMAL SHOCK RESISTANCE.	• NONE
6. PREFIRING MULLITE FIBERS TO REDUCE PERMANENT EXPANSION OF BASE COATING.	• NONE	• NO IMPROVEMENT.
7. MODIFIED BASE COATINGS FOR IMPROVED STABILITY (NSM_p AND MP_A).	• LOW DIMENSIONAL CHANGE AFTER FIRING. • IMPROVED THERMAL SHOCK RESISTANCE. • IMPROVED THERMAL EXPANSION MATCH.	• NONE
• NEW BASE COATING		
1. SILICATE BONDED SILICON CARBIDE.	• EXPANSION MATCHES MULLITE HCF.	• NO IMPROVEMENT IN THERMAL CYCLING.
2. SILICATE BONDED CHROMIC OXIDE.	• NONE	• NO IMPROVEMENT IN THERMAL CYCLING.
3. ONE-STEP COATING ($MoSi_2$, SiC, B_4Si + GLASS.	• EXCELLENT THERMAL SHOCK RESISTANCE AND WATERPROOFING. • REQUIRES ONE OR TWO COATING APPLICATIONS COMPARED TO FOUR FOR THE M25A7.	• MUST BE FIRED RAPIDLY TO PREVENT OXIDATION OF PIGMENT.
4. SILICATE BONDED SILICA	• NONE	• NO IMPROVEMENT IN THERMAL CYCLING.
• DIFFUSION BARRIER DEVELOPMENT		
1. REDUCE PARTICLE SIZE OF DIFFUSION BARRIER PARTICLES.	• NONE	• NO IMPROVEMENT IN THERMAL CYCLING OR LIQUID WATERPROOFING.
2. MULTIPLE APPLICATIONS OF DIFFUSION BARRIER (CHROMIC OXIDE).	• IMPROVED THERMAL CYCLING RESISTANCE AND LIQUID WATERPROOFING.	• INCREASED COATING WEIGHT.
3. PLATINUM COATED ALUMINA PARTICLES IN LIEU OF CHROMIC OXIDE IN BARRIER COATING.	• IMPROVED THERMAL SHOCK RESISTANCE AND LIQUID WATERPROOFING.	• COST PROHIBITIVE.
4. $MoSi_2$ PIGMENT SUBSTITUTED FOR CHROMIC OXIDE IN THE BARRIER COATING.	• IMPROVED THERMAL SHOCK RESISTANCE AND LIQUID WATERPROOFING	• NONE
5. FLAME SPRAYED $MoSi_2$ AND Cr_2O_3.	• IMPROVED THERMAL SHOCK RESISTANCE AND WATERPROOFING.	• DEPOSITION OF COATING HARD TO CONTROL. • CRACKING ASSOCIATED WITH APPLICATION.
• NEW GLASS SEALER		
1. BOROSILICATE GLASS	• GOOD THERMAL SHOCK RESISTANCE. • REHEALS CRACKS • SMOOTH, WATERPROOFING COATING.	• EXPANSION COEFFICIENT TOO LOW COMPARED TO HCF. • TENDS TO BLISTER WHEN FIRED TOO RAPIDLY.
2. ALUMINOSILICATE GLASS	• GOOD THERMAL SHOCK RESISTANCE. • DOES NOT BLISTER. • SMOOTH, WATERPROOF COATING.	• EXPANSION COEFFICIENT TOO LOW COMPARED TO HCF. • HIGHER SOFTENING POINT THAN BOROSILICATE GLASS. • DOESN'T HEAL CRACKS AS WELL AS THE BOROSILICATE GLASSES.
3. NEW BOROSILICATE GLASS	• BETTER EXPANSION MATCH. • IMPROVED THERMAL SHOCK RESISTANCE AND WATERPROOFING.	• REQUIRES TWO APPLICATIONS TO FORM A WATERPROOF COATING.
• NONGLASSY SEAL COATINGS		
1. COAT M25 BASE COAT WITH PLATINUM RESINATES.	• NONE	• NONWATERPROOF • NOT COST EFFECTIVE.
2. VAPOR DEPOSITED PLATINUM ON THE M25 BASE COATING.	• NONE	• NONWATERPROOF • NOT COST EFFECTIVE
3. PLATINUM FOIL BONDED TO M25 BASE COATING.	• WATERPROOF	• FOIL DELAMINATED ON ENTRY CYCLING. • NOT COST EFFECTIVE.
• ORGANIC COATINGS (APPLIED TO BARE HCF OR IN PLACE OF GLASS SEALER ON THE BASE COATING).	• DOES NOT REQUIRE HIGH TEMPERATURE PROCESSING. • CAN BE EASILY APPLIED. • LIGHTER THAN INORGANIC COATINGS. • WATERPROOFING EASILY ACHIEVED.	• MUST BE REAPPLIED AFTER EACH ENTRY CYCLE. • DIFFICULT TO APPLY TO JOINT AREAS.
• PLATINUM WIRE REINFORCED M25A7 COATING	• SHOWS PROMISE FOR CRACK STOPPING IN THE COATING. • HOLD HCF TOGETHER IF CRACKS PROPAGATE INTO THE HCF.	• DIFFICULT TO FABRICATE. • INCREASE COATING WEIGHT (0.6 LB FT^2). • NOT COST EFFECTIVE. • NOT AERODYNAMICALLY SMOOTH SURFACE.
• GROOVES IN COATING	• SHOWS PROMISE FOR CRACK STOPPING. • IMPROVED THERMAL CYCLING RESISTANCE FOR SMALL SPECIMENS.	• NOT EASILY SEALED FOR LIQUID WATERPROOFING.

FIGURE 4–1

SUMMARY OF EARLY COATING DEVELOPMENTS

one-step system is illustrated in Figures 4-2 and 4-3. Rather than having three discrete layers, the one-step coating has a single layer of uniformly distributed pigment particles in a glass matrix. The pigment particle size is maintained at larger than 325 mesh to prevent excessive oxidation of the non-oxide pigments such as $MoSi_2$, B_4Si, SiC.

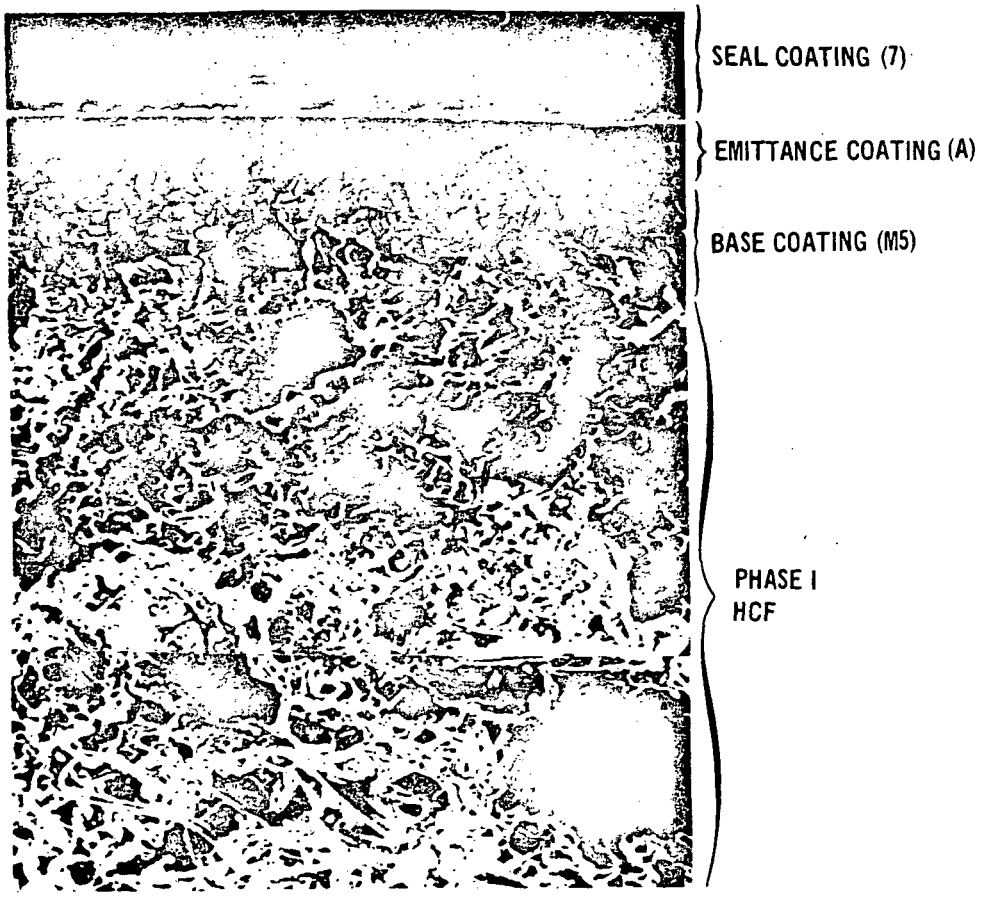

457-1340

FIGURE 4-2
M25A7 COATED PHASE I MULLITE HCF (120X)

4.2 SCALE-UP TO FULL-SIZE TILES - Coating improvements listed in Figure 4-1 were applied to 6 by 6 by 2-inch and 3-inch Mod III A HCF tiles for evaluation in the quartz lamp facility. The early work was conducted on 2-inch thick Mod III material and later work was on 3-inch thick Mod III A tiles. Figure 4-4 summarizes the early work on 6 by 6 by 2-inch Mod I and Mod III A tiles.

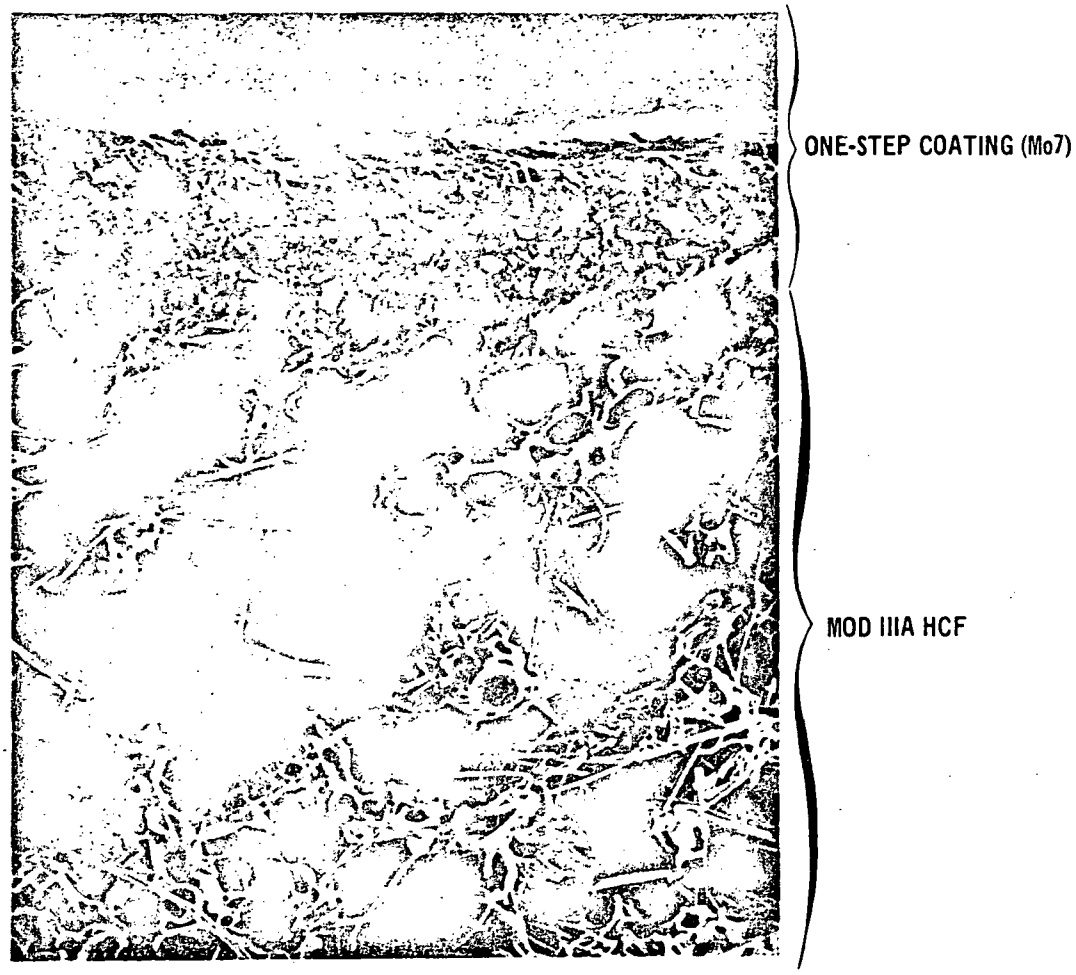

457-2442

FIGURE 4-3

Mo7 COATED MOD IIIA MULLITE HCF (100X)
TESTED 20 CYCLES AT 2500°F IN TORCH

The tiles, equipment and test setup are shown in the following figures. The three basic configurations of test tiles are shown in Figure 4-5. HCF tiles were usually 2 or 3-inch thick and were coated on 5 sides or on 1 surface only, as pictured. These tiles were bonded with RTV-560 silicone adhesive to titanium with a 1/4-inch thick silicone sponge layer for strain isolation. A "Data Trak" Controller (Figure 4-6) programmed the power input to the quartz lamps shown in Figures 4-7 and 4-8. The surface temperatures on the specimen and the bondline temperatures

COATING	COATING LB/FT^2	NO. OF CYCLES AT 2300°F	COMMENTS
$M5_{23}A7$ (top only)	0.190	30 (wp)*	Slight blistering on coating after 10 cycles, single small crack noted on one edge (uncoated) after 10 cycles.
$M5_{23}P7$ (top only)	0.200	30 (wp)	Few secondary bubbles in glass after 20 cycles. No cracks noted.
$M5_{23}A7$ (5 sides)	0.185	30 (wp-20 cyc SWP-25 cyc)	Slight blistering on coating after 5 cycles. No cracks noted.
$M5_{23}A7056$ (top only)	0.218	30 (wp)	No blistering, slight crack on one side (uncoated)
$M5_{23}A7056$ (5 sides)	0.200	30 (wp)	Slight crack on edge and top of tile. No blistering.
$M5_{23}A7$ (5 sides)	0.180	30 (wp)	Moderate blistering. No cracks.
MMpP7	0.145	30 (wp)	No blisters, no cracks.

*(wp) = waterproof

FIGURE 4-4
FULL SCALE COATING IMPROVEMENT TEST RESULTS

Note: All HCF tiles were bonded to titanium (.03-inch) plate with RTV-560 silicone adhesive and a 1/4-inch thick strain isolation silicone sponge insert.

were plotted as a function of time on the recorder (Figure 4-9). The same time/temperature entry profile (Section 5.2) used in the low pressure tests which describes the predicted surface temperature history on one area of the Shuttle Orbiter was used. Figures 4-10, 4-11, and 4-12 show the HCF tile in place in the quartz lamp test fixture before, during and after testing, respectively. Glass sealed 6 by 6-inch HCF tiles have been cycled up to 100 times using this facility. The standard $M5_{23}A7$ coating which uses a phosphate bonded chromium oxide (A) emittance coating tends to blister to various degrees as a result of heating

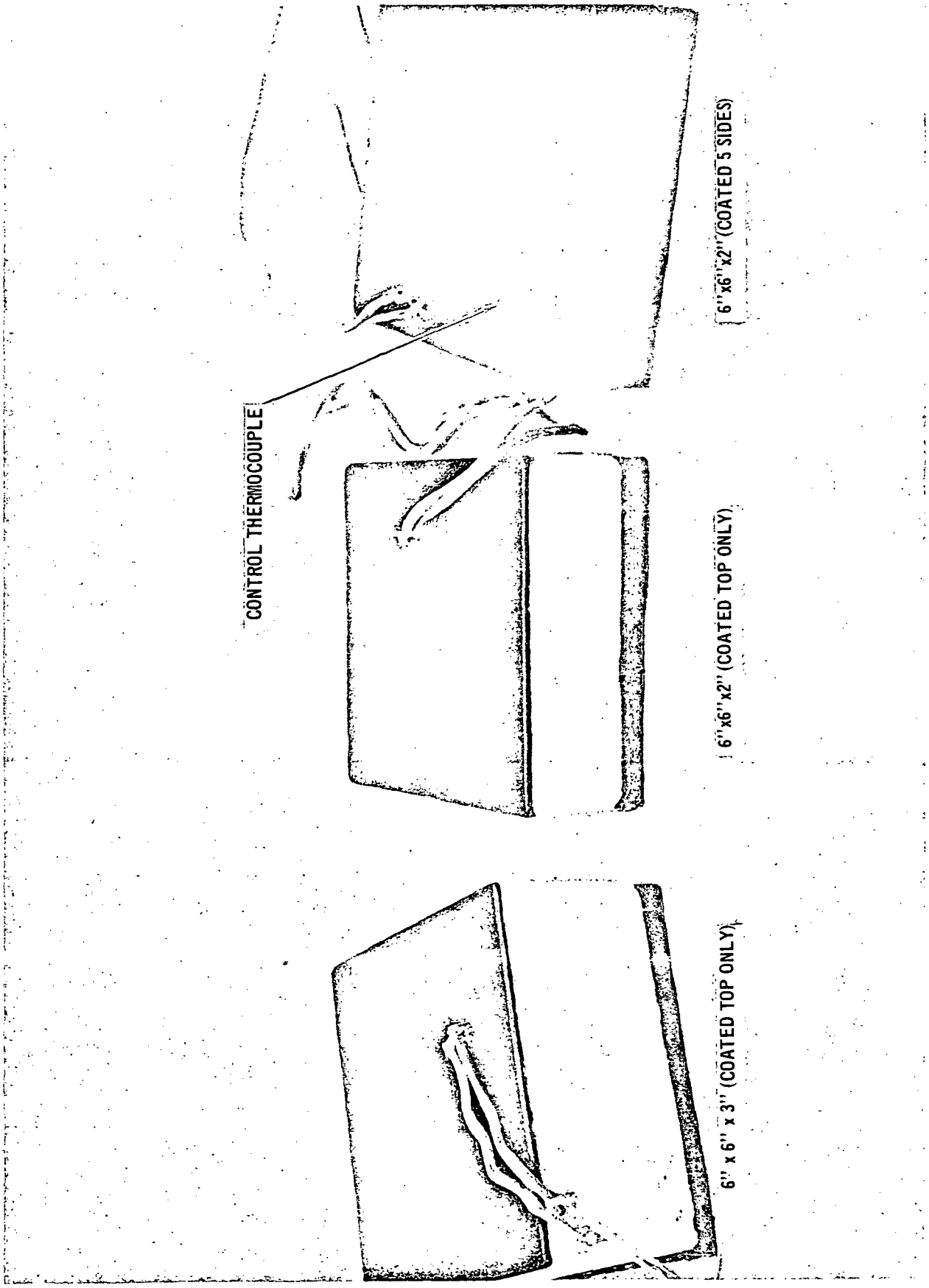

FIGURE 4-5
COATED MULLITE HCF QUARTZ LAMP TEST SPECIMENS

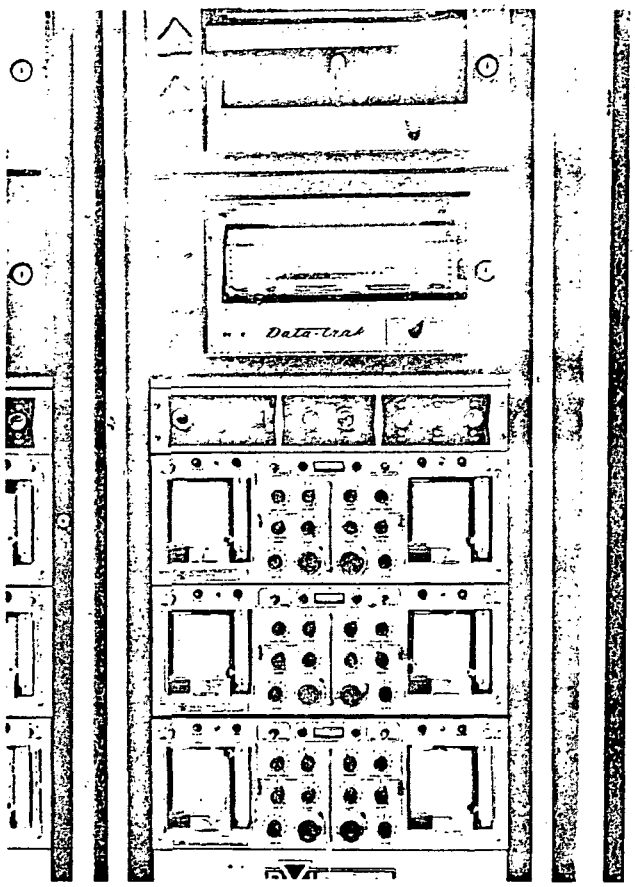

FIGURE 4-6

QUARTZ LAMP CONTROLLER BANK

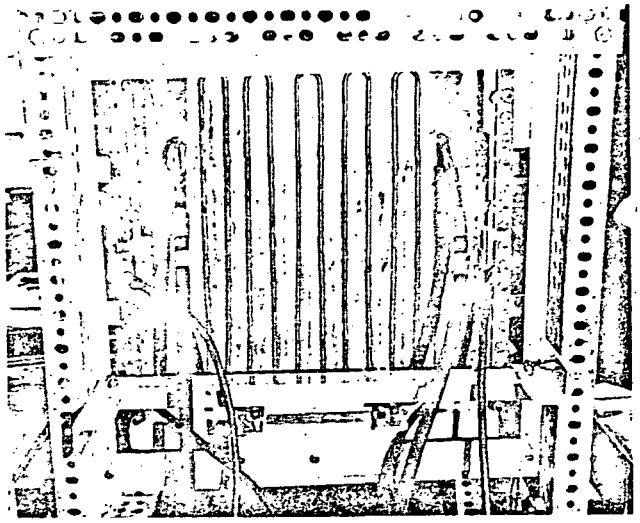

FIGURE 4-8

REAR VIEW OF QUARTZ LAMP BANK SHOWING WATER-COOLED REFLECTOR

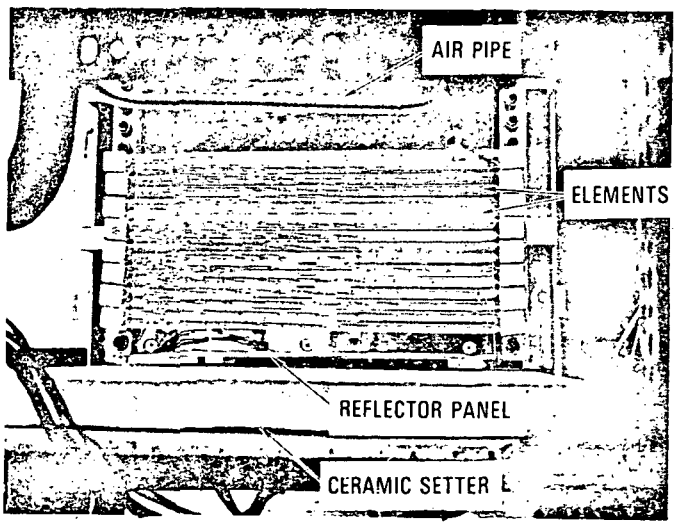

FIGURE 4-7

FRONT VIEW OF QUARTZ LAMP BANK SHOWING ELEMENTS

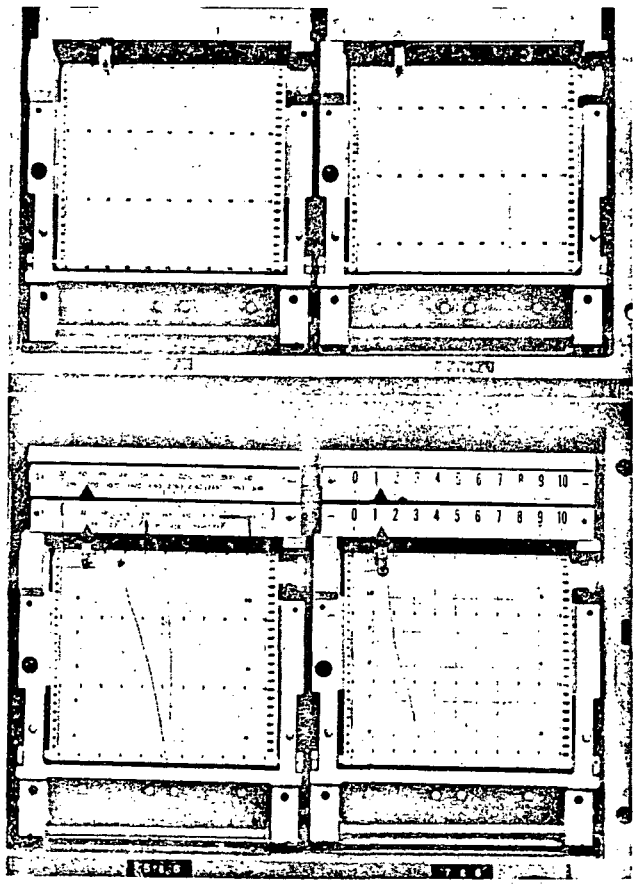

FIGURE 4-9

QUARTZ LAMP RECORDER BANK

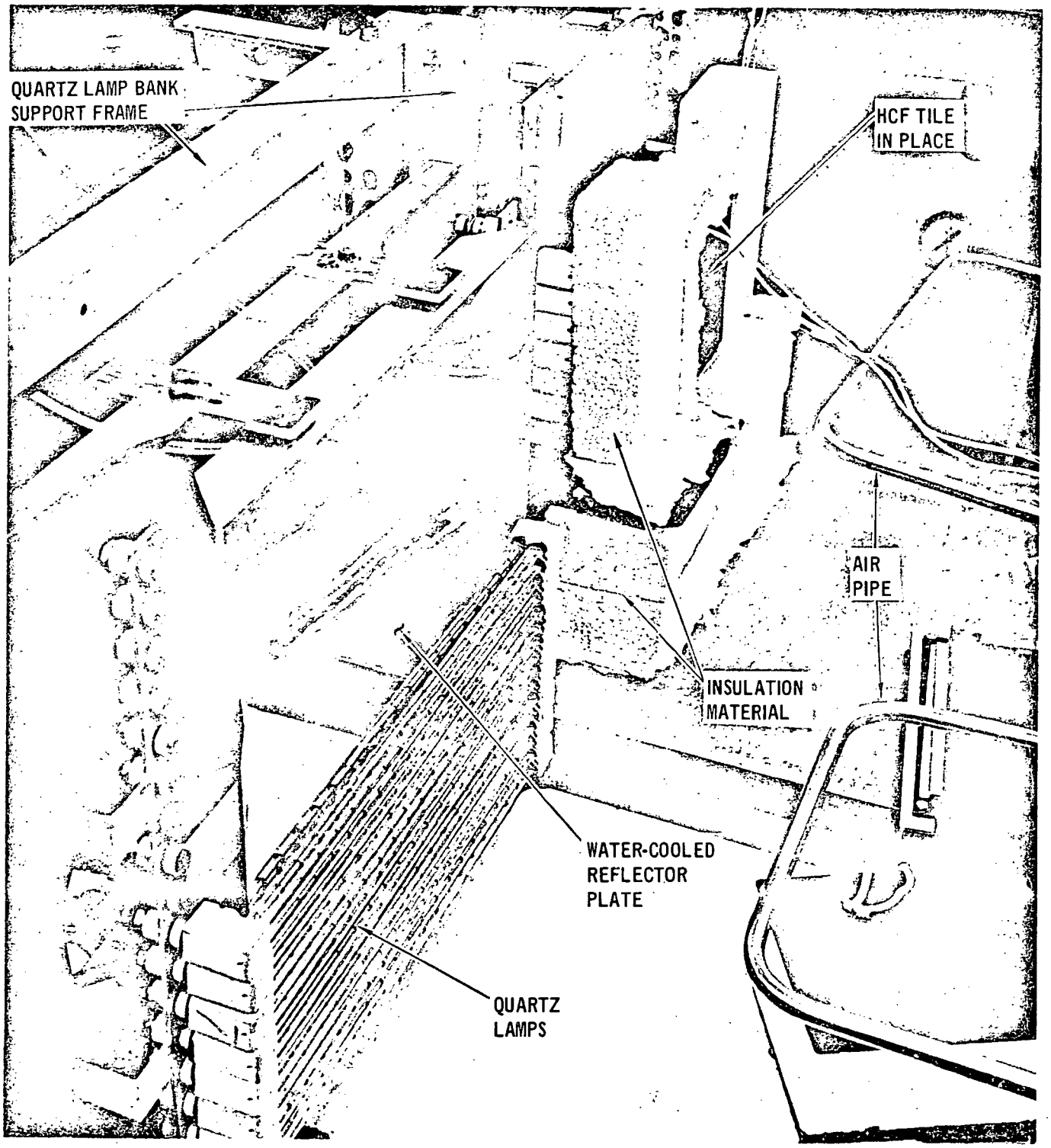

FIGURE 4–10

HCF SPECIMEN "IN PLACE" IN FRONT OF QUARTZ LAMP BANKS

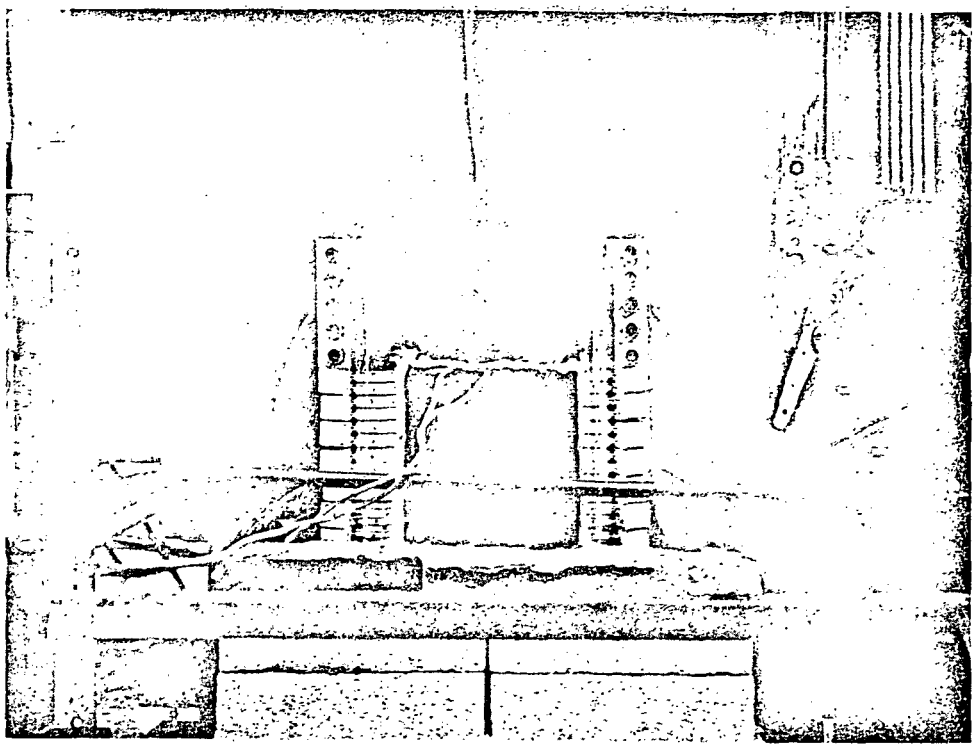

FIGURE 4–11
HCF TILE "IN PLACE" DURING HEAT-UP PHASE OF TEST
(Insulation Removed)

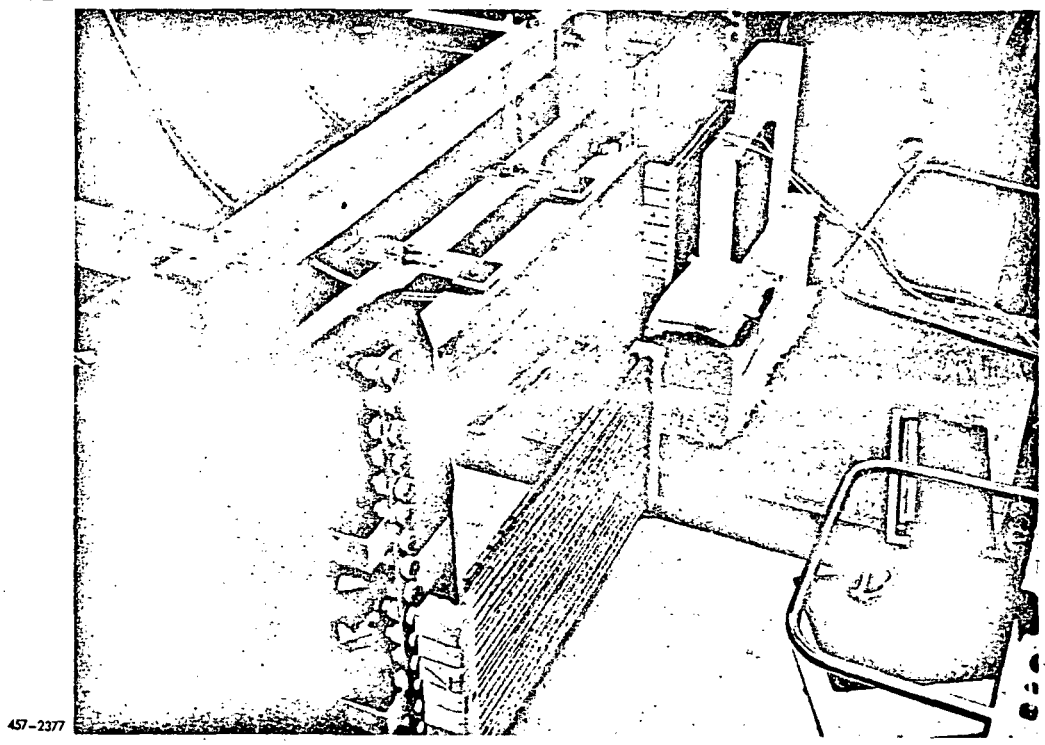

FIGURE 4–12
HCF TILE AFTER TEST WITH INSULATION PARTIALLY REMOVED

above 2300°F. The $M5_{23}P7$ coatings, with a silicate bonded chromium oxide (P) emittance coating, showed a marked improvement in blister reduction. The $M5_{23}A7$ did not blister using a different borosilicate glass, but two coats were required to waterproof the tiles. The MM_pP7 coated tile did not blister or crack and was tested to a total of 100 cycles in the quartz lamps without failure or loss of waterproofing.

The next step was to scale-up the most improved coatings to 3 and 3.5-inch thick tiles. Early attempts to increase HCF tile thickness resulted in tile failure which occurred in two basic modes. The first mode was cracking or delamination of the basic HCF material due to strength and density gradients through the tile thickness and the second mode was cracking of the coating on the top and sides of the tile due to the high thermal stresses in the coating. Typical locations of these cracks are shown in Figure 4-13. Poor strength HCF tends to propagate cracks which initiate in the coating. The cracks arising in the coating are mainly a result of the stresses induced by thermal gradients across the tile thickness. Slots, machined in the coating, stop cracks and provide stress relieving mechanisms for the coating. Tiles have been tested with slots cut on the sides in parallel and orthogonal grid patterns. Cracks did not propagate across the slots but, in some cases, did run along the slots in the HCF material. The overall cracking was greatly reduced by the slots.

Further scale-up work included the coating of full-size tiles which were bonded to a copper support plate and to a titanium 1/2-size panel. The copper support plate, shown in Figure 4-14, was tested in the graphite heater facility shown in Figure 4-15. The specimens, positioned face-down on top of the heater elements are shown in Figure 4-15. The test results (for the titanium 1/2-size panel), shown in Figure 4-16, show the relative stability of coatings in a low pressure (10-torr air) environment. The $MoSi_2$/Borosilicate (Mo7) and SiC/aluminosilicate coatings did not blister or react at 2300°F. The MMp $P_{cr}7P_{700}$

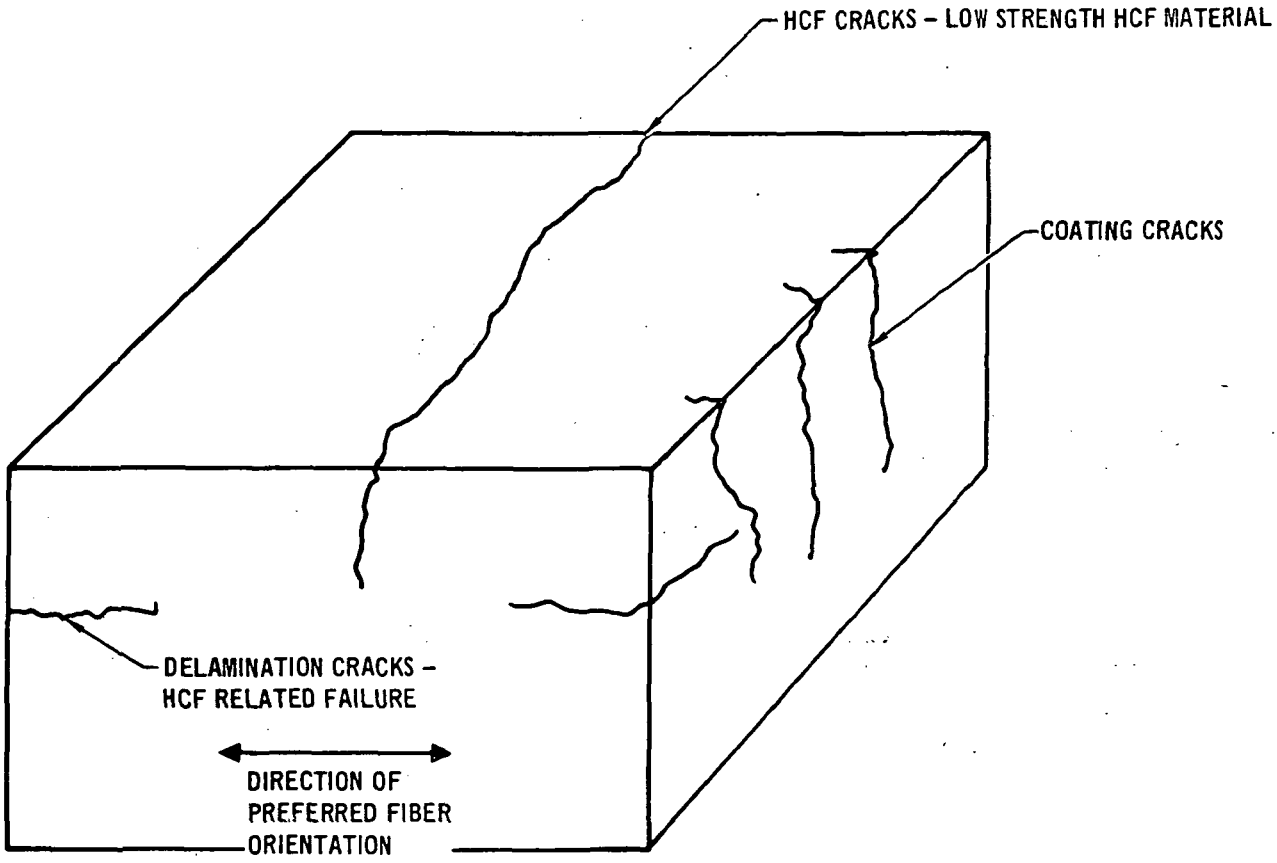

FIGURE 4-13
THERMAL-MECHANICAL FAILURE MODES OF COATED HCF TILES

coating (baseline) did exhibit slight blistering. The P_{700} coating was applied to increase the coating emittance; however, it produced higher surface temperature during plasma arc testing (which is related to the degree of surface catalycity).

Full size tiles with the B-7 coating were also tested in low pressure (10-torr) at 2300°F to 2500°F without forming blisters. This was done after it was discovered that the Mo7, Mo76 and $MMpP_{cr}7$ coatings blistered. However, it was found that for the B-7 coating, a boron silicide/glass mixture tended to hydrate after a few test cycles in air. A summary of the full-scale coating developments is presented in Figure 4-17.

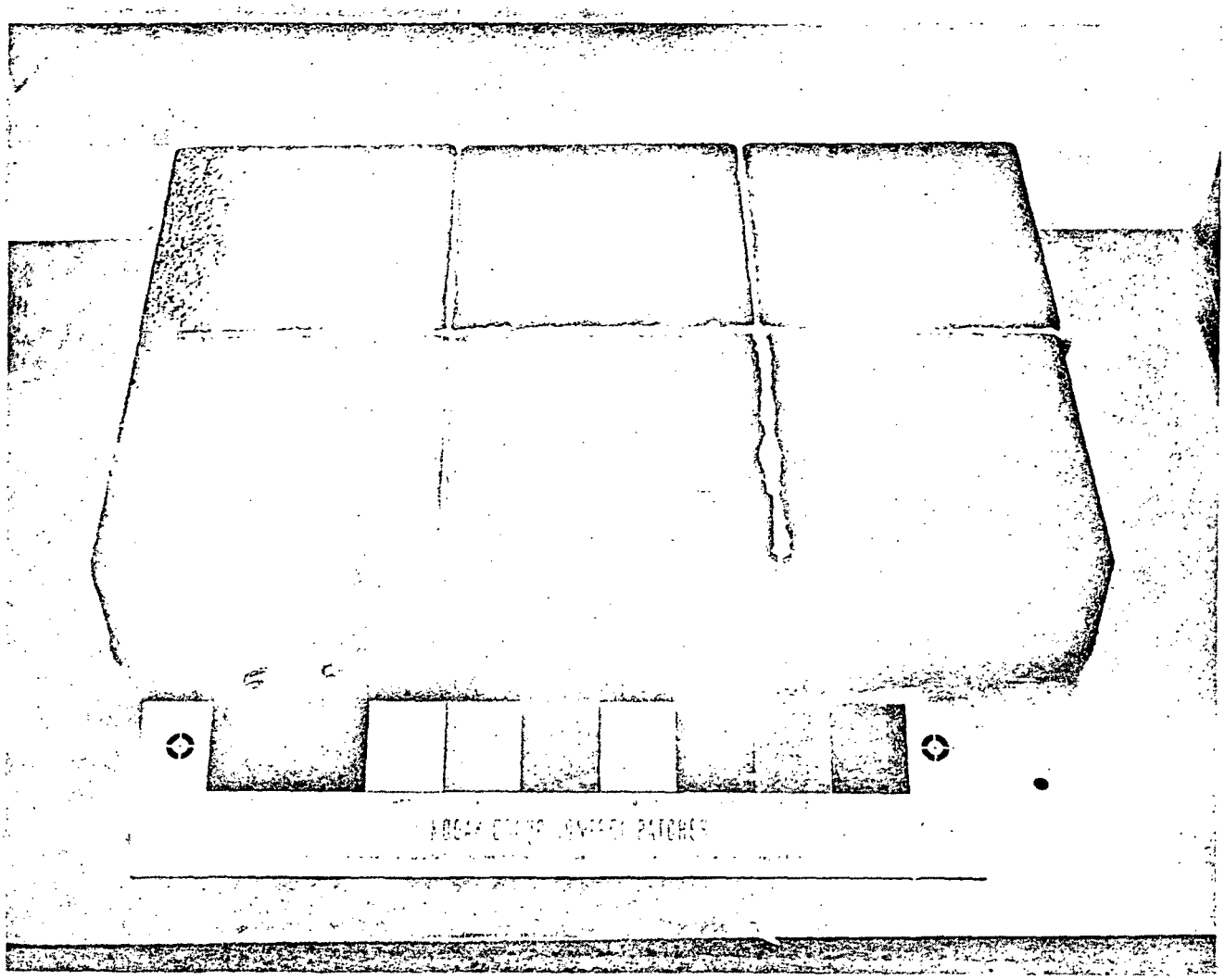

FIGURE 4-14

FULL SIZE TEST TILES BONDED TO COPPER SUPPORT PANEL

457-2573

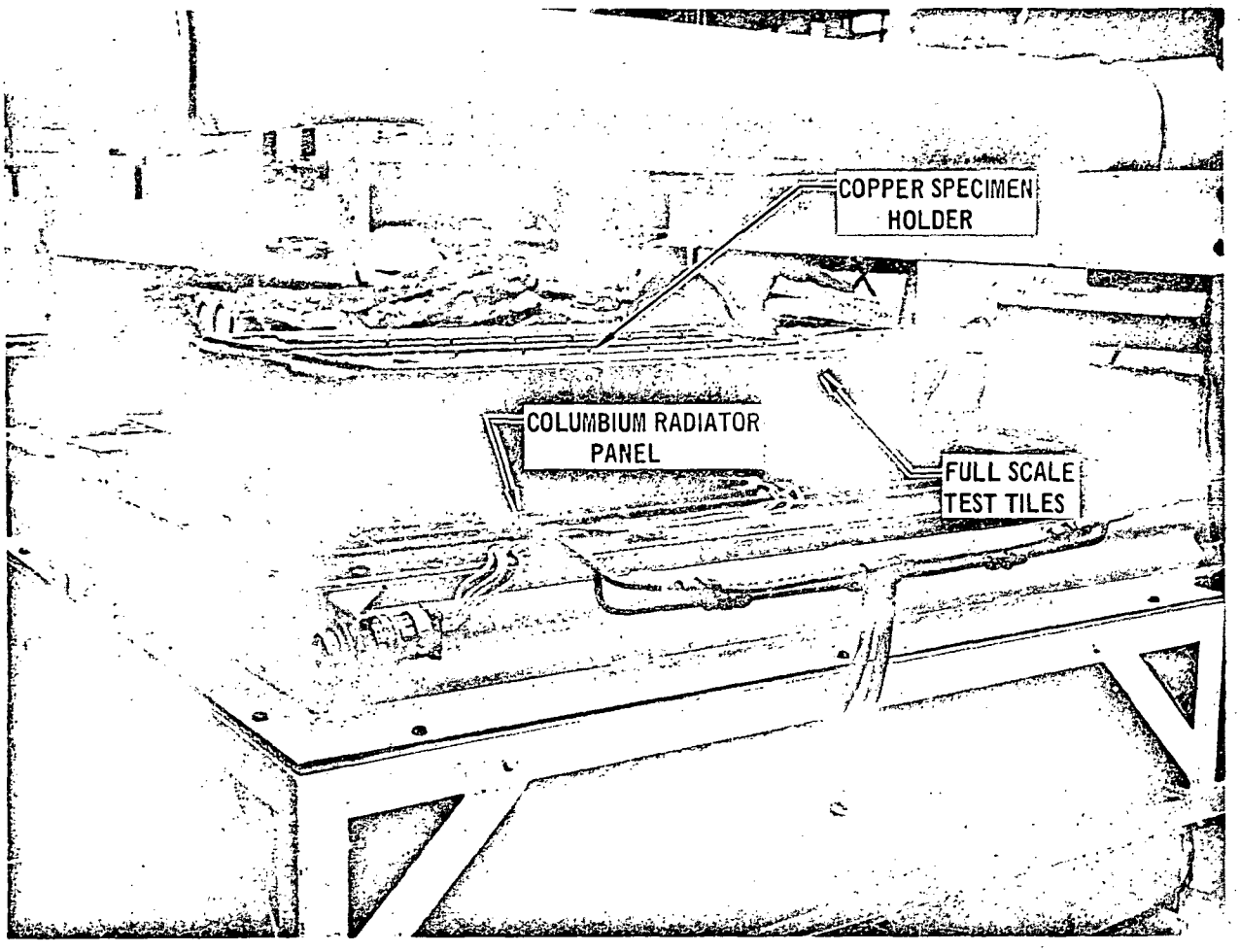

FIGURE 4-15

FULL SIZE PANELS IN POSITION ABOVE THE GRAPHITE HEATER

457-2574

TILE NO.	COATING	TEST COMMENTS (EXAMINED AFTER: 1 CYCLE AT 70% AREA 2P) (1 CYCLE AT 90% AREA 2P) (4 CYCLES AT 100% AREA 2P)*
B-67-2 (DUMMY TILE)	MMS450-I 5 SIDES COATED	NO CHANGE, NOT W/P**
409-1	$MM_pP_{Cr}7P_{700}$ 5 SIDES COATED	EMITTANCE OVERCOATING SPALLED EXTENSIVELY. W/P WHERE P_{700} DID NOT SPALL. SOME BLISTERS ON TOP. NOT W/P ON SPALLED AREA
409-3	MM_p SiC/1717 5 SIDES COATED	COATING W/P. NO REACTION OR BLISTERING
425-1	2 SiC/1717 (1 COAT) 5 SIDES COATED	COATING W/P. NO REACTION OR BLISTERING
442-2	2 Mo Si_2/7740 (1 COAT) (UNCOATED ON ONE END)	COATED W/P. NO REACTION OR BLISTERING
445-1	MM_p SiC/1717 5 SIDES COATED	COATING W/P. NO REACTION OR BLISTERING
445-2	2 SiC/1717 (1 COAT) 5 SIDES COATED	NO CHANGE AFTER 4 - 2300°F CYCLES. NO REACTION OR BLISTERING
445-3	2 Mo Si_2/7740 (1 COAT) 5 SIDES COATED	COATING W/P. NO REACTION OR BLISTERING

*70% - 1500°F T_{MAX} 90% - 2000°F T_{MAX} 100% - 2300°F T_{MAX}

** W/P - WATERPROOF

FIGURE 4-16

TEST RESULTS ON TITANIUM 1/2 SIZE AREA 2P PANEL WITH 2.88 IN. THICK HCF

457-2529

COATING	HCF TILE SIZE	COMMENTS
M25A7	APPLIED TO FULL SIZE TILES 12 BY 12 BY 1.5 – INCH	• TESTED 50 CYCLES UP TO 2500°F IN QUARTZ LAMPS. • ORIGINAL COATING APPLIED TO PHASE I MATERIAL. • FOUR STEP APPLICATION.
$M5_{23}A7$	APPLIED TO 6 BY 6 BY 2-INCH TILES (MOD I)	• ELIMINATED INTERMEDIATE COATING, LIGHTER WEIGHT. • COATING BLISTERED DURING PROCESSING. • PREFIRED FIBERS IN BASE COAT TO REDUCE PERMANENT EXPANSION.
$M5_{23}P7$	APPLIED TO 6 BY 6 BY 2-INCH (MOD I)	• REDUCED SEALER COATING BLISTERING.
MM_pP7	APPLIED TO 6 BY 6 BY 2-INCH AND 3 TO 3.5-INCH THICK TILES. (MOD I, MOD IIIA)	• ELIMINATE PERMANENT EXPANSION IN BASE COAT. • TESTED 100 CYCLES IN QUARTZ LAMPS(6''x6''x2'') AT 2300°F. • BLISTERS AT LOW PRESSURE AT 2500°F. • THICKER TILES CRACK ON SIDES.
Mo7, Mo76	APPLIED TO 6 BY 6 BY 3 TO 3.5-INCH TILES. (MOD IIIA, MOD V)	• ONE-STEP COATING. • HEALS CRACKS DURING ENTRY. • TESTED 20 CYCLES UP TO 2500°F IN QUARTZ LAMPS. • BLISTERS AT LOW PRESSURE AT 2500°F. • THICKER TILES CRACK ON SIDES.
B7	APPLIED TO 6 BY 6 BY 3 TO 3.5-INCH TILES, 5 SIDES COATED. (MOD IIIA, MOD V)	• ONE-STEP COATING. • HEALS CRACKS DURING ENTRY. • TESTED 20 CYCLES UP TO 2500°F IN QUARTZ LAMPS. • DOES NOT BLISTER AT LOW PRESSURE AT 2500°F. • THICKER TILES CRACK ON SIDES. • COATING HYDRATES.
SiC17	APPLIED TO 6 BY 6 BY 3 TO 3.5-INCH TILES, 5 SIDES COATED. (MOD IIIA)	• ONE-STEP COATING, FIRE AT 2500°F • TESTED 6 CYCLES UP TO 2300°F IN QUARTZ LAMPS. • DOES NOT BLISTER AT LOW PRESSURE AT 2500°F. • THICKER TILES CRACK ON SIDES. • COATING BLOATS WHEN TESTED AT 2500°F IN AIR.

FIGURE 4-17

SUMMARY OF FULL SCALE COATING DEVELOPMENT

457-2564

5.0 COATING PROPERTIES

Both mechanical and thermal properties were determined to assist in analysis and thereby aid in the improvement of the various vitreous coating systems.

Again, as in the work with the HCF materials, new test methods had to be developed and tested before they could be used to actually determine the coating's mechanical properties. These methods and the test results will be discussed in this section.

The thermal properties, or the properties after exposure to thermal environments, were determined in two phases; The developmental phase in which new coating candidates were applied to small (2 by 2-inch), and a scale-up phase in which the new coatings, showing the improvements were applied to 6 by 6 by 3-inch HCF tiles. The specimens were tested at reduced pressure, and through a simulated time/temperature profile. Samples were evaluated for smoothness, cracks, blisters and bloating, and liquid-water proofness.

Emittance and thermal expansion measurements were made over the expected environmental spectra as a further aid in the analyses which were made on the coating systems.

5.1 MECHANICAL PROPERTIES - One goal of this program was to develop methods for accurately determining coating mechanical properties. Previous mechanical property tests of coating, reported in Reference (b), utilized coated HCF dog-bone shaped specimens. Strain gages, bonded to the coating, were used to determine elastic modulus. Since strain gages could not be used above 500°F it was impossible to measure elevated temperature strains. In this program, flexure specimens were coated, and the flexure data were then used to estimate room and elevated temperature properties of the coating. Tests reported in this section were conducted at MDAC-W using the M25A7 coating. Properties were measured to 1500°F.

Test Methods - The coating mechanical property test specimen geometry is illustrated in Figure 5-1. Specimens consisted of HCF bars coated on two sides and loaded in flexure. The flexure test setup is illustrated in Figure 5-2. The four point graphite load fixture had an overall span length of 2.500 inches and applied loads were separated by 0.833 inch. Loads and reactions were applied through 0.25-inch diameter pins. Crosshead travel was recorded during the flexure tests to determine specimen deflection. At the low loads used (less than 6-lb) no correction for deflection of the load train was necessary.

All tests were conducted in the elevated temperature fixture shown in Figure 5-2 mounted on an Instron test machine. Specimens were loaded to failure at a loading rate of approximately 0.05 inch/minute. Load rods are closely fitted to guide bushings in the yoke to insure good alignment. The yoke and guide bushings are water cooled for dimensional stability.

Heating was provided by radiation from electrically heated graphite bars. The furnace was purged with argon for 2 hours prior to heating the specimens to the test temperature. Heat was applied slowly (approximately 30 minutes) and the temperature was held approximately 20 minutes before applying loads. A chromel-alumel thermocouple, imbedded in a small block of HCF clamped to the loading fixture, was used to measure temperature.

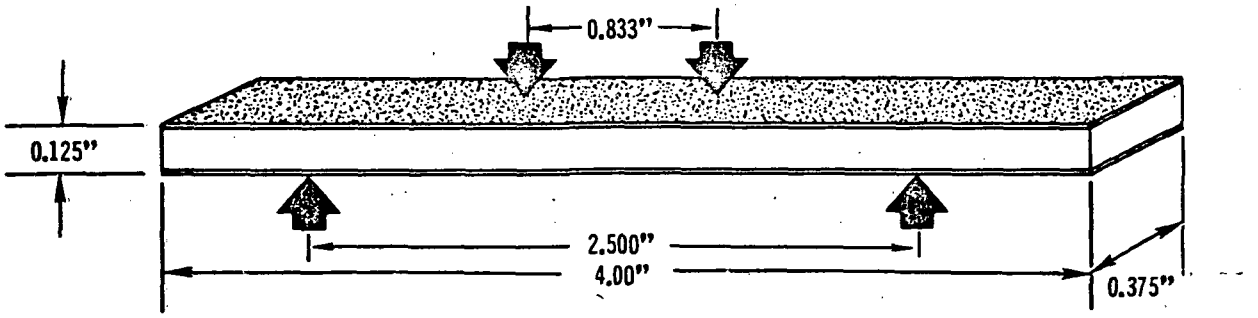

FIGURE 5-1
COATING MECHANICAL PROPERTY SPECIMENS

457-2554

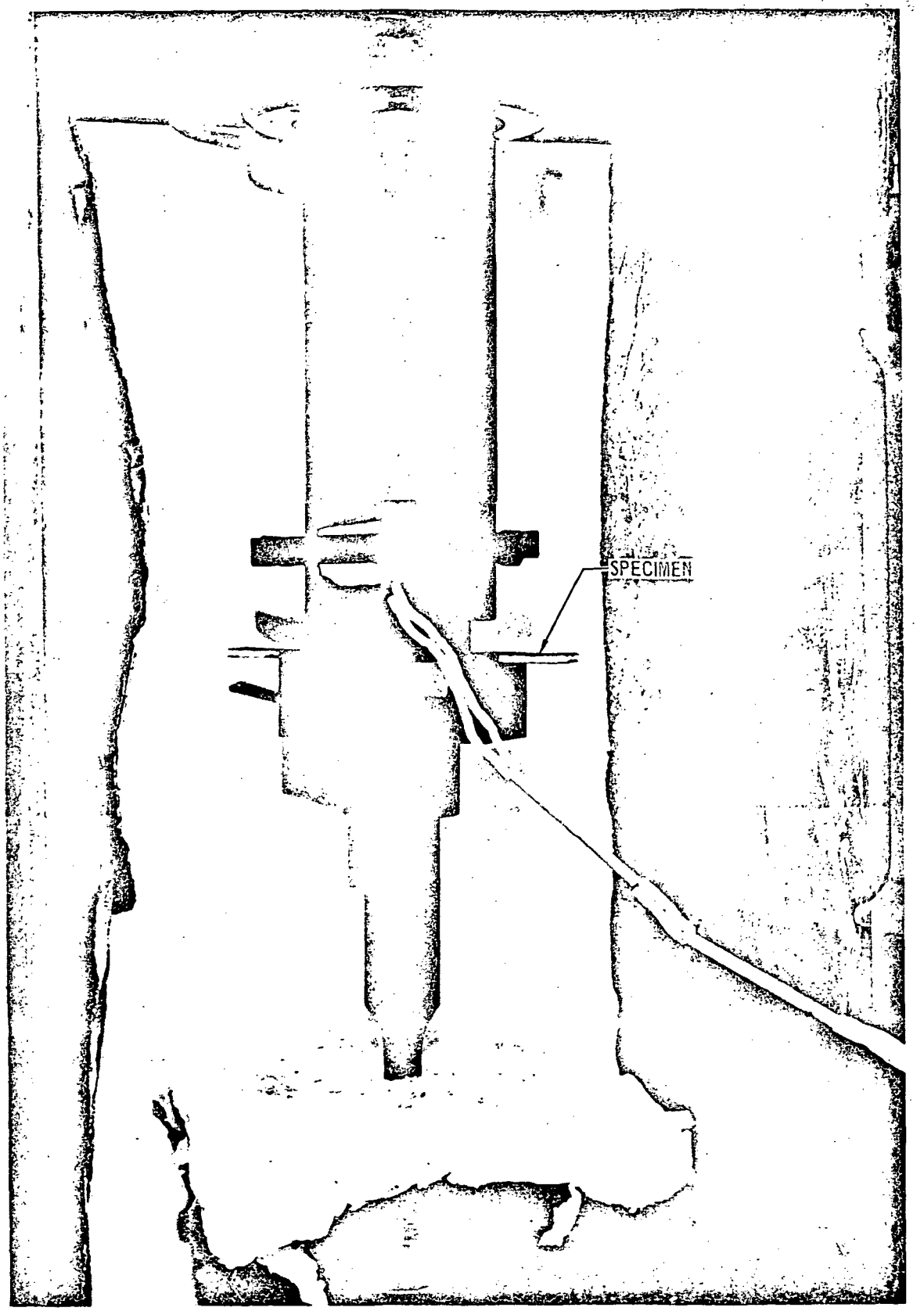

FIGURE 5-2

COATING TEST SETUP

457-2559

Test Results - Results of flexure tests are presented in Figure 5-3. All specimens were tested in the "as fabricated" condition and all specimens were loaded to failure. Specimen geometry, ultimate strength, and elastic modulus are listed for each specimen tested.

The tensile strength and modulus of elasticity of the coating were computed from the test data using linear-elastic beam theory. Thickness of coating on each specimen was measured. It was not possible to tell during the test if the first surface to fail was in tension or compression. However, previous tests of coated tension and compression specimens, reported in Reference (b), indicated the compressive strength to be much larger than the tensile strength. Coating strengths were, therefore, assumed to be tensile.

The coating elastic modulus was assumed to be the same in tension and compression and much greater than the HCF modulus. The coating modulus was determined from the flexure specimen load deflection curve. Calculations indicated that HCF shear deflections were a significant part of total specimen deflections. Deflections due to shear were therefore calculated and subtracted from measured deflections to determine modulus.

Coating tensile strength and elastic modulus are plotted in Figures 5-4 and 5-5. Also shown are results of tests conducted during the Reference (b) program. A computer program entitled "General Least Squares Analysis" was used to fit the curves.

5.2 THERMAL PROPERTIES - Various coatings in different phases of development were exposed to the expected shuttle thermal environment, then surface characteristics such as smoothness, etc., were evaluated. Selected coatings were applied to full sized tiles and were then further tested. Other necessary properties such as emittence of high temperature, and thermal expansion characteristics were also determined; these are discussed in this section along with the thermal exposure results.

TEST TEMPERATURE (°F)	SPECIMEN NO.	t_t (IN.)	t_1 (IN.)	t_2 (IN.)	b (IN.)	ULTIMATE STRENGTH LB/IN^2	ELASTIC MODULUS LB/IN^2
ROOM TEMPERATURE	12	0.132	0.014	0.012	0.367	2378	13.1×10^6
	21	0.124	0.012	0.015	0.364	2276	6.6×10^6
	16	0.133	0.012	0.014	0.366	1939	8.2×10^6
	10	0.134	0.009	0.013	0.372	2080	6.6×10^6
	9	0.129	0.010	0.011	0.365	1815	28.5×10^6
	2	0.127	0.010	0.010	0.367	2290	10.4×10^6
	AVERAGE	-	-	-	-	2130	12.2×10^6
900	1	0.123	0.010	0.010	0.358	6202	13.5×10^6
	8	0.142	0.010	0.012	0.371	1954	10.1×10^6
	15	0.135	0.012	0.013	0.368	1807	9.5×10^6
	AVERAGE	-	-	-	-	3321	11.0×10^6
1200	3	0.129	0.015	0.012	0.369	2836	-
	5	0.136	0.010	0.012	0.368	4268	6.6×10^6
	22	0.130	0.012	0.013	0.369	3076	8.0×10^6
	AVERAGE	-	-	-	-	3393	7.3×10^6
1500	4	0.134	0.013	0.014	0.367	1214	1.0×10^6
	6	0.136	0.014	0.012	0.370	1627	1.7×10^6
	25	0.131	0.010	0.010	0.367	1943	2.5×10^6
	AVERAGE	-	-	-	-	1595	1.7×10^6

FIGURE 5-3

457-2527 COATING MECHANICAL PROPERTY TEST RESULTS

line least squares curves to the test results. The large scatter in test results is typical of brittle ceramics.

Low-Pressure, High-Temperature Testing - This work was conducted in two phases: the developmental phase in which new coatings were applied to 2 by 2 by 2-inch HCF test specimens, and the scale-up phase in which the new coatings showing the improvements were applied to 6 by 6 by 3-inch or 3.5-inch thick HCF tiles. The specimens were tested in the graphite heater facility at 2300°F and at 2500°F maximum temperature and at 10-torr air pressure. The test chamber and graphite heater assembly are shown in Figure 5-6. The time/temperature profiles used for these tests are shown in Figure 5-7.

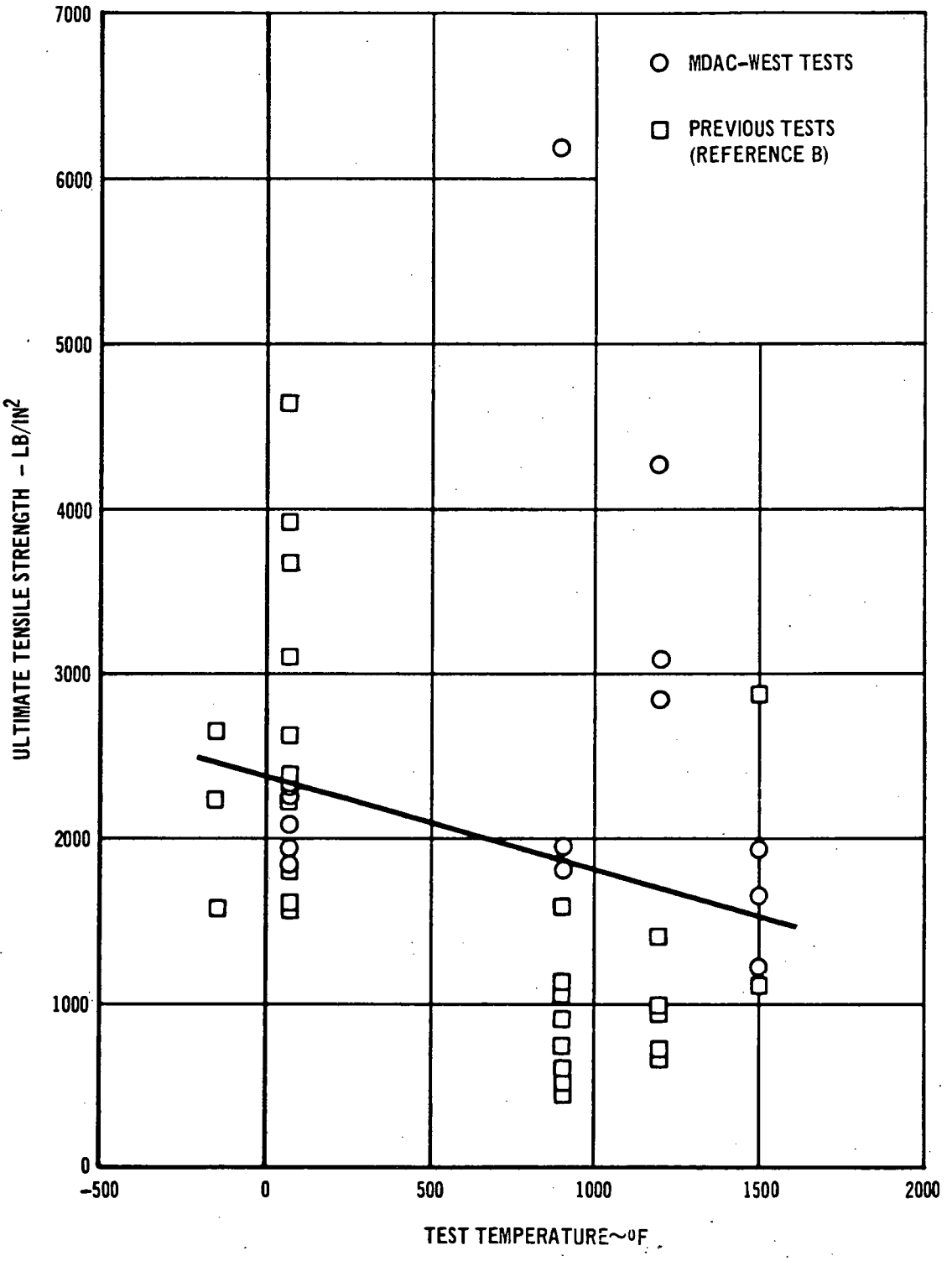

FIGURE 5-4
COATING TENSILE STRENGTH

457-2555

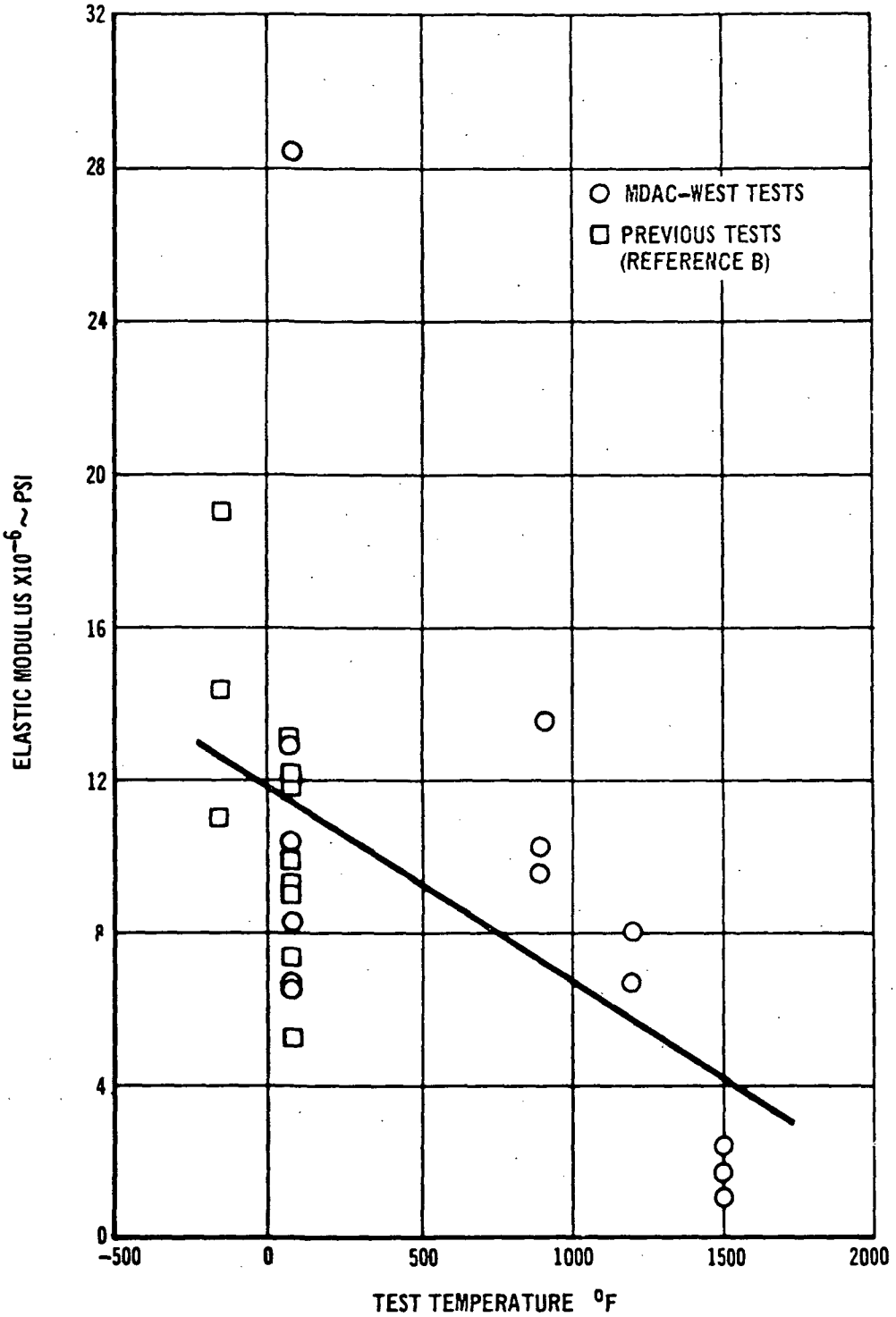

FIGURE 5-5

COATING ELASTIC MODULUS

457-2546

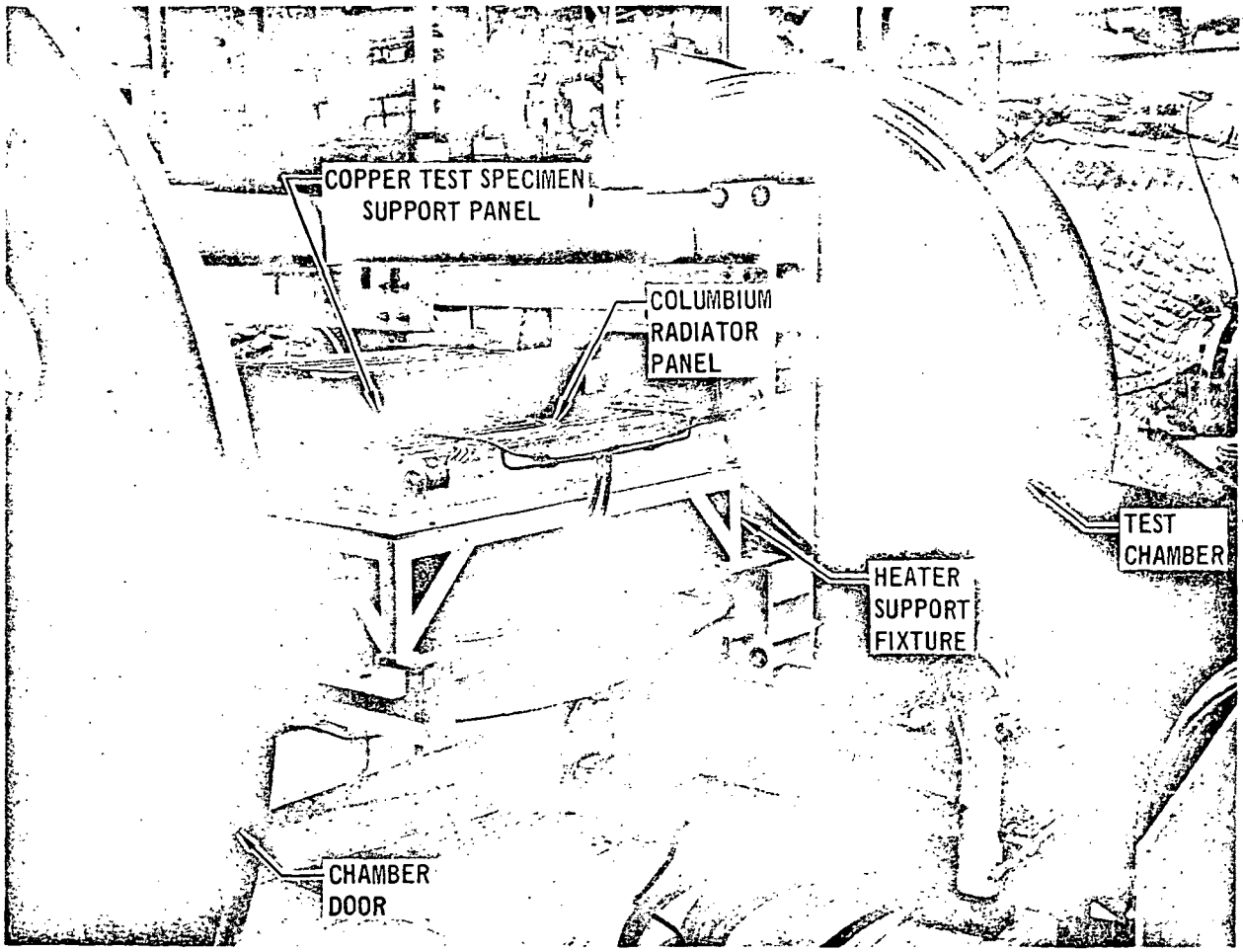

457-2575

FIGURE 5-6
ENVIRONMENTAL TEST CHAMBER AND SUPPORT FIXTURE

The developmental and full-scale test specimens were bonded to a water-cooled copper plate which holds the specimens in position above a columbium susceptor panel. The susceptor panel is, in turn, heated by the graphite resistance heating elements which are kept in a vacuum. The time/temperature profile was controlled according to Space Shuttle requirements.

A test panel shown in Figure 5-8, containing the 2 by 2-inch development test specimens, was used to determine the high-temperature, low pressure stability of the new one-step coatings compared with our standard MMpP_{cr}7 coating. The basic function of the test was to determine what constitutents, either pigment or glass,

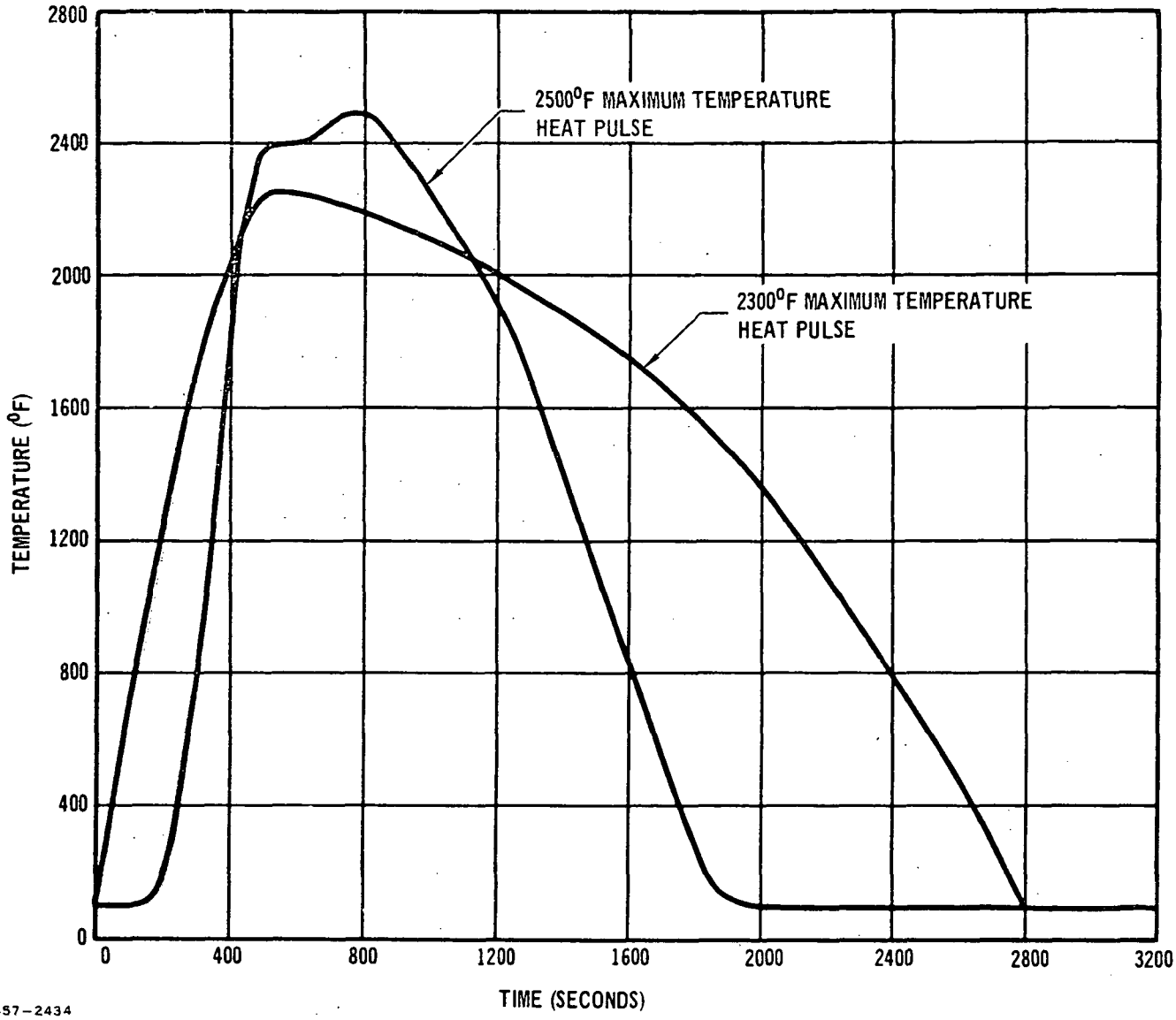

FIGURE 5-7
TEMPERATURE – TIME PROFILES FOR SHUTTLE ENTRY SIMULATION

would be volatile and would cause blistering at 2500°F, 10-torr air conditions. The following one-step coatings were tested: SiC, $MoSi_2$, ZrB_2, WSi_2, and B_4Si pigments in conjunction with borosilicate and aluminosilicate glasses. Silica (SiO_2) was added to the one-step coatings to reduce blistering at low pressure and high temperatures. Testing on the $MMpP_{cr}7$ and Mo7 coatings at low pressure and high temperature had resulted in blistering of the coatings at 2500°F. Also, the

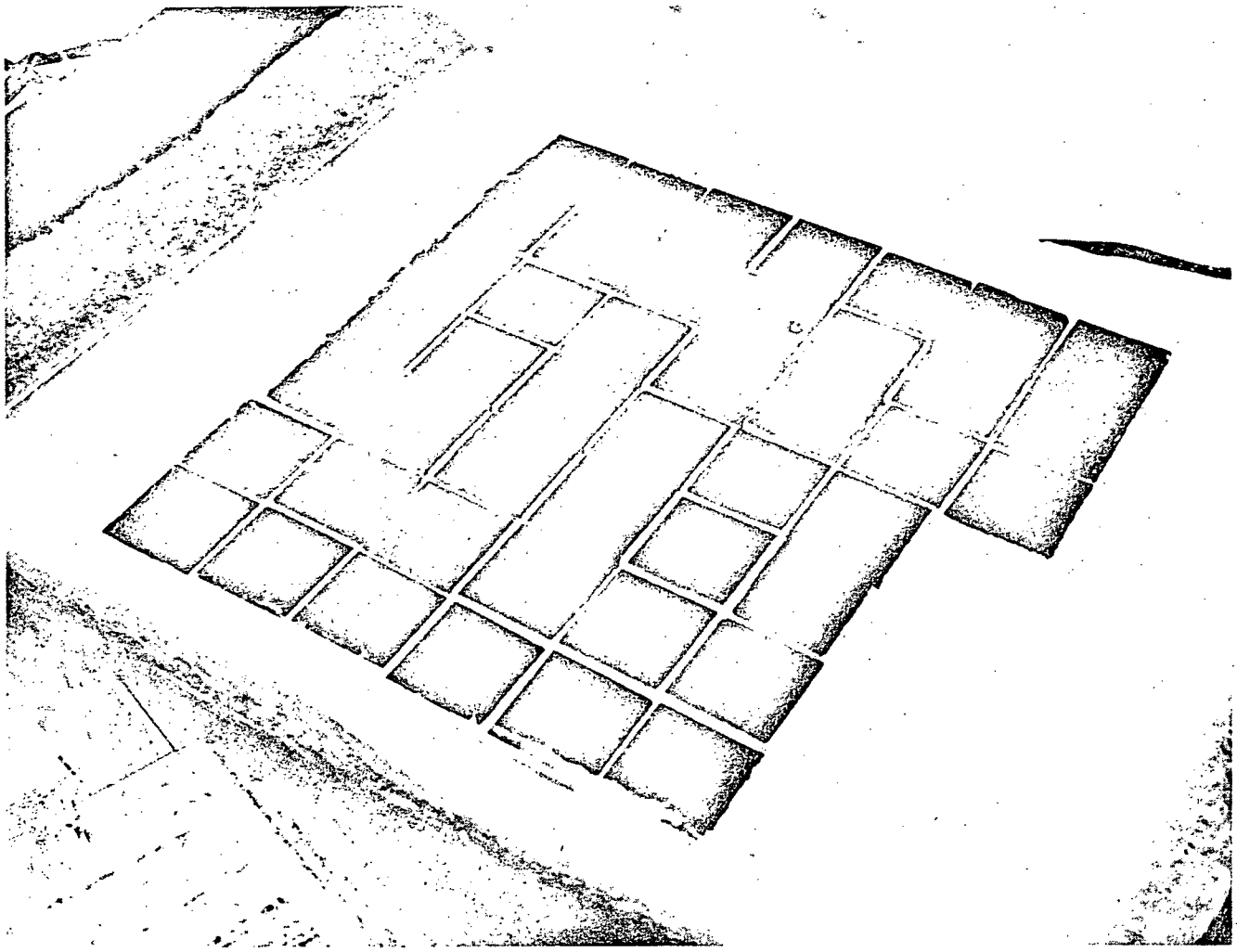

457-2572

FIGURE 5-8
DEVELOPMENTAL COATING SPECIMENS FOR LOW PRESSURE TESTING

ability of the coatings to remain liquid waterproof during the test was a major test criterion in selection of an improved coating. The developmental specimens were then heated on a total of six cycles to peak temperatures of 2300°, 2400°, and 2500°F under 10-torr air pressure conditions. The coatings were inspected after each cycle for oxidation, cracking, blistering, and retention of liquid waterproofing. The coating formulations showing the most promise were as follows:

	PIGMENT	GLASS	OTHER
a.	B_4Si	Borosilicate	
b.	B_6Si	Borosilicate	

c.	B_4Si	Borosilicate	SiO_2 (reduce blisters)
d.	SiC (fired @ 2300°F)	Aluminosilicate	
e.	SiC (fired @ 2500°F)	Aluminosilicate	
f.	SiC (fired @ 2300°F)	Aluminosilicate	PbO (flux)
g.	WSi_2	Borosilicate	

The earlier $MoSi_2$/borosilicate glass mixtures and the $MMpP_{cr}7$ baseline coating both blistered after 2500°F exposure at 10 torr, although the latter did not blister severely and remained waterproof. The SiC/Aluminosilicate glass coatings were fired at 2500°F to achieve liquid waterproof coatings because firing at 2300°F did not result in a waterproof coating. The addition of flux, lead oxide (PbO) to this coating provided a waterproof coating after firing at 2300°F. During testing at 2500°F (low pressure), the SiC17 coatings which were fired at 2300°F became liquid waterproof. These coatings thereafter remained smooth and waterproof during test. The B_4Si and B_6Si/glass mixtures exhibited some discoloration, but did not blister or lose liquid waterproofing during testing. The WSi_2/glass coating performed in a similar manner.

After the low-pressure testing, the specimens with the most promising coatings were subjected to oxyacetylene torch testing in air at 2300° and 2500°F for 5-minute cycles to determine the effect of high-temperature exposure at one atmosphere on the coatings. The B_4Si/glass coatings remained waterproof throughout the testing. The SiC/glass coatings which had been fired at 2300°F lost their liquid waterproofing ability and began to bloat. The SiC/glass coatings which had been fired at 2500°F did not bloat, but the coating delaminated from the HCF. Overall, the best coating composition was the B_4Si/SiO_2/7740 mixture, designated B-7, which exhibited little change through the torch testing. The WSi_2/glass coating oxidized extensively and was eliminated. The B-7 coating and modifications of the $MoSi_2$/glass and SiC/

glass coatings (to reduce blistering and bloating) will be scaled up as a future developmental activity.

Emittance Measurement - The total normal spectral emittance of coated and uncoated Mod IIIA mullite HCF was measured using a push-pull apparatus (shown in Figure 5-9) heated by an Astro tube furnace.

The total normal emittance of coated HCF was measured by a method that is based upon the comparison of the energy emitted by the test specimen and a black-body cavity at the same temperature. The specimen is mounted at the rear of a heated cavity on the end of a pushrod. In this position, the specimen can be moved to any location within the cavity up to the aperture. The emitted energy is detected by a fast response thermopile. The energy received when the thermopile "sees" the black-body cavity (specimen at initial position) is considered as 1.0 and as zero when the field of view is closed (specimen at final position). The specimen is moved rapidly to the aperture and is "seen" by the thermopile. This action corresponds to the time interval ΔT and is typically 0.2 second. Specimen cooling then begins as it radiates to the water-cooled sight port. It is important to account for specimen cooling effects since the ratio of emitted energy from the specimen in the two locations is used as the basis for the emittance determination (Figure 5-10). This cooling effect can be estimated by extrapolating the cooling curve through the ΔT time span. Except for specimens where cooling is very rapid, the error introduced in emittance determinations is typically $\pm$ 0.02 emittance units.

The Model 2570C Astro furnace is resistance heated using a graphite tube as the heating element. Two components make up the pushrod mechanism: a stainless steel rod with a water cooling tube through the center, and a coated graphite rod. One end of the graphite rod is machined to form a sample holder. A stainless steel stud is used to connect the two parts of the pushrod mechanism, and sealing rings are

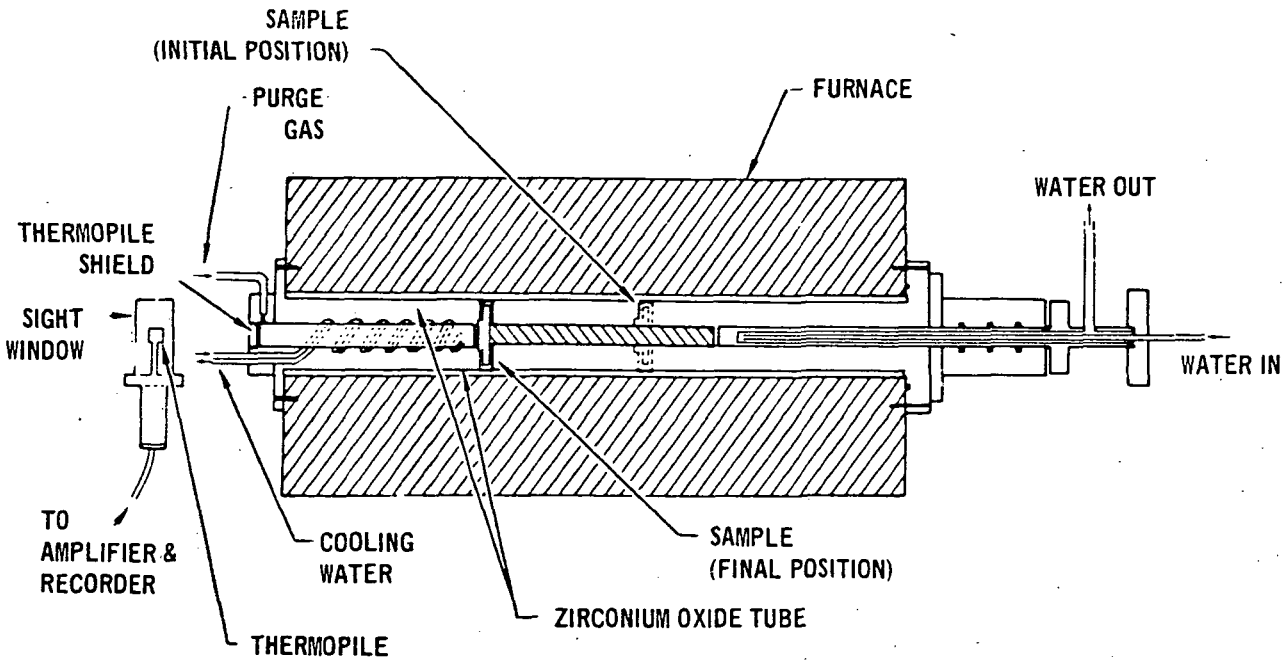

FIGURE 5–9

TOTAL NORMAL EMITTANCE ACCESSORY

457–2524

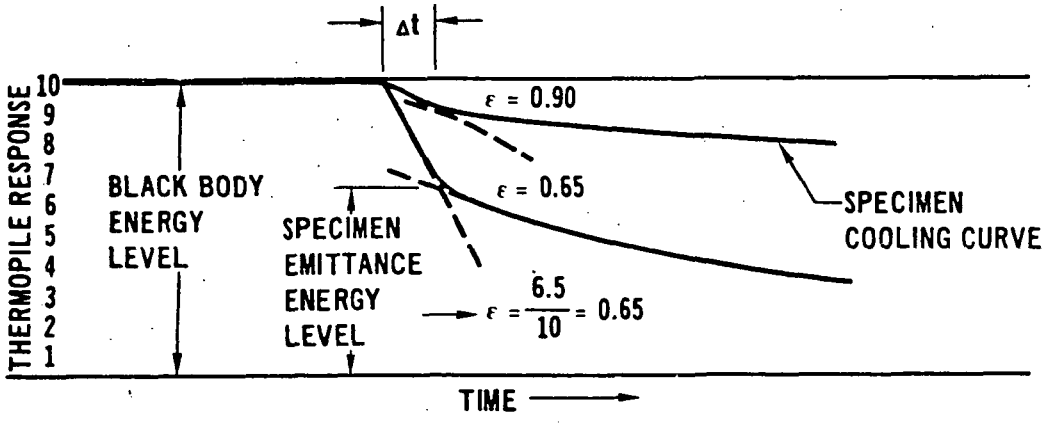

FIGURE 5–10

THERMOPILE RESPONSE CURVE FOR $\epsilon = 0.65$ AND $\epsilon = 0.9$

provided around the pushrod and under the cover plate to enable furnace depressurization.

The emittance of all the new coatings was not measured, however, the emittance as a function of temperature of the SiC17, $MiSi_2$ and $MMpP_{cr}7$ coatings can be closely estimated from test data on the M25A7 coating, Figure 5-11 and from data on the overcoatings for the M5A7 coating containing the emittance of pigments ($MoSi_2$, SiC, Co-Fe-Cr oxide mixture).

The emittances of these surface overcoatings as a function of test temperature are shown in Figure 5-12 and is compared with uncoated HCF material. The emittance of boron silicide pigments was not measured, but the emittance of this material is estimated to be in excess of 0.8.

Note that the SiC and $MoSi_2$ pigments have greater emittance values at lower temperature than the standard M25A7. The M25A7 emittance should be equivalent to that of the $MMpP_{cr}7$ system because both utilize a chromic oxide pigment. The inorganic bonded P-700 pigment (Co-Cr-Fe oxide) used as an overcoating increases the emittance from 0.78 to 0.82 when applied to the M25A7 or $MMpP_{cr}7$.

Although the nonoxide pigments possess high emittance at lower temperature, elevated temperatures result in a marked decrease in emittance due to oxidation. The current one-step coatings are mixtures of glass and nonoxide pigments; the glass provides oxidation protection for the pigment and the high emittance is maintained at higher temperatures. As an example, the SiC pigmented coating without glass protection shows a degradation of emittance, but the SiC/17 glass mixture retains its original emittance and is an improvement over the standard coating. From these data, the predicted emittance data for the temperature range of 2000° to 2500°F for the new coatings are given in Figure 5-13.

Coating Thermal Expansion Measurement - The linear thermal expansion as a function of temperature of the various coatings and the Mod IIIA mullite HCF from

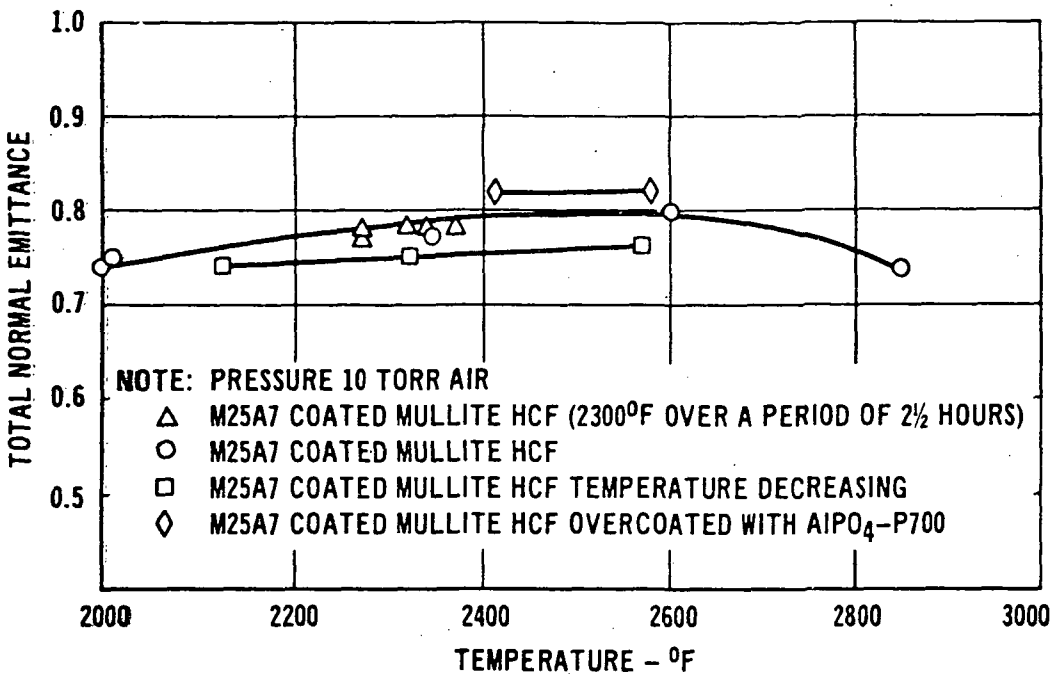

457-2580

FIGURE 5-11

TOTAL NORMAL EMITTANCE OF COATED MULLITE HCF vs TEMPERATURE

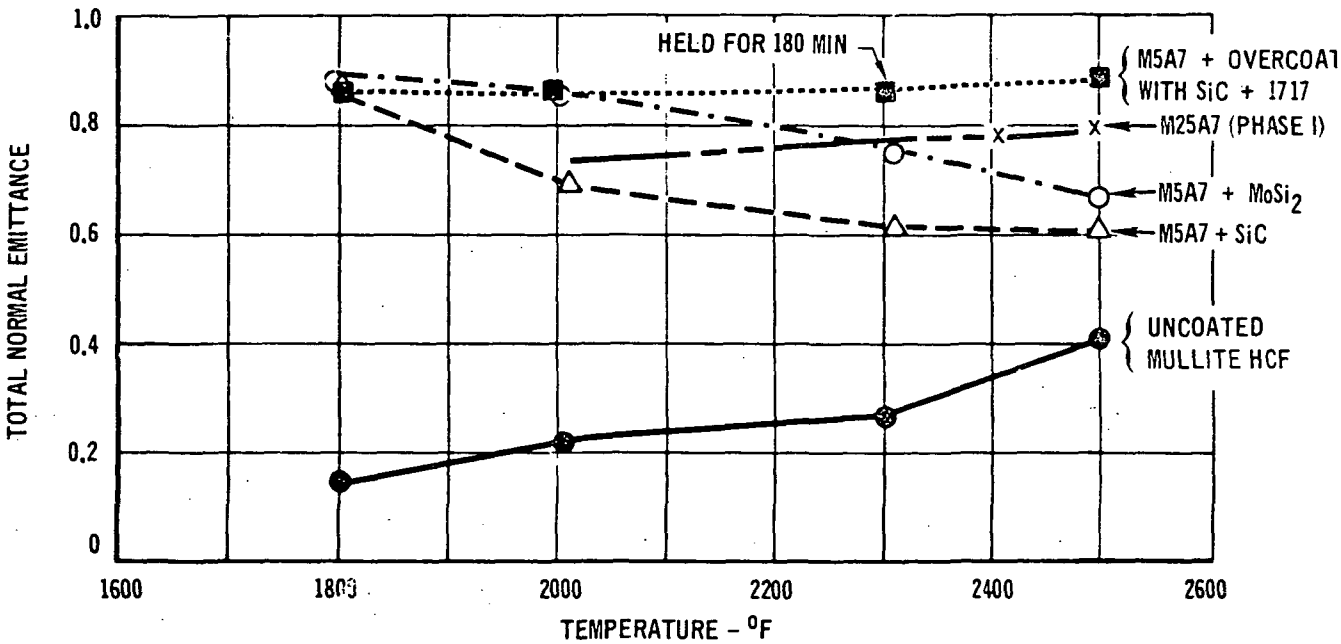

457-1963

FIGURE 5-12

EMITTANCES OF SURFACE COATINGS FOR MULLITE HCF

COATING	(TOTAL NORMAL EMITTANCE)	
	2000°F	2500°F
M25A7	0.73	0.80
$MM_pP_{cr}7$*	0.73	0.80
$MM_pP_{cr}7P_{700}$ (OVERCOATED)*	0.82	0.82
Mo7 (MOLYBDENUM DISILICIDE PIGMENT)*	0.88	0.84
SiC17 (SILICON CARBIDE PIGMENT)*	0.88	0.88
B7 (BORON SILICIDE PIGMENT)*	GREATER THAN 0.80	

*PREDICTED FROM FIGURES 3-26 AND 3-27

457-2565

FIGURE 5-13

ACTUAL AND PREDICTED EMITTANCES FOR HCF COATINGS

room temperature to 2500°F and back to room temperature was measured using a modified Astro tube furace. This apparatus can provide expansion measurements from 500°F to 5000°F. The expansion of 3 by 0.25 by 0.25-inch test specimens was measured optically using a calibrated telescope to observe the change in distance between two slots which were machined in the bars; the expansion was determined by dividing the expansion or contraction by the distance between the slots.

The thermal expansion of a coating should closely match the expansion of the HCF material to reduce stresses between the coating and the HCF. A comparison of the thermal expansion coefficients of the various coatings developed is presented in Figure 5-14. Note that the Mod IIIA material exhibited very little dimensional change after the 2500°F test exposure. The thermal expansion of the Mod IIIA in both orthogonal directions of fiber orientation is plotted in Figure 5-15. The expansion in the X-Y plane of the HCF material could possibly be attributed to grain growth in the mullite fibers. The thermal expansion of the mullite fiber based M5 base coating was developed to match closely that of the HCF and is plotted as a function of temperature in Figure 5-16. A large permanent expansion which occurred in this coating at 2200°F was decreased by altering the binder used in the base coating.

By comparison, the thermal expansion as a function of temperature of the MMp base coating is also shown in Figure 5-16. This binder change was found to be more effective in stabilizing the base coating than was prefiring the mullite fibers (at 2300°F) used in the M5 composition.

The thermal expansion as a function of temperature for the one-step coatings is a function of the glass phase which is also the major phase of the coating (see Figure 5-17). The SiC, $MoSi_2$ or B_4Si pigment particles are uniformly distributed throughout the glass matrix. These coatings, therefore, soften at 1250°F to 1700°F and valid expansion data can be measured only below 1250°F. Considering the three most promising one-step coatings, the SiC17 composition most closely matches the thermal expansion of the HCF. The Mo7 coating, with a higher expansion coefficient, would present the greatest mismatch with the HCF.

MATERIAL	$\alpha \times 10^{-6}/°F$	COMMENTS
HCF (MOD IIIA)		
PARALLEL TO FIBER ORIENTATION	3.2 (2500°F) (1)	0.6% PERMANENT EXPANSION AFTER TEST
PERPENDICULAR TO FIBER ORIENTATION	3.0 (2300°F)	0.5% PERMANENT CONTRACTION AFTER TEST
BASE COATINGS:		
M5 (MULLITE FIBERS + ALUMINA CEMENT)	3.2 (2200°F)	2.2% PERMANENT EXPANSION AFTER TEST
MM_P (MULLITE FIBERS + MULLITE FILLER + PHOSPHATE BINDER)	3.1 (2400°F)	NEGLIGIBLE CHANGE AFTER TEST.
ONE-STEP COATINGS		
Mo7 ($MoSi_2$ + BOROSILICATE GLASS)	6.7 (1250°F)	COATING SOFTENED AT 1700°F. 1.3% PERMANENT CONTRACTION AFTER TEST.
SiC17 (SiC + ALUMINOSILICATE GLASS)	2.2 (1500°F)	COATING SOFTENED AT 1700°F. 1.2% PERMANENT CONTRACTION AFTER TEST.
B-7 (BORON SILICIDE + SILICA + BOROSILICATE GLASS)	2.0 (1250°F)	COATING SOFTENED AT 1500°F. SPECIMEN WARPED.

(1) MAX. TEMPERATURES USED TO CALCULATE α.

457-2569

FIGURE 5-14

THERMAL EXPANSION COEFFICIENTS OF HCF AND COATING MATERIALS

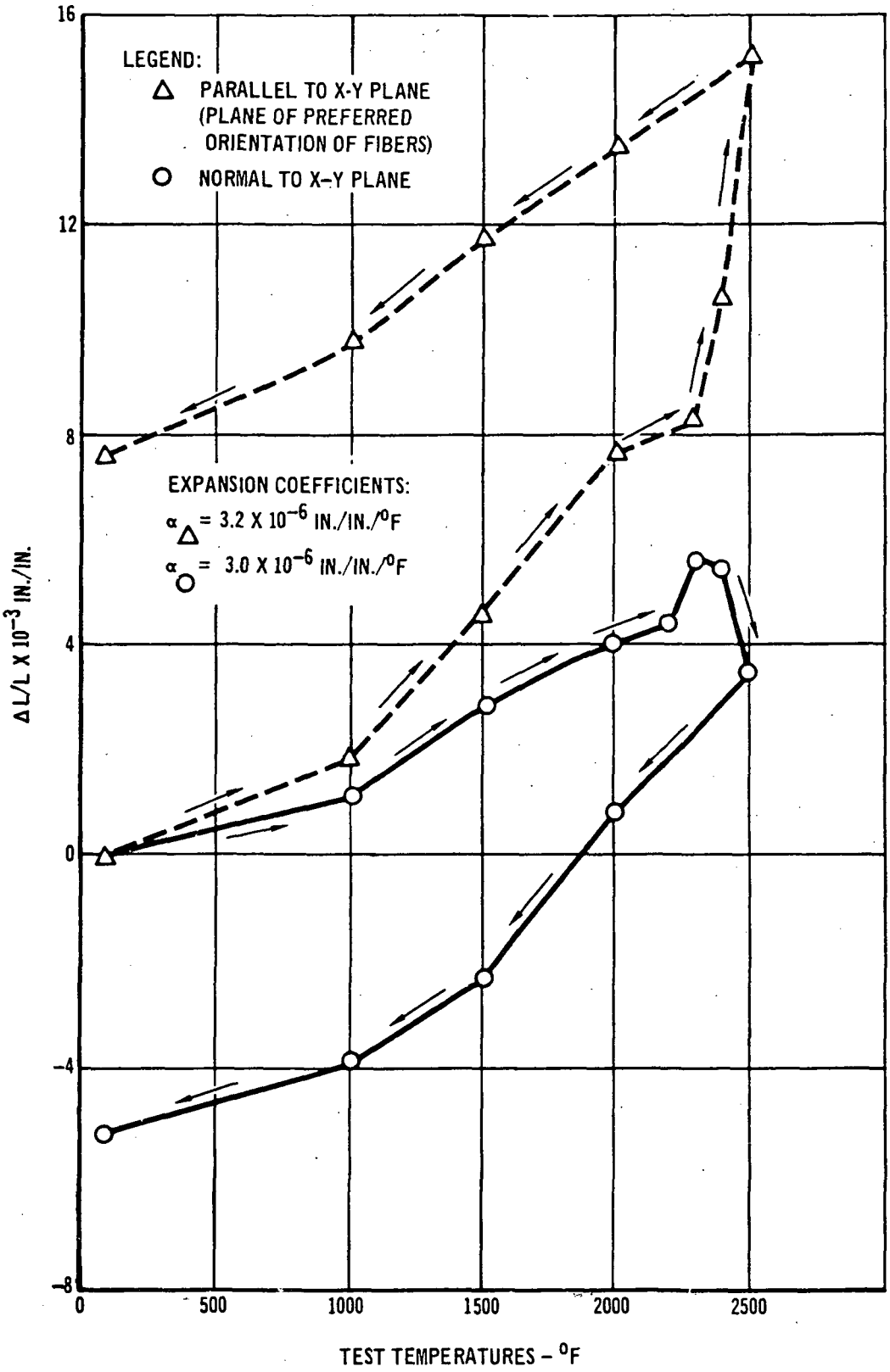

457-2528

FIGURE 5-15

ΔL/L OF MOD IIIA AS A FUNCTION OF TEMPERATURE AND SPECIMEN ORIENTATION

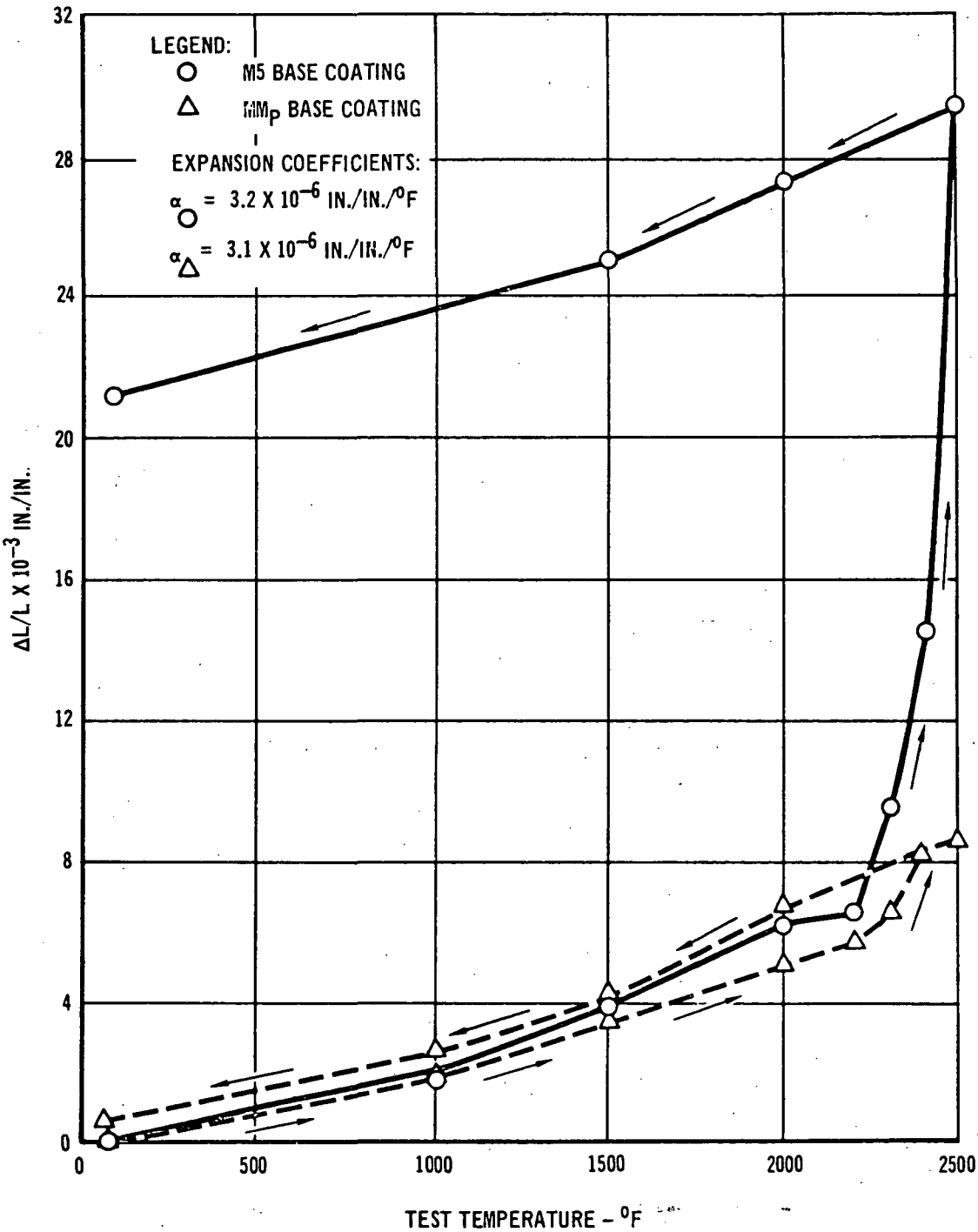

FIGURE 5-16
COMPARISON OF THERMAL EXPANSION OF M5 BASE COAT WITH MMp BASE COAT

457-2570

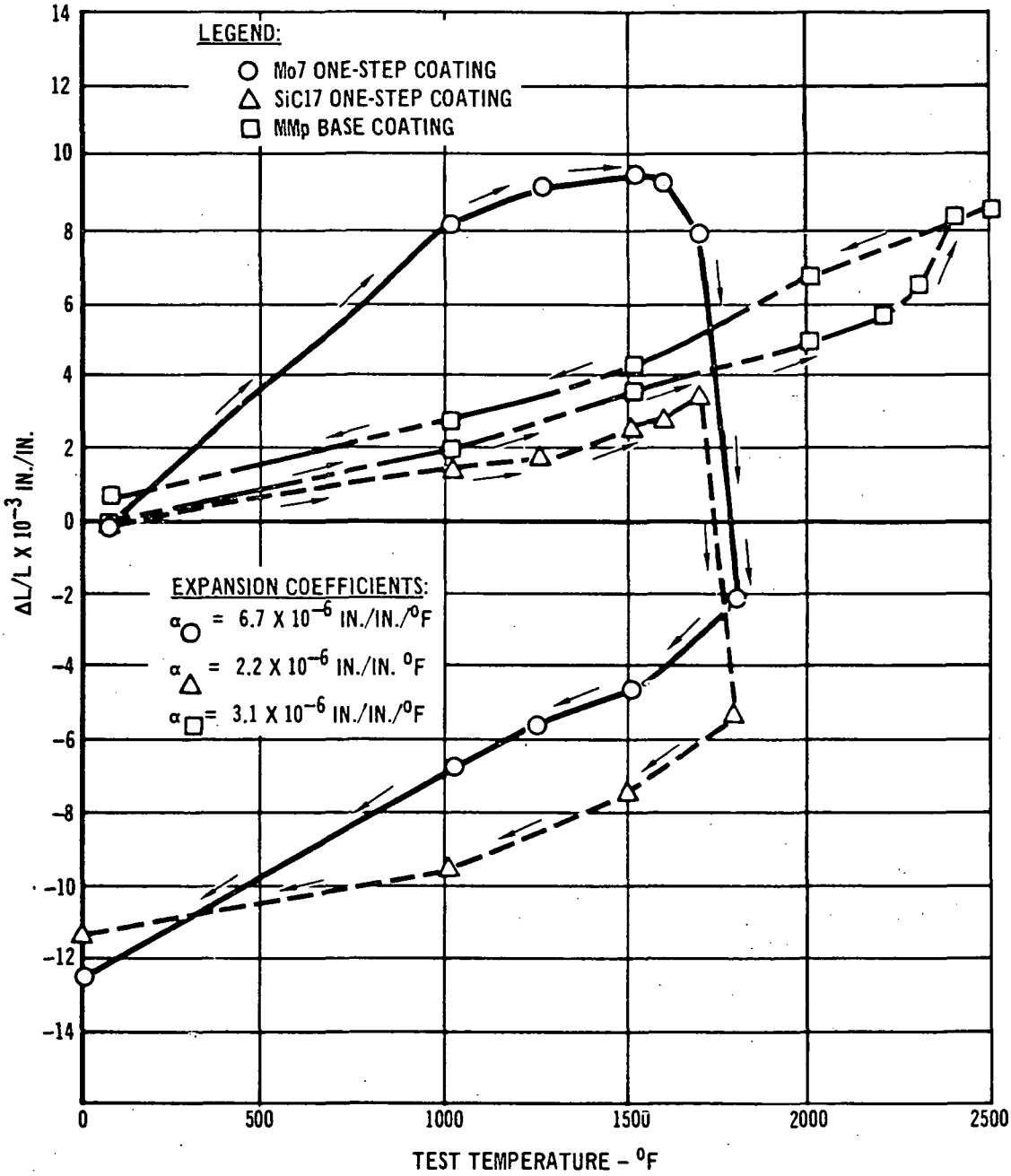

FIGURE 5-17

COMPARISON OF THERMAL EXPANSION OF Mo7 AND SiC17 ONE-STEP COATINGS WITH MMp BASE COATING

457-2563

6.0 REINFORCEMENT

The objective of reinforcing HCF is to hold the material together in case of cracking. The approach taken was to emplace a reliable, continuous, high strength filament. Although reinforcement may also increase the ultimate strength of the HCF material, this was not the goal of our effort.

6.1 MATERIALS CONSIDERED - Astroquartz* (SiO_2) and Zircar** (ZrO_2) threads, which have breaking strengths of approximately 20 pounds and 4 pounds, respectively, were considered for reinforcement materials because of their oxidation resistance, temperature resistance, and availability in thread form. Small test samples of these threads in HCF were fabricated and heat treated to 2150°F. Both the SiO_2 and ZrO_2 threads became brittle and lost all appreciable strength when fired to 2150°F.

Columbium, platinum, nickel-chromium, and Kovar wires were then considered as HCF reinforcements; however, only Cb and nichrome specimens were fabricated.

6.2 CERAMIC THREAD REINFORCEMENT - Figure 6-1 shows the fixture used to hold the silica thread in place during the felting operation. The threads were strung with 3/4-inch spacings in three orthogonal directions. Using conventional felting techniques, the HCF slurry was poured through the fixture. The felt formed around the reinforcement threads into a continuous block without voids. The block of material was cured before removing the sides and top of the mold. The block was then fired at 2150°F in 16 hours. Figure 6-2 shows the HCF block reinforced with the threads before machining.

The material used to construct the supporting frame tooling was commercial acrylic sheet, The box frame was constructed of 1/4-inch thick acrylic sheets, 3 inches wide and 7-1/2 inches long, to form the four sides of the frame. One-eighth-inch holes were drilled on three-quarter-inch centerlines laterally and longitudinally, to allow insertion of the thread in two axes. Positioning in the

* J. P. Stevens Co.
** Union Carbide

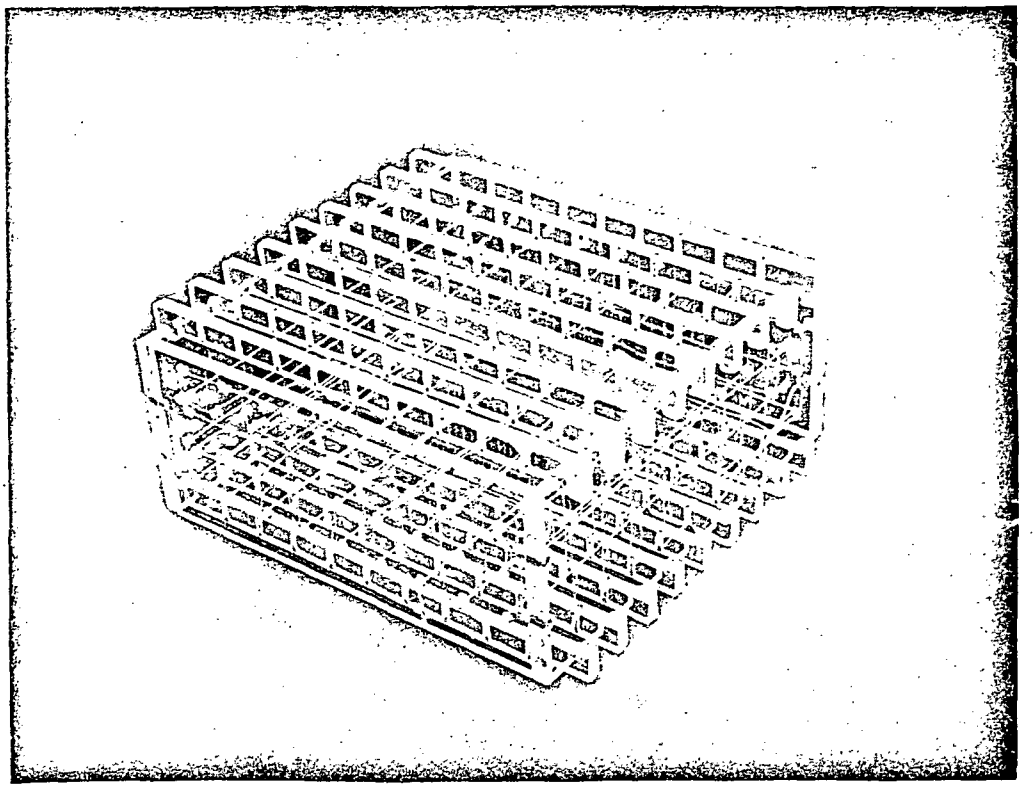

FIGURE 6-1
3-D ARRAY OF REINFORCEMENT THREADS IN TOOL BEFORE FILLING

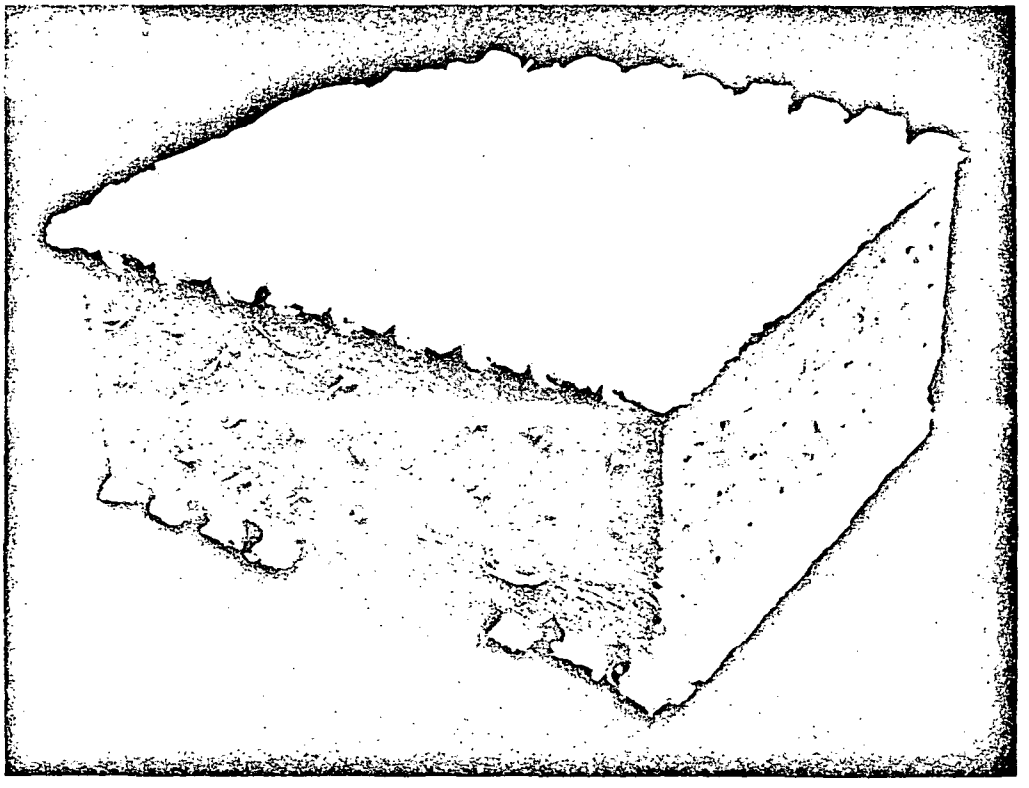

FIGURE 6-2
ASTOQUARTZ 3-D REINFORCED HCF AFTER REMOVAL FROM TOOL

457-1261

assembly of the four sides was accomplished by 3/16-inch diameter acrylic dowels. Fiber tension provided mechanical fastening of the mold. A series of 1/2-inch wide, 1/4-inch thick acrylic bars with 1/8-inch holes in 3/4-inch centers drilled through the 1/2-inch width provided a grid support for the fibers in the Z axis.

The box frame was assembled and Dacron polyester thread was used in a trial fabrication. The fiber insertion or "string up" method used was an 8-inch long needle passed back and forth through the holes provided. The fibers were first pulled through the two sides parallel to the locator dowels (to be referred to as the X axis) to provide mechanical assembly of the four frame (or box) sides. Next, the fiber was strung through the two sides perpendicular to the X axis. The 1/4 by 1/2-inch acrylic bars were progressively added as thread was inserted in the Z axis, resulting in a cubic lattice. Notches were provided in the box sides of the X axis to locate the Z axis support bars. The assembly method described above was chosen because it provided simple disassembly of the completed specimen by cutting exterior loops without potential damage to the completed HCF composite. The actual Astroquartz thread (#300-4/4) specimen was fabricated as outlined above.

Preliminary cost estimates indicated that an additional 20 manhours would be required to produce one cubic foot of silica thread reinforced HCF compared to unreinforced material. This included only the time required for threading the reinforcement through the tool on 3/4-inch centers. Tooling, planning, and other related costs were not included.

6.3 NICHROME WIRE REINFORCEMENTS - The first wire reinforcement concept evaluated used reinforcement only across the thickness. It was felt that this reinforcement would provide support if delaminations should occur in the weaker HCF plane (parallel to the moldline).

Initial specimens were fabricated using nichrome wire inserted in predrilled holes in fired HCF. It was found that pulling the wires into position with a small

force could easily cut through HCF. It was thought that vibration might cause this cutting in service. An alternate method was devised to hold the reinforcement wires using 99-percent alumina tubes. These tubes provide a wire path during insertion and also a bearing surface to prevent cutting (Figure 6-3). The ceramic bearing concept was dropped because coating application was difficult and the alumina tubes tended to work loose during thermal cycling.

Using a 3-D orthogonal array of 0.010-inch diameter nichrome wires, two felts were fabricated, one using the RSB-2 binder system and a second using precursor silicone binder. In both cases it was found that the wires could be easily pulled out of the part. It was thought that if these wires were to provide reliable retention of large, cracked pieces of HCF, the wires should be welded at their intersections to prevent possible pullout. Radiographs were taken in two directions of 3-D wire reinforced HCF to detect any possible voids which might be present due to the wire reinforcements. No voids were detected, as shown in Figure 6-4. It was concluded that sound HCF felts can be fabricated with 3-D wire reinforcements using our present felting processes.

3-D Welded Nichrome Wire Reinforcement Concept - One 3-D reinforced HCF specimen was fabricated using 0.030-inch diameter nichrome wire. The nichrome trusswork was 7 by 7 by 1/2-inch and the wires were spaced on 3/4-inch centers. Each intersection of wires was welded. Figure 6-5 shows the 14.2 lb/ft^3 tile, including the weight of the support pads. The silicone precursor technique was used to form this reinforced HCF block. The part was cured at 150°F for 2 hours and then fired for 2 hours at 1500°F. The part was trimmed to final dimension and coated with a high emittance ceramic. Figure 6-6 shows that no voids in the HCF are detectable by X-ray.

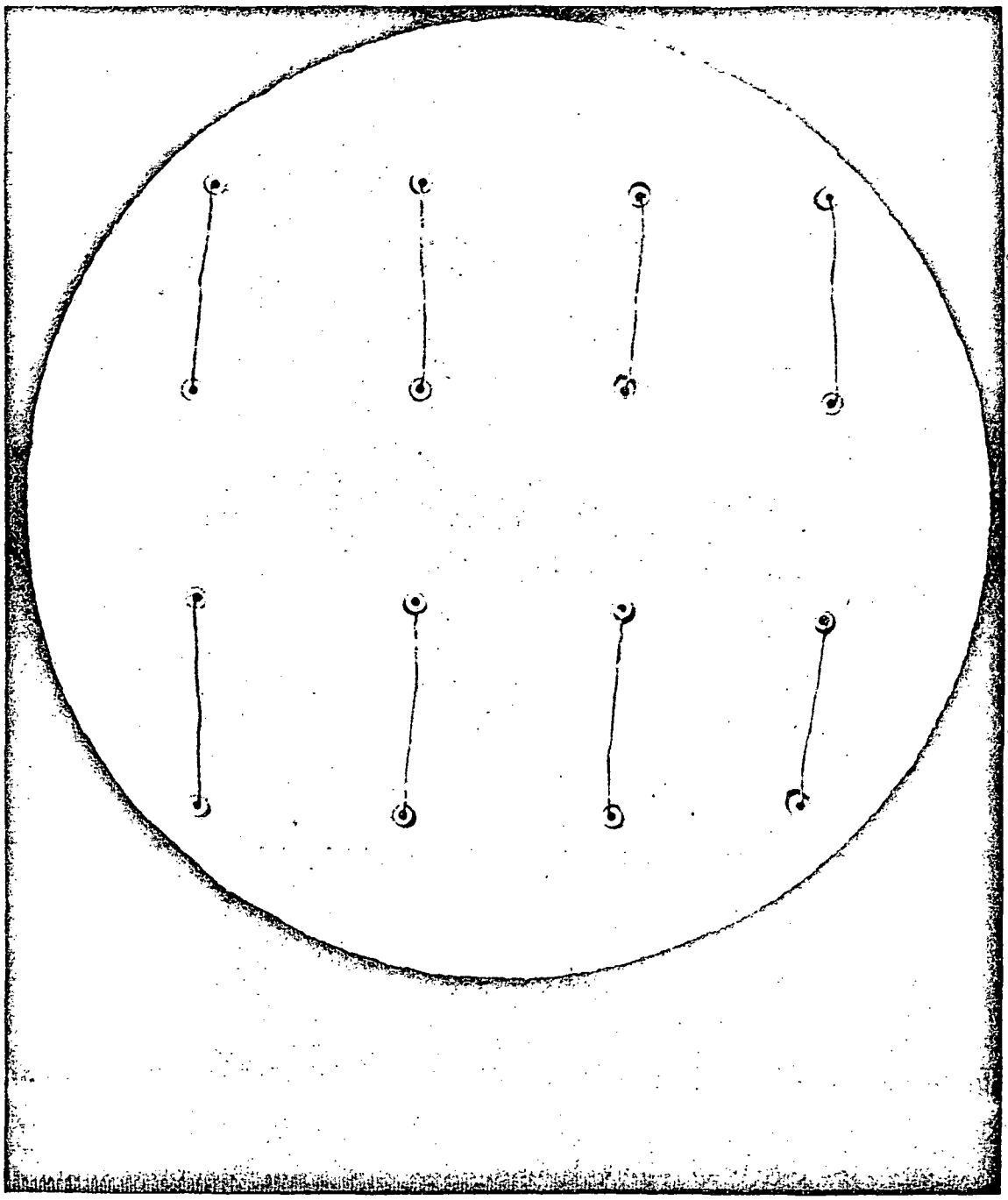

FIGURE 6-3
ONE DIMENSION WIRE REINFORCED HCF WITH ALUMINA TUBE BEARING SURFACES

457-1767

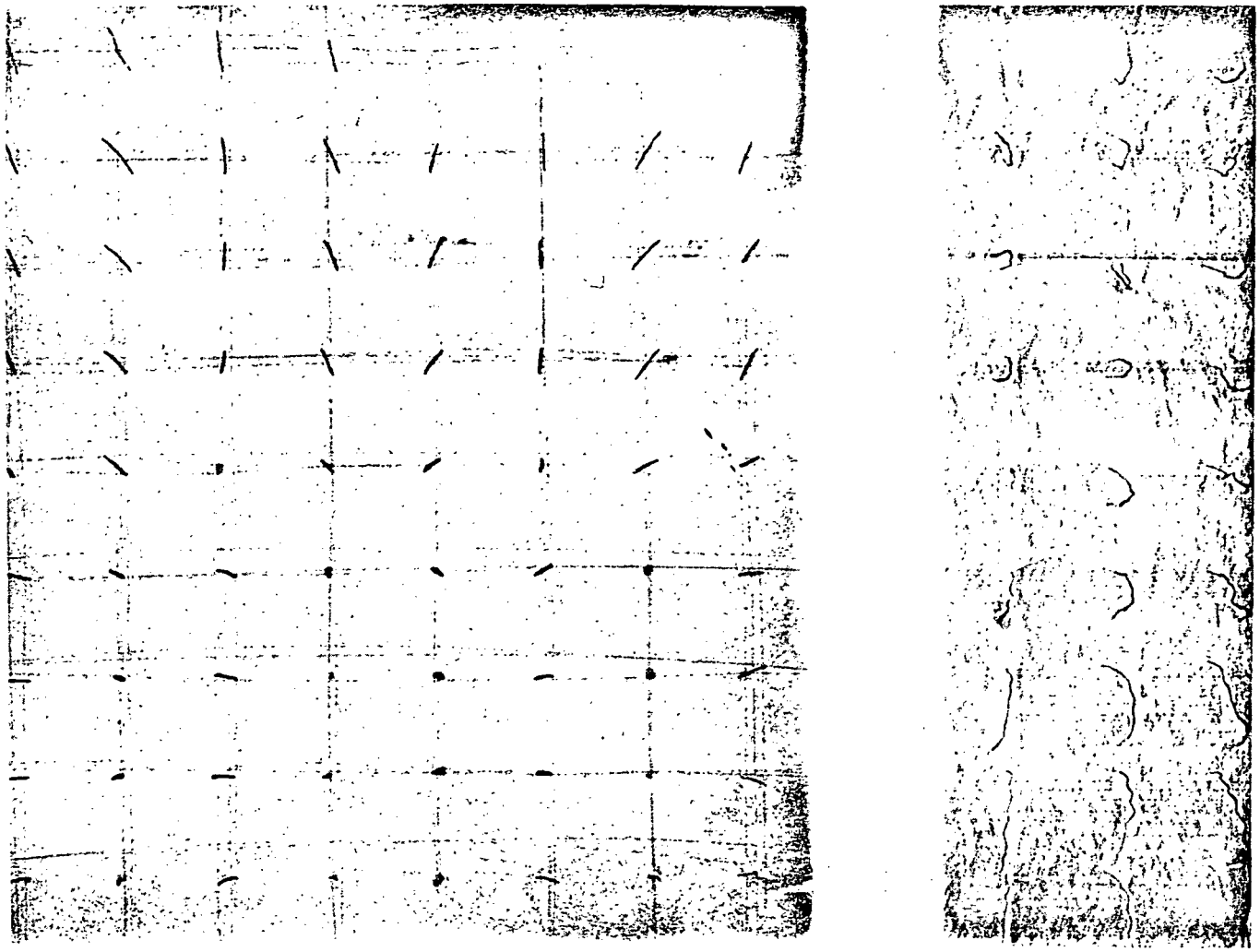

PLAN VIEW EDGE VIEW

457-1772

FIGURE 6-4

TWO VIEW X-RAYS OF 3-D WIRE REINFORCED HCF SHOWING VOID-FREE TEXTURE

6.4 COLUMBIUM WIRE REINFORCEMENT - Three columbium wire arrays were fabricated to reinforce HCF. Coated columbium was selected as the best candidate wire material because it most closely matches the thermal expansion of HCF and is usable to 2500°F.

Partial Depth Columbium Wire Array - A layer of packaged insulation (Hastelloy X metal foil and Microquartz insulation) was included in the partial depth columbium wire grid design. Figure 6-7 shows the columbium wire reinforcement, the insulation package, and the substructure. The attachment points of the

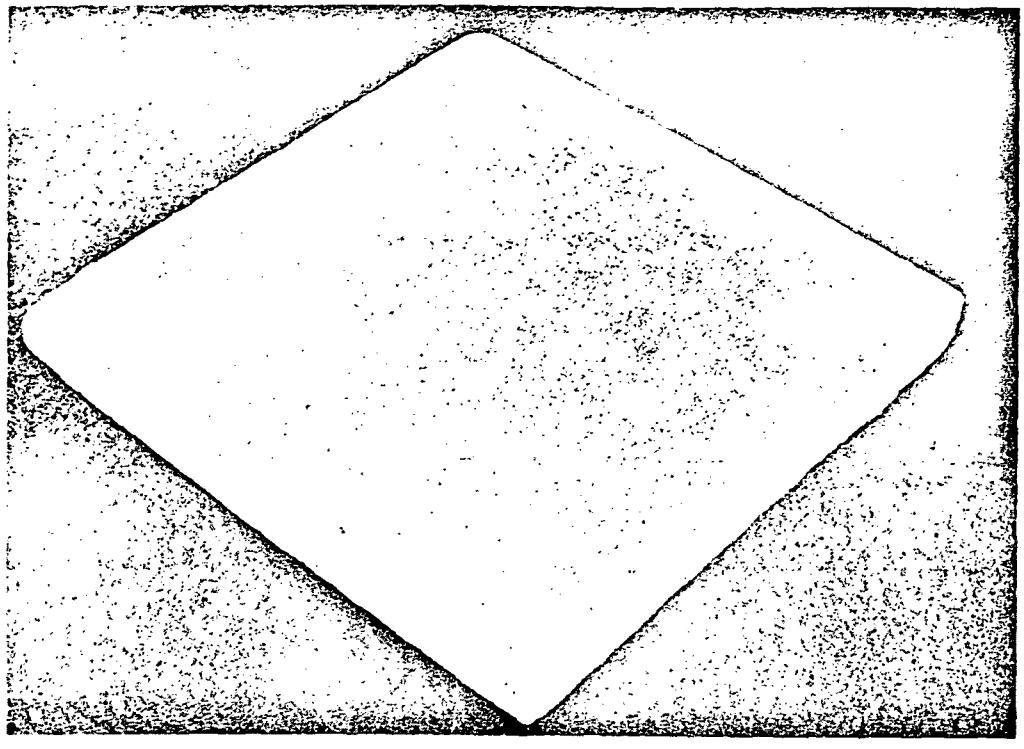

Top View

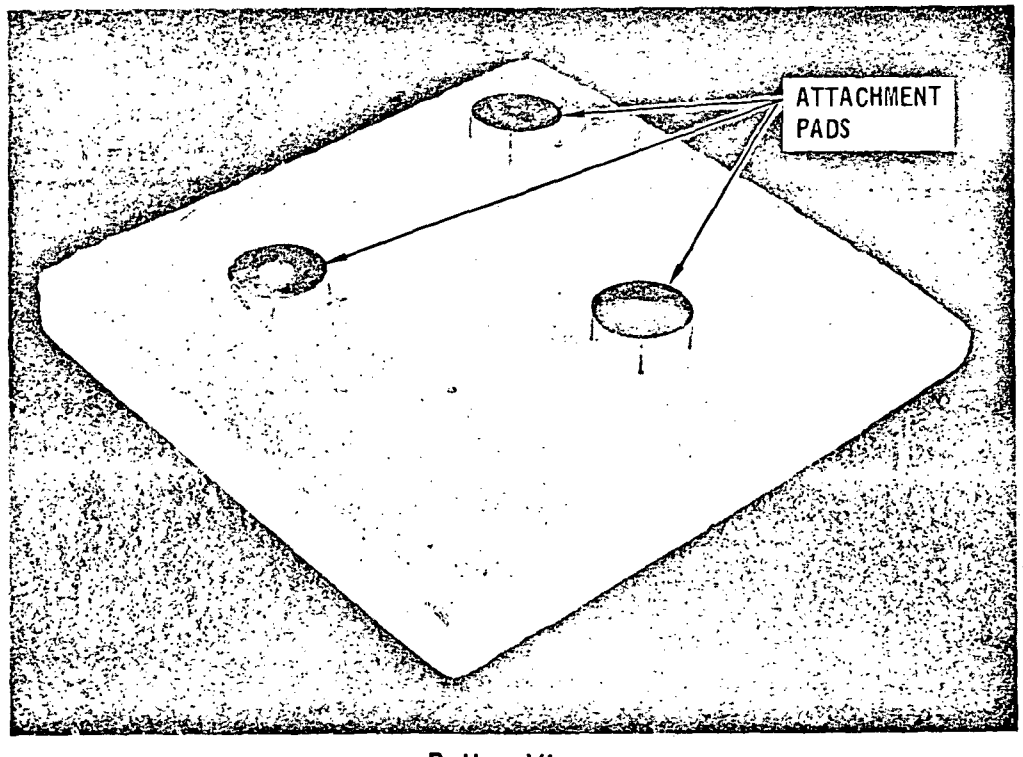

Bottom View

457-2369

FIGURE 6-5

3-D NICHROME WIRE REINFORCED HCF

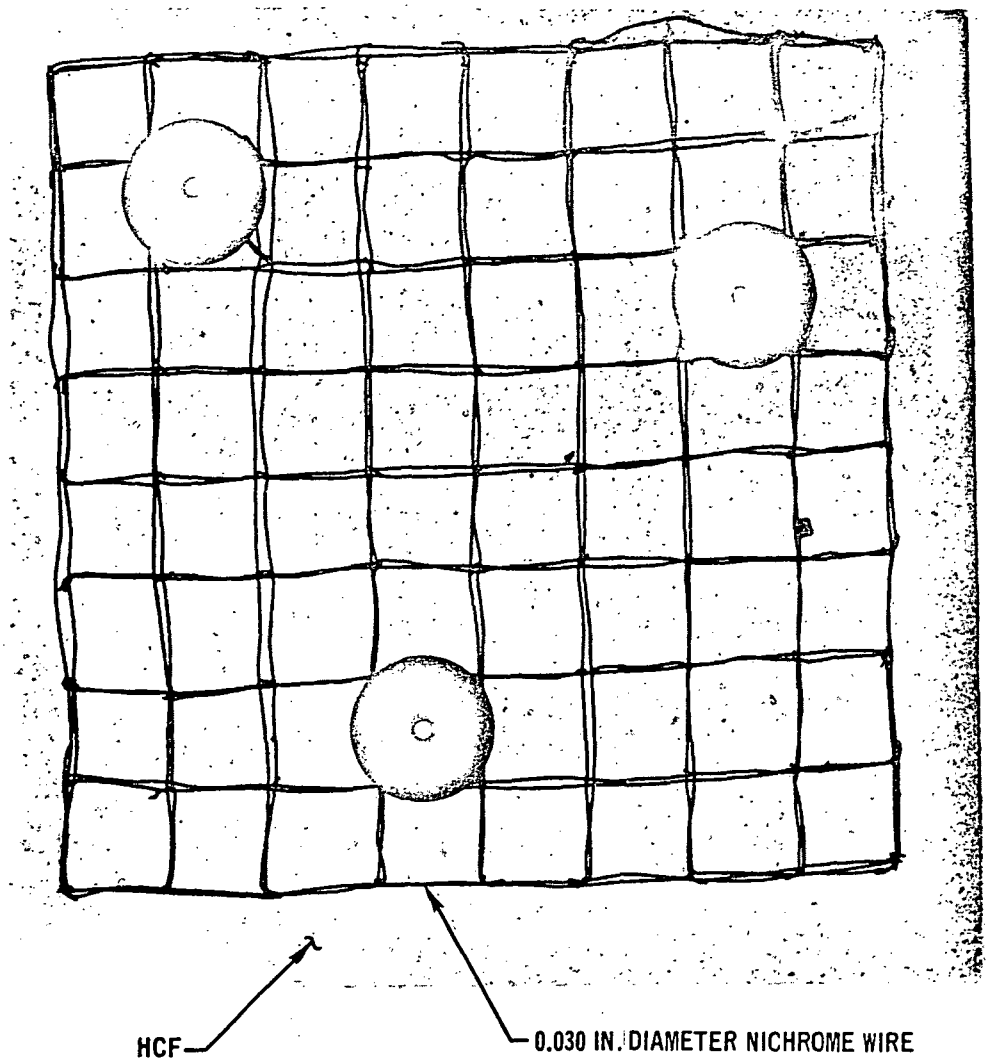

FIGURE 6-6
X-RAY OF NICHROME WIRE REINFORCED HCF
Improved RSI

columbium reinforcement extended through the packaged insulation and were mechanically attached to the primary structure. In order to prevent high temperature oxidation of the columbium alloy (Cb-752) wire structure, a coating was applied A fused slurry silicide coating (60 Si-20Cr-20Fe) was applied by dipping; it was fired in an argon atmosphere in a graphite furnace at 2600°F for one hour. The coating obtained was the desired thickness 3 $\pm$0.5 mils per side, but the columbium base metal remaining was so embrittled that the wire structure could not be handled without breaking some wires. Two broken pieces of wire, one 15

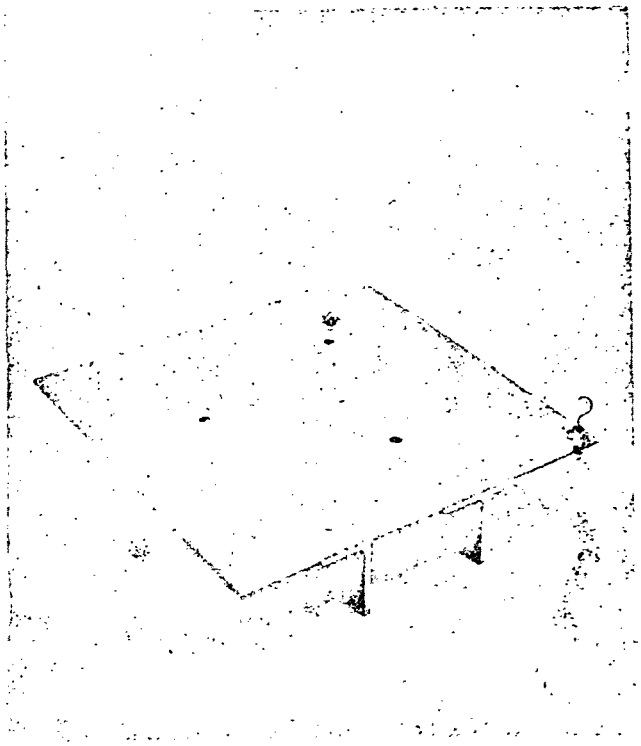

Primary Structure

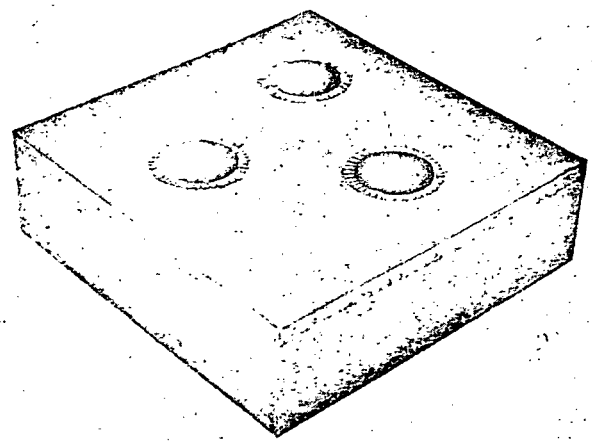

Packaged Insulation

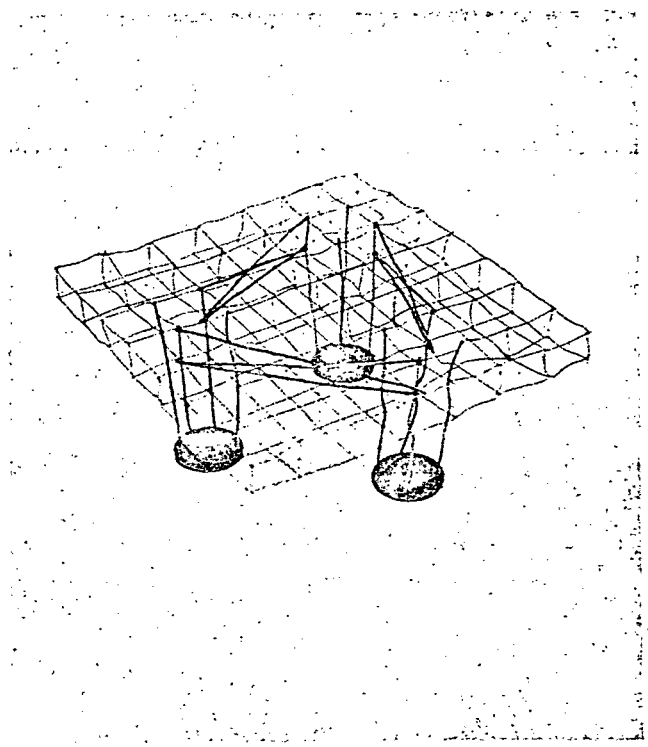

Cb Wire Grid

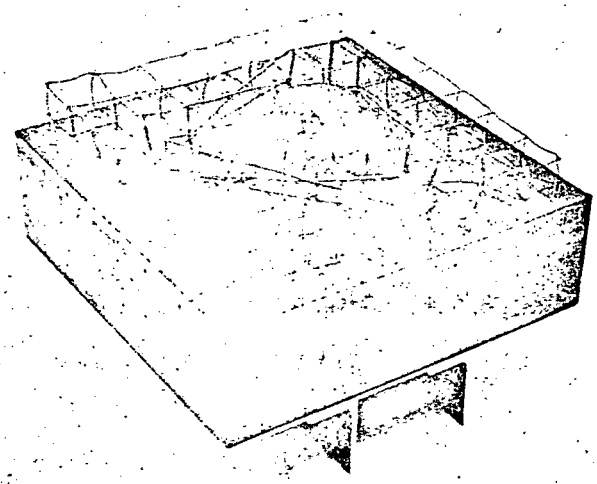

Total System

FIGURE 6-7
3D COLUMBIUM WIRE REINIFORCEMENT FOR HCF

mils in diameter and the other 40 mils in diameter, were submitted for metallographic cross-sectioning in an attempt to determine the cause for embrittlement. Photomicrographs are shown in Figures 6-8 and 6-9. There are many indications of carbides which are much more predominant than would be expected in wire products as supplied by the manufacturer. Oxides and nitrides are not as easily identified as carbides by visual observation, but are suspected of being major contributors to the embrittlement which was experienced due to poor atmospheric control during diffusion coating.

Full Depth Columbium Wire Array - An oxidation protective coating was applied to this array by Sylvania. The array had a full depth (thickness) HCF compared with the first columbium array which had a half-thickness reinforced HCF. In the first array, a space was provided below the array for efficient thermal insulation.

A one-inch spacing was used in making the second array using 0.032-inch diameter columbium wire. The bracing and legs were made from 0.04-inch diameter columbium wire. The legs were welded to columbium pads which were 0.063 by 1.375 inches in diameter. Each pad contained a 0.312-inch diameter hold which was provided for mechanical attachment to the airframe structure.

All intersections of wires were welded. Welding of this second array was more simply done because the larger diameter wires were used. The wires in the first array were 0.015-inch in diameter. The oxidation protective coating was applied by the fused slurry silicide process and was composed of 60 percent Si, 20 percent Cr, and 20 percent Fe. No embrittlement problems, such as had occurred on the first array were observed.

The array was visually inspected and appeared to be free of excess coating; it was quite smooth and uniform in color. All welds were tight before and after coating. The array was filled with mullite HCF and then dried and fired in the normal manner for HCF. The results of filling the array were excellent. See

100X

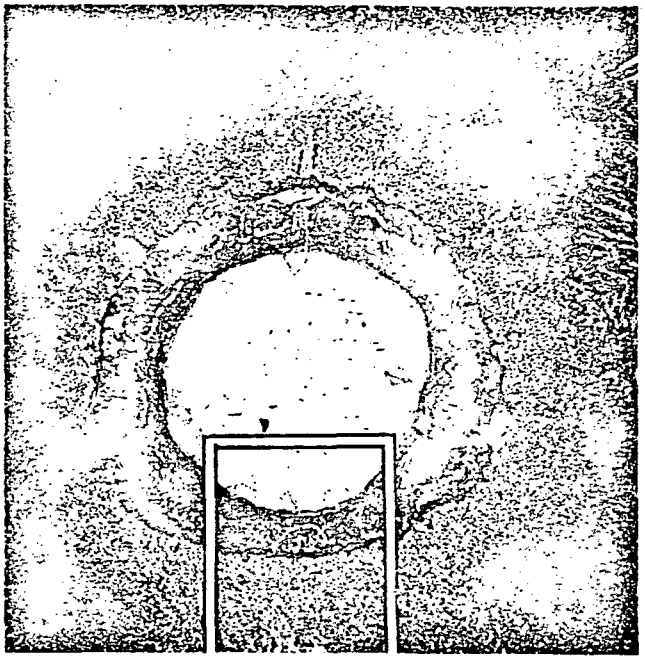

500X

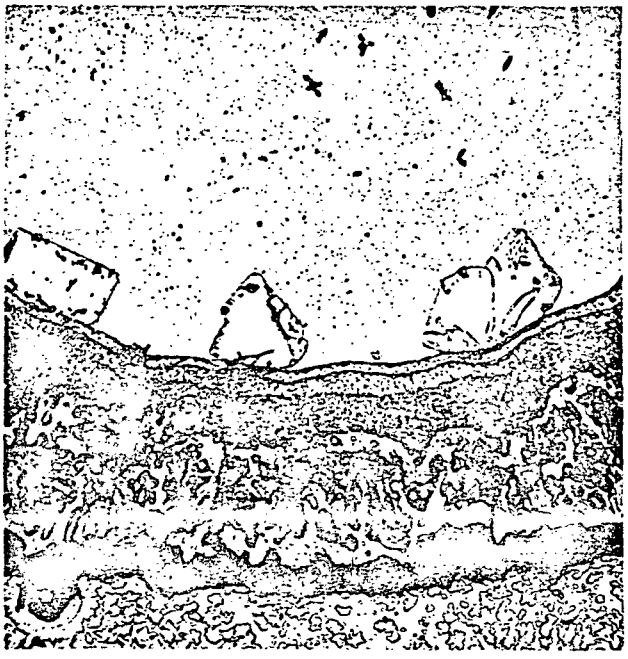

457-2439

FIGURE 6-8
CROSS SECTION OF 15 MIL DIAMETER, EMBRITTLED, COATED COLUMBIUM WIRE

100X

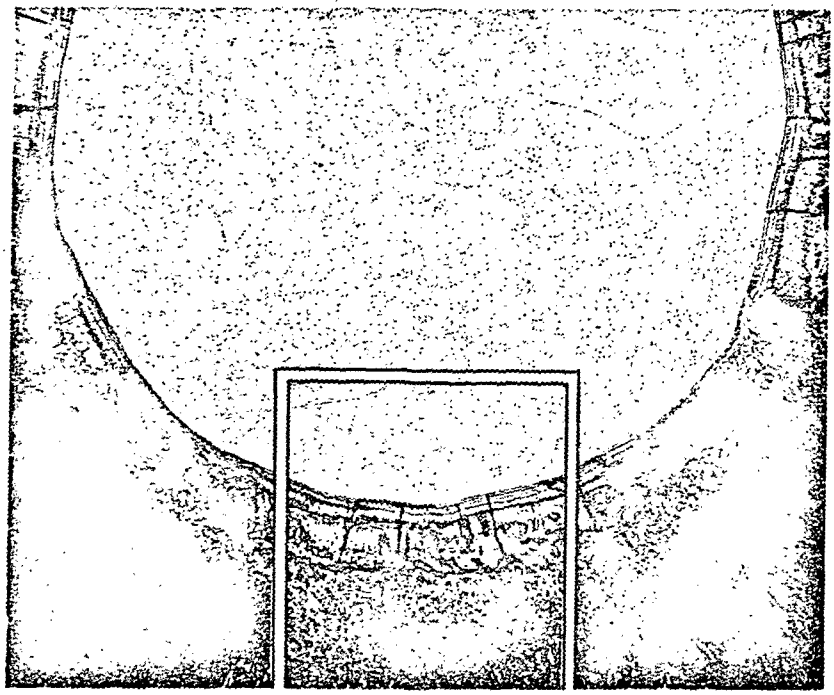

500X

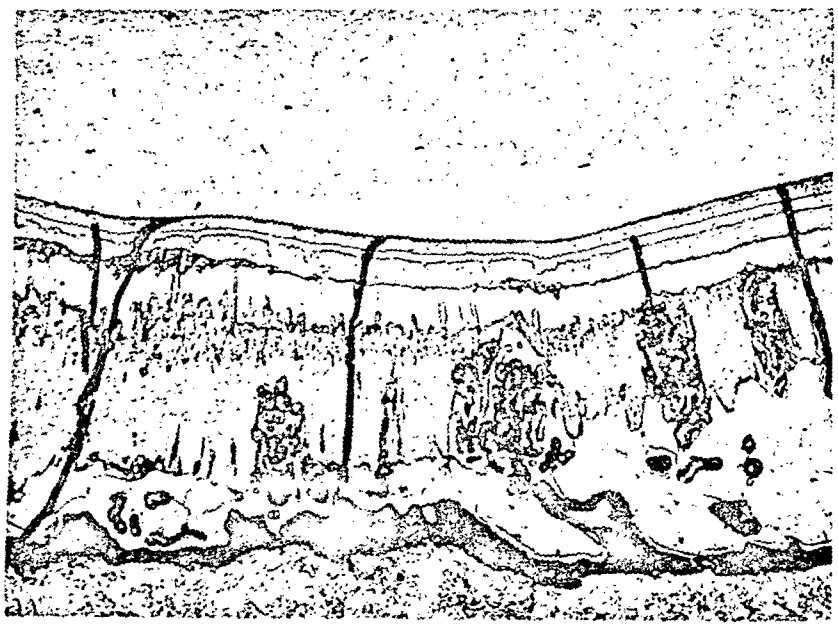

457-2438

FIGURE 6-9

CROSS SECTION OF 40 MIL DIAMETER,
EMBRITTLED, COATED COLUMBIUM WIRE

Figure 6-10. A complete visual and X-ray inspection revealed no voids, cracks, or inclusions. However, during repair of a defect in the coating on the columbium wire array, the HCF block developed a crack, probably due to the wire rapidly conducting the heat to the interior and causing internal stresses and the cracking. The type of localized heating used to effect the repair is not representative of an actual Shuttle use.

Modified Columbium Wire Array - A columbium wire array of modified design was fabricated as shown in Figure 6-11. The objective of this design was to optimize

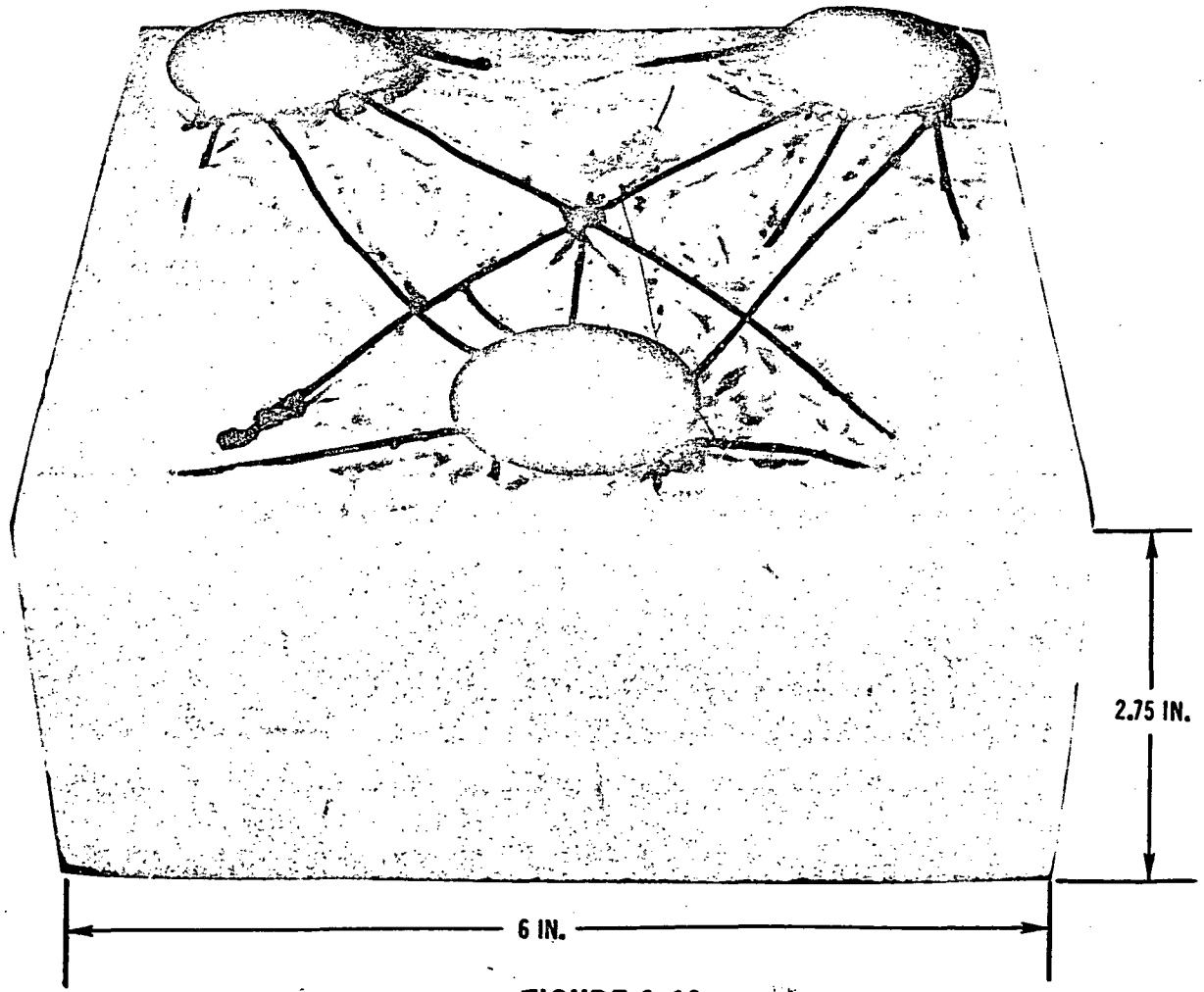

FIGURE 6-10
FULL DEPTH COLUMBIUM WIRE REINFORCED HCF AFTER FIVE CYCLES AT 2300°F/2500°F

4572566

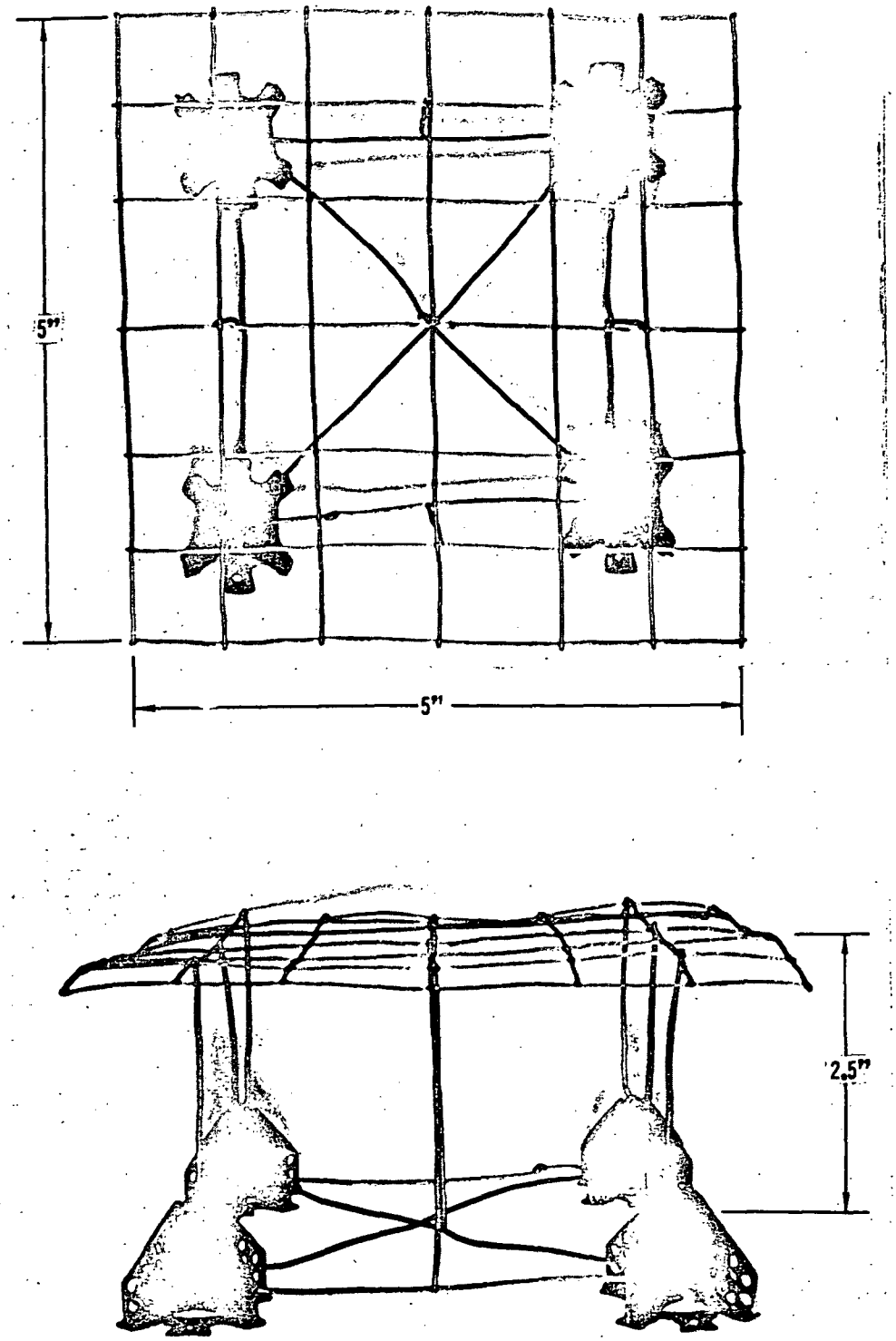

FIGURE 6-11
MODIFIED COLUMBIUM WIRE ARRAY

457-2534

the reinforcement by eliminating some unnecessary trusses and supports, while better distributing the loads at the attachment points.

6.5 THERMAL RESPONSE TO FULL-DEPTH COLUMBIUM WIRE REINFORCED HCF SPECIMEN - The full-depth columbium wire reinforced HCF specimen was exposed to five thermal cycles. The first four cycles peaked at 2300°F and the last at 2500°F (Figures 6-12 and 6-13). The specimen was inspected between and during test cycles for crack propagation and growth. The crack induced during processing did not grow and no further cracks were observed. It may be concluded that the columbium wires successfully reinforced the specimen by inhibiting crack growth.

In an attempt to measure the magnitude of "heat shorts" due to the wire reinforcements, one chromel-alumel thermocouple was placed on the bottom surface of the culumbium fastener foot and another was placed on the cold face of the HCF specimen in an area away from the wires. As shown in Figures 6-12 and 6-13, the foot was cooler than the HCF in both the 2300°F and 2500°F cases. These results were probably due to cooling from the 0.060-inch thick titanium face plate to which the reinforcement pads were bolted and to small heat conduction paths from the hot HCF tile to the attachment pads. From this test, the conclusion was drawn that the "heat short" consideration in our reinforced HCF concept is negligible. This is in agreement with earlier calculations which indicated a "heat short" of under one percent.

6.6 STRENGTHENED AND REINFORCED HCF - As an outgrowth of the reinforced HCF concept, an approach was conceived which could save considerable HCF thermal protection system weight.

This concept, shown in Figure 6-14, uses a truss system which transfers air pressure loads to three attachment points. The trusses are welded to the finer diameter wires which form the standard reinforcements. An early model using 0.035-inch diameter stainless wire is shown in Figure 6-15.

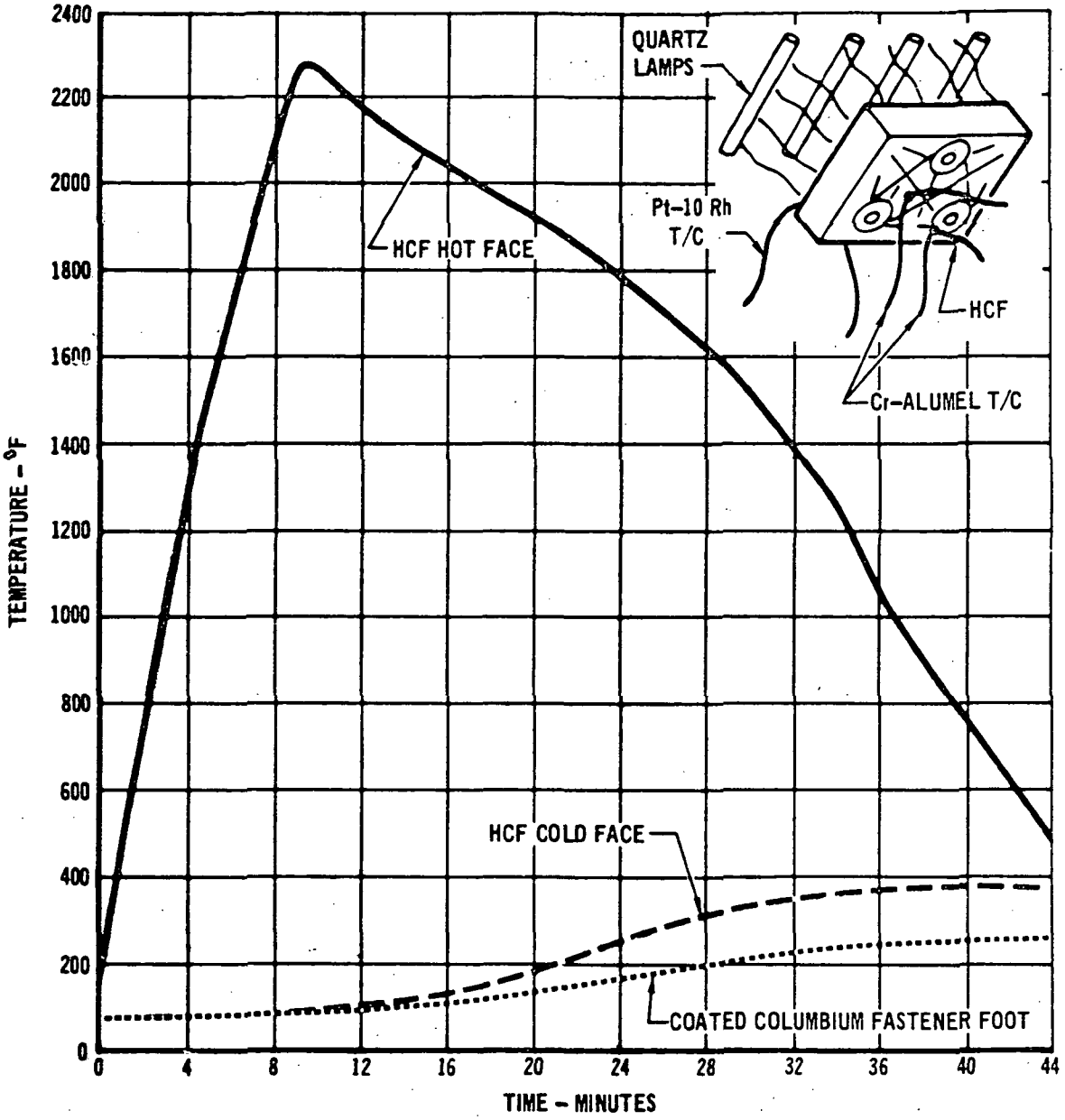

FIGURE 6-12

THERMAL RESPONSE OF COATED COLUMBIUM WIRE REINFORCED HCF DURING FIRST CYCLE AT 2300°F

457-2535

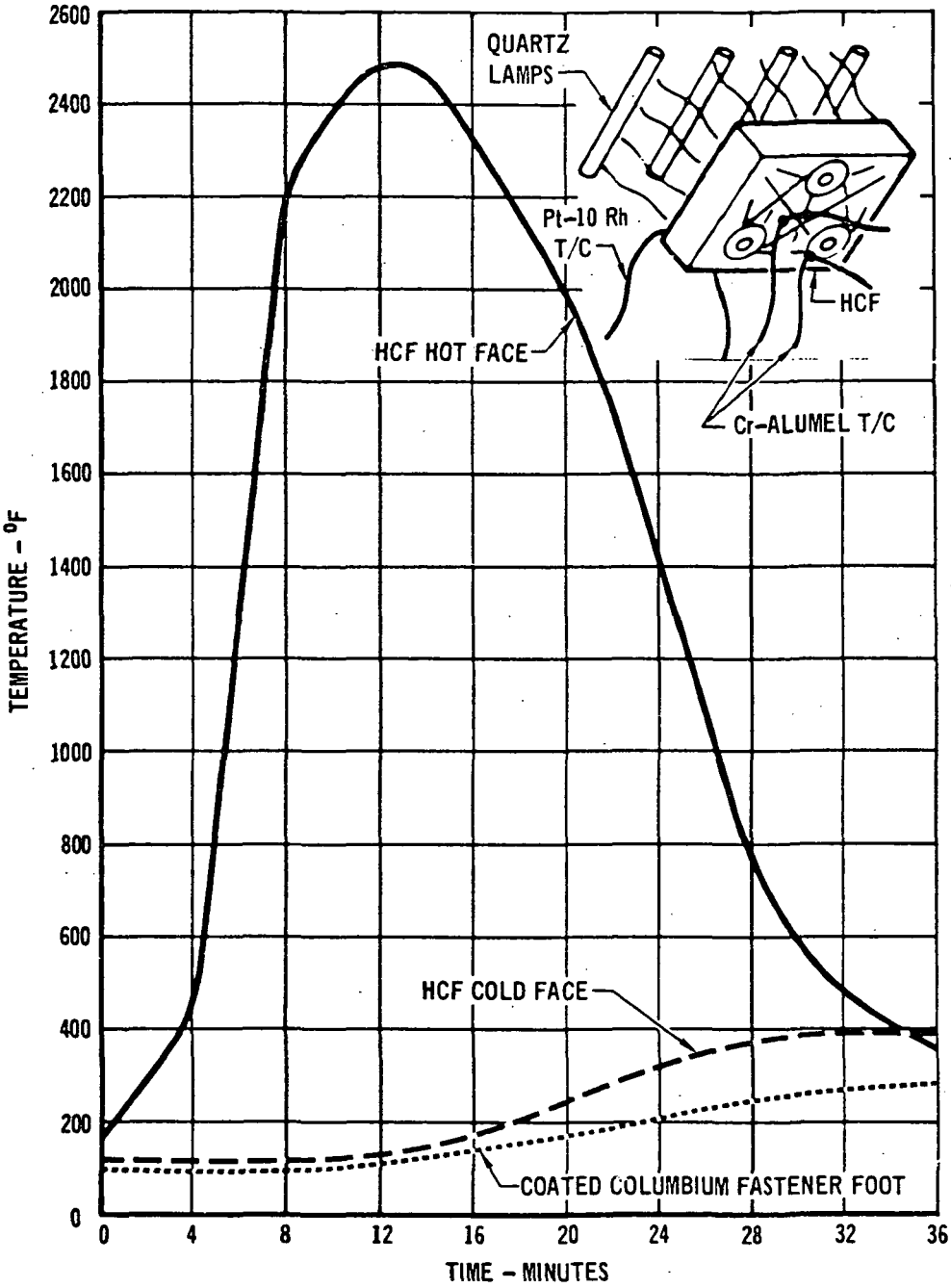

FIGURE 6–13

THERMAL RESPONSE OF COATED COLUMBIUM WIRE REINFORCED HCF DURING FIFTH CYCLE AT 2500°F

457–2536

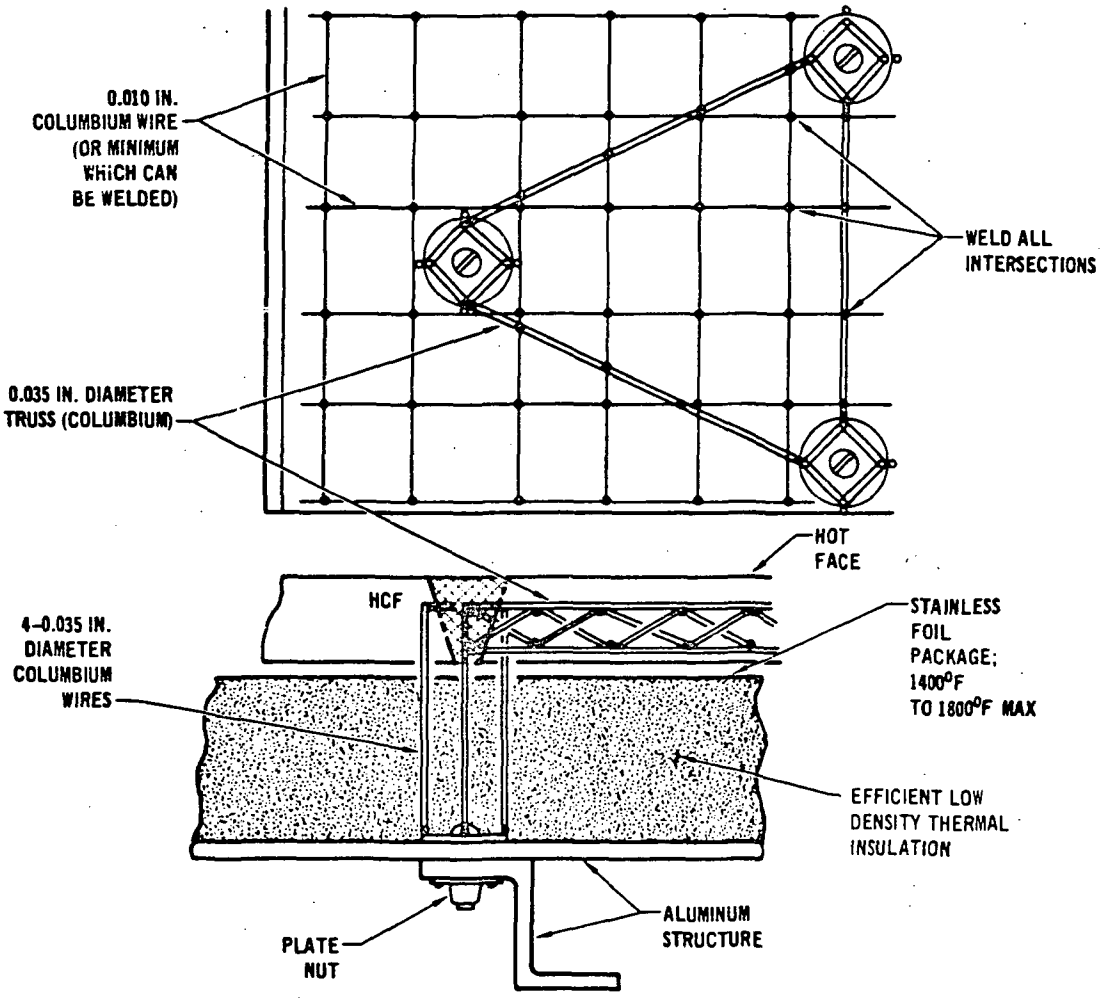

FIGURE 6-14

STRENGTHENED AND REINFORCED HCF THERMAL INSULATION PROTECTION SYSTEM

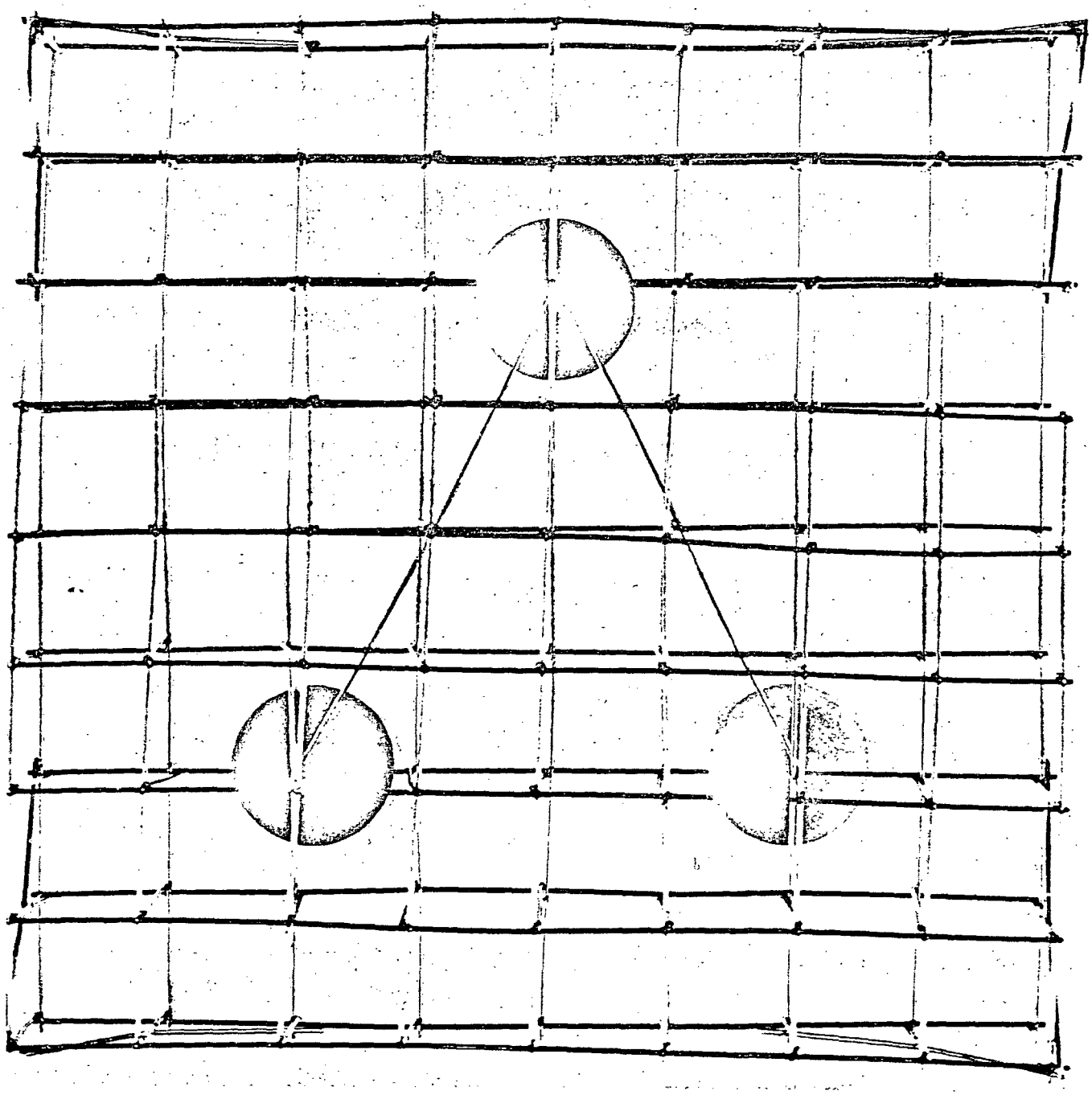

FIGURE 6–15

EARLY MODEL OF WIRE TRUSS STRENGTHENING SYSTEM

457–1777

The weight reduction is achieved by trading HCF very efficient low density insulation between the reinforced HCF tile and the airframe.

6.7 SUMMARY OF REINFORCEMENT ACCOMPLISHMENTS - The accomplishments and conclusions from the reinforcement effort are summarized below:

- Metal wires are the best reinforcement material; SiO_2 and ZrO_2 threads became brittle.
- Columbium (Cb-752) wires are better than nickel-chromium and platinum because of thermal expansion compatibility with HCF and temperature resistance.
- Wire reinforced HCF was felted, dried, and fired in the conventional manner with no difficulty.
- A simplified welded array of wires with load distribution attachment points has evolved.
- Reinforcement inhibited separation of cracked HCF during five thermal cycles.
- The "heat short" consideration in wire reinforcement was proven to be negligible during thermal cycling.

7.0 CONCLUSIONS AND RECOMMENDATIONS

The following conclusions and recommendations are based on the work performed in this program and the related work in References (a) and (b) of Section 8.

7.1 Strength - Improvements can be made in the strength of mullite HCF material by control of the processing variables, with values of up to 250-lb/in^2 in tension possible for 16-lb/ft^3 material. Strength and modulus of elasticity are dependent on density. The strength of HCF is anisotropic because of the preferred orientation of the fibers.

7.2 Density - Average density can be controlled to 15 $\pm$ 1-lb/ft^3 from felt to felt, and $\pm$ 1 PCF within a single tile by formulation and processing control. Each new fiber type and diameter, filler and binder material processes differently. Various blending times and speeds, and resulting viscosities, are examples of the types of parameters which must be adjusted and then controlled to produce good quality felts. Also, various organic processing aids can be added to control the quality and uniformity of the final products.

7.3 Thermal Performance - Thermal performance efficiency can be improved on the order of 20 percent by substituting about 20 percent of smaller diameter, less than 2-μ fibers for standard 6-μ diameter fibers.

Our Mod V composition, which is an 80-20 mixture of mullite and silica fibers, offers the thermal performance improvement described above and possible higher strength, compared to our Mod IIIA material. This is based on laboratory size felts.

Small diameter (1.6-μ) aluminosilicate fibers (SKX type) have shown to be efficient in thermal performance when tested in an HCF type formulation; however, they are not as temperature resistant as mullite fibers.

Small diameter (2.5-μ) mullite has also recently been produced by B&W, and evaluated by us to a limited degree. These fibers should also be efficient thermal insulators.

Mixtures of fibers, such as silica and mullite, and combinations of fine and medium diameter mullite fibers, are areas in which RSI could be further improved.

7.4 Coatings - A smoother inorganic surface coating can be obtained by first filling the HCF surface irregularities and then overspraying. The surface density of the coating can be decreased to 0.15-lb/ft^2 by eliminating one layer of the coating. This system still remains waterproof and reusable but its strain to failure could not be increased.

The following areas are suggested for future work on coatings:

- Develop a low modulus reusable inorganic coating that is sealed from liquid water with an organic coating that would be refurbished after entry. The inorganic coating would provide handling abrasion resistance when the organic coating is absent. This would eliminate the high modulus glass seal coating that is a shortcoming of that type coating system.
- Develop an inorganic glassy sealed coating that is self-healing. This would provide waterproofing of cracked coating upon cool-down. The present coating systems that provide this feature, blister at reduced pressure and at temperatures around 2500°F.
- Evaluate organic coatings that provide liquid waterproofing of the gaps in the RSI tiles and that can be refurbished after different temperature exposures up to 2500°F.
- Evaluate organic impregnants which provide waterproofing for several flights by pyrolysis/condensation mechanisms.

7.5 Reinforcements - Metal wires are an effective means of preventing the separation of cracked pieces of HCF and do not cause appreciable heat shorts. Reinforced HCF can be made void free, by standard felting techniques. An increase in density of 1.5-lb/ft^3 resulted from the use of a coated columbium wire reinforcement.

This reinforcement effort led to the concept of strengthening HCF by including metallic trusses in the HCF. When combined with the use of efficient low-density insulation, these trusses could save up to 50 percent of the weight of an unreinforced RSI thermal protection system.

8.0 REFERENCES

Reference (a): High Temperature Insulation Materials for Reradiative Thermal Protection Systems, MDC Report E0666, 19 July 1972.

Reference (b): Reusable Surface Insulation (RSI) Thermal Protection Development for Shuttle, MDC Report E0557, Volume I, 21 March 1972.

Page Intentionally Left Blank

MCDONNELL DOUGLAS ASTRONAUTICS COMPANY - EAST
Saint Louis, Missouri 63166 (314) 232-0232

MCDONNELL DOUGLAS
CORPORATION

Page Intentionally Left Blank